Alfred-Wegener-Institut für Polar- und Meeresforschung
Forschungsstelle Potsdam
Arbeitsgruppe 'Periglazialforschung'

Freshwater ostracods as bioindicators in Arctic periglacial regions

Dissertation
zur Erlangung des akademischen Grades
"doctor rerum naturalium"
(Dr. rer. nat.)
in der Wissenschaftsdisziplin "Geowissenschaften"

eingereicht an der
Mathematisch-Naturwissenschaftlichen Fakultät
der Universität Potsdam

von
Sebastian Wetterich

Potsdam, Dezember 2008

Table of contents

Kurzfassung

Grosse Gebiete der kontinentalen Erdoberfläche sind von Permafrost unterlagert, d.h. von ständig gefrorenen Untergrund, der in Periglazialregionen mit negativen Jahresmitteltemperaturen auftritt. Der kontinuierliche Permafrost, umfasst in den arktischen und subarktischen Tiefländern der nördlichen Hemisphäre Tundra-, Waldtundra- und Taigalandschaften. Er ist dort ein dominierender Umweltfaktor, der die Vegetation, die Hydrologie, die Böden und das Relief einer periglazialen Landschaft durch den jahreszeitlichen Wechsel von Abkühlen, Gefrieren, Erwärmen und Auftauen in der obersten aktiven Schicht (Auftauzone) sowie durch längerfristige Dynamik bestimmt. Da Permafrosteigenschaften und Permafrostdynamik von langfristigen Klimabedingungen abhängen, werden entsprechende gefrorene Sedimentabfolgen, die während des Quartärs akkumulierten, als Archiv von Klima- und Umweltveränderungen der Vergangenheit betrachtet.

Basierend auf der Tatsache, dass die heute fortschreitende globale Erwärmung die arktischen Gebiete weit mehr als andere Regionen der Erde beeinflusst, ist die Untersuchung von klimaempfindlichen Organismen in der modernen und in der vergangenen polaren Umwelt von großer Bedeutung, sowohl für das Verständnis der heutigen Wechselwirkungen als auch für die Abschätzung zukünftiger Auswirkungen des Klimawandels. Frühere Umweltveränderungen in arktischen Periglazialgebieten können mit Hilfe gut erhaltener Tier- und Pflanzenfossilien aus Permafrostabfolgen rekonstruiert werden. In der hier vorgelegten Arbeit werden Ostracoden als ein neuer Bioindikator für das Umweltarchiv Permafrost eingeführt, wobei taxonomische und geochemische Untersuchungsmethoden genutzt werden. Ostracoden sind Kleinkrebse mit einem zweiklappigen Kalzitgehäuse. Diese aquatischen Organismen reagieren sensibel auf sich ändernde Lebensbedingungen. Die hohe Anzahl von Ostracodenschalen in lakustrinen Sedimenten machen sie zu nützlichen Anzeigern vergangener Umweltbedingungen. Die geochemischen Eigenschaften im Kalzit der Ostracodenschalen, d.h. stabile Isotopenverhältnisse von Sauerstoff ($\delta^{18}O$) und Kohlenstoff ($\delta^{13}C$) und molare Elementverhältnisse von Strontium, Magnesium und Kalzium (Sr/Ca, Mg/Ca) widerspiegeln die Wasserzusammensetzung in den jeweiligen Habitaten.

Moderne Ostracodenassoziationen wurden in Nordost-Sibirien im Norden (Lenadelta), im Nordosten (Moma-Gebiet) und im zentralen Teil (Lena-Amga-Gebiet) Jakutiens untersucht. Referenzdatensätze zu Süßwasserostracoden Nordost-Sibiriens waren bisher kaum vorhanden, so dass die vorgelegte Arbeit einen ersten umfassenden regionalen Datensatz präsentiert. Diese Datensammlung umfasst Ergebnisse von Untersuchungen der modernen Ostracodetaxonomie und -geochemie exemplarischer Standorte, die auf

fossile Ostracoden-Vergesellschaftungen angewendet wurden. Die periglazialen Gewässer jeder Untersuchungsregion (Polygontümpel, Tau-Seen und Thermokarstseen) erbrachten umfangreiche Originaldaten zur Artenverbreitung und den entsprechenden ökologischen Bedingungen in Nordost-Sibirien. Insgesamt wurden 42 Taxa in modernen und fossilen Ostracodenvergesellschaftungen gefunden. Davon wurden 10 Taxa sowohl modern als auch fossil nachgewiesen, 18 Taxa sind nur in modernen Habitaten präsent und 14 Taxa, einschließlich einiger heute ausgestorbener Arten, wurden nur fossil gefunden.

Die fossilen Ostracoden sind zahlreich in spätquartären Permafrostabfolgen, die in interglazialen Warmzeiten und gemäßigten interstadialen Perioden akkumulierten (Eem-Interglazial, Mittelweichsel-Interstadial, Spätweichsel/Frühholozän einschließlich des Allerød, Spätholozän). In Ablagerungen aus Kaltzeiten hingegen wurden kaum Ostracoden gefunden. Insbesondere die in modernen Habitaten weitverbreitete Art *Candona muelleri jakutica,* konnte fossil in Ablagerungen aus dem Früh- und Mittelweichsel, wie auch aus dem Spätholozän zahlreich nachgewiesen werden. Außer in früh- und spätweichselzeitlichen Sedimenten findet sich die Art *Fabaeformiscandona harmsworthi* in allen untersuchten Abfolgen, wobei diese Ostracodenart wahrscheinlich endemisch für die Arktis ist und auch heute in Nordjakutien vorkommt. Fossile Schalen der Art *Fabaeformiscandona rawsoni*, die heutzutage in Zentraljakutien anzutreffen ist, wurden in Sedimenten unterschiedlicher Warmphasen gefunden. Zwei weitere häufig fossil vorkommende Arten, *Limnocytherina sanctipatricii* und *Ilyocypris lacustris*, fehlen allerdings in den modernen Gewässern oder sind dort nur sehr selten. Vier typische Arten der fossilen Ostracodenassoziationen aus warmzeitlichen Sedimenten (*Limnocythere falcata*, *L. goersbachensis*, *L. suessenbornensis,* and *Eucypris dulcifons*) konnten ebenfalls in modernen Habitaten nicht wiedergefunden werden.

Die geochemischen Eigenschaften des Ostracodenkalzits werden als zeitlich und räumlich begrenzte Indikatoren der entsprechenden Gewässerzusammensetzung zum Zeitpunkt der Schalenbildung betrachtet. Da bisher keine regionalen Vergleichsdaten verfügbar waren, wurde ein entsprechender Datensatz erhoben, um erste Interpretationen der Zusammenhänge zwischen der Wasserzusammensetzung und Schalenkalzit einzelner Ostracodenarten vorzunehmen. Solche Zusammenhänge konnten nachgewiesen werden, wenn die untersuchten Individuen in höherer Zahl vorlagen und die gemessenen Umweltparameter einen ausreichend hohen Gradienten aufwiesen. Die Beziehungen zwischen $\delta^{18}O$, Sr/Ca, Mg/Ca auf der einen und der elektrischen Leitfähigkeit (bzw. Salinität) der Gewässer als Ausdruck der verdunstungskontrollierten Ionenkonzentrationen auf der anderen Seite, sind komplex und konnten aufgrund der begrenzten Datenlage noch nicht umfassend geklärt werden. Mehrere

Steuermechanismen (z.B. Temperatur- und Stoffwechseleffekte), die bei der Kalzitbildung die Aufnahme der Isotope und Elemente in die Ostracodenschale beeinflussen konnten daher für die untersuchten periglazialen Habitate noch nicht ausreichend beurteilt werden. Für die Rekonstruktion regionaler quartärer Umweltbedingungen bestätigen die fossilen Ostracoden die Existenz von stabilen Flachwasserstandorten und ergänzen zudem die Rekonstruktion polygonaler Tundren und thermokarst-geprägter Landschaften. Die geochemische Zusammensetzung der Ostracodenschalen und die Artvorkommen widerspiegeln dabei auch das hydrologische und hydrochemische Regime der quartären Periglazialgewässer. Neue stratigraphische und paläoökologische Ergebnisse in der vorgelegten Arbeit unterstreichen die Bedeutung von Rekonstruktionen der interstadialen und interglazialen Umweltbedingungen. Weiterführende Untersuchungen moderner und fossiler Ostracoden werden ihre zukünftige Anwendung als Bioindikatoren für die sibirische Arktis verbessern.

Abstract

Large areas of the continental Earth's surface are underlain by permafrost, i.e. frozen ground that exists in periglacial regions with negative mean annual air temperatures. Continuous permafrost in arctic and subarctic lowlands including tundra, forest-tundra, and taiga periglacial landscapes of the Northern Hemisphere is a dominant environmental factor; it affects vegetation, hydrology, soils, and morphology via seasonally alternating freezing, cooling, and thawing of the ground (cryogenic processes) as well as long-term variations. Due to the dependence of permafrost characteristics and dynamics on long-term climatic conditions, permafrost sequences which accumulated during the Quaternary past are regarded as an archive of palaeoenvironmental and palaeoclimatic changes.

Based on the fact that the current, ongoing global warming affects arctic regions to a greater degree than other Earth environments, studies of climate-sensitive organisms in modern and past polar environments are of great value for enabling us to understand current interactions and to estimate the impact of future climate changes. Past environmental changes in arctic periglacial regions can be deduced from well-preserved floral and faunal remains in permafrost deposits. In this study, freshwater ostracods are established as a new bioindicator for understanding permafrost as a palaeoarchive; environmental interpretations are reinforced using taxonomical and geochemical methods. Ostracods are small crustaceans whose bivalved shells consist of calcite. These aquatic organisms are sensitive to environmental conditions, and the high frequency at which their valves occur in lacustrine sediments makes them a useful palaeoproxy. Geochemical properties, i.e. stable isotopes of oxygen and carbon ($\delta^{18}O$, $\delta^{13}C$) and element ratios of strontium and magnesium to calcium (Sr/Ca, Mg/Ca) in ostracod calcite reflect the host water composition.

The modern ostracod records presented are from North (Lena Delta), Northeast (Moma region), and Central (Lena-Amga region) Yakutia (Northeast Siberia). Reference freshwater ostracod data were previously rare for Northeast Siberia; thus a comprehensive dataset has been introduced for this region. This dataset includes studies of modern ostracod taxonomy and geochemistry, which are based on exemplary sites and have been applied to fossil records. Each study site reveals original data of ostracod species distribution and environmental conditions in Northeast Siberia; sites comprise different types of periglacial waters (polygonal ponds, thaw lakes, and thermokarst lakes). A total of 42 ostracod taxa were identified in modern and fossil records; ten taxa could be found in both the modern and the fossil periglacial environments studied, whereas 18 taxa only occur today and 14 taxa, including some extinct species, have only been described from fossil records.

The fossil ostracods in late Quaternary permafrost sequences are numerous in deposits from warm stages and temperate periods (i.e. Eemian Interglacial, Middle Weichselian Interstadial, Late Weichselian/early Holocene including the Allerød period and late Holocene) whereas cold-period deposits are almost free of ostracods.

In particular, the species *Candona muelleri jakutica,* wide-spread in modern records, has been indentified in deposits from the Early and Middle Weichselian and the Late Holocene. Except for Early and Late Weichselian sediments all lacustrine records contain shells of *Fabaeformiscandona harmsworthi*, a species likely endemic to the Arctic that occurs today in North Yakutia. Fossils of the species *Fabaeformiscandona rawsoni*, present today in Central Yakutia, have been obtained from warm-stage deposits. Other common fossil ostracods belong to the species *Limnocytherina sanctipatricii* and *Ilyocypris lacustris,* which are rare or lacking in the modern environments studied. Four species without a modern record (*Limnocythere falcata*, *L. goersbachensis*, *L. suessenbornensis,* and *Eucypris dulcifons*) were also frequently found in the warm-stage sediments.

Geochemical properties of ostracod calcite that precipitates from the host water at the time of shell secretion are regarded as a spatially- and temporally-restricted reflection of the host water composition. No regional reference data were previously available; thus, a new data set has been compiled to allow initial interpretation of the linkage between the composition of host waters and ostracod calcite of single species. It is valid for studied species that were found in higher frequencies and over considerable ranges in the values of measurable environmental properties. The relationships between $\delta^{18}O$, Sr/Ca and Mg/Ca ratios, and electrical conductivity (salinity) as an expression of solute concentrations in the waters that are mainly controlled by evaporation are more complicated, and the limited database is insufficient to clarify these relationships. Several controls on the uptake of isotopes and elements into ostracod calcite (i.e. temperature and metabolic effects) clearly exist but cannot yet be assessed for the studied periglacial habitats.

Ostracod fossils support the reconstruction of stable shallow aquatic conditions in regional palaeoenvironmental records and complete landscape reconstructions, especially for polygonal tundra plains and thermokarst-affected landscapes. The composition of fossil freshwater ostracod calcite and distribution of species also mirror the hydrological and hydrochemical regime of periglacial inland waters in the Quaternary past. New here presented stratigraphic and palaeoecological results highlight the usefulness of reconstructions of interglacial and interstadial environments. Further comprehensive studies in both modern and fossil research directions will allow reliable future applications of ostracods as bioindicators in Arctic Siberia.

1 Introduction

1.1 Scientific background

1.1.1 Arctic environmental dynamics

Worldwide, substantial climate warming has occurred during the second half of the 20th century (IPCC 2007). This warming has been particularly intense in the Arctic, a phenomenon known as the “polar amplification” (Serreze et al. 2000; ACIA 2005; McGuire et al. 2007).

Accompanying pronounced changes in climate, pronounced changes in permafrost conditions have been observed in Russian arctic regions with increasing air and permafrost ground temperatures (Oberman and Mazhitova 2001; Richter-Menge et al. 2008) as well as increasing greenness of the arctic region as snow melts earlier in spring and the shrub and tree lines expand to the North (Richter-Menge et al. 2008). Warmer summer air temperatures and deeper winter snows over permafrost result in an increase of the maximum seasonal thaw depth (Lemke et al. 2007).

Simultaneous changes of climate and permafrost conditions in the Russian Arctic have also been inferred on longer time scales. Permafrost has been present in the arctic Siberian lowlands since the Late Pliocene (Arkhangelov et al. 1996) and has persisted there over the entire Pleistocene, although it strongly degraded during warm periods (e.g. during the Eemian Interglacial; Kienast et al. 2008). During the Holocene a dramatic decrease of the permafrost zone occurred together with large-scale flooding of arctic shelf areas (Romanovskii et al. 2004).

Continental arctic freshwater bodies ranging from small, shallow polygonal ponds to large thermokarst lakes occupy huge areas of the arctic and subarctic lowlands and provide an integrated, climate-sensitive inventory of changes in the surrounding landscape. Seasonal shifts in water flow, ice cover, precipitation surplus, and sediment and nutrient input have all been identified as climate-related factors that control the biodiversity, storage regime, and greenhouse gas exchange of these water bodies (Wrona et al. 2005). Using satellite-, air-, and ground-borne remote sensing methods, Yoshikava and Hinzman (2003) and Smith et al. (2005) showed for Alaska and Siberia, respectively, that initial permafrost melting leads to thermokarst and lake expansion, followed by lake drainage and shrinkage as the permafrost degrades further. Such examples highlight the climate sensitivity of arctic freshwater bodies.

Permafrost degradation is already leading to changes in surface relief and drainage patterns. Thermokarst poses a serious threat to arctic biota through either inundation (when the lake forms) or desiccation (when the lake drains) (Hinzman et al. 2005; Walsh et al. 2005). Satellite data reveal that in the past three decades the total lake area in the

continuous permafrost zone of Siberia has increased by 12 % whereas the number of lakes rose by 4 % (Smith et al. 2005).

Beside thermokarst lakes, polygonal ponds are widely distributed in wetland landscapes of the arctic lowlands. These shallow, small waters are often highly productive, and form hotspots of biodiversity for microorganisms, plants, and animals in this otherwise hostile environment (Smol et al. 2005). Polygonal ponds are especially susceptible to the effects of climatic change because of their small water volume and large surface area to depth ratio (Smol and Douglas 2007). Current studies from the Canadian High Arctic document the disappearance of polygonal ponds due to increasing evaporation/precipitation ratios that are probably associated with climatic warming (Smol and Douglas 2007).

Based on the fact that the ongoing global climate warming affects arctic regions to a greater degree than other Earth environments, studies of climate-sensitive organisms in modern and past polar environments will be of great value for estimating the impact of future climate changes. In this context, freshwater ostracods from arctic periglacial waters are regarded as valuable bioindicators, and are the subject of the studies presented in this thesis.

1.1.2 Freshwater ostracods and their use in palaeoenvironmental studies

Ostracods are small aquatic organisms mostly ca. 1 mm long (different species range in size from 0.3 to 30 mm; Athersuch et al. 1989). In phylogenetic systematics ostracods are classed within the Metazoa and belong to the Phylum Arthropoda LATREILLE, 1829, Subphylum Crustacea PENNANT, 1777. The Class Ostracoda LATREILLE, 1806 is separated from other Crustacea such as lobsters and crabs by a laterally compressed body, undifferentiated head, five to eight limbs, and a bivalved carapace lacking growth lines (e.g. Horne et al. 2002). Micro-crustacean ostracods are considered to be the most diverse Crustacea with probably at least 25,000 extant species, of which roughly 12,000 have been described (3,000 freshwater and 9,500 marine species; Cohen et al. 2007). Ostracods inhabit a wide range of marine and non-marine (freshwater) habitats including both temporary and stable inland waters, lakes, rivers, springs, and even groundwater. They can be divided into pelagic (free-swimming) and benthic (crawling in or on the substrate) forms. Both forms receive their nutrition from a wide range of sources including diatoms, bacteria, and detritus. Benthic ostracods are commonly detritivores or filter feeders. The reproduction of ostracods includes asexual (parthenogenetic) and sexual modes. Sexual reproduction enables selection for sexual dimorphism; males and females of the same species may have carapaces of slightly differing form.

Early fossil records of marine ostracods are known from the Cambrian (e.g. Athersuch et al. 1989), whereas the first freshwater forms occurred in the Carboniferous. Since the

Jurassic, freshwater ostracods have become common. Along with marine, brackish water, and (semi-) terrestrial species all freshwater ostracods belong to the Order Podocopida SARS, 1866 (Meisch 2000). However, freshwater ostracods do not belong to one phylogenetic group, but arose from three different lineages; the Darwinuloidea, Cypridoidea, and Cytheroidea occupied inland waters independently (Martens et al. 2007). The research presented here is focused on freshwater species from modern habitats and from Quaternary permafrost sequences in Yakutia (Northeast Siberia, Russia).

As in other Arthropoda, a distinctive morphological feature of ostracods is the two-sided symmetry of their body shape. The paired parts of the soft body are enclosed in a dorsally-hinged carapace which consists of a right and a left valve; various appendages protrude from the carapace for locomotion, feeding, and reproduction (Figure 1-1). The podocopid ostracods produce a calcified, overlapping flange called a duplicature around the ventral margin.

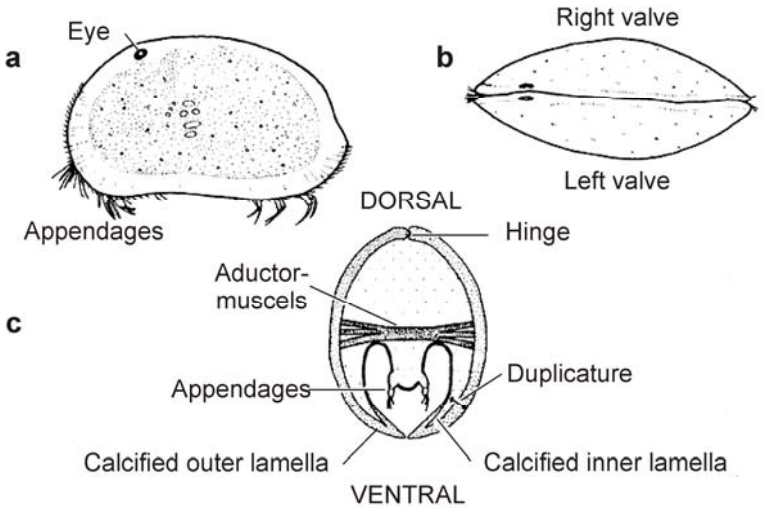

Figure 1-1: General structure of a typical podocopid ostracod: (a) carapace seen from the left side with appendages protruding ventrally; (b) carapace seen dorsally; (c) schematic cross section (modified after Athersuch et al. 1989)

The term ‘ostracod’ derives from the Greek word ‘*όστρακον*’ (*ostrakon*) which means ‘shell’ or ‘mussel’ and describes the outer structure of the animal. The classification of living ostracods is mostly based on variations in their soft body parts and appendages, but fossil ostracods usually lack well-preserved, intact soft parts; therefore, the morphological characteristics of the carapace have become essential to palaeontological classification.

The carapace of ostracods consists of low-magnesium calcite (Kesling 1951); these valves are commonly preserved as fossils in marine and lacustrine sediments. A fossil ostracod assemblage is often composed of numerous valves from juvenile specimens and

fewer valves from adults, implying lower adult numbers. However, during ostracod ontogeny, the individuals pass through nine moult (growth) stages between egg and adult and every stage leaves a calcareous carapace which may be preserved in the fossil record; therefore, each individual adult may also be represented by eight juvenile specimens.

Broad knowledge of taxonomy, species distribution, and ecology is prerequisite for using ostracods in palaeoenvironmental research. Ostracod species have distinct ecological requirements for water salinity, water temperature, dissolved oxygen supply, and additional habitat parameters such as area, water depth, and water permanency and type (e.g. Hiller 1972; Boomer et al. 2003). Due to this sensitivity of freshwater ostracods to environmental conditions and the high frequency at which their valves occur in lacustrine sediments, freshwater ostracods have been frequently and effectively used as palaeoenvironmental indicators mainly based on three approaches (Mischke 2001):

- ⇒ assuming that the ecological requirements of modern assemblages also apply to fossil records (e.g. Viehberg 2006; Horne 2007; Mischke et al. 2007, 2008);
- ⇒ investigating the effects of environmental physical and chemical parameters on the shape and structure of the carapace (e.g. Vesper 1975; van Harten 2000); and
- ⇒ analysing the geochemical properties of ostracod shells (e.g. Xia et al. 1997a; Holmes and Chivas 2002).

The later approach includes measuring element ratios of magnesium and strontium to calcium (Mg/Ca, Sr/Ca) as well as stable isotope ratios of oxygen ($\delta^{18}O$) and carbon ($\delta^{13}C$) in ostracod calcite; these ratios are increasingly used in palaeoenvironmental reconstructions of temperature, salinity, and lake productivity (e.g. Griffiths and Holmes 2000).

Freshwater ostracods have already been successfully used as indicators of Holocene and late Quaternary palaeoenvironmental changes. Numerous convincing studies combining ecological and/or geochemical methods were presented in the last decades, such as by Dettman et al. (1995) for North America, Schwalb et al. (1999) for South America, von Grafenstein et al. (1999) for Europe, Keatings et al. (2006a) for Africa, Mischke and Wünnemann (2006) for Tibet and Holmes et al. (1992) for India.

Whereas fossil and modern ostracod fauna and their ecology at mid-latitudes are relatively well known due to numerous investigations, there are only very rare records from high latitudes or from Siberia, where the studies presented here were carried out.

For the area covering the former USSR modern ostracods were summarised by Bronshtein (1947), Kurashov (1995), and Semenova (2005). However, the occurrence of

Arctic freshwater species is only briefly mentioned. Several studies on modern ostracods have been presented from high latitude environments, including the Faroe Islands (Jeppesen et al. 2002), Greenland (Anderson and Bennike 1997), Svalbard (Svenning et al. 2006), Canada (Delorme 1970a-c; Delorme et al. 1977; Bunbury and Gajewski 2005), Central Yakutia (Pietrzeniuk 1977), and Arctic Siberia (Alm 1914; Neale 1969), but environmental and geochemical data are mostly lacking. Moreover, the identification of Arctic species is complicated by inconsistent nomenclature since in the past American, Russian, and European researchers have used different classifications (e.g. Delorme 1967).

1.1.3 Permafrost and the periglacial environment

Any ground on the Earth which remains at temperatures of 0 °C or less for two or more consecutive years is defined as permafrost (van Everdingen 1998). According to this definition, about 20 to 25 % of the continental Earth's surface is underlain by permafrost (Zhang 2003). As one moves from far northern to more southern latitudes, permafrost, expressed as the percentage of frozen ground on the land surface, occurs in continuous, discontinuous, sporadic, and isolated distribution (e.g. Yershov 1990). Continuous permafrost is one of the dominant environmental factors in the arctic lowlands of Alaska, Canada, and Siberia; it affects vegetation, hydrology, soils, and morphology in these periglacial landscapes via cryogenic processes.

The occurrence of permafrost in periglacial regions depends on climatic conditions, in particular on annual mean air temperatures below 0 °C; the summer, when temperatures are positive, is short and complete thawing of the ground which is frozen during winter does not occur. Therefore, the existence of deep permafrost indicates that stable, cold climatic conditions have reigned over long periods of time. The oldest permafrost indications in East Siberia are known from upper Pliocene deposits at the Krestovka River in the Kolyma lowlands (Sher 1971) and also in the Val'karai lowlands on the northern coast of Chukotka (Arkhangelov et al. 1985) in the form of frost crack pseudomorphs. Actually, Froese et al. (2008) reported middle Pleistocene relict ground ice within the discontinuous permafrost zone of Central Yukon Territory, Canada dated to 740,000 +/- 60,000 yrs BP.

Permafrost degradation (thermokarst) caused by extensive thawing of ground ice is climatically driven and intensified during warm periods in the Quaternary, especially since the Holocene (e.g. Katasonov et al. 1979). It is responsible for the formation of numerous depressions in the landscape surface (alases), which are often occupied by thermokarst lakes.

Late Pleistocene permafrost sequences are widely distributed in the arctic lowlands. Such deposits are of epigenetic or syngenetic type (e.g. Dostovalov and Kudryavtsev 1967). Epigenetic permafrost forms when sediments or rocks freeze singly after their deposition; syngenetic permafrost forms when sediments freeze approximately simultaneously during their accumulation. The latter is commonly accompanied by migration of moisture into the freezing ground and, depending on the original water content, syngenetic permafrost may be enriched in ground ice. The resulting ice structures (cryostructures) are of different types and patterns and indicate the temperature and moisture regime at the time of freezing (Katasonov 1954). Syngenetic ice wedges are large ground ice bodies. They begin as frost cracks generated by rapid temperature drops below 0°C; afterwards these cracks are filled by melt water, which freezes immediately because of the negative temperatures in the ground. Syngenetic ice wedges are formed by successive annual cycles of this process and are composed of vertical ice veins; they grow in a polygonal pattern, while at the same time upward sedimentation occurs

During the late Pleistocene, the continuous growth of polygonal ice-wedge systems and the synchronous accumulation and freezing of sediments composed ice-rich sequences which are widely distributed in the Siberian arctic lowlands. These frozen sediments are called Ice Complex (e.g. Kunitsky 1989).

Because the existence of permafrost depends on the temperature regime and has therefore been sensitive to climate changes during the Quaternary past, such frozen deposits are regarded as an archive of palaeoenvironmental changes. The high content of well-preserved floral and faunal remains as well as the sedimentological and cryological parameters enable these permafrost sequences to be used in reconstructing the palaeoenvironment. Numerous multidisciplinary publications have already focused on permafrost deposits as late Quaternary palaeoclimate archives in the Siberian Arctic (e.g. Hubberten et al. 2004; Pitulko et al. 2004; Sher et al. 2005; Grosse et al. 2007; Schirrmeister et al. 2008a), in Alaska (e.g. Anderson and Lozhkin 2001), and in Canada (e.g. Murton 2001, 2005). Various palaeoproxies in frozen deposits such as pollen (e.g. Andreev et al. 2004, 2008), plant macrofossils (Yurtsev 2001; Kienast et al. 2005, 2008), rhizopods (e.g. Bobrov et al. 2004), chironomids (e.g. Ilyashuk et al. 2006), insects (e.g. Kiselyov 1981; Kuzmina and Sher 2006), diatoms (Pirumova 1968), and mammal bones (e.g. Vartanyan et al. 1993; Guthrie 2001) as well as stable isotope records of ground ice (Vasil'chuk 1992; Meyer et al. 2002a, b) have been used for reconstructions of late Quaternary palaeoenvironments and palaeoclimate in Northeast Siberia. Such studies have contributed to reconstructing the environmental history of Beringia, the huge arctic landmass connecting East Siberia and Alaska during several Pleistocene periods.

1.2 Aims and approaches

Up to now, although ostracods bear indicator potential for modern and past environments, neither modern nor fossil assemblages have been studied in detail in the huge areas of Northeast Siberia. The first goal of this thesis, therefore, is to elucidate the abundance and diversity of modern ostracods in periglacial environments by performing an inventory of species present today. In order to apply modern reference data to the analysis of fossil assemblages, the interactions between relevant environmental parameters and ostracod occurrence have been studied by combining ecological, taxonomic, and geochemical data (Table 1-1).

Table 1-1: Generalised overview of methods applied in studies of modern and fossil freshwater ostracods and their habitats

	Modern approach	**Fossil approach**
Field studies	Site characteristics	Exposure characteristics
	Water body size and depth	Profile description
	Vegetation	Stratigraphy and general structure
	Ground substrate	Cryostructures
	Fingerprint hydrochemistry	
	Air and water temperatures	
Laboratory studies	Sedimentology	Sedimentology
	Hydrochemistry and element ratios	Geochronology
	Stable isotopes in water (δD, $\delta^{13}C$, $\delta^{18}O$)	
	Taxonomy	Taxonomy
	Stable isotopes and element ratios of valves ($\delta^{13}C$, $\delta^{18}O$, Sr/Ca, Mg/Ca)	Stable isotopes of valves ($\delta^{13}C$, $\delta^{18}O$)

The following questions should be answerable using this approach:

- ⇒ Which environmental parameters are directly or indirectly related to ecological and taxonomical ostracod characteristics?
- ⇒ How does the geochemistry of ostracod shells reflect the natural modern aquatic environment?
- ⇒ How do environmental gradients in space and time control the occurrence of ostracods in polygonal ponds and thermokarst lakes in Siberian tundra and taiga landscapes?

⇒ What is the significance of freshwater ostracods within the permafrost palaeoarchive, and what does the presence of their fossil remains indicate?

The second goal of this thesis is to interpret Quaternary ostracod records from North Yakutian permafrost exposures based on the modern dataset (Table 1-1). This goal was pursued through multidisciplinary studies using a variety of bioindicators and sedimentological, geocryological, and geochronological methods. Studies of fossil ostracods from permafrost deposits were performed on deposits from the Holocene and Eemian Interglacials, and from the Middle Weichselian and Late Weichselian (Allerød) Interstadials. These studies sought to answer the following questions:

⇒ Which information about the late Quaternary past can be deduced from fossil ostracod assemblages?
⇒ What are the potentials and limits to the application of geochemical methods (element ratios and stable isotopes) to fossil ostracod shells for understanding the palaeoenvironmental record present in archive permafrost?
⇒ How does the ostracod record fit into multiproxy palaeoenvironmental reconstructions?

1.3 Study region

1.3.1 Study sites

The studies of modern and fossil ostracods presented here were performed on material which was collected during several joint Russian-German expeditions to Yakutia (Figure 1-2; Northeast Siberia, Russia); Russian partners from several institutions participated along with researchers from the German Alfred Wegener Institute for Polar and Marine Research.

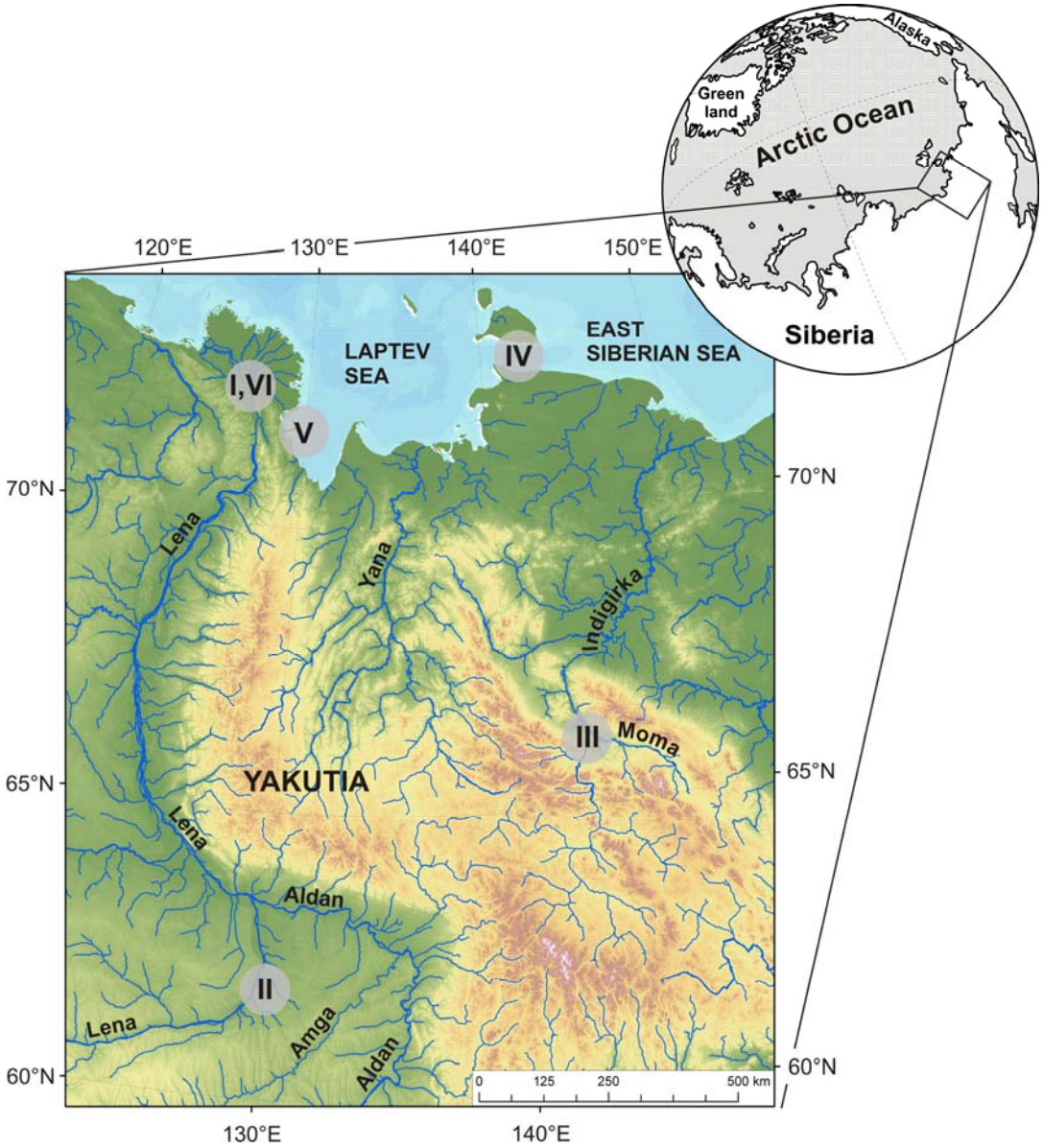

Figure 1-2: Position of study sites in Yakutia (Northeast Siberia, Russia). Modern ostracod records were obtained (I) in the Lena River Delta (North Yakutia), (II) on the Lena-Amga-interfluve (Central Yakutia), and (III) in the Moma River region (Northeast Yakutia). Fossil records from Quaternary permafrost deposits in North Yakutia were studied from coastal exposures at (IV) the Dimitri Laptev Strait (East Siberian Sea), (V) the Bykovsky Peninsula (Laptev Sea), and (VI) Kurungnakh Island (Lena River Delta). Map compiled by G. Grosse (University of Alaska Fairbanks) using data from Hastings et al. (1999)

Three study regions in the North, Northeast, and Central Yakutia were investigated for modern ostracod assemblages and the environmental parameters affecting their life conditions in 2002 (Lena River Delta) and 2005 (Central Yakutia and Moma regions) (Figure 1-2). The material for the fossil records from Quaternary permafrost sequences was sampled on riverside or coastal exposures in 1998 (Bykovsky Peninsula, Laptev Sea), in 2002 (Kurungnakh Island, Lena River Delta), and in 2007 (Dimitri Laptev Strait, East Siberian Sea) (Figure 1-2).

1.3.2 Geological characteristics

The geology in the studied regions is generally structured by three major elements with diverse stratigraphic and lithological successions: the Siberian craton, which belongs to the Eurasian plate, and the Verkhoyansk-Kolymian orogen and the Laptev Rift system, both of which belong to the North American plate (Fujita et al. 1997).

The western and southern parts of Yakutia fit in the Siberian craton which is further divided into the Lena-Yenisey plate, the Anabar massif, and the Aldan shield (Figure 1-3).

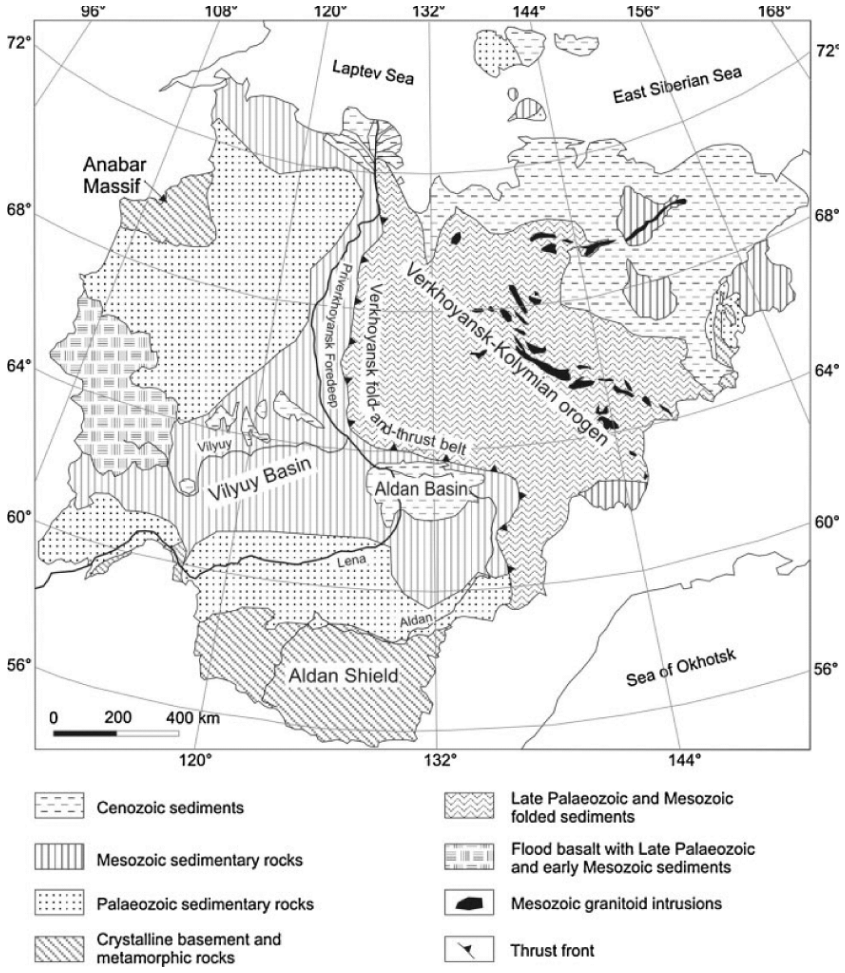

Figure 1-3: Generalised geological map of Yakutia (Popp et al. 2007, based on Sedenko et al. 2001)

The basement is mainly composed of early Archean metamorphic series which are structured by numerous basin, uplift, and graben units. Several hundred metres of Neogene to late Pleistocene aged sediment successions in the Aldan basin underlie the study sites in Central Yakutia. The eastern and northern parts of Yakutia are dominated by the Verkhoyansk-Kolymian orogen (Figure 1-3) which resulted from the collision of the Eurasian plate with the Kolyma-Omolon microcontinent along the eastern margin of the Siberian craton in Mesozoic times (Parfenov 1991). The folded Paleozoic and Mesozoic sediments of the Verkhoyansk-Kolymian orogen are penetrated by Jurassic and Cretaceous granitoid intrusions. The study sites in the Moma region in the valleys of the Indigirka and Moma rivers are situated between the Cherskii and Moma ridges which are of Cretaceous and Jurassic origin.

The study sites in the Lena River Delta, at the Bykovsky Peninsula, and along the Dimitri Laptev Strait are situated on Cenozoic sediments which belong in the western part to the Siberian craton, and in the eastern part to the Verkhoyansk-Kolymian orogen. In the range of the Laptev rift system both structures are separated by the Lyakhov-South Anyui suture (Drachev et al. 1998). The Laptev rift system is known for neotectonic activity. Due to the presence of different basement levels for late Pleistocene and Holocene sediments in the region of the Lena River Delta, formerly and presently active block tectonics are assumed to influence the delta formation and orientation of the main outlets (Grigoriev et al. 1996; Are and Reimnitz 2000).

1.3.3 Climate

The climate of all Yakutian study sites is characterised by continental conditions (Gavrilova 1998): great seasonal contrasts, high temperature amplitudes over the year, and low precipitation (Figure 1-4; Table 1-2).

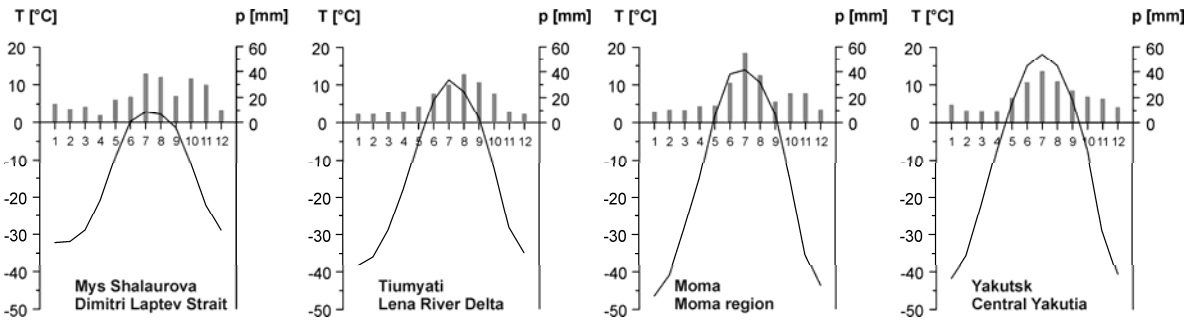

Figure 1-4: Long-term climatic data from meteorological stations next to the study sites (data compiled using Rivas-Martínez 2007)

Short, cool summers follow long, very cold winters; periods with air temperatures above 0 °C range from three to five months from North to South (Figure 1-4). Consequently,

shallow lakes and ponds are covered with ice and frozen to the bottom during seven to nine months of the year; this short time period circumscribes the period of active growth for annual aquatic organisms such as ostracods at high latitudes.

Table 1-2: Summarised climatic data from meteorological stations next to the study sites (Rivas-Martínez 2007)

Study region	Station	Coordinates °N	°E	T_{mean} [°C]	ΔT [°C]	p_{mean} [mm]
North Yakutia (Dimitri Laptev Strait)	Mys Shalaurova	73°11'	143°56'	-15.1	35.0	253.0
North Yakutia (Lena River Delta)	Tiumyati	72°30'	123°50'	-14.5	49.5	206.0
Northeast Yakutia (Moma region)	Moma	66°27'	143°14'	-15.3	60.3	256.6
Central Yakutia (Lena-Amga interfluve, Yakutsk)	Yakutsk	62°05'	129°45'	-10.4	59.8	247.5

T_{mean}: mean annual temperature; ΔT: absolute annual amplitude between mean temperatures in January and July; p_{mean}: mean annual precipitation

The continental effect in Northeast Siberia strengthens southwards and causes absolute annual amplitudes between mean January and July temperatures of about 60 ºC in Central Yakutia and the Moma region, whereas the North Yakutian sites in the Lena River Delta and at the Dimitri Laptev Strait are influenced by ameliorating maritime conditions. The extreme climate conditions are caused by the northern position and the huge landmass of Eurasia, and the position of mountainous systems leading to a relative isolation of the area with respect to maritime humid air masses except for the Arctic Ocean (Tumel 2002). In winter, in response to strong radiation-caused cooling of the Earth's surface, a stable high pressure system (Siberian high) develops over Central Siberia (40-55 °N, 90-110 °E), accompanied by a second high over the Yana-Indigirka lowlands (65-70 °N, 140-150 °E) (Shahgedanova 2002). Like the temperature-induced winter Siberian high, the heating of air masses and high insolation during summer leads to the development of low pressure areas in East Siberia. The pressure decrease from West to East over Eurasia assists the transport of Atlantic maritime air across the continent and leads to higher precipitation rates in the summer months.

The mean precipitation averages about 200 to 250 mm at all study sites (Table 1-2). Obviously, the annual precipitation pattern is controlled by the seasonally-occurring cyclones and anticyclones in Northeast Siberia. For this reason the precipitation during the winter months is clearly lower than in the summer; in particular, July and August are the wettest months. However, evaporation exceeds precipitation during the summer (Gavrilova 1973). The moisture deficit amounts to more than 220 mm per year in all study

regions due to approximately twofold higher potential evapotranspiration than real precipitation (Rivas-Martínez 2007); in consequence, arid conditions are maintained.

1.3.4 Periglacial freshwaters

The tundra, forest-tundra, and taiga landscapes within the zone of continuous permafrost are mainly affected by the deeply frozen ground which thaws in its upper part several centimeters to meters during summer. Because of the seasonally alternating freezing, cooling, and thawing of the ground, several periglacial (cryogenic) processes form a periglacial relief on different scales. Such relief-forming processes are frost cracking and ice wedge growth leading to a polygonal wedge relief, frost heave and frost mounds, thermokarst, thermoerosion, geli-solifluction, and patterned ground (French 2007). The occurrence of lakes, ponds, and other water bodies in periglacial landscapes is directly connected to those cryogenic processes that form depressions on the land surface. Polygonal ice wedge systems often contain so-called polygonal ponds, shallow waters only several meters in diameter whose development may, however, lead to the initial formation of thermokarst lakes, so-called thaw lakes, which continuously expand in depth and size (Soloviev 1959; Billings and Peterson 1980). Polygonal ponds and thermokarst lakes are the most frequent inland water bodies in arctic lowlands and serve as habitats for aquatic organisms, whose fossil remains are also present in Quaternary deposits.

In the course of the work presented in this thesis, in the Lena River Delta sites of North Yakutia, modern ostracods primarily from small polygonal ponds and thaw lakes of the arctic polygonal tundra were studied, while in the central Yakutian taiga, mainly dominated by alas landscapes, ostracods were primarily studied from large thermokarst lakes. The study sites in the mountainous Moma region of Northeast Yakutia were mostly small, water-filled lowland depressions and old branches (distributaries) of the Moma and Indigirka Rivers.

1.4 Synopsis

This thesis is composed of an introductory chapter with background information, followed by three main chapters and a synthesis. The three main chapters and appendices I and II contain original research papers which have been published or are in the process of being published (Table 1-3).

Chapters 2 and 3 deal with modern ostracod assemblages, their life conditions and the geochemical properties of periglacial waters on islands of the Lena River Delta (Wetterich et al. 2008a), and in Central and Northeast Yakutia (Wetterich et al. 2008b). Studies of Holocene and Eemian fossil ostracods from permafrost sequences at the Dimitri Laptev Strait (East Siberian Sea) presented in Chapter 4 are currently being prepared for

publication in the journal Palaeogeography, Palaeoclimatology and Palaeoecology. Based on sedimentological, geocryological, and geochronological as well as palynological analyses, taxonomical and stable isotope records of ostracods have been used for palaeoecological interpretations. The appendix contains two late Quaternary palaeoreconstructions from permafrost deposits of the Bykovsky Peninsula in the Laptev Sea (Wetterich et al. 2005) and Kurungnakh Island in the Lena River Delta (Wetterich et al. 2008c). Ostracods were used as a bioindicator in both these multidisciplinary studies of the palaeoarchive permafrost.

Table 1-3 Overview of publications presented within the thesis

Publication	Chapters
Wetterich S, Schirrmeister L, Meyer H, Viehberg FA and Mackensen A (2008a) Arctic freshwater ostracods from modern periglacial environment in the Lena River Delta (Siberian Arctic, Russia): Geochemical applications for palaeoenvironmental reconstructions. *Journal of Paleolimnology* 39: 427-449 (DOI 10.1007/s10933-007-9122-1)	Chapter 2
Wetterich S, Herzschuh U, Meyer H, Pestryakova L, Plessen B, Lopez CML and Schirrmeister L (2008b) Evaporation effects as reflected in freshwaters and ostracod calcite from modern environments in Central and Northeast Yakutia (East Siberia, Russia). *Hydrobiologia* 614: 171-195 (DOI 10.1007/s10750-008-9505-y)	Chapter 3
Wetterich S, Schirrmeister L, Andreev A, Pudenz M, Plessen B, Meyer H and Kunitsky VV (in preparation) Eemian and Late Glacial/Holocene palaeoenvironmental records from permafrost sequences at the Dimitri Laptev Strait (NE Siberia, Russia). *Palaeogeography, Palaeoclimatology, Palaeoecology*	Chapter 4
Wetterich S, Schirrmeister L and Pietrzeniuk E (2005) Freshwater ostracodes in Quaternary permafrost deposits from the Siberian Arctic. *Journal of Paleolimnology* 34: 363-376 (DOI 10.1007/s10933-005-5801-y)	Appendix I
Wetterich S, Kuzmina S, Andreev AA, Kienast F, Meyer H, Schirrmeister L, Kuznetsova T and Sierralta M (2008c) Palaeoenvironmental dynamics inferred from late Quaternary permafrost deposits on Kurungnakh Island (Lena Delta, Northeast Siberia, Russia). *Quaternary Science Reviews* 27: 1523-1540 (DOI 10.1016/j.quascirev. 2008.04.007)	Appendix II

The results and implications of all five publications are summarised in the Chapter 5 synthesis that also includes an outlook for further development and application of ostracod research in the context of palaeoecology and permafrost sciences.

Taking into account the multidisciplinary character of the studies, each co-author contributed to his own field of experience (Table 1-3). As first author, S. Wetterich initiated, wrote and coordinated the publications. In particular, he contributed to all data collections, analyses and interpretations related to modern and fossil ostracods.

2 Arctic freshwater ostracods from modern periglacial environments in the Lena River Delta (Siberian Arctic, Russia): geochemical applications for palaeoenvironmental reconstructions

Sebastian Wetterich[1], Lutz Schirrmeister[1], Hanno Meyer[1], Finn Andreas Viehberg[2] and Andreas Mackensen[3]

(1) Alfred Wegener Institute for Polar and Marine Research, Research Unit Potsdam, Telegrafenberg A43, 14473 Potsdam, Germany; (2) Laboratoire de Paléolimnologie-Paléoecologie, Université Laval, Centre d'Études Nordique, Pavillon Abitibi-Price, G1K 7P4 Sainte-Foy, QC, Canada (current address: Institute for Environmental Geology, Technical University Braunschweig, Postbox 3329, 38023 Braunschweig, Germany); (3) Alfred Wegener Institute for Polar and Marine Research Bremerhaven, Am Alten Hafen 26, 27568 Bremerhaven, Germany

Journal of Paleolimnology 39: 427-449 (DOI 10.1007/s10933-007-9122-1)

2.1 Abstract

The aim of this study is to describe ostracods from freshwater habitats in the Siberian Arctic in order to estimate the present-day relationships between the environmental setting and the geochemical properties of ostracod calcite. A special focus is on the element ratios (Mg/Ca, Sr/Ca), and the stable isotope composition ($\delta^{18}O$, $\delta^{13}C$), in both ambient waters and ostracod calcite. The most common species are *Fabaeformiscandona pedata* and *F. harmsworthi* with the highest frequency in all studied waters. Average partition coefficients *D*(Sr) of *F. pedata* are 0.33 ± 0.06 (1σ) in females, and 0.32 ± 0.06 (1σ) in males. A near 1:1 relationship of $\delta^{18}O$ was found, with a mean shift of Δ_{mean} = 2.2‰ ± 0.5 (1σ) to heavier values in ostracod calcite of *F. pedata* as compared to ambient waters. The shift is not dependent on $\delta^{18}O_{water}$, and is caused by metabolic (vital) and temperature effects. Temperature-dependence is reflected in the variations of this shift. For ostracod calcite of *F. pedata* a vital effect as compared to inorganic calcite in equilibrium was quantified with 1.4‰. Results of this study are valuable for the palaeoenvironmental interpretation of geochemical data of fossil ostracods from permafrost deposits.

2.2 Introduction

Freshwater ostracods are crustaceans, usually less than 3 mm long, with a bivalved carapace made of low magnesium-calcite. During their ontogeny, the individuals run through nine moult stages (Kesling 1951). After each moult, ostracods calcify new shells

within a short time, probably within a few days (Chivas et al. 1983). The ions for the calcite formation are incorporated directly from the ambient water at this time (Turpen and Angell 1971). Therefore, element ratios of magnesium, strontium and calcium (Mg/Ca, Sr/Ca) as well as stable isotope ratios of oxygen ($\delta^{18}O$) and carbon ($\delta^{13}C$) in ostracod calcite are related to the geochemistry of the ambient water (e.g. Chivas et al. 1986; Xia et al. 1997b, c; von Grafenstein et al. 1999). The understanding of these relationships is a prerequisite for interpreting geochemical information in fossil ostracod calcite for palaeoenvironmental reconstructions.

Due to the sensitivity of freshwater ostracods to environmental changes and the high durability of their remains in lacustrine sediments, ostracods serve as good indicators for palaeoclimatic reconstructions (e.g. Anadón et al. 2006; Poberezhnaya et al. 2006; Xia et al. 1997a). The ecology of freshwater ostracods is defined by water chemistry, water temperature and additional habitat parameters such as area, water depth, and water permanency and type. Environmental changes influence the diversity of freshwater ostracods as well as the morphology and the geochemical composition of the ostracod shells (e.g. Griffiths and Holmes 2000). Coupled element and stable isotope measurements in fossil ostracod calcite are being increasingly used in palaeoenvironmental reconstructions of temperature, salinity and productivity (e.g. De Deckker and Forester 1988; Griffiths and Holmes 2000). Whereas fossil and modern ostracod fauna and their ecology in mid-latitudes are relatively well known due to numerous investigations, there are only a few records concerning freshwater ostracods in Siberia, or in (sub-) Arctic permafrost regions (e.g. Alm 1914; Bunbury and Gajewski 2005; Pietrzeniuk 1977; Semenova 2005).

Numerous multidisciplinary studies have focused on permafrost deposits with well preserved remains of palaeoindicative fossils and have highlighted their potential and significance as Quaternary palaeoclimate archives in the Siberian Arctic (e.g. Schirrmeister et al. 2002a, b, 2003; Hubberten et al. 2004), especially since other long-term records such as lake sediment cores or inland glacier ice cores are rare or not available in this vast region. Various palaeoproxies in the frozen deposits, such as pollen (Andreev et al. 2002), rhizopods (Bobrov et al. 2004), plant macrofossils (Kienast et al. 2005), insects (Kuzmina and Sher 2006) and mammal bones (Sher et al. 2005), as well as stable isotope records of ground ice (Meyer et al. 2002a), have already been used, while ostracods were introduced as a valuable palaeoindicator only recently by Wetterich et al. (2005).

Still, knowledge about the ecology and biology of Arctic freshwater ostracods needs improvement to apply modern analogues to fossil records. Thus, the key question is how do ostracod associations and/or the geochemistry of their valves reflect the natural setting

of a modern aquatic environment in the periglacial Arctic, which is characterised by widely distributed polygons and thermokarst lakes in a tundra landscape. It should be mentioned that this study presents the species distribution and life conditions of ostracods at the sampling time. Nevertheless, our results increase the value of using freshwater ostracods from permafrost deposits as palaeoindicators and, when combined with planned geochemical studies on element ratios (Mg/Ca, Sr/Ca) and stable isotopes ($\delta^{18}O$, $\delta^{13}C$), will enable us to interpret signals from fossil ostracod calcite in this region.

2.3 Study area and types of water bodies

The Lena River has the largest delta in the Arctic, located at the Laptev Sea shore between Taimyr Peninsula and the New Siberian Islands (Figure 2-1a). The delta covers an area of about 32,000 km^2, where more than 1,500 islands of various size were formed by a network of rivers and channels (e.g. Are and Reimnitz 2000). The islands are composed of Quaternary sediments. They are subdivided into three terraces of different ages and height levels above the modern flood plain of the Lena River (e.g. Grigoriev 1993; Schwamborn et al. 2002).

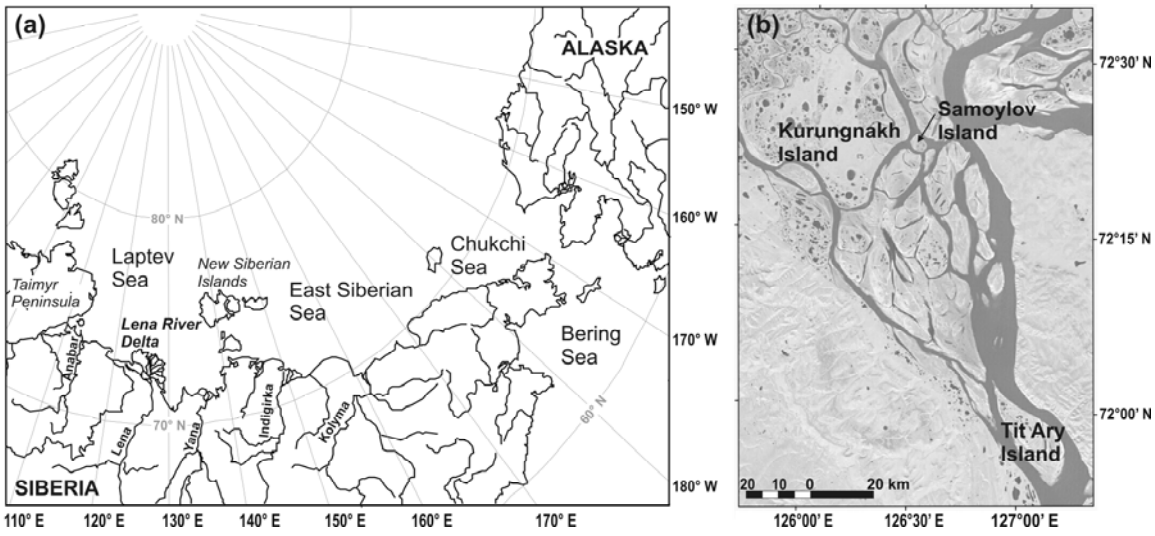

Figure 2-1 (a) Location of the Lena River Delta on the Laptev Sea coast in northeast Siberia; (b) the study area in the southern part of the delta (Satellite image provided by Statens Kartverk, UNEP/GRID-Arendal and Landsat 2000)

The modern climatic conditions of the Lena River Delta are extreme. Short and cool summers follow long and very cold winters. The mean July air temperature varies between +4°C and +8°C and the mean January air temperature varies between −36°C and −32°C (Atlas Arktiki 1985). The mean annual air temperature averages −14°C (Kunitsky 1989). Only 4 months of the year are mean air temperatures above 0°C. Consequently, shallow lakes and ponds are covered with ice and frozen to the bottom

during at least eight to nine months of the year, which circumscribes the period of active growth for annual aquatic organisms such as ostracods in this region. The mean annual precipitation (about 200 mm) is low, but still higher than evaporation, because of the predominance of freezing temperatures through the year (Kunitsky 1989). Data from 2002 by an automatic soil and meteorology measurement station on Samoylov Island (Friedrich and Boike 1999; Wille et al. 2003) recorded mean air temperatures 0.5 m above the ground and mean soil temperature 0.15 m below the ground as the following: in May (T_{Air} = −9.0°C; T_{Soil} = −10.5°C), in June (T_{Air} = 6.2°C; T_{Soil} = −0.1°C), in July (T_{Air} = 10.7°C; T_{Soil} = 6.1°C) and in August (T_{Air} = 10.0°C; T_{Soil} = 7.4°C). The precipitation totalled 65 mm (J. Boike, AWI Potsdam, unpublished data).

The entire Lena River Delta is located in the zone of continuous permafrost, with a permafrost thickness of 400–700 m in the western part and 300–500 m in the eastern part (Kondrat'eva and Solov'ev 1989). The occurrence of permafrost is expressed on the landscape microrelief as widespread patterned ground dominantly formed by ice wedge polygons in different stages of development. The formation of lakes, ponds, and other water bodies on islands of the Lena River Delta is directly connected to permafrost processes like ice wedge growth, thermokarst, and thermoerosion, as well as to the fluvial dynamics of the Lena River on the flood plain.

The patterned ground of the polygonal tundra is dominated by ponds and thaw lakes (Figure 2-2). In winter, initial frost cracks are generated by rapid temperature drops below 0°C (Figure 2-2a). In spring, these cracks are filled by melt water, which freezes immediately because of the negative temperatures in the ground. Ice wedges, formed by successive annual cycles of this process, grow in a polygonal pattern. The polygon rim is usually higher than the polygon centre. Intrapolygon ponds (Figure 2-2b) are situated in these so-called low-centre polygons (French 1996). Later, the degradation of the polygon rims and changes in the hydrological regime may cause the formation of so-called high-centre polygons (French 1996), which are often accompanied by interpolygon ponds and thaw lakes (Figure 2-2c,d). Shallow intrapolygon ponds have a water depth between about 0.5–1 m, but are characterised by different diameters (Meyer 2003). The size of intrapolygon ponds can be up to 30 m in diameter, depending on the polygon in which they occur. Interpolygon ponds delineate the location of polygon rims and are underlain by ice wedges. Thaw lakes are also shallow with a water depth of up to 1.5 m and cover areas of up to several hundred m^2. Thermokarst processes cause extensive melting of the underlying permafrost and large depressions thus develop, which often form lakes. Thermokarst lakes occur over areas up to several km^2 with water depths up to 5 meters. On the lower floodplain, shallow cut-off river branches (up to 1 m water depth) expand during spring flooding and form stream-oriented shallow depressions.

Recent ostracods were found during limnological investigations in 40 shallow lakes and ponds on Samoylov (72° 22′ N, 126° 28′ E), Kurungnakh (72° 20′ N, 126° 10′ E), and Tit Ary Islands (71° 58′ N, 127° 04′ E) in the southern part of the Lena River Delta (Figure 1b). Here, we present data from 23 lakes and ponds situated on Samoylov (on the first Lena River terrace and lower flood plain) and Kurungnakh Islands (on the third Lena River terrace), where ostracods were found in sufficient numbers for further geochemical analyses. The studied waterbodies included three intrapolygon ponds, three interpolygon ponds, 13 thaw lakes and one river branch on Samoylov Island as well as one intrapolygon pond and two thermokarst lakes on Kurungnakh Island (Appendix III-1).

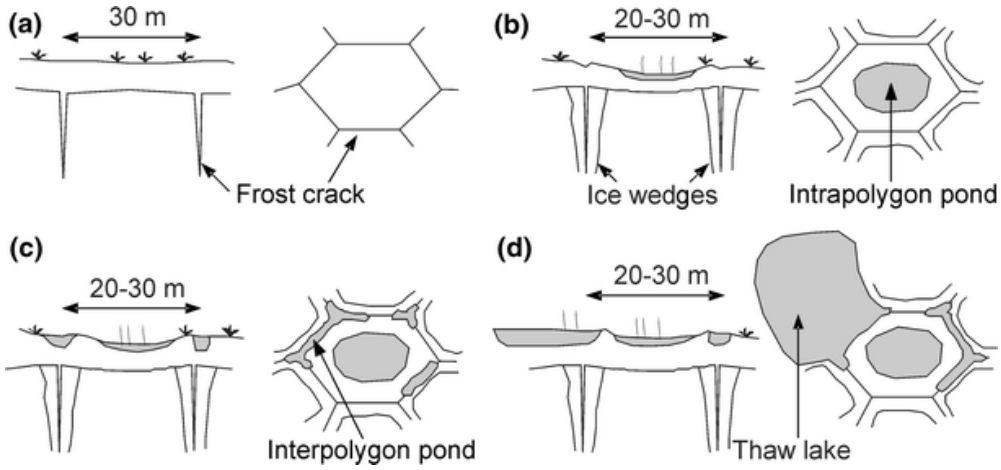

Figure 2-2 The formation of ice wedges and the resulting changes on the landscape surface with different types of shallow waterbodies depending on the polygon degradation state in the Lena River Delta (modified after Meyer 2003). (a) Juvenile polygon type with very small height differences between polygon wall and the centre; no waterbody; (b) Mature low-centre polygon type with height differences between 0.5 m and 1 m between polygon wall and the centre; intrapolygon ponds develop in poorly drained sites; (c) Polygon type of initial degradation with height differences between 0.5 m and 1 m between polygon wall and the centre; interpolygonal ponds on the polygon wall are present as triangular ponds in the triple junctions or elongated ponds along the frost crack; (d) Polygon type of final degradation with height differences of up to 1.5 m between polygon wall and polygon centre; thaw lake of variable size and polygonal structure are present

2.4 Materials and methods

Hydrochemical variables such as pH, the content of nutrients (NH_4, NO_2, NO_3, PO_4) and oxygen (O_2) were analysed during the fieldwork by means of a compact laboratory (Aquamerck). All water samples and measurements were performed at the margin of the water bodies at water depths of about 0.5 m, where near-bottom water was taken or measured, respectively. Water temperature and electrical conductivity were measured

with a conductivity meter (WTW Cond 330i). Water was sampled for ionic (Ca, K, Mg, Sr, Na, Cl, SO_4, HCO_3) and stable isotope (δD, $\delta^{18}O$, $\delta^{13}C$) analyses.

Samples for cation analyses were acidified with HNO_3, whereas samples for anion analyses and residue samples were preserved by freezing until analysis. Before conservation, samples for cation and anion analyses were passed through a cellulose-acetate filter (0.45 µm pore size). Upon return to the main laboratory, the element (cation) content of the waters was analysed by Inductively Coupled Plasma-Optical Emission Spectrometry (ICP-OES, Perkin–Elmer Optima 3000 XL), while the anion content was determined by Ion Chromatography (IC, Dionex DX-320). The hydrogen carbonate concentrations (alkalinity) of the waters were determined by titration with 0.01 M HCl using an automatic titrator (Metrohm 794 Basic Titrino).

The lake water samples for oxygen and hydrogen stable isotope analysis (δD, $\delta^{18}O$) were stored cool and later analysed by equilibration technique (Meyer et al. 2000) using a mass-spectrometer (Finnigan MAT Delta-S). The reproducibility derived from long-term standard measurements is established with 1σ better than ±0.1‰ (Meyer et al. 2000). All samples were run at least in duplicate. The values are expressed in delta per mil notation (δ, ‰) relative to the Vienna Standard Mean Ocean Water (VSMOW). The water samples for carbon isotope analysis ($\delta^{13}C$) on total dissolved inorganic carbon (TDIC) were preserved by freezing until analysis using a mass-spectrometer (Finnigan MAT 252). The reproducibility derived from standard measurements over a 1-year period is ±0.1 ‰ (1σ). TDIC was extracted from lake water with 100% phosphoric acid in an automatic preparation line (Finnigan Gasbench I) coupled online with the mass-spectrometer. All samples were run at least in duplicate. The values are expressed in delta per mil notation (δ, ‰) relative to the Vienna Pee Dee Belemnite standard (VPDB).

Samples from the upper layer of bottom sediments (up to 5 cm) were analysed for nitrogen, organic and total carbon contents by CNS-Analyser (Elementar Vario EL III), as well as for grain-size distribution by Laser-Granulometry (Coulter LS 200).

Living ostracods were collected using an exhaustor (Viehberg 2002), then preserved in 70% alcohol and finally counted and identified under a binocular microscope (Zeiss SV 10) by soft body and valve characteristics described in Alm (1914), Bronshtein (1947), Neale (1969), and Meisch (2000). In samples with sufficient numbers of living ostracods, the most common species were prepared for element (Mg, Sr, Ca) and stable isotope ($\delta^{18}O$, $\delta^{13}C$) analyses. Additionally, subfossil valves from the upper layer of the bottom sediments were analysed in order to relate these data to that of the ostracods caught alive. The valves of these ostracods were cleaned by removing the soft body under the binocular microscope, and then washed in distilled water and air-dried. The subfossil valves were picked from the wet sieved 250 µm fraction of the upper layer of bottom

sediments under the binocular microscope. Only clean valves of adult specimens were used for analysis. Particles adhered to valves were removed with a fine brush. Prior to analysis, up to four single valves from the same sample were weighed using an electronic micro-balance (Sartorius micro) in order to check the reliability of the $CaCO_3$ Nominal Shell Weight (NSW). The $CaCO_3$ NSW is calculated from total Ca concentrations of each sample solution (Chivas et al. 1986). The single valve samples were placed in a reaction vial and dissolved in 30 µl of 20% HNO_3 (Baker Ultrex). Afterwards, 3 ml of distilled water were added. For analysis of Ca, Mg, and Sr contents we used Inductively Coupled Plasma-Optical Emission Spectrometry (ICP-OES, Varian Vista-MPX) at the Research Centre for Geosciences Potsdam (GFZ Potsdam, Germany). The ICP-OES was calibrated with three multi-element standards prepared by mono-element standard solutions for ICP (Alfa Aesar Specpure 1,000 µg/ml). Standard solution 1 contained 1 ppm Ca, 0.02 ppm Mg, and 0.01 ppm Sr. The concentrations in standard solutions 2 and 3 were twice and three times higher, respectively. Three determinations were made from each sample to check machine precision. Contaminant (blank) concentrations in the solvent acid were analysed for each batch of 10 samples to determine detection limits of the measurements. The detection limits in solution (3σ above background in µg/l or ppb, e.g. Doerfel 1966) are 1.51 for Ca (wavelength 422.673 nm), 0.05 for Mg (279.553 nm), and 0.03 for Sr (407.771 nm). Standard 1 provided a consecutive reference for each batch of 10 samples analysed, and confirmed an internal 1σ error of less than ±2.3% for Ca, ±1.0% for Mg, and ±1.2% for Sr. The results for Mg and Sr are expressed as µg/g (ppm) in calcite following Chivas et al. (1986). From these results, molar ratios of Mg/Ca × 10^{-2} and Sr/Ca × 10^{-3} were calculated. In total, 47 samples of recent ostracods and 18 samples of subfossil ostracods from 23 water bodies were used for the determination of Mg/Ca and Sr/Ca ratios.

The ostracod valves for oxygen isotope ($\delta^{18}O$) and carbon isotope ($\delta^{13}C$) analysis were prepared and cleaned in the same way as for the element analysis. To ensure enough material for isotope analysis (80–100 µg $CaCO_3$), 10–18 single valves of one species and sex from one waterbody were aggregated to create one sample. The aggregated samples were analysed by an isotope ratio gas mass-spectrometer (Finnigan MAT 251) directly coupled to an automated carbonate preparation device (Kiel II). The reproducibility, as determined by standard measurements over a 1-year period, is ±0.08‰ (1σ) for $\delta^{18}O$ and ±0.06‰ (1σ) for $\delta^{13}C$. The values are expressed in delta per mil notation (δ, ‰) relative to the VPDB. In total, 46 samples of recent ostracods and 14 samples of subfossil ostracods from 23 water bodies were analysed for $\delta^{18}O$ and $\delta^{13}C$ stable isotopes.

2.5 Results

2.5.1 Physico-chemical characteristics of the ostracod habitats

During the summer period, when no ice covers the lakes and ponds, the water bodies are defined as polymictic. Because of the shallow water depth and the wind driven mixing, the water temperature is tightly correlated to the air temperature and ranged from 5.9°C to 15.3°C during the fieldwork period (Appendix III-1). Dissolved oxygen concentrations were between 5.3 mg/l and 11.3 mg/l. The waters were oligotrophic (with phosphate values <0.1 ppm, below the detection limit), slightly acid to neutral (pH 6.5–7.6), and had alkalinities between 13.4 ppm and 148 ppm (Appendix III-1). The electrical conductivity was very low and ranged from 27 µS/cm to 254 µS/cm. The waters were dominated by Mg–Ca or Ca–Mg, and HCO_3 (Figure 2-3), but the ion content was generally low in all studied waters (Appendix III-1). The molar Mg/Ca ratios ranged from 0.53 to 1.40 and the Sr/Ca ratios from 2.63×10^{-3} to 4.83×10^{-3} (Appendix III-2).

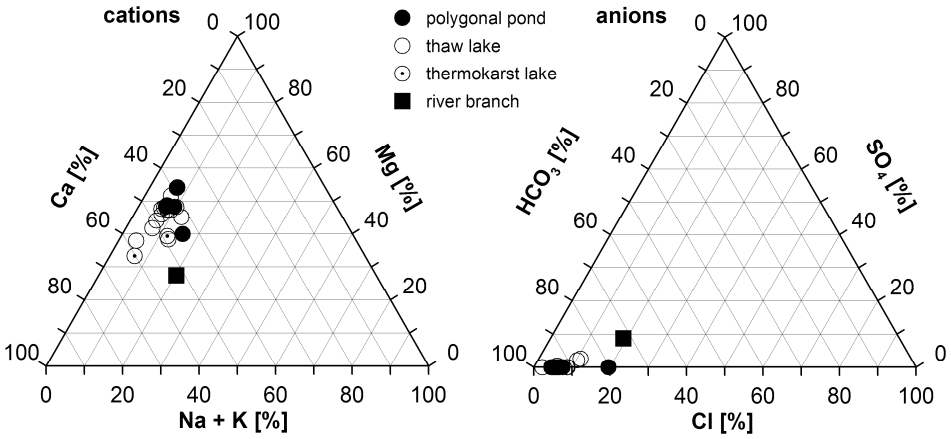

Figure 2-3 Ionic composition in waters of lakes and ponds in the Lena River Delta

The results of oxygen and hydrogen isotope analyses of the lake waters are presented in a $\delta^{18}O$–δD plot (Figure 2-4a) with respect to the Global Meteoric Water Line (GMWL), which correlates fresh surface waters on a global scale (Craig 1961).

The studied lakes and ponds are mainly fed by precipitation waters. The isotope values of three rain water samples from the beginning of August 2002 and one sample of Lena River water are given in Figure 2-4a. Whereas the local rain water samples and the river water are close to the GMWL, samples from the studied lakes and ponds are shifted below the GMWL. The deviation of the data from the GMWL reflects evaporation in the studied water bodies, as indicated by a slope of 5.56 (R^2 = 0.96; excluding the cut-off river branch) shown in Figure 2-4a. The isotopic composition of one cut-off river branch (sample SAM-14) shows the influence of the Lena River with relatively lighter $\delta^{18}O$ (Figure 2-4a).

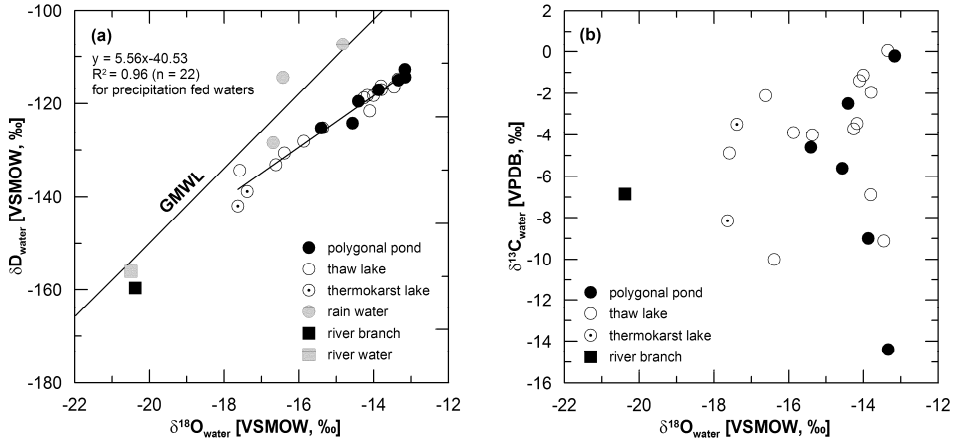

Figure 2-4 Isotopic composition in natural waters in the Lena River Delta: (a) Plot of oxygen and hydrogen isotopes ($\delta^{18}O$ and δD) in lake water and precipitation in summer 2002 as well as in Lena River water; (b) Plot of oxygen and carbon isotopes ($\delta^{18}O$ and $\delta^{13}C$) in lake water

The plot of $\delta^{18}O$–$\delta^{13}C$ (Figure 2-4b) shows no distinct differentiation in $\delta^{13}C$ between lakes and ponds situated on Samoylov and Kurungnakh islands. The waters varied between +0.1‰ and −14.4‰ for $\delta^{13}C$. The $\delta^{13}C$ of the cut-off river branch observed on Samoylov Island (sample SAM-14) lies within this range. The wide range in $\delta^{13}C$ obviously reflects the influence of several biotic and abiotic factors on this parameter. The minimum value of −14.4‰ for $\delta^{13}C$ comes from an intrapolygon pond (sample SAM-13) on Kurungnakh Island. In this pond a pH-value of 6.5 was measured in the field. It had the lowest pH and consequently the lowest HCO_3 value of all the studied waters (Appendix III-1). At constant temperatures a decrease in pH leads to a decrease in HCO_3 and therefore the composition of $\delta^{13}C$ in TDIC tends to become lighter (e.g. Clark and Fritz 1997).

The bottom sediments at the sites consisted primarily of minerogenic, sandy deposits with an organic cover. The main fraction of the studied sediments was composed of fine-grained sand (0.125–0.25 mm) or medium-grained sand (0.25–0.5 mm) (Figure 2-5a). Furthermore, the sediments were characterised by C/N ratios from 9.8 to 17.9 (Figure 2-5b), which are typical for polyhumic sediments with a low rate of decomposition (Hansen 1961) as is expected in high-latitude regions. The organic carbon content of the sediment varied between 0.7% and 17.3%. Highest values of more than 15% were found in sediments from two water bodies on Kurungnakh Island, which may be linked to higher organic carbon contents in the late Pleistocene Ice Complex deposits on the third Lena River terrace compared to those in the Holocene deposits on the first Lena River terrace (Schirrmeister et al. 2003).

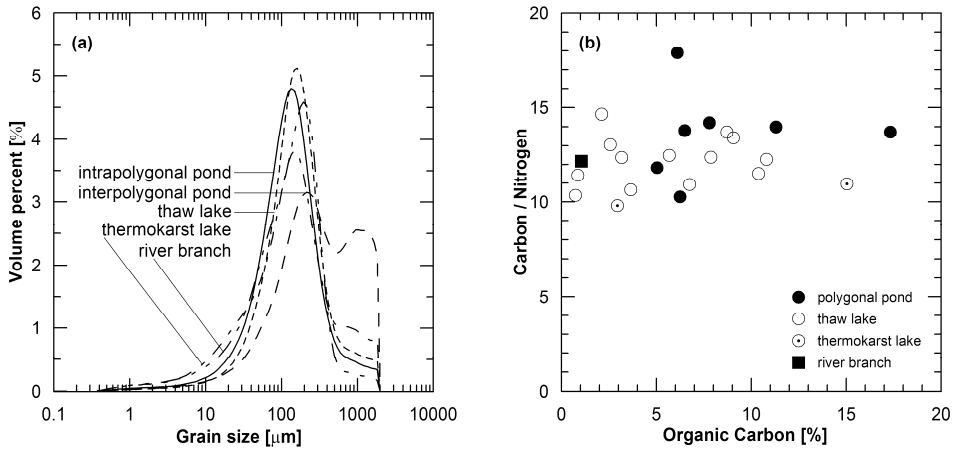

Figure 2-5 Sedimentological properties of bottom sediments for the studied types of lakes and ponds: (a) Grain size distributions of examples for intrapolygon ponds (SAM-30); interpolygon ponds (SAM-37), thaw lakes (SAM-28), thermokarst lake shores (SAM-38) and river branches (SAM 14); (b) Plot of C/N ratios and organic carbon content in bottom sediments

2.5.2 Ostracod taxonomy and environmental ranges of their habitats

Among the 14 observed ostracod taxa, 11 taxa were identified down to the species level and two taxa to the genus level, whereas one taxon comprises indeterminate juvenile Candoninae. Here, we present the species from lakes and ponds that were used in describing the geochemical applications (Figure 2-6).

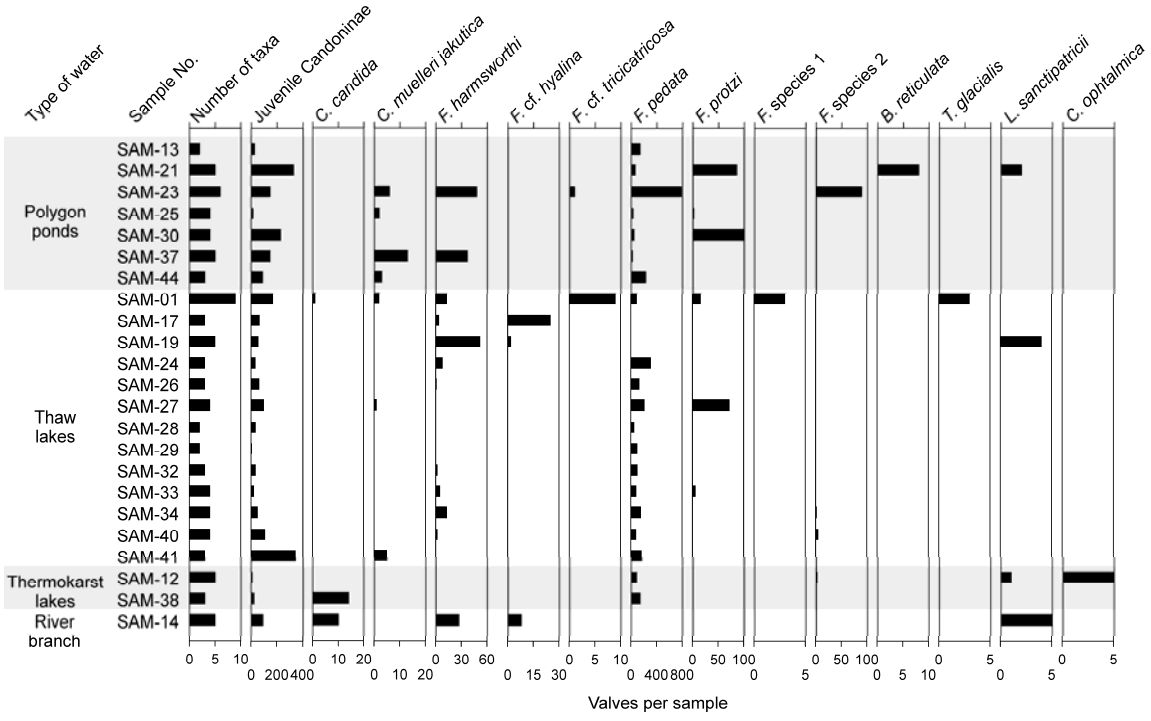

Figure 2-6 Ostracod species frequency (in absolute numbers) in different types of lakes and ponds in the Lena River Delta. Note varying scales

The ostracod assemblage in the shallow water bodies of the Lena River Delta consists partly of cosmopolitian species like *Candona candida* (O.F. MÜLLER, 1776), *Fabaeformiscandona* cf. *hyalina* (BRADY & ROBERTSON, 1870), *Fabaeformiscandona* cf. *tricicatricosa* (DIEBEL & PIETRZENIUK, 1969), *Fabaeformiscandona protzi* (HARTWIG, 1898), *Bradleystrandesia reticulata* (ZADDACH, 1844), *Limnocytherina sanctipatricii* (BRADY & ROBERTSON, 1869), and *Cypria ophtalmica* (JURINE, 1820). The second group of ostracods found in lakes and ponds of the Lena River Delta are typical species for the Subarctic and Arctic of Siberia like *Candona muelleri jakutica* PIETRZENIUK, 1977, *Fabaeformiscandona harmsworthi* (SCOTT, 1899), *Fabaeformiscandona pedata* (ALM, 1914), and *Tonnacypris glacialis* (SARS, 1890). The two taxa *Fabaeformiscandona* sp. 1 and *Fabaeformiscandona* sp. 2 still remain in open nomenclature. Bisexual populations were found for all species except for *C. candida*, *C. ophtalmica*, and *T. glacialis*. The ostracod species frequency for the studied lakes and ponds is shown in Figure 2-6.

The species *C. muelleri jakutica*, *F. protzi*, *F.* sp. 2, and *B. reticulata* were mostly found in ponds and small lakes of polygonal genesis. A further dependence of species distribution on the water body type was not observed. The most common species in our study were *F. pedata* and *F. harmsworthi*. In Figure 2-7 the ecological range is shown according to the environmental parameters at the sampling site, when the species occurred. Anyway, these data do not reflect the species tolerance as the only a limited gradient is covered by the studied waters. In general, the gradient of the environmental parameters during the sampling time in August 2002 is quite low due to the very low ionic content of the studied water. The broadest ranges were found for the most common species in our study *F. pedata* and *F. harmsworthi*.

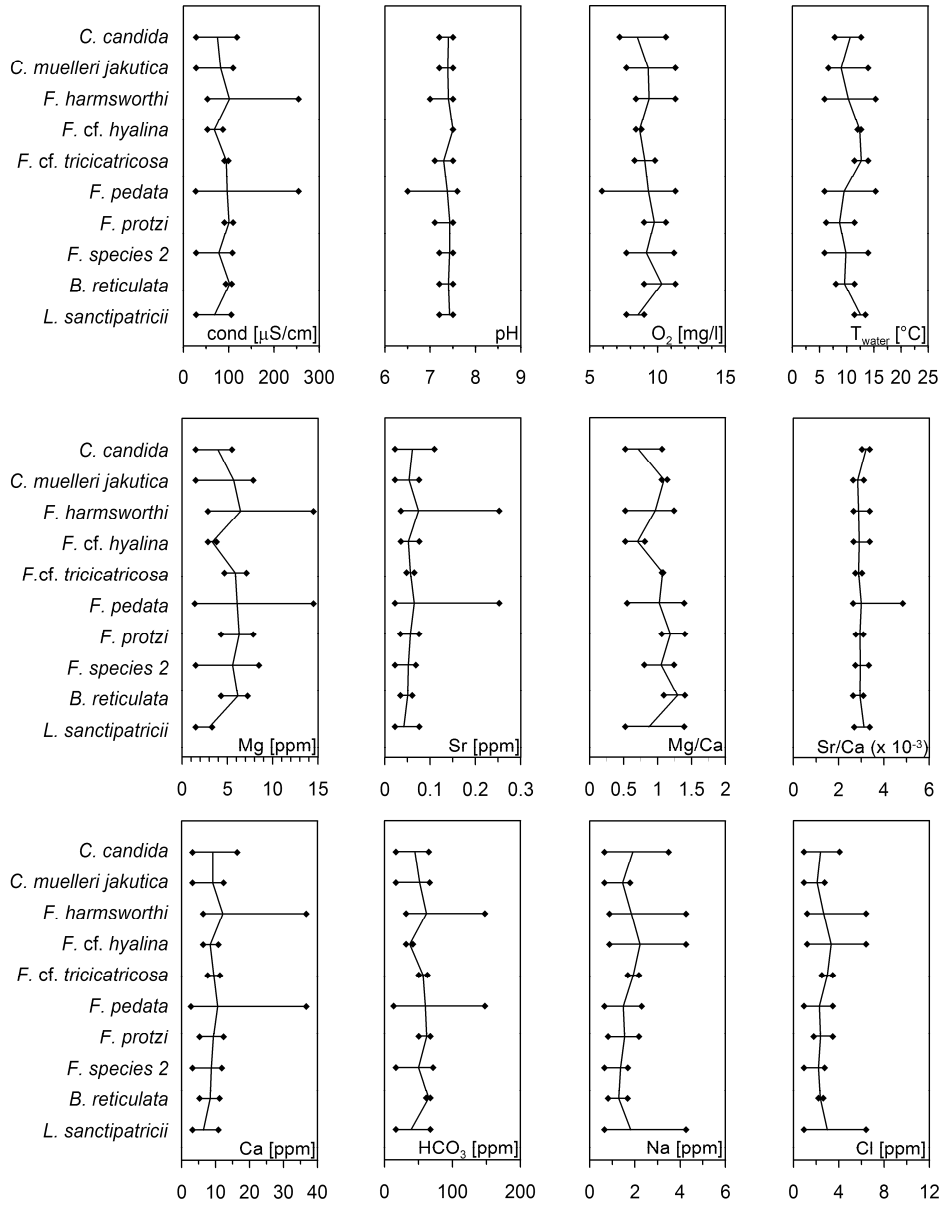

Figure 2-7 Ranges of environmental parameters of ostracod habitats for most current taxa found in the studied shallow lakes and ponds. Horizontal lines connect the minimum and the maximum, and the vertical line is the mean. *C. candida* (n = 3), *C. muelleri jakutica* (n = 7), *F. harmsworthi* (n = 12), *F.* cf. *hyalina* (n = 3), *F. levanderi* (n = 2), *F. pedata* (n = 21), *F. protzi* (n = 6), *F.* sp. 2 (n = 4), *B. reticulata* (n = 3) and *L. sanctipatricii* (n = 4). Note varying scales

2.5.3 Ostracod geochemistry

The correlation between the $CaCO_3$ Nominal Shell Weight (NSW) and the measured valve weights is shown in Figure 2-8. In general, the valve weights determined by micro-balance are higher than the calculated $CaCO_3$ NSW since ostracod valves consist of 80–90% $CaCO_3$ (Sohn 1958). Distinct or systematic differences between weights of recent and subfossil valves of any one species were not observed. The reliability of the preparation method (soft body extraction) of the modern ostracods for geochemical analyses is therefore assumed.

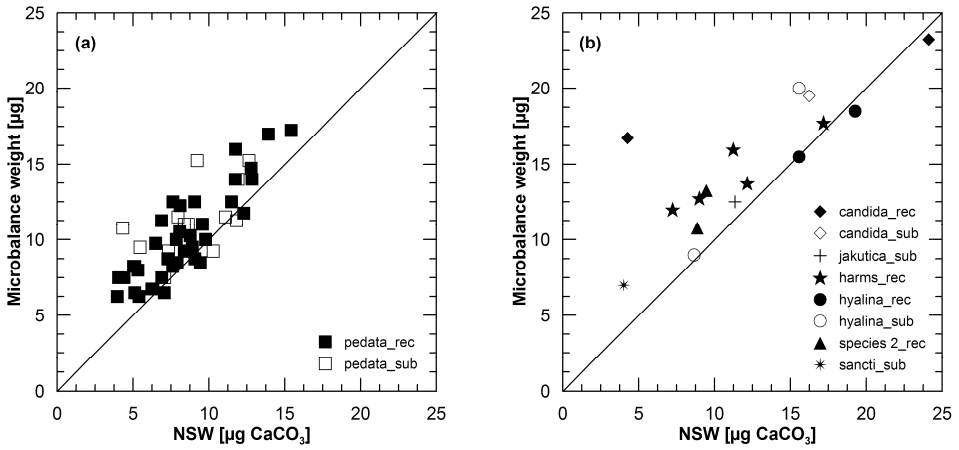

Figure 2-8 Correlation of the calculated Nominal Shell Weight (NSW, Ca content by ICP-OES) and the measured weight (by micro-balance) of recent and subfossil single valves of: (a) *F. pedata*; (b) *C. candida*, *C. muelleri jakutica*, *F. harmsworthi*, *F*. cf. *hyalina*, *F*. sp. 2 and *L. sanctipatricii*. The species identification follows the key: species (e.g. *F. pedata* → pedata) and state (recent → rec or subfossil → sub)

The element ratios (Mg/Ca, Sr/Ca) in ostracod calcite are listed in Appendix III-2. In Figure 2-9 the relationship of element ratios in calcite for several species are shown. The highest variation in the Mg/Ca ratio is found in recent valves of *F. harmsworthi*, ranging from 0.35 to 0.97 × 10^{-2} (mean 0.7 × 10^{-2}; n = 5), whereas Mg/Ca ratios from the most common species in our dataset, *F. pedata*, range between 0.21 and 0.8 × 10^{-2} (mean 0.45 × 10^{-2}; n = 49). The Sr/Ca ratios for *F. harmsworthi* vary between 0.66 and 0.96 × 10^{-3} (mean 0.78 × 10^{-3}; n = 5), and for *F. pedata* between 0.69 and 1.94 × 10^{-3} (mean 1 × 10^{-3}; n = 49). Element ratios of subfossil valves lie within the ranges of recent valves (Figure 2-9).

The plot of stable isotopes ($\delta^{18}O$, $\delta^{13}C$) in ostracod calcite reflects a differentiation with regard to the origin of water (Figure 2-10). The isotopic composition of ostracod calcite from lakes and ponds on Samoylov Island fed by precipitation shows heavier isotopic composition, with values between −1.6‰ and −6.3‰ for $\delta^{13}C$, and between −10.4‰ and −15.1‰ for $\delta^{18}O$ (Figure 2-10). The waters on Kurungnakh Island are situated on the up to 40 m high third Lena River terrace and are not influenced by river water. The isotope record of ostracods from this location is lighter in comparison to the data from Samoylov Island in $\delta^{18}O$ or in both $\delta^{18}O$ and $\delta^{13}C$ (Figure 2-10). The isotopic composition of ostracod calcite from one cut-off river branch on Samoylov Island (sample SAM-14) is characterised by relatively light values (−17.7 and −18.5‰ for $\delta^{18}O$) as compared to those from precipitation-fed waters, whereas the $\delta^{13}C$ in ostracod calcite from the river branch does not differ (Figure 2-10).

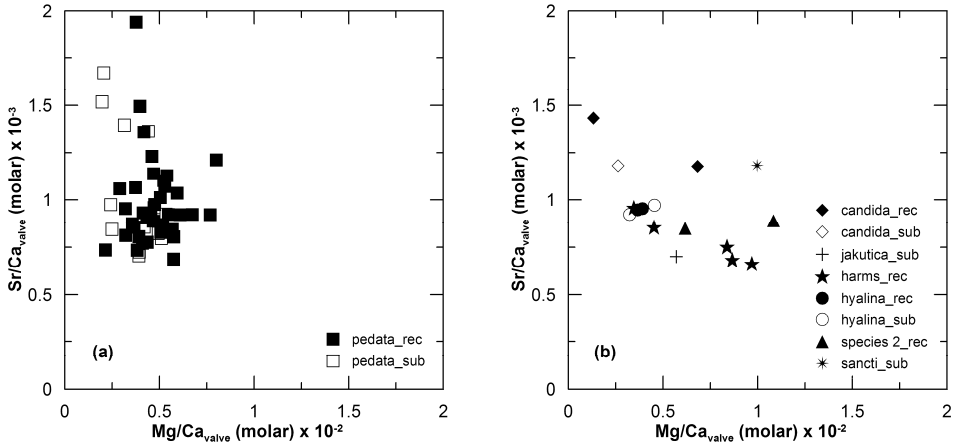

Figure 2-9 Element ratios (Sr/Ca and Mg/Ca) of recent and subfossil single valves of: (a) *F. pedata*; (b) *C. candida*, *C. muelleri jakutica*, *F. harmsworthi*, *F.* cf. *hyalina*, *F.* sp. 2 and *L. sanctipatricii*. The species identification follows the key: species (e.g. *F. pedata* → pedata) and state (recent → rec or subfossil → sub)

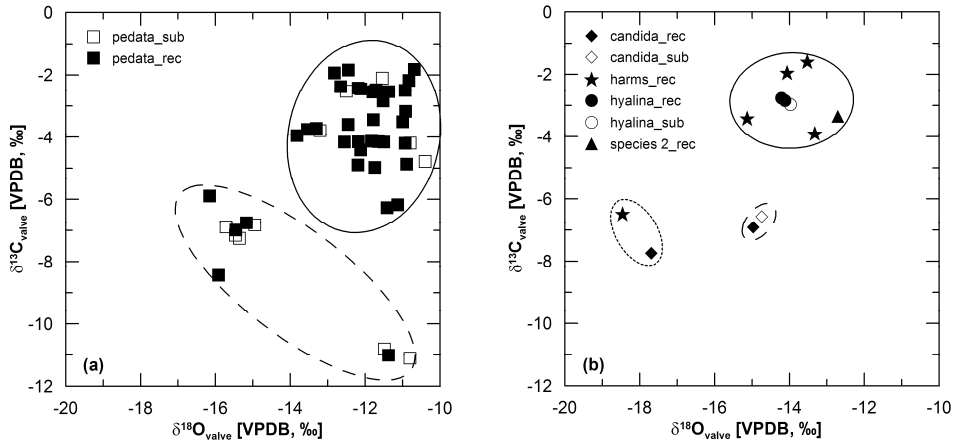

Figure 2-10 Isotopic composition ($\delta^{18}O$ and $\delta^{13}C$) in ostracod calcite for recent and subfossil single valves of: (a) *F. pedata*; (b) *C. candida*, *F. harmsworthi*, *F.* cf. *hyalina* and *F.* sp. 2. The species identification follows the key: species (e.g. *F. pedata* → pedata) and state (recent → rec or subfossil → sub). Full circles mark precipitation fed waters on Samoylov Island. Dashed circles mark precipitation fed waters on Kurungnakh Island. The dotted circle marks a river fed branch water on Samoylov Island

2.6 Discussion

2.6.1 Taxonomy and ecology of ostracods

The species *C. candida*, *F.* cf. *hyalina*, *F. protzi*, *B. reticulata*, *C. ophtalmica*, and *L. sanctipatricii* are known from mid-latitude regions to be broadly distributed and tolerant to a wide range of environmental factors, but with a preference or at least a tolerance for cooler water temperatures (Hiller 1972; Meisch 2000; Viehberg 2006). Their occurrence in Arctic environments shows their great ability for adaptation to extreme climatic conditions where the time for ontogenic cycles is very short. Semenova (2005) listed these species

as commonly distributed in East Siberia. Furthermore, *C. candida*, *F. hyalina*, and *B. reticulata* were found in thermokarst lakes in permafrost regions of Central Yakutia (Pietrzeniuk 1977). *C. candida* and *B. reticulata* were also described from Arctic environments on Greenland and in North Siberia (Alm 1914).

Species with preferences for (sub-) Arctic environments are *C. muelleri jakutica*, *F. harmsworthi*, *F. pedata*, and *T. glacialis*. The subspecies *C. muelleri jakutica* was first described by Pietrzeniuk (1977) from thermokarst lakes in Central Yakutia, whereas *F. harmsworthi* is commonly distributed in East Siberia (Semenova 2005) and known from Arctic environments on the Novaya Zemlya Archipelago and Franz Josef Land (Neale 1969). Another typical representative of Arctic freshwater ostracods is *F. pedata*, which was originally described as *Candona pedata* by Alm (1914). The genus *Fabaeformiscandona*, defined by Krstić (1972), did not originally include *F. pedata*, but the structure of the externo-distal seta (γ-seta) of the penultimate segment of the mandibular palp (which is smooth, not pulmose), and a carapace longer than 0.6 mm confirm the attribution of *F. pedata* to this genus. *T. glacialis* is known from East Siberia (Semenova 2005) and is considered to be endemic to most parts of the Arctic (Griffiths et al. 1998).

Some of the recently found species in the study area are known from Quaternary permafrost deposits in northeast Siberia, and therefore hold potential for aiding in regional palaeoenvironmental reconstructions. *C. candida*, *F. harmsworthi*, *F. pedata*, *L. sanctipatricii*, and *T. glacialis* are documented by Pietrzeniuk (unpublished data) in Late Pleistocene Ice Complex deposits in the Lena River Delta, and *C. muelleri jakutica*, *F. harmsworthi*, *F.* cf. *hyalina*, and *L. sanctipatricii* were collected in permafrost deposits on Bykovsky Peninsula to the east of our study sites (Wetterich et al. 2005).

2.6.2 Element ratios in ostracods and ambient waters

A relationship between the element content in ostracod calcite and water properties controlling the uptake of elements was established by studies in laboratory cultures and field collections of freshwater ostracods (e.g. Engstrom and Nelson 1991; Xia et al. 1997c; Wansard et al. 1998). This relationship is usually expressed as the partition coefficient D(M): $D(M) = (M/Ca)_{valve} / (M/Ca)_{water}$ (1)

where M can either be Mg or Sr, and M/Ca ratios are molar ratios. This function reflects the environmental conditions of the host water (temperature, Mg/Ca, Sr/Ca) expressed as the Mg/Ca and Sr/Ca ratio of the valves of any one species at the time of calcification to the corresponding ratio in ambient water, and it is used for palaeoenvironmental reconstructions which are based on ostracod geochemical data (e.g. Chivas et al. 1986; Ricketts et al. 2001). Other factors which may also control the element composition of ostracod calcite, such as the biological effect of temperature dependent metabolic rates

and ionic uptake also have to be taken into account (e.g. Dettmann et al. 2002). Presently the relationships between the element composition in host waters and ostracod calcite are not fully understood (Ito et al. 2003).

The magnesium uptake during valve calcification is a function of both the Mg/Ca ratio and the temperature of the water. Therefore, Mg/Ca ratios have the potential for being used as palaeothermometer (Chivas et al. 1986; Boomer et al. 2003). The observed Mg/Ca ratios in waters and ostracod calcite reach 1.39 in waters and 1.08×10^{-2} in valves. The lack of covariance between Sr and Mg (Figure 2-9) can be explained by these low Mg/Ca ratios of the ambient waters and the narrow range of Mg/Ca in ostracod calcite (Xia et al. 1997c). The plot of Mg/Ca ratios for *F. pedata* versus water shows no covariance within the observed ranges due to the temperature-dependence of Mg partitioning and the very low Mg/Ca ratios in the ambient waters (Figure 2-11a). For *F. harmsworthi*, which was investigated in much lower numbers, higher Mg/Ca ratios in waters seem to lead to higher ratios in valves (Figure 2-11b). Partition coefficients for magnesium *D*(Mg) were not calculated because of their temperature-dependence, and therefore should be investigated in laboratory cultures under controlled temperatures only. Furthermore, water temperatures measured during fieldwork at the time of ostracod sampling were likely different from those at the time of calcification of the valves. Strontium uptake into ostracod calcite and consequently the resulting Sr/Ca ratios correlate with the Sr/Ca ratio (mostly depending on salinity) of the ambient water (Chivas et al. 1986; Engstrom and Nelson 1991). De Dekker et al. (1999) presented preliminary data that suggest the possibility of a small thermodependence of Sr uptake in ostracod calcite of Cyprideis. This relationship underscores the potential of using Sr/Ca ratios as a salinometer in palaeoenvironmental reconstructions based on the geochemistry of fossil ostracods (e.g. Chivas et al. 1986; Boomer et al. 2003). The Sr/Ca ratios observed in ostracod calcite in the Lena River Delta seem to be positively correlated with their ambient waters (Figure 2-12). However, the variation in electrical conductivity in our data is too small to assume a strong correlation between changes in Sr/Ca ratio and electrical conductivity (salinity). The Sr/Ca ratio varies between 0.66 and 1.94×10^{-3} in ostracod calcite and between 2.63 and 4.83×10^{-3} in waters (Figure 2-12). For the most common species in our study, *F. pedata*, average partition coefficients D(Sr) for living caught specimens were calculated according to equation (1) and were 0.33 ± 0.06 (1σ) for female adults (n = 19) and 0.32 ± 0.06 (1σ) for male adults (n = 18). Xia et al. (1997c) discussed a Mg dependence of *D*(Sr), where *D*(Sr) increases with Mg concentration because of the large physiological energy needed to exclude Mg (and Sr) during shell calcification in waters of high Mg/Ca. Following this assumption, in our data the calculated low partition coefficients *D*(Sr) correspond to the

low Mg/Ca ratios of the ambient waters. *D*(Sr) values for other species were not calculated due to the low numbers of individuals.

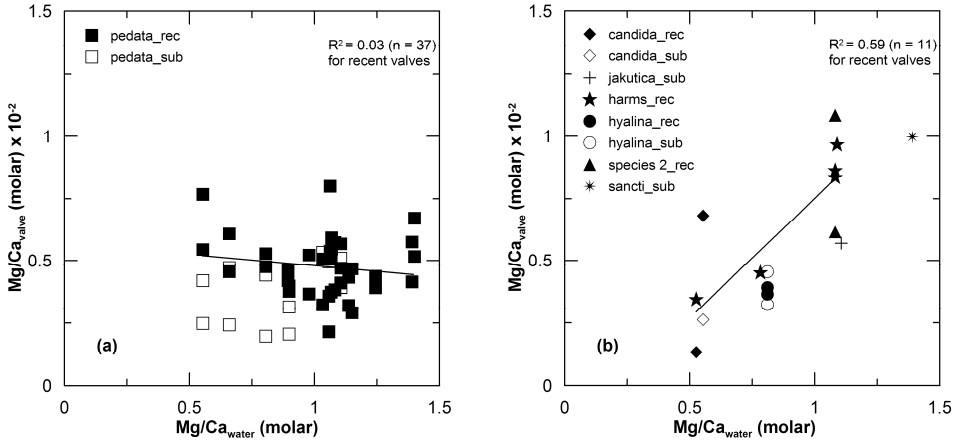

Figure 2-11 Plot of Mg/Ca ratios in ostracod calcite and ambient waters for recent and subfossil single valves of: (a) *F. pedata*; (b) *C. candida, C. muelleri jakutica, F. harmsworthi, F.* cf. *hyalina, F.* sp. 2 and *L. sanctipatricii*. The species identification follows the key: species (e.g. *F. pedata* → pedata) and state (recent → rec or subfossil → sub)

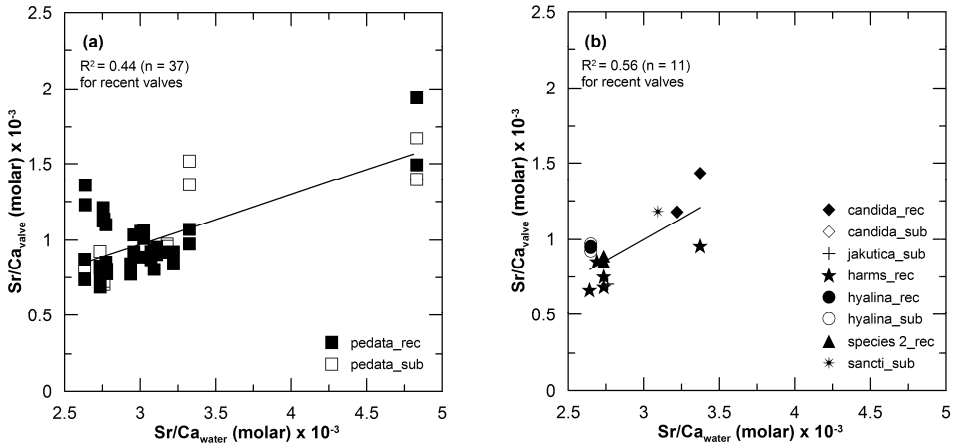

Figure 2-12 Plot of Sr/Ca ratios in ostracod calcite and ambient waters for recent and subfossil single valves of: (a) *F. pedata*; (b) *C. candida, C. muelleri jakutica, F. harmsworthi, F. cf. hyalina, F.* sp. 2 and *L. sanctipatricii*. The species identification follows the key: species (e.g. *F. pedata* → pedata) and state (recent → rec or subfossil → sub)

Arctic ostracods are observed to produce only one population in the open water season (Semenova 2003), which lasts about 3 months in the Lena River Delta. That implies that the adults will hatch first in July. So the time lag between shell secretion and time of our sampling (in August) was quite short, while hydrochemical characteristics of the host waters were fairly stable. We therefore assume that shell chemistry at sampling time was similar to the one at secretion time. Nevertheless, it is clear that our results do not reflect the exact Mg/Ca and Sr/Ca ratios of host waters during shell secretion, because of

laboratory manipulations, as shown in other experiments (Xia et al. 1997c). Furthermore, we emphasise strongly that the very low ionic content of the waters of the polygonal tundra does not allow a safe interpretation of the relationship between the element chemistry of the waters and the ostracod calcite. We refer to the fact that the observed variability does not allow us to calculate transfer functions.

In comparison with other studies on element chemistry in waters and ostracods (Engstrom and Nelson 1991; Xia et al. 1997c; Wansard et al. 1998, 1999; Wansard and Mezquita 2001), our data are likely to represent one endmember on the scale of hydrochemical information preserved in ostracods. It should be complemented by further investigations in (sub-) Arctic waters with higher ionic contents, where continental climatic conditions favour higher evaporation rates that alter the hydrochemical setting of fresh waters.

2.6.3 Stable isotopes in ostracods and ambient waters

Like element ratios, the isotopic composition of ostracod calcite ($\delta^{18}O$, $\delta^{13}C$) can be linked to the composition of the ambient water at the time of valve formation. (e.g. Chivas et al. 1993; Xia et al. 1997b, b; von Grafenstein et al. 1999). Therefore, $\delta^{18}O$ and $\delta^{13}C$ records of ostracod calcite provide a highly localised and temporally restricted reflection of the isotopic composition of water and TDIC, making them useful proxies in palaeolimnology (Holmes 1996). The isotopic composition of ostracod calcite shows both interspecific and intraspecific variations, mainly because of species-dependent metabolic effects on isotope fractionation, the timing of shell calcification in different seasons and at different temperatures, and species-dependent preferences for different microhabitats (e.g. Heaton et al. 1995; von Grafenstein et al. 1999). The $\delta^{18}O$ of ostracod carbonates is used as a proxy for temperature and isotopic composition of the water from which they precipitated (e.g. Chivas et al. 1993; Xia et al. 1997b; von Grafenstein et al. 1999). Factors affecting the oxygen isotope composition of lake water are the isotopic composition of precipitation, drainage basin hydrology, groundwater input, the precipitation/evaporation ratio, the residence time of water, the size of the waterbody, as well as the hydrochemical properties and temperature of the lake water (e.g. Kelts and Talbot 1990; Schwalb 2003; Leng and Marshall 2004).

Water bodies mostly fed by precipitation are common on the Lena River terraces above the floodplain and are generally not deep enough for extensive melting of the permafrost. Therefore, the influence of river water and meltwater from the frozen ground is of minor importance for most of the waterbodies. The main water source is summer precipitation. The $\delta^{18}O$ of these waterbodies ranged between −13.1‰ and −17.6‰ $\delta^{18}O$ (mean −15.1‰; n = 23) with a slope of 5.56 (Figure 2-4a). According to Meyer et al. (2002a), rain water samples from the Bykovsky Peninsula ranged between −11.4‰ and −17.0‰ $\delta^{18}O$

(mean −14.8‰; n = 10) with a slope of 6.77 and lie nearer to the GMWL than the data from lakes and ponds, which confirms the noticeable influence of evaporation on the $\delta^{18}O$ signal in waterbodies fed by precipitation. In general, the smaller polygonal ponds show a stronger deviation from the GMWL than thaw lakes, which in turn deviate more than thermokarst lakes (Figure 2-4a); this is obviously caused by lower evaporation rates per volume in deeper waters. Furthermore, deeper thaw lakes and thermokarst lakes reflect a mixed isotopic signal of precipitation waters and meltwater from the underlying ground ice. The latter is known to have a mean $\delta^{18}O$ isotopic ratio of −25‰ in Holocene ground ice and −30‰ in late Pleistocene ground ice (Meyer et al. 2002a). The isotopic signal of one cut-off river branch on Samoylov Island (sample SAM-14, −20.4‰ for $\delta^{18}O$ and −159.6‰ for δD) corresponds to the relatively light isotopic composition of the river water (−20.5‰ for $\delta^{18}O$ and −156‰ for δD; Schirrmeister et al. 2003). Obviously, this waterbody was flooded by the Lena River during spring flooding.

A strong covariance is shown between $\delta^{18}O$ in ostracod calcite of *F. pedata* (Figure 2-13a) and of other species (Figure 2-13b) with the water in which the valves were formed. The data show a near 1:1 relationship of $\delta^{18}O$ with a systematic shift to heavier values in ostracod calcite than in the respective ambient waters. According to Xia et al. (1997b), this shift (Δ) reflects the dependence between the $\delta^{18}O$ of ostracod calcite and of water with respect to water temperature, and is defined as: $\Delta = \delta^{18}O_{valve} - \delta^{18}O_{water}$ [‰] (2)

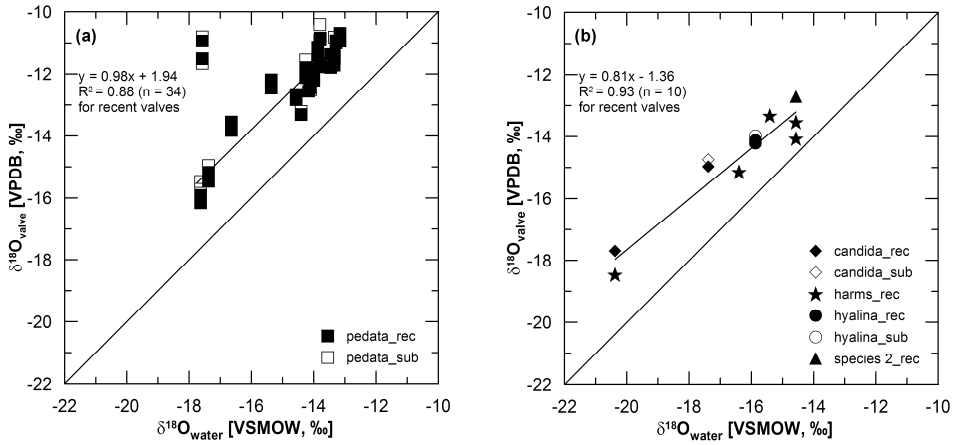

Figure 2-13 Plot of $\delta^{18}O$ in ostracod calcite and ambient waters for recent and subfossil single valves of: (a) *F. pedata*; (b) *C. candida*, *F. harmsworthi*, *F.* cf. *hyalina* and *F.* sp. 2. The species identification follows the key: species (e.g. *F. pedata* → pedata) and state (recent → rec or subfossil → sub)

The shift varies between Δ_{min} = + 1.1‰ and Δ_{max} = + 3.2‰ (excluding two outliers), with a mean of + 2.2‰ ± 0.5 (1σ) for living caught female and male specimens of *F. pedata* (Figure 2-13a). Two outliers with shifts of −6.1‰ and −6.7‰ were observed in valves of living female and male *F. pedata* caught in one thaw lake (SAM-24) on Samoylov Island.

This thaw lake drained into the river, had a water depth less than one meter, and the highest electrical conductivity and ionic contents of all studied waters (Appendix III-1). Probably because of the very shallow water in this lake, evaporation had a stronger influence than in other waterbodies and led to the unusual isotopic composition. These samples were therefore not included in further interpretation.

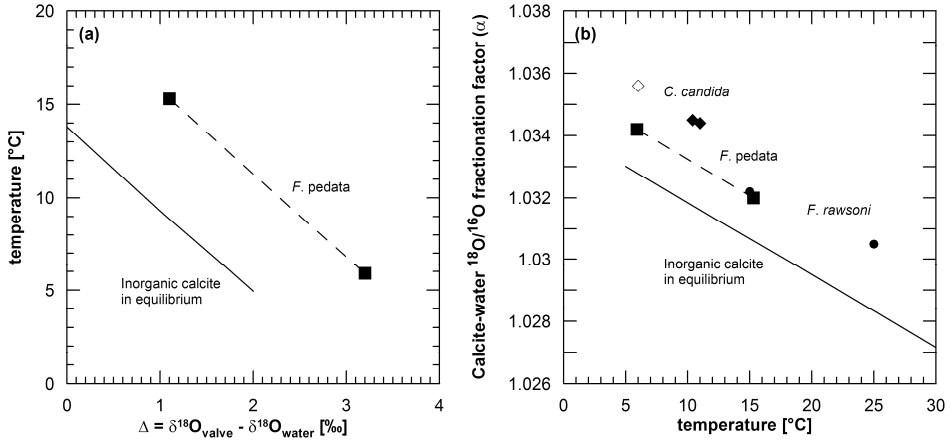

Figure 2-14 Temperature-dependent $\delta^{18}O$ fractionation in *Fabaeformiscandona pedata* expressed as: (a) variations in the calcite-water oxygen isotope fractionation shift Δ (T [°C] = 20.22–4.48($\delta^{18}O_{valve}$–$\delta^{18}O_{water}$)) in comparison with that of inorganic carbonates (T [°C] = 13.8–4.58($\delta^{18}O_{valve}$–$\delta^{18}O_{water}$) + 0.08($\delta^{18}O_{valve}$–$\delta^{18}O_{water}$)^2) by Kim and O'Neil (1997), re-expressed by Leng and Marshall (2004); (b) variations in the calcite-water oxygen isotope fractionation factor α for ostracods of the genera *Candona* and *Fabaeformiscandona*: closed dots for *F. rawsoni* (Xia et al. 1997b); open diamond for *C. candida* (von Grafenstein et al. 1999); closed diamonds for *C. candida* (Keatings et al. 2002) and closed squares for *F. pedata* (this study) in comparison with data of equilibrium fractionation in inorganic calcite at 5 mM Ca^{2+} solution (Kim and O'Neil 1997) given as a solid line. The dashed line reflects the slope in the data of this study

The parameters ($\delta^{18}O_{valve}$, $\delta^{18}O_{water}$) were measured in duplicate with high-precision of about ±0.1‰ (1σ) and therefore measurement errors can be ruled out. The isotopic composition of the water is more negative than that of the valves. However, the water was sampled in summer after the ostracod calcite had formed and $\delta^{18}O_{water}$ should consequently rather be heavier (more summer precipitation, more evaporation) than the measured one. This leads to the assumption that the systematic deviation of about 2‰ is not related to $\delta^{18}O_{water}$. The shift of about 2‰ (Figure 2-13a) between $\delta^{18}O_{water}$ and $\delta^{18}O_{valve}$ includes most likely metabolic (vital) and temperature effects which cause this systematic deviation. A metabolic or vital offset as compared to inorganic calcite in equilibrium was quantified to about 1.4‰ for *F. pedata* (Figure 2-14a). Vital offsets were already proposed by von Grafenstein et al. (1999), where a temperature-independent deviation (vital offset) of Δ = +2.2‰ ± 0.15 (1σ) was inferred for several species of

Candoninae. Other studies already showed the influence of vital effects on the isotopic composition of ostracod calcite of modern *F. rawsoni* (Xia et al. 1997b) and of *C. candida* (Keatings et al. 2002).

Our dataset is based on sampling of ostracods from shallow waterbodies with a high daily temperature range. Hence, it is difficult to relate our temperature data directly to $\delta^{18}O_{water}$ and $\delta^{18}O_{valve}$. Therefore, we correlated the minima and maxima of temperatures (T_{min}, T_{max}) and of shifts (Δ_{min}, Δ_{max}) in our dataset (Figure 2-14). Water temperatures and $\delta^{18}O_{water}$ measured at the time of ostracod sampling may have been different from those at the time of valve calcification. Nevertheless, we assume that field data reflect potential temperature variations between about 6 and 15°C over the summer period. Due to the lack of continuous water temperature measurements over the ice free period, we use field observations as well as air and soil temperature measurements from Samoylov Island in summer 2002 (Wille et al. 2003) to support the relevance of water temperature variations. The temperature regime of the studied shallow polymictic ponds and lakes is controlled by air and soil temperatures and should range between them. Hourly mean temperatures in July 2002 varied from 0°C to 25°C in the air and from 3°C to 10°C in the soil. In August 2002, the temperature variation ranged from 1°C to 24°C in the air and from 4°C to 10°C in the soil (J. Boike, AWI Potsdam, unpublished data). The studied shallow water bodies frozen down to the bottom in winter usually start thawing in the middle of June and refreeze in the middle of September (G. Stoof, AWI Potsdam, pers. comm.). The ostracods from these habitats most likely start their ontogeny not earlier than the waters are free of ice at the end of June when water temperature should be distinctly above 0°C. After this ostracods certainly need some time to reach adulthood. From these presumptions we conclude that a range of near bottom water temperature between about 6°C and 15°C which was measured during ostracod sampling seems to be quite realistic.

The temperature-dependence of $\delta^{18}O$ fractionation is reflected by the variation of the shift within a species, where increased temperatures correspond to smaller shifts (e.g. Leng and Marshall 2004). Xia et al. (1997b) showed a clear and consistent temperature-dependence of oxygen isotope fractionation during biological calcification by the species *Fabaeformiscandona rawsoni* (TRESSLER, 1957) in culture experiments at 15°C and 25°C. The 15°C cultures were about 2‰ heavier than the 25°C cultures, which confirms with the expected deviation of about 2‰ for a temperature difference of 10°C in inorganic carbonates (Xia et al. 1997b). The observed variation in the shift for modern *F. pedata* (between Δ_{min} = + 1.1‰ and Δ_{max} = + 3.2‰) over a temperature range of 9.4°C (T_{min} = 5.9°C and T_{max} = 15.3°C) during the fieldwork in summer 2002 can be explained by different temperatures of the water at the time of calcification (Figure 2-14a). The equation relating $\delta^{18}O$ of ostracod calcite to temperature is: $T\ [°C] = 20.22–4.48(\delta^{18}O_{valve}–$

$\delta^{18}O_{water}$), defined according to the standard palaeotemperature scale by Epstein et al. (1953).

From the two samples where maximal and minimal shifts are found, the calcite-water oxygen isotope fractionation factors (α) are calculated based on the definition:

$\alpha = \delta^{18}O_{valve} + 1{,}000 / \delta^{18}O_{water} + 1{,}000$

(3)

The results are α = 1.0342 at 5.9°C and α = 1.0320 at 15.3°C ($\delta^{18}O_{valve}$ and $\delta^{18}O_{water}$, relative to VSMOW). The temperature-dependence between ostracod calcite and ambient water, expressed as oxygen isotope fractionation factors (α), is given in Figure 2-14b, along with results for inorganic calcite (Kim and O'Neil 1997) and for ostracod calcite from other studies (Xia et al. 1997b; von Grafenstein et al. 1999; Keatings et al. 2002) which dealt with species of the genera *Candona* and *Fabaeformiscandona*. The oxygen isotope fractionation factors for inorganic calcite in equilibrium are given as solid line for a 5 mM Ca^{2+} solution which was assumed as most representative for equilibrium fractionation (Kim and O'Neil 1997). The other data plotted in Figure 2-14b derive from an in vivo study of *C. candida* in small shallow ponds in southern England (α = 1.0345 at 11°C; Keatings et al. 2002), and otherwise from an in vivo study of the same species in a large, deep lake in southern Germany (α = 1.0356 at 6°C, calculated by Keatings et al. 2002, based on data of von Grafenstein et al. 1999). Furthermore, data of an in vitro study of is shown for *F. rawsoni* (α = 1.0322 at 15°C and α = 1.0305 at 25°C; Xia et al. 1997b). The authors stated that *F. rawsoni* incorporate relatively more ^{18}O relative to inorganic calcite at 25°C than at 15°C, probably due to slower or less robust calcification, and to stress at the lower temperature. Therefore, the *F. rawsoni* data are closer to equilibrium fractionation line of inorganic calcite and reflect lower fractionation at a given temperature (Xia et al. 1997b).

Even though the comparison of data from different environments and laboratory experiments is highly speculative, the results are instructive since presently there are only a few studies on modern ostracods of different taxa and some aspects are worth discussing. Since the slope of temperature-dependence of the *F. pedata* data is defined by just two points (Figure 2-14b), and our species is different, we only assume a general accordance with the results of the studies cited above. The effect of lower calcification probably due to temperature-stress conditions as described by Xia et al. (1997b) is not seen in our data and most likely due to coldwater adaptation by the Arctic species *F. pedata*. The slope between the two data points of *F. pedata* is parallel to that of equilibrium fractionation of inorganic calcite, but systematically shifted. Both data points are arranged between that of *Candona* species and inorganic calcite. Possible explanations of lower fractionation in *F. pedata* can be attributed to species-dependent vital effects which result in different fractionation factors. Up to now the mechanisms of

ostracod calcification still remain unclear (e.g. Keatings et al. 2002). Furthermore, the different fractionation can be also caused by habitat-specific characteristics of Arctic environments, which are not fully understood up to now.

In summary, the variation in $\delta^{18}O$ ostracod calcite corresponds to the isotopic composition of ambient waters, which is affected by the general climatic setting of the region, the water source feeding the waterbody (precipitation or river water), and the influence of meltwater from the frozen ground. For the $\delta^{18}O$ of ostracods adapted to cold environments such as *F. pedata*, a temperature-dependence is reflected in the variations of calcite-water oxygen isotope fractionation factor (α) and shift (Δ). Additionally, the deviation to equilibrium fractionation is most likely influenced by metabolic (vital) effects. These vital effects are also seen in the deviation of the $\delta^{18}O$ signal in ostracod calcite of other species.

The $\delta^{13}C$ of carbonates is not very influenced by temperature variations but is rather understood to be a response to changes in the isotopic ratio of the total dissolved inorganic carbon (TDIC) from which the carbonates precipitated (Holmes 1996). Commonly, changes in $\delta^{13}C$ are attributed to changes in carbon and productivity within a lake (e.g. Schwalb 2003; Leng and Marshall 2004). Rates of exchange of CO_2 with the atmosphere, photosynthesis/respiration of aquatic plants, organic decay, and bacterial processes are the main controlling factors for the $\delta^{13}C$ of TDIC (e.g. von Grafenstein et al. 1999; Schwalb 2003; Leng and Marshall 2004).

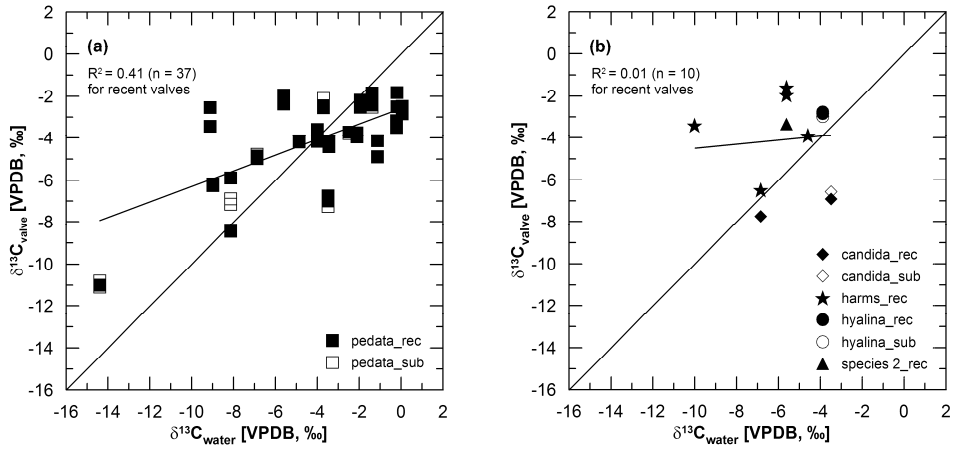

Figure 2-15 Plot of $\delta^{13}C$ in ostracod calcite and ambient waters for recent and subfossil single valves of: (a) *F. pedata*; (b) *C. candida*, *F. harmsworthi*, *F.* cf. *hyalina* and *F.* sp. 2. The species identification follows the key: species (e.g. *F. pedata* → pedata) and state (recent → rec or subfossil → sub)

In Figure 15 the relationship between $\delta^{13}C$ in ostracod calcite of different species and in water is shown. The $\delta^{13}C$ of the waters ranges between +0.1‰ and −14.4‰, and waters fed by precipitation cannot be distinguished from that in the old branch. The considerable scatter in $\delta^{13}C$ indicates the influence of complex abiotic and biotic effects on $\delta^{13}C$

fractionation as is expected in natural lacustrine systems (Leng and Marshall 2004). The most probable explanation for the observed $\delta^{13}C$ variation at the studied shallow ponds and lakes is the daily variation of water plant photosynthesis and seasonal variations during the summer.

2.7 Conclusions

For the first time, this study deals with the geochemical properties of modern freshwater ostracods from northeast Siberia. The geochemical record in ostracod calcite (Mg/Ca, Sr/Ca; $\delta^{18}O$, $\delta^{13}C$) was investigated in comparison with data from ambient waters. Over the years, several studies on this branch of ostracodology have been undertaken, but even more recent studies do not fully explain the relationships between water and shell chemistry (e.g. Wansard et al. 1998, 1999; Griffiths and Holmes 2000; Boomer et al. 2003). Our study was the first attempt to expand knowledge about the geochemistry of freshwater ostracods in Arctic regions. The results show the potential of Arctic freshwater ostracods, which are often preserved in Quaternary permafrost deposits, as geochemical proxies for regional reconstructions of palaeoenvironments. The following conclusions can be drawn from our study:

(1) The ostracod assemblages in the Lena River Delta include typical Arctic species like *Candona muelleri jakutica*, *Fabaeformiscandona harmsworthi*, *Fabaeformiscandona pedata*, and *Tonnacypris glacialis*, but also cosmopolitan species like *Candona candida*, *Fabaeformiscandona* cf. *hyalina*, *Fabaeformiscandona* cf. *tricicatricosa*, *Fabaeformiscandona protzi*, *Bradleystrandesia reticulata*, *Cypria ophtalmica*, and *Limnocytherina sanctipatricii* were found. The most common species are *F. pedata* and *F. harmsworthi*.

(2) Due to the very low ionic content of the waters of the Arctic tundra, the observed element ratios of ostracod calcite (Mg/Ca, Sr/Ca) in recent valves of female and male specimens of different species range in very narrow arrays. Therefore, our data represent one endmember on a scale of hydrochemical information preserved in ostracods.

(3) No distinct differentiations are observed in Mg/Ca, Sr/Ca, $\delta^{18}O$, and $\delta^{13}C$ between female and male or recent and subfossil valves, either within one species or between different species.

(4) Average partition coefficients D(Sr) for living caught specimens of *F. pedata* were calculated, with 0.33 ± 0.06 (1σ) for female adults (n = 19), and 0.32 ± 0.06 (1σ) for male adults (n = 18).

(5) The $\delta^{18}O$ data of the waters, and consequently of ostracod calcite, indicate the water

source in the watershed is either precipitation or the Lena River.

(6) A near 1:1 relationship of $\delta^{18}O$ in waters and valves was found, with a mean shift of Δ_{mean} = 2.2‰ ± 0.5 (1σ) to heavier values for calcite of modern *F. pedata* (n = 34) as compared to ambient waters. The shift is not dependent on $\delta^{18}O_{water}$, and caused by vital and temperature effects. Temperature-dependence is reflected in the variations of Δ (between Δ_{min} = +1.1‰ and Δ_{max} = +3.2‰). A vital effect as compared to inorganic calcite in equilibrium was quantified with 1.4‰ for *F. pedata*.

3 Evaporation effects as reflected in freshwaters and ostracod calcite from modern environments in Central and Northeast Yakutia (East Siberia, Russia)

Sebastian Wetterich[1], Ulrike Herzschuh[1], Hanno Meyer[1], Lyudmila Pestryakova[2], Birgit Plessen[3], C. M. Larry Lopez[4] and Lutz Schirrmeister[1]

(1) Alfred Wegener Institute for Polar and Marine Research, Telegrafenberg A43, 14473 Potsdam, Germany; (2) Department of Biology and Geography, Yakutsk State University, Belinskogo 58, 677000 Yakutsk, Russia; (3) GeoForschungsZentrum Potsdam, Section 3.3, Telegrafenberg, 14473 Potsdam, Germany; (4) The United Graduate School of Agricultural Sciences, Iwate University, 020-8550 18-8, Ueda 3 chome, Morioka, Japan

Hydrobiologia 614: 171-195 (DOI 10.1007/s10750-008-9505-y)

3.1 Abstract

Taxonomical and geochemical investigations on freshwater ostracods from 15 waters in Central and Northeast (NE) Yakutia have been undertaken in order to estimate their potential usefulness in palaeoenvironmental reconstructions based on regional fossil records. Higher variability in environmental factors such as pH, electrical conductivity, and ionic content was observed in thermokarst-affected lakes in Central Yakutia than in NE Yakutia lakes. Species diversity of freshwater ostracods reached up to eight taxa per lake, mostly dominated by *Candona weltneri* HARTWIG, 1899, in Central Yakutia, whereas in NE Yakutian waters the diversity was lower and *Candona muelleri jakutica* PIETRZENIUK, 1977 or *Fabaeformiscandona inaequivalvis* (SARS, 1898) had highest frequencies. Coupled analyses of stable isotopes ($\delta^{18}O$, $\delta^{13}C$) and element ratios (Sr/Ca, Mg/Ca) were performed on both host waters and ostracod calcite, aiming to estimate the modern relationships. Correlations between host waters and ostracod calcite of single species were found for $\delta^{18}O$, $\delta^{13}C$ and Sr/Ca and Mg/Ca ratios. The relationships between $\delta^{18}O$, Mg/Ca and Sr/Ca ratios and electrical conductivity (salinity) as an expression of solute concentrations in the waters mainly controlled by evaporation are more complicated but evident, and may be useful in future interpretation of geochemical data from fossil Siberian ostracods.

3.2 Introduction

Knowing the physico-chemical properties of lake water is a prerequisite for understanding relationships between environmental conditions and the significance of bioindicators such as freshwater ostracods for interpreting fossil records in palaeoenvironmental

reconstructions. Therefore, we studied relevant environmental parameters controlling ostracod diversity and the geochemical properties of their shells in order to apply modern reference data in future studies of fossil assemblages.

The most characteristic feature of micro-crustacean ostracods is a bi-valved carapace made of low-magnesium calcite. Changes in environmental parameters alter the composition of freshwater ostracod assemblages and the geochemical composition of ostracod calcite that precipitates from the host water at the time of shell secretion (e.g. Griffiths and Holmes 2000). In particular, stable isotopes of oxygen and carbon ($\delta^{18}O$, $\delta^{13}C$) as well as molar element ratios of strontium and magnesium to calcium (Sr/Ca, Mg/Ca) in ostracod calcite provide a highly localised and temporally restricted reflection of the host water composition (Griffiths and Holmes 2000).

In East Siberia, two palaeo-archives have been used mainly for reconstructions of palaeoclimatic changes: lake sediments (e.g. Katamura et al. 2006; Lozkhin et al. 2007) and permafrost deposits (e.g. Hubberten et al. 2004). The scientific interest in palaeoclimatic and palaeoenvironmental reconstructions from East Siberian records is based on current understanding that permafrost is a climate-driven phenomenon and Arctic regions are sensitive to the ongoing climate change. In this context, the Siberian Arctic is experiencing a large impact from global warming (ACIA 2005; IPCC 2007). The permafrost system reacts to warming with intensified thermokarst processes which lead to changes in matter and energy cycles, and also influence relief and hydrology in the Arctic. Understanding past environmental history can enable us to explain and estimate future environmental dynamics in Arctic permafrost areas.

Remains of fossil freshwater ostracods have been obtained from Siberian lacustrine sediments and used as proxy for climatic and hydrological conditions during the Late Quaternary (Wetterich et al. 2005; Wetterich et al. 2008c). However, modern and fossil Siberian freshwater ostracods have seldom been studied. The first description of modern ostracods from Yakutia was given by Pietrzeniuk (1977). More recent data on ostracod occurrence in Siberia was summarised by Semenova (2005). The first geochemical studies on shells of Yakutian freshwater ostracods were carried out on samples from waters located on islands in the Lena River Delta, Laptev Sea (Wetterich et al. 2008a).

In this article we present taxonomical and geochemical data of ostracods and their habitats from two study regions in East Siberia in order to apply modern analogues to fossil records. Further studies of East Siberian fossil ostracod assemblages and their palaeoecological interpretation will benefit from the modern reference data offered here since the understanding of fossil records is impossible without knowledge of recent relationships and processes. Therefore, we focus our research on climate-relevant

parameters such as evaporation, solute concentration and temperature regime in lakes as they are reflected in geochemical composition of both host waters and ostracod calcite.

3.3 Study area

Our limnological study in East Siberia includes two regions: (1) Central Yakutia (61° N to 62° N and 129° E to 132° E) at the Lena River, and (2) NE Yakutia (66° N and 143° E) at the mouth of the Moma River where it flows into the Indigirka River (Figure 3-1).

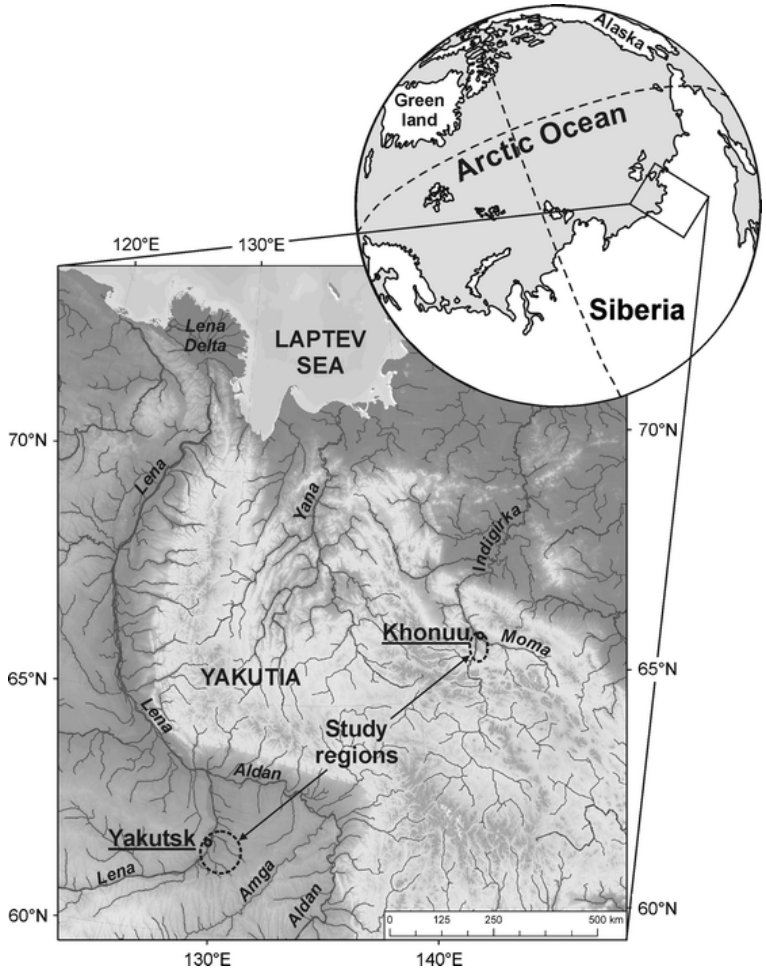

Figure 3-1 Location of the two study regions in Central and Northeast Yakutia in East Siberia. Map compiled by G. Grosse (UAF) using data from Hastings et al. (1999)

The study regions belong to the boreal coniferous forest zone (taiga) and to the zone of continuous permafrost. The permafrost thickness in both regions reaches up to 500 m (Geocryological Map 1991). The climatic conditions are strongly continental, with high annual temperature amplitudes (Gavrilova 1998). The mean annual air temperatures are −10.4°C in Yakutsk ($T_{January}$ −41.7°C; T_{July} +18.1°C) and −15.3°C in Khonuu ($T_{January}$ −46.3°C; T_{July} +13.9°C; Rivas-Martínez 2007). The mean precipitation averages about 250 mm in both regions (Rivas-Martínez 2007). About 75–85% of the annual precipitation occurs from April to October, and evaporation exceeds precipitation during the summer

(Gavrilova 1973). The moisture deficit amounts to more than 220 mm per year in both study regions due to approximately twofold higher potential evapotranspiration than real precipitation (Gavrilova 1969; Rivas-Martínez 2007).

Thermokarst, an important landscape-forming feature of the permafrost zone, is mainly caused by extensive melting of ground ice in the formerly underlying permanently-frozen loose sediments (van Everdingen 1998). Widespread thermokarst processes form numerous depressions in the landscape surface (Alases), which are often occupied by thermokarst lakes. This thermokarst landscape is typical of Central Yakutia (e.g. Soloviev 1973). Due to the continental climate conditions, the lakes of Central Yakutia are likely to experience changing water levels and desiccation (e.g. Nemchinov 1958; Bosikov 2005; Pestryakova 2005). Water level changes and depth in thermokarst lakes are also controlled by geomorphological features (e.g. Bosikov 2005). Solute concentrations in these waters are influenced by the ionic composition of thawed ground ice from the underlying permafrost (e.g. Lopez et al. 2007), but the main source of such waters is precipitation. Thermokarst lakes are sensitive to any variations in climate, vegetation, or anthropogenic influence (e.g. Kumke et al. 2007; Pestryakova et al. 2007). Except of river branches where periodic flooding may alter the isotope and ionic composition all other studied waters are mainly fed by precipitation since visible inflows and outflows have not been observed. In summer, commonly the upper 0.5 to 2.0 m of the ground is unfrozen. The thickness of the so-called active layer mainly depends on substrate, exposition and vegetation covers and controls the melt water flow above the permafrost table within the seasonal thawed ground.

3.4 Material and methods

All presented samples and data were obtained in frame of a joint Russian–German expedition to Yakutia in summer 2005. A total of 56 lakes and other waters were sampled for several limnological purposes during the fieldwork in two study regions. Here, we present the limnological data from all sampled lakes and focus on ostracod data from 15 sites where enough ostracod material could be obtained for further taxonomical and geochemical analyses.

3.4.1 Field work

In July 2005, fieldwork was performed in Central Yakutia; 12 sites around Yakutsk and 27 sites on the Lena-Amga interfluve east of Yakutsk were sampled (Figure 3-1). The studied waters, including thermokarst lakes in different development stages, lakes in thermo-erosion depressions, one Tukulan (dune) lake and old branches of the Lena River (Appendix III-3), are situated on denudation plains and different flood plain levels

(terraces) of the Lena River. The classification of thermokarst lakes comprises of the following stages Soloviev (1959): Dyuedya (initial thermokarst), Tyympy (first stage of Alas development) and mature Alas lake. In August 2005, 17 sites in total were sampled in NE Yakutia near the Khonuu settlement (Figure 3-1) on the flood plain and the lower terraces of the Indigirka and the Moma rivers. Kerdyugen ponds (ponds in areas of burned forests) as well as lakes in lowland depressions and anthropogenic water basins were studied (Appendix III-3).

Studies of water chemistry and physics in lakes were undertaken in order to describe recent environmental variables affecting life conditions of ostracods. For hydrochemical analyses conducted while still in the field and afterwards in the laboratory, lake water was sampled from each site in Central Yakutia in the lake centre at 0.5–1 m water depth using an inflatable dinghy. Because we did not have a dinghy in NE Yakutia, the lake water was sampled at the lake margin at a water depth of 0.5–1 m.

Total hardness, alkalinity and acidity were determined using titrimetric test kits (Macherey-Nagel, Visocolor series). We quantified pH, temperature, oxygen concentration and electrical conductivity (EC) using a handheld multi-parameter instrument (WTW 340i) equipped with appropriate sensors (pH: SenTix 41; Oxygen: CellOx 325; EC and temperature: Tetracon 325). In August, due to technical problems with the oxygen sensor these measurements were continued using a titrimetric test kit (Aquamerck, Oxygen Test). These field measurements were performed on water samples directly after sampling. Our investigations included measuring water depth using an echo sounder (Appendix III-3). Continuous measurements of water temperature, EC and water level fluctuations (HM-500 series, Hi-net) were performed from May to September 2005 at the Japanese–Russian research station Neleger, west of Yakutsk (62°05′ N, 129°45′ E) in an Alas lake (2 m deep) at a water depth of ca. 0.4 m using a datalogger (Campbell, CR10X).

3.4.2 Water analyses

Water samples were analysed for stable isotopes and hydrochemistry at the Alfred Wegener Institute (Potsdam and Bremerhaven, Germany).

The lake water samples for $\delta^{18}O$ determination were stored cool and afterwards analysed by an equilibration technique (Meyer et al. 2000) using a mass-spectrometer (Finnigan MAT Delta-S). The water samples intended for analysis of $\delta^{13}C$ in total dissolved inorganic carbon (TDIC) were preserved by adding $HgCl_2$ until analysis; carbon was extracted from lake water with 100% phosphoric acid in an automatic preparation line (Finnigan Gasbench I) coupled online with the mass-spectrometer (Finnigan MAT 252). The reproducibility of these data derived from standard measurements is better than ±0.1‰ (1σ). The stable isotope water data are expressed in delta per mil notation (δ, ‰) relative

to the Vienna Standard Mean Ocean Water (VSMOW) for water isotopes ($\delta^{18}O$, δD), and relative to the Vienna Pee Dee Belemnite (VPDB) standard for $\delta^{13}C$ in TDIC.

Water samples for ion analysis were passed through a cellulose-acetate filter (pore size 0.45 µm) in the field. Afterwards, samples for element (cation) analyses were acidified with HNO_3, whereas samples for anion analysis and residue samples were stored cool. Upon return to the laboratory, the element content of the water was analysed by Inductively Coupled Plasma-Optical Emission Spectrometry (ICP-OES, Perkin-Elmer Optima 3000 XL), while the anion content was determined by Ion Chromatography (IC, Dionex DX-320). The bi-carbonate concentrations of the water were calculated from the alkalinity measurements in the field. To ensure the reliability of the analytical methods, the ion balance of each sample was calculated, resulting in deviations of better than ±10% for most samples. Poor charge balances were obtained in single samples, that are caused likely by underestimated bi-carbonate concentrations. Molar ratios in the water were calculated from the concentrations of magnesium, strontium and calcium as Mg/Ca and Sr/Ca ($\times 10^{-3}$).

3.4.3 Ostracod analyses

Living ostracods were captured from the upper 5 cm of the lake margin sediment in about 0.5–1 m water depth using an exhaustor system (Viehberg 2002), and were preserved in 70% alcohol. This method allows representative and qualitative sampling of living specimens, enables further preparation of the soft body needed for taxonomical work, and preserves the undamaged valves needed for geochemical analyses of ostracod calcite. In samples with sufficient number of living ostracods, the most common species were prepared for element (Mg, Sr, Ca) and stable isotope ($\delta^{18}O$, $\delta^{13}C$) analyses.

The species were identified under a binocular microscope (Zeiss SV 10) by the soft body and valve characteristics described in Bronshtein (1947), Pietrzeniuk (1977), and Meisch (2000), and following the taxonomic nomenclature given by Meisch (2000). The total number of caught and identified individuals per lake reaches more than 100 in most lakes except of Yak-31 (69 individuals) Yak-22 (92 individuals) and Yak-12 (99 individuals). Maximal number of ostracods was caught in Yak-49 (911 individuals). From the total number of individuals per lake percentage data of species frequencies were calculated as shown in Figure 7. Scanning Electron Microscopy (SEM, Zeiss Digital Scanning Microscope 962) with ×40, ×80, or ×100 magnification, depending on valve sizes, was used at the GeoForschungsZentrum (Potsdam, Germany) for imaging valves of the most common ostracod species.

Altogether, 34 samples of modern ostracods from 15 water bodies were analysed for $\delta^{18}O$ and $\delta^{13}C$ stable isotopes and for Mg/Ca and Sr/Ca ratios. In order to create sufficient

material (ca. 50 µg) for isotope analyses we compiled two to four valves of one species and sex for mostly two samples per lake (Appendix III-5). In total, 112 valves were used for isotope analyses. The analyses on element content (Sr, Mg, Ca) of ostracod calcite were carried out mostly on two single-valve samples from one species and sex per lake (Appendix III-5). In total, 34 valves were used for element analyses. The analytical work on ostracod valves was performed at the GeoForschungsZentrum laboratories. Following Keatings et al. (2006b) the ostracod valves were manually cleaned by removing the soft body under the binocular microscope, and then washed in distilled water and air-dried. Only clean valves of adult specimens were used for analysis. Particles adhering to valves were removed with a fine brush. The prepared valves were dissolved with 103% phosphoric acid and analysed for $\delta^{18}O$ and $\delta^{13}C$ by a mass-spectrometer (Finnigan MAT 253) directly coupled to an automated carbonate preparation device (Kiel IV). The reproducibility as determined by standard measurements is better than ±0.06‰ (1σ) for $\delta^{18}O$ and ±0.04‰ (1σ) for $\delta^{13}C$. The stable isotope ostracod calcite ($\delta^{18}O$, $\delta^{13}C$) data are expressed in delta per mil notation (δ, ‰) relative to VPDB.

For analysis of Ca, Mg and Sr we used an ICP-OES (Varian Vista-MPX) at the GeoForschungsZentrum. The single valve samples were placed in a reaction vial, dissolved in 30 ml of 20% HNO_3 (Baker Ultrex), and 3 ml of distilled water were added. The ICP-OES was calibrated with three multi-element standards prepared from mono-element standard solutions for ICP (Alfa Aesar Specpure 1,000 µg/l). Standard solution 1 contained 1 ppm Ca, 0.02 ppm Mg and 0.01 ppm Sr. Concentrations in standard solutions 2 and 3 were two and three times higher, respectively. For samples with calcium concentrations more than 3 ppm standard solutions of 2, 4 and 6 ppm Ca were used. Three determinations were made from each sample to check machine precision. Contaminant (blank) concentrations in the solvent acid were analysed for each batch of 10 samples to determine detection limits of the measurements. The detection limits in solution (3σ above background in µg/l (ppb), e.g. Doerfel 1966) are 0.55 for Ca (wavelength 422.673 nm), 0.11 for Mg (279.553 nm) and 0.01 for Sr (407.771 nm). The results for Mg, Sr and Ca are expressed as µg/g (ppm) in calcite following Chivas et al. (1986). From these results, molar ratios in ostracod calcite were calculated as Mg/Ca ($\times 10^{-2}$) and Sr/Ca ($\times 10^{-3}$).

3.5 Results

3.5.1 Physico-chemical characteristics of the lakes and ponds

Results of limnological investigations and observations during the fieldwork and later in the laboratory are summarised in Appendix III-3 and Appendix III-4.

The studied lakes are shallow with maximal depths of about 4 m. Lake area varies from 2 × 5 m to 30 × 1000 m. The pH ranges from 6.6 to 10.2 in mostly slightly alkaline to alkaline waters in Central Yakutia and from 6.0 to 9.1 in mostly neutral waters in NE Yakutia. Electrical conductivity differs between the regions, with generally higher values in Central Yakutia (0.10 to 5.71 mS/cm) than in NE Yakutian waters (0.03 to 0.93 mS/cm). The water temperature varies from 8.0 to 26.3°C at different times and sites of sampling. The data obtained at the Neleger Site from continuous monitoring of water temperature, EC and lake level fluctuations in one Alas lake reflect clear trends during summer 2005 (Figure 3-2).

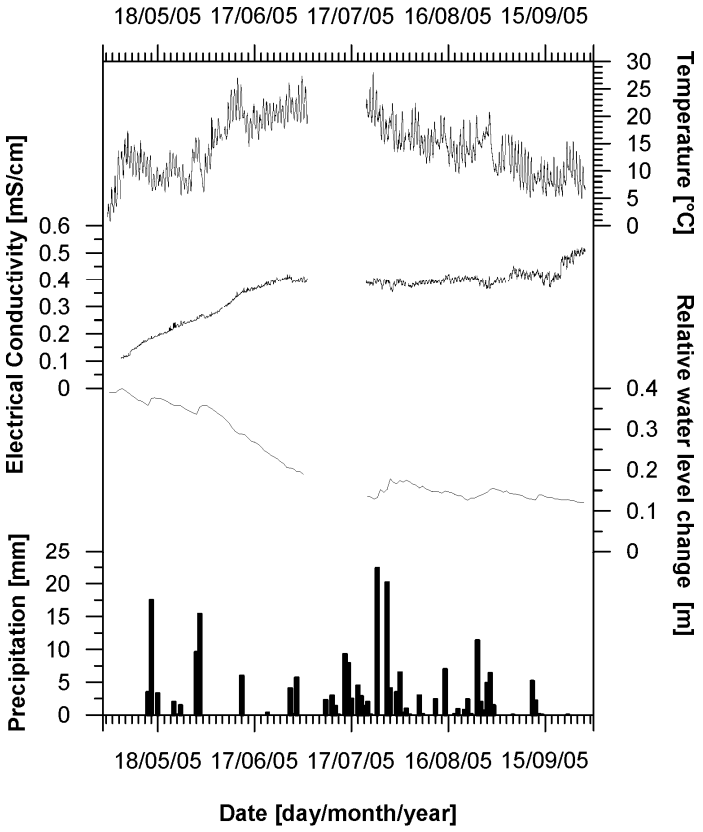

Figure 3-2 Continuous temperature and conductivity measurements in an Alas lake at the Japanese–Russian research station Neleger from May 2 until September 27, 2005. Note lacking data due to technical problems in the first half of July 2005

The water temperature record is characterised by daily high amplitudes of up to 11°C with mean temperatures of 9.8°C in May, 19.1°C in June, 19.2°C in the second half of July (data from 03 to 21 July 2005 are lacking), 14.9°C in August and 9.6°C in September. Electrical conductivity increases continuously from the beginning of May until the end of June, rising fourfold from 0.1 to 0.4 mS/cm, and likely stays at the upper end of this range during July and August; the highest value (0.5 mS/cm) is reached in the second half of September (Figure 3-2).

The measured lake level fluctuations are consistent with the changes in conductivity; they decrease from May to June and remain fairly stable from July to September (Figure 3-2). Lake levels briefly increased after larger rainfall events (Figure 3-2); in total, 217 mm precipitation was measured during the monitoring period.

As shown in Figure 3-3, the ionic composition of Central Yakutian lakes is dominated by Mg or Na + K and HCO_3. In contrast, lakes studied in NE Yakutia are dominated by Ca and HCO_3.

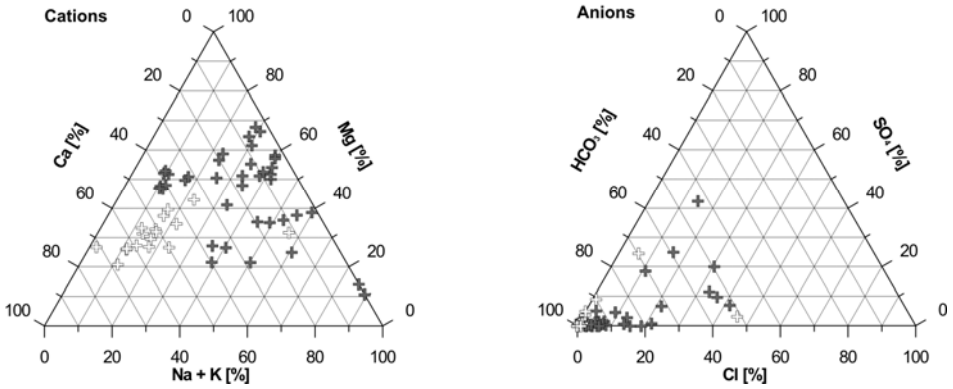

Figure 3-3 Ionic composition of lake and pond waters in Yakutia. Data from Central Yakutia are shown by grey symbols and those from NE Yakutia by white symbols

The results of oxygen and hydrogen isotope analyses of the lake waters are presented in a $\delta^{18}O$-δD plot (Figure 3-4) with respect to the Global Meteoric Water Line (GMWL) that correlates fresh surface waters on a global scale (Craig 1961).

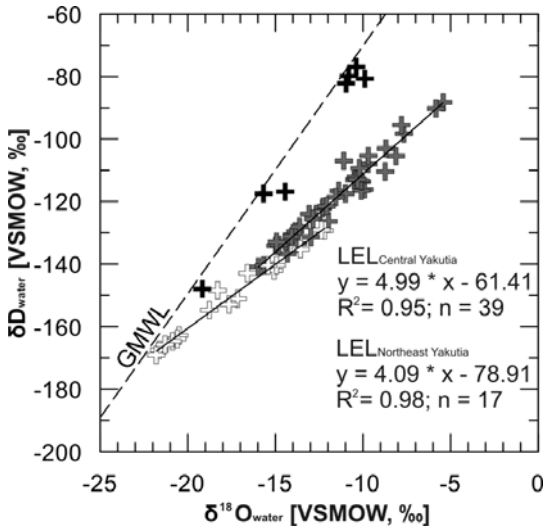

Figure 3-4 Isotopic composition of natural Yakutian waters; plot shows oxygen and hydrogen isotopes in lake water and summer 2005 precipitation. Data from Central Yakutia are shown by grey symbols and those from NE Yakutia by white symbols. Precipitation data are given by black symbols. Regional evaporation effects on the waters are expressed as Local Evaporation Lines (LELs)

The studied lakes are mainly fed by precipitation. The isotope values of seven August 2005 rain water samples from Yakutsk are given in Figure 3-4. Whereas the local rain water samples are close to the GMWL, samples from the studied lakes are shifted to lower values. The $\delta^{18}O$ values from Central Yakutian lake samples range between about −15.7 and −5.5‰, differing from NE Yakutian lakes with values between about −21.3 and −12.2‰ (Figure 3-5). The $\delta^{13}C$ data from both regions show a similar and considerable scatter, and range between about −11.2 and +11.0‰ (Figure 3-5). We did not detect a correlation between $\delta^{18}O$ and $\delta^{13}C$.

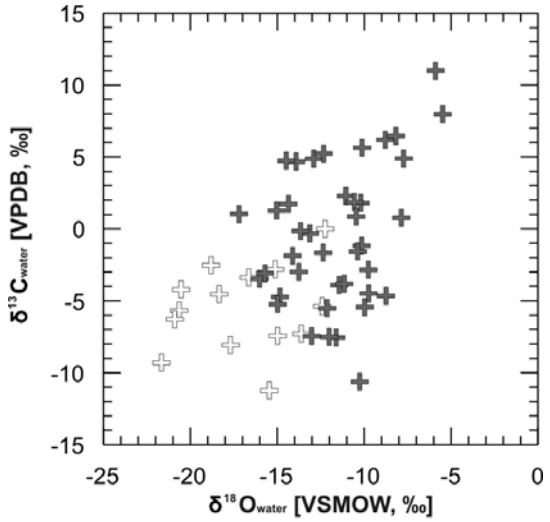

Figure 3-5 Isotopic composition of natural Yakutian waters; plot shows oxygen and carbon isotopes in lake water in summer 2005. Data from Central Yakutia are shown by grey symbols and those from NE Yakutia by white symbols

3.5.2 Ostracod taxonomy and environmental ranges

Among the 18 ostracod taxa observed, 16 taxa were identified to the species level, one taxon (*Cyclocypris* sp.) to the genus level, and one taxon is represented by undetermined juvenile Candoninae. SEM images of the most common species are presented in Figure 3-6.

Most of the adult specimens belong to species of the subfamily Candoninae including the genera *Candona*, *Fabaeformiscandona* and *Pseudocandona* (Figure 3-7). With up to eight taxa per lake, the number of species is generally higher in Central Yakutian lakes than in NE Yakutia. In our Central Yakutian collection the dominant species in most samples is *Candona weltneri* HARTWIG, 1899, but *Candona candida* (O.F. MÜLLER, 1776), *Candona muelleri jakutica* PIETRZENIUK, 1977, and *Fabaeformiscandona rawsoni* (TRESSLER, 1957) are most common in single lakes (Figure 3-7). NE Yakutia lakes are dominated by *C. muelleri jakutica* or *F. inaquivalvis* (SARS 1898) except for two lakes, where *F. acuminata* (FISCHER, 1851) or *Physocypria kraepelini* G.W. MÜLLER, 1903 are most

abundant. *F. inaquivalvis* was first described as *Candona inaequivalvis* by Sars (1898) from the environs of Verkhoyansk in Yakutia and also listed by Semenova (2005) as a rare species in East Siberia. Other species such as *Pseudocandona compressa* (KOCH 1838), *F. fabaeformis* (FISCHER, 1851), *F. hyalina* (BRADY & ROBERTSON, 1870), *Limnocythere inopinata* (BAIRD, 1843) and *Cyclocypris ovum* (JURINE, 1820) are recorded as common in Central Yakutia by Pietrzeniuk (1977), but are found in lower quantities in our data set.

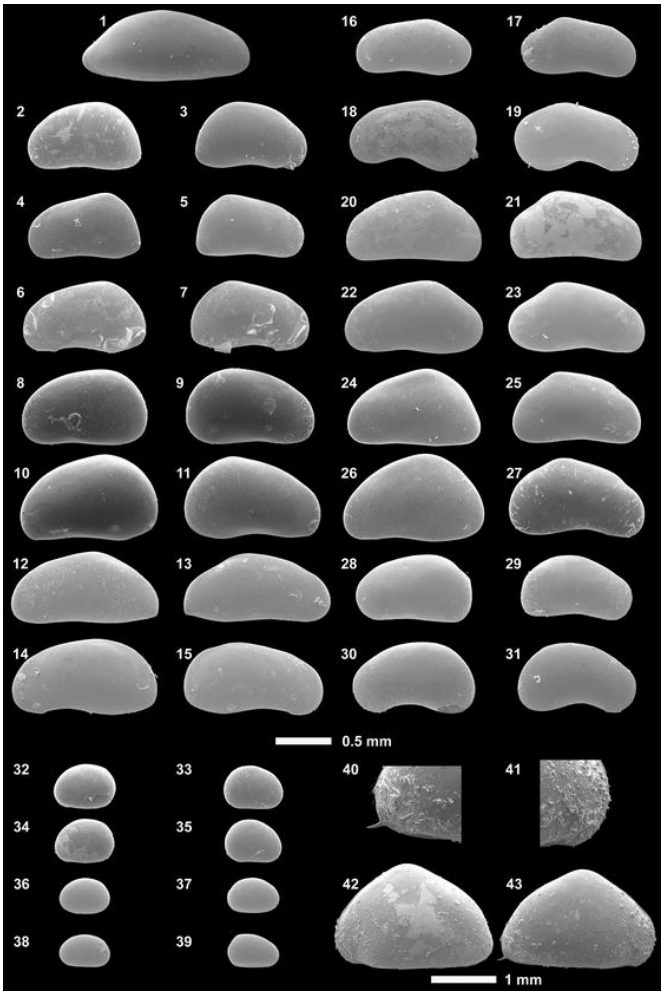

Figure 3-6 SEM images of Yakutian ostracod valves (LV - left valve, RV - right valve). *Dolerocypris fasciata*: (1) female RV; *Candona candida*: (2) female LV, (3) female RV; *C. muelleri-jakutica*: (4) female LV, (5) female RV, (6) male LV, (7) male RV; *C. weltneri*: (8) female LV, (9) female RV, (10) male LV, (11) male RV; *Fabaeformiscandona acuminata*: (12) female LV, (13) female RV, (14) male LV, (15) male RV; *F. fabaeformis*: (16) female LV, (17) female RV, (18) male LV, (19) male RV; *F. hyalina*: (20) female LV, (21) female RV, (22) male LV, (23) male RV; *F. inaequivalvis*: (24) female LV, (25) female RV, (26) male LV, (27) male RV; *F. rawsoni*: (28) female LV, (29) female RV, (30) male LV, (31) male RV; *Physocypria kraepelini*: (32) female LV, (33) female RV, (34) male LV, (35) male RV; *Cyclocypris ovum*: (36) female LV, (37) female RV, (38) male LV, (39) male RV; *Cypris pubera*: (40) postero-ventral RV margin, (41) antero-ventral RV margin, (42) female LV, (43) female RV. Note varying scales: 0.5 mm scale for number 1-41 and 1 mm scale for number 42-43

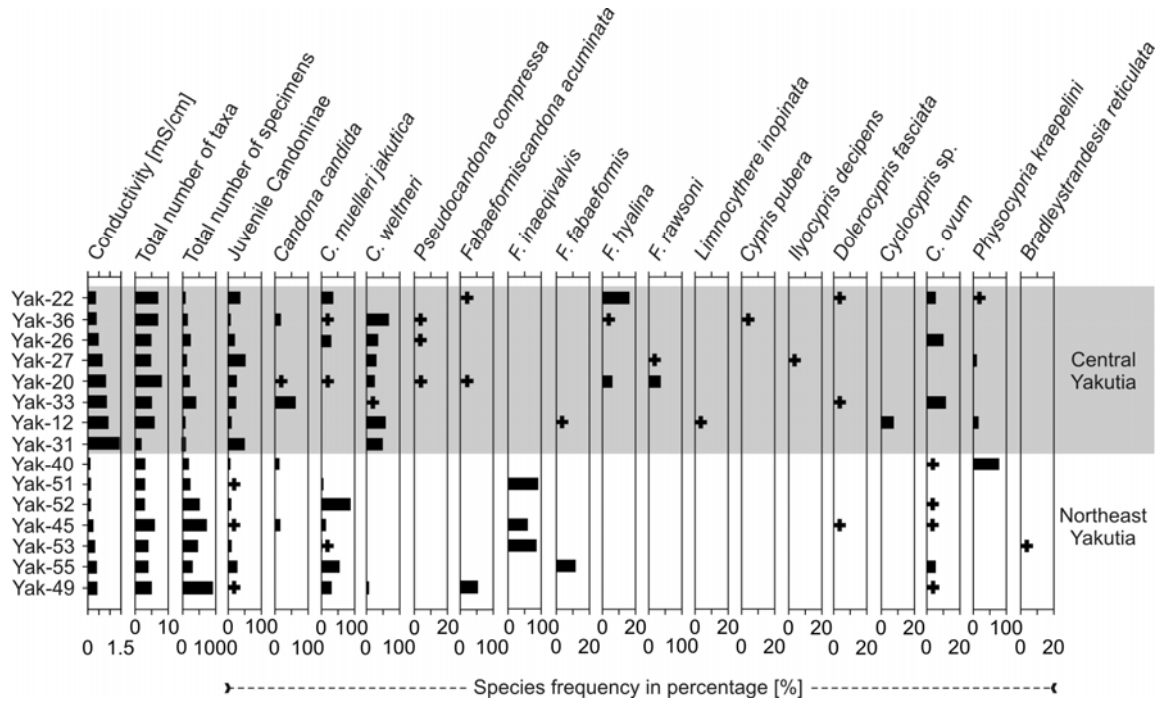

Figure 3-7 Ostracod taxa and specimens (in absolute numbers) as well as species frequency (in percentage) in waters of Northeast and Central Yakutia (highlighted in grey). Frequencies of single species <5% are marked by a cross. Note varying scales. The data are arranged by increasing electrical conductivities for each region

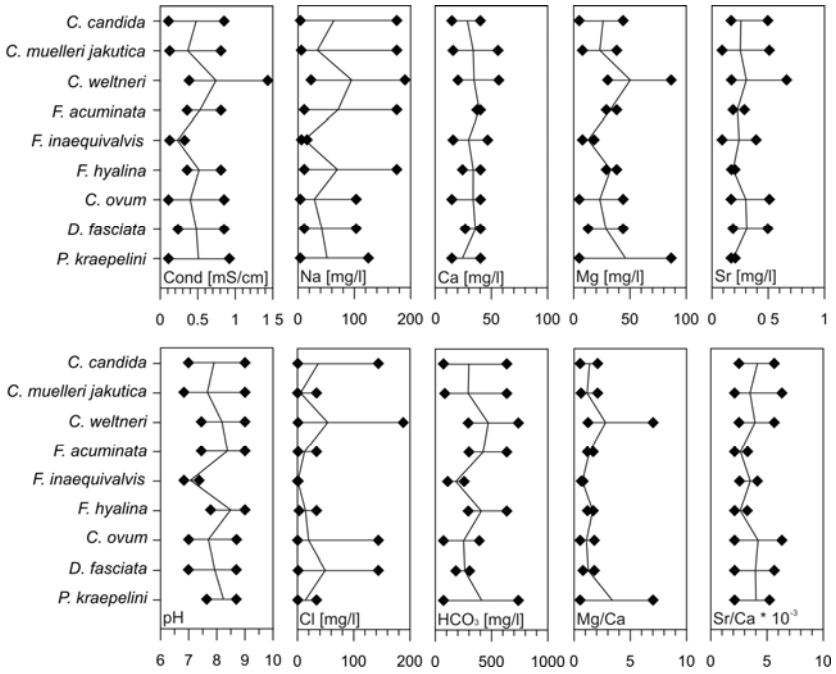

Figure 3-8 Ranges of environmental parameters of ostracod habitats for most current taxa found in the studied lakes. Horizontal lines connect the minimum and the maximum, and the vertical line connects the mean values. Species include *Candona candida* (n = 5), *C. muelleri jakutica* (n = 10), *C. weltneri* (n = 8), *Fabaeformiscandona acuminata* (n = 3), *F. hyalina* (n = 3), *F. inaequivalvis* (n = 3), *Cyclocypris ovum* (n = 8), *Dolerocypris fasciata* (n = 3), and *Physocypria kraepelini* (n = 4). Note varying scales

In Figure 3-8 the ecological ranges of the species that occur in three or more lakes are shown according to environmental parameters measured at the sampling time and site. The broadest ranges in most of the presented parameters were found for the species *C. candida* (at 5 sites) and *C. weltneri* (at 8 sites), which are common in our collection. *F. inaequivalvis* (at 3 sites) was found exclusively in NE Yakutia, within relatively small ranges in most of the measured environmental parameters; its rarity underscores the differentiation in the environmental setting (e.g. pH, ionic content) between study regions.

3.5.3 Stable isotopes in host waters and ostracod calcite

Analyses of the stable isotope content were performed on valves of the most common species and their host waters (Appendix III-5). The $\delta^{18}O$ values vary between about −18.5 and −10‰ in lake water where either *C. candida* or *C. muelleri jakutica* were abundant; the $\delta^{18}O$ values of the valves of both species taken together ranges from −16 to −9‰ (Figure 3-9a).

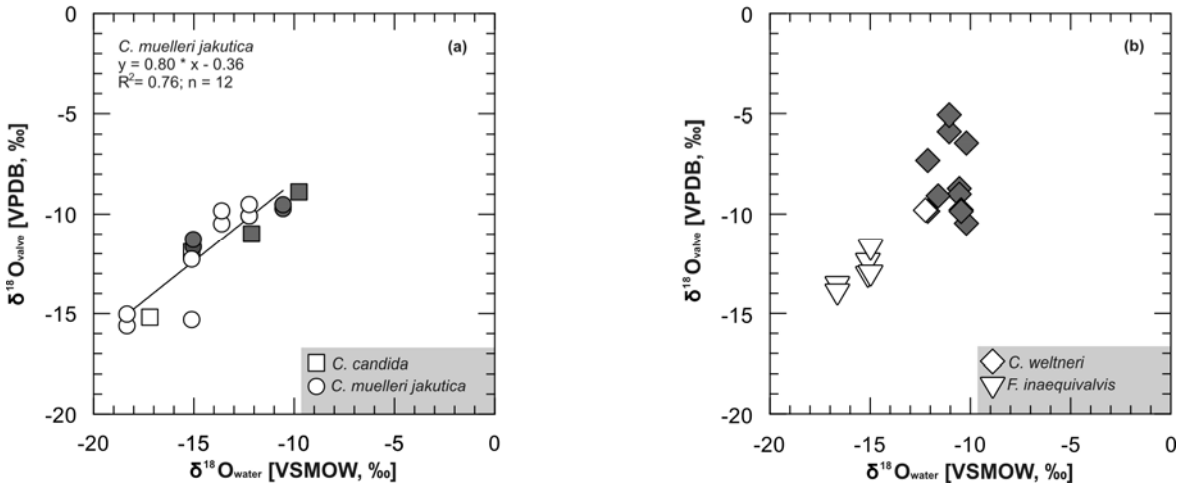

Figure 3-9 Stable oxygen isotopes in host waters and ostracod calcite of: (a) *C. candida* (squares) and *C. muelleri jakutica* (circles); (b) *F. inaequivalvis* (triangles) and *C. weltneri* (diamonds). Data from Central Yakutia are shown by grey symbols and those from NE Yakutia by white symbols

A positive correlation between the $\delta^{18}O$ of six lakes and of *C. muelleri jakutica* valves was found ($R^2 = 0.76$, n = 12; Figure 3-9a). The species *F. inaequivalvis* (typical for NE Yakutia) shows small variations in valve $\delta^{18}O$ from −14 to −12‰, corresponding to host waters from −17 to −15‰ (Figure 3-9b). Whereas the $\delta^{18}O$ values range from about −12 to −10‰ in host waters where *C. weltneri* (typical for Central Yakutia) occurs, the $\delta^{18}O$ range in valves of this species was about 6‰, from −11 to −5‰ (Figure 3-9b).

The relationship between the $\delta^{13}C$ in host waters and in ostracod valves is illustrated in Figure 3-10. The overall variation in water $\delta^{13}C$ amounts to more than 9‰, ranging between about −7 and +2‰ (Figure 3-10). The $\delta^{13}C$ in valves of *C. muelleri jakutica* co-

varies with values between about −6 and 0‰ (R^2 = 0.82, n = 12; Figure 3-10a). The variation of $\delta^{13}C$ in valves of *C. candida* and *F. inaequivalvis* are within the same range, whereas *C. weltneri* values are widely scattered between about −8 and +5‰ (Figure 3-10a, b). Nevertheless, the *C. weltneri* data also seem to show the same trend; higher $\delta^{13}C$ values in ostracod calcite correspond to higher $\delta^{13}C$ values in host waters.

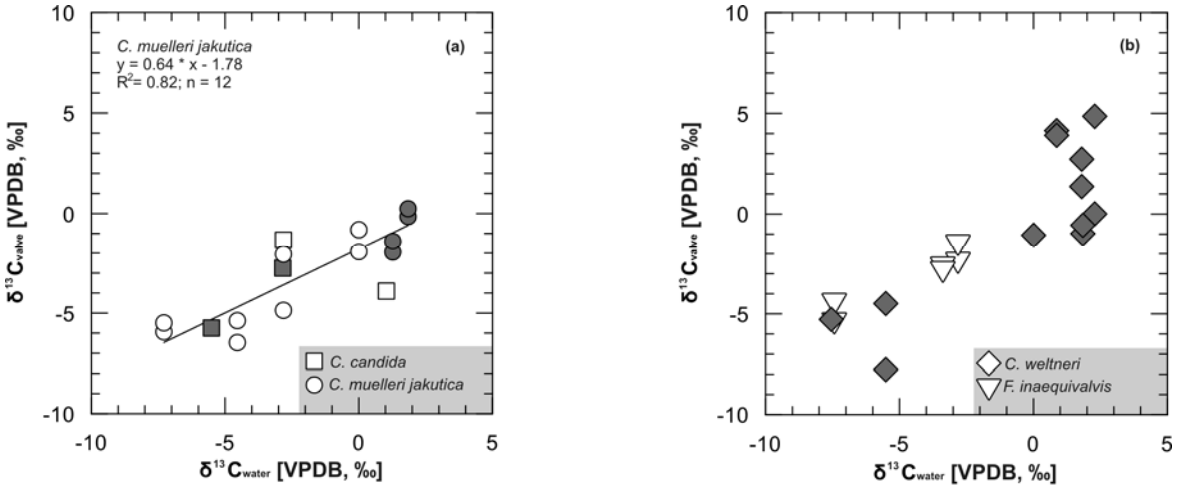

Figure 3-10 Stable carbon isotopes in host waters and ostracod calcite of (a) *C. candida* (squares) and *C. muelleri jakutica* (circles), and (b) *F. inaequivalvis* (triangles) and *C. weltneri* (diamonds). Data from Central Yakutia are shown by grey symbols and those from NE Yakutia by white symbols

3.5.4 Element ratios in host waters and ostracod calcite

The element ratios in host waters and in the ostracod calcite of several species are listed in Appendix III-5. The Sr/Ca of host waters in both study regions ranges from about 2 to 6.5 ($\times 10^{-3}$), corresponding to Sr/Ca ratios in calcite of *C. muelleri jakutica*, which varies from about 0.7 to 1.8 ($\times 10^{-3}$) (R^2 = 0.92, n = 12; Figure 3-11a). The Sr/Ca of the other studied species *F. inaequivalvis* and *C. weltneri* are within the range mentioned above, whereas Sr/Ca ratios in *C. candida* reach about 2.3 ($\times 10^{-3}$) (Figure 3-11a, b). The Sr/Ca ratios in seven lakes and in *C. weltneri* valves is correlated (R^2 = 0.74, n = 12; Figure 3-11b). A positive correlation between the Sr/Ca in host waters and ostracod calcite is obvious for all species.

The Mg/Ca of host waters show a wide range between about 0.4 and 7 (Figure 3-12a, b). The species *C. candida*, *F. inaequivalvis* and *C. muelleri jakutica* are found in waters with low Mg/Ca ratios of about 2 or less. Only *C. weltneri* inhabits waters with Mg/Ca of about 5 to 7 (Figure 3-12b). For this species, we found a correlation of Mg/Ca in water to Mg/Ca in ostracod calcite (R^2 = 0.66, n = 12; Figure 3-12b).

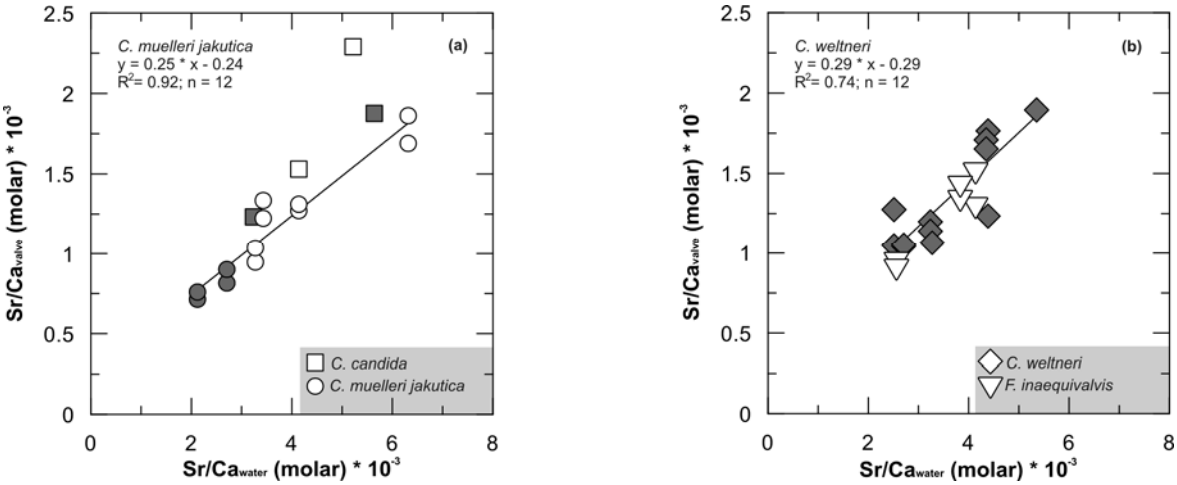

Figure 3-11 Molar strontium/calcium (Sr/Ca) ratios in host waters and ostracod calcite of (a) *C. candida* (squares) and *C. muelleri jakutica* (circles), and (b) *F. inaequivalvis* (triangles) and *C. weltneri* (diamonds). Data from Central Yakutia are shown by grey symbols and those from NE Yakutia by white symbols

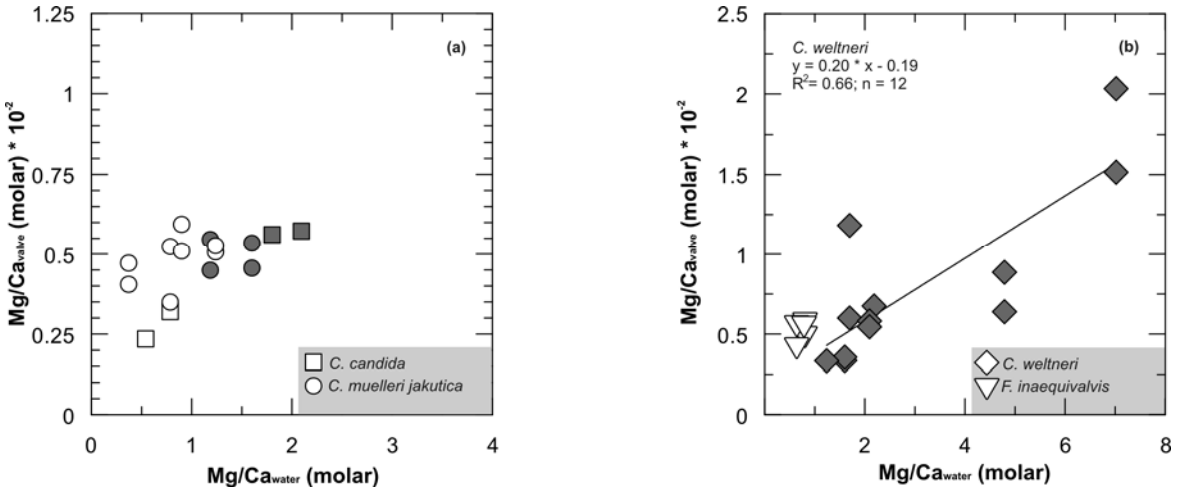

Figure 3-12 Molar magnesium/calcium (Mg/Ca) ratios in host waters and ostracod calcite of (a) *C. candida* (squares) and *C. muelleri jakutica* (circles), and (b) *F. inaequivalvis* (triangles) and *C. weltneri* (diamonds). Data from Central Yakutia are shown by grey symbols and those from NE Yakutia by white symbols. Note varying scales in Figure 3-12a and b

3.6 Discussion

3.6.1 Physico-chemical characteristics of the lakes and ponds

In comparison to NE Yakutian lakes the studied Central Yakutian lakes are characterised by higher pH (slightly alkaline to alkaline), higher electrical conductivity (up to 5.71 mS/cm) and an ionic composition dominated by Mg or Na + K and HCO_3, not by Ca and HCO_3 as in NE Yakutian waters (Figure 3-3). Central Yakutian limnological features reported by Kumke et al. (2007) include alkaline conditions with mean pH 8.5 and mean electrical conductivities of 0.5 mS/cm with maxima of up to 3.6 mS/cm in Yakutsk environments. From these data, it is obvious that physico-chemical characteristics of

Central Yakutian lakes are strongly influenced by the climatic setting (i.e. high continentality) resulting in strong evaporation and a negative moisture balance. Therefore, decreasing water levels in lakes are common and, as a consequence, the enrichment of soluble salts at different stages of lake development (e.g. Pestryakova et al. 2007). Limnological records from North Yakutia report neutral pH values and generally low EC of maximum 0.25 mS/cm in lakes and ponds in the headwaters region and in the delta of the Lena River (Duff et al. 1999; Wetterich et al. 2008a). The NE Yakutian data show higher ionic contents than in the North, with EC up to 0.93 mS/cm; Central Yakutian data show EC up to 5.71 mS/cm, reflecting increasing continentality from the North to the South.

Seasonal changes in water properties are obvious in the record of evaporation-relevant parameters (temperature, EC and lake level fluctuations) from data of an Alas lake in Central Yakutia at the Neleger site (Figure 2). Increasing EC and decreasing water level point to a major influence of evaporation during the summer. In addition, the ongoing thawing of deeper ground layers with higher ionic contents below and around the lake during the summer (Lopez et al. 2007) likely explains the increase in EC from 0.4 to 0.5 mS/cm in the second half of September. Although monitoring data over several years is lacking, it is assumable that the lake level will rise again and the EC will decline again during the next spring due to winter precipitation and snow melt.

The influence of evaporation on lake waters is reflected in stable oxygen–hydrogen isotope compositions which show distinct local evaporation effects on lake waters, evidenced by the Local Evaporation Lines (LELs) with low slopes of 4.99 (R^2 = 0.95, n = 39) for Central Yakutian lakes and 4.09 (R^2 = 0.98, n = 17) for NE Yakutian lakes (Figure 3-4). The initial precipitation source for both regions show a similar isotope signature as indicated by similar slopes and very narrow points of intersection with the GMWL (Figure 3-4). The small differences in LELs can be explained by varying local conditions such as low recharge rates, repeating precipitation–evaporation cycles and generally shallower water bodies in the mountainous region of NE Yakutia. The lower summer mean temperature in NE Yakutia is reflected by generally lower $\delta^{18}O$ values in lake water between about −21.3 to −12.2‰ as compared Central Yakutian lake water data which are higher than −15‰ (Figure 3-4).

3.6.2 Ostracod taxonomy, biogeography, and environmental ranges

Ostracod species compositions differ between the two study regions, most likely because of differences in the environmental parameters that affect ostracod habitats (Figure 3-7). Higher diversity in environmental conditions, and accordingly in species, was recorded in Central Yakutian waters where, in total, 15 species were found. The dominating species *Candona weltneri* has only been recorded once in a NE Yakutian lake. Other common

Central Yakutian species are *Cyclocypris ovum*, *Candona candida* and *C. muelleri jakutica*. The later seems to be widely distributed and was already recorded from several modern environments of North Yakutia, in the Lena River Delta (Wetterich et al. 2008a) and in Central Yakutia (Pietrzeniuk 1977). Fossil records of *C. muelleri jakutica* are known from Central Yakutia (Wetterich et al. 2008d) and also from North Yakutia, Lena River Delta (Wetterich et al. 2008c) and Bykovsky Peninsula (Wetterich et al. 2005).

Most species such as *C. compressa*, *Fabaeformiscandona acuminata*, *F. fabaeformis*, *F. rawsoni*, *Limnocythere inopinata*, *Cypris pubera*, *Ilyocypris decipens* and *Dolerocypris fasciata* are very rare, with one or two records and low frequencies in the studied waters (Figure 7). Except for *F. acuminata* all species are already described for the region by Pietrzeniuk (1977), who counted 24 species in Central Yakutia. The higher number of Central Yakutian species recorded by Pietrzeniuk (1977) is most likely caused by additional sampling of sediments in order to expand the live-caught collection. Most species which have not been found in 2005 are represented in the dataset of Pietrzeniuk (1977) by valves (*Pseudocandona sucki*, *P. hartwigi*, *Cyprois marginata*, *Plesiocypridopsis newtoni* and *Paralimnocythere cf. diebeli*) or by rare, sometimes juvenile, individuals (*Cypria exsculpta*, *Cypridopsis vidua* and *Notodromas monarcha*). Generally, we believe that every careful ostracod sampling in the low studied waters of Yakutia would expand the total species number.

Nine species were found in NE Yakutia; *C. muelleri jakutica* and *F. inaequivalvis* occur at the highest frequencies. The latter species, previously known as *Candona inaequivalvis* SARS 1898, should be re-described as belonging to the genus *Fabaeformiscandona*. This genus, defined by Krstić (1972), did not originally include *F. inaequivalvis*, but the structure of the externo-distal seta (γ-seta) of the penultimate segment of the mandibular palp (which is smooth, not pulmose), and a carapace longer than 0.6 mm with the carapace width/length ratio (W/L) less than 0.4 confirm this attribution. This determination should be confirmed by further detailed taxonomical studies.

An ostracod community studied in lakes and ponds in North Yakutia (Lena River Delta, Laptev Sea) was clearly dominated by the typical Arctic species *F. harmsworthi* and *F. pedata* (Wetterich et al. 2008a). In addition, *C. candida* and *C. muelleri jakutica*, known from more southern regions of Yakutia (Pietrzeniuk 1977), occurred there. Obviously, both species are adapted to the harsh conditions of the Siberian Arctic.

The observed modern ostracod assemblages are dominated by species preferring, in general, lower water temperatures and low ionic content (e.g. *C. candida*, *C. muelleri jakutica* and *C. welterni*). *C. weltneri*, the most common species in Central Yakutia, is described as cold stenothermal to oligothermophilic and oligohalophilic (Meisch 2000). However, a broad spectrum of species was observed with different adaptations to

temperature and salinity, ranging from cold stenothermal (e.g. *F. hyalina*) to mesothermophilic (e.g. *P. compressa* and *D. fasciata*), and from oligohalophilic (e.g. *F. acuminata*) to mesohalophilic (e.g. *C. ovum*). Therefore, care should be taken when interpreting the temperature and salinity environments of fossil ostracod assemblages.

The observed environmental gradients (Figure 3-8) do not determine the overall distribution of the ostracods species since species distribution surely depends on more environmental parameters than observed in course of the study presented here. Especially, detailed sampling of ostracods in different water depths, lake zones and types as well as estimations of parameters such as the presence and type of the aquatic vegetation, the substrate type, the turbidity of the water and the duration of the ice-free period in relation to the length of the life cycle are required to be studied in detail at monitoring sites for better understanding of the complex environmental dependencies of species distribution. In this context, our record is more focussed on stable isotope and hydrochemical properties of the sampled lakes in comparison to the geochemical properties in ostracod calcite. Actually, detailed discussion on modern ostracod species distribution and their environmental habitat parameters in Yakutia is impossible since data sets needed for these purposes are lacking except of the already mentioned publications of Pietrzeniuk (1977) and Wetterich et al. (2008a). However, within the Yakutian data set, *C. candida*, *C. muelleri jakutica*, *C. weltneri* and *C. ovum* are the most common species, probably suggesting higher tolerance to solute composition in lakes within the observed ranges (Figure 3-8). In contrast, *F. inaequivalvis* was only found in very narrow ranges of pH and electrical conductivity in NE Yakutian waters.

3.6.3 Stable isotopes in ostracod calcite

The relationship between the isotopic composition of ostracod calcite ($\delta^{18}O$, $\delta^{13}C$) and of host waters has already been examined in numerous laboratory and field studies (e.g. Xia et al. 1997b; Keatings et al. 2002, 2006a, b). The $\delta^{18}O$ of lake water is affected by environmental factors, such as the isotope composition of the input water (precipitation and groundwater), the climate-driven precipitation to evaporation (P/E) ratio, and the hydrochemical properties and temperature of the lake water (e.g. Leng and Marshall 2004). Commonly, $\delta^{18}O$ and $\delta^{13}C$ records of ostracod calcite are thought to provide a restricted reflection of the isotopic composition of water and TDIC at the time of shell secretion, making them helpful proxies in palaeolimnology (Griffiths and Holmes 2000). However, the $\delta^{18}O$ and $\delta^{13}C$ composition of ostracod calcite is influenced by interspecific and intraspecific variations, caused by species-dependent metabolic effects on isotope fractionation (vital effects) and preferences for different microhabitats, as well as by the timing of shell calcification in different seasons and at different temperatures (e.g. Heaton

et al. 1995; von Grafenstein et al. 1999). Temperature-independent vital effects (in comparison to anorganic calcite precipitated in equilibrium to the isotopic composition of the water) for species of Candoninae from different field and laboratory collections were estimated to be +2.2‰ (von Grafenstein et al. 1999) and +2.5 to +3‰ for *C. candida* (Keatings et al. 2002), 1.5 to 2‰ for *C. subtriangulata* (Dettman et al. 1995), about +2‰ for *F. rawsoni* (Xia et al. 1997b), and 1.4‰ for *F. pedata* (Wetterich et al. 2008a).

In our study, the species *C. muelleri jakutica* was observed at six localities in numbers sufficient for stable isotope analyses, and over great ranges of about 8‰ for water $\delta^{18}O$. The corresponding stable isotope values of this species' ostracod calcite show good correlations (Figure 9). Similar results were obtained from the species *F. pedata* common in lakes and ponds in the North Yakutian Lena Delta (Wetterich et al. 2008a), where the stable oxygen isotopes in host waters and ostracod calcite were also well correlated. The lack of such correlation in other species (*C. candida*, *C. weltneri* and *F. inaequivalvis*) is likely because they are less frequent and they occurred in more restricted stable isotope ranges during our fieldwork. The vertical stack of $\delta^{18}O$ values in calcite of *C. weltneri* probably reflects different isotope compositions in host waters at the time of calcification and at the sampling time. Monitoring of ostracod development and seasonal changes in water properties at selected sites is needed for detection of such relationships.

Compared to Arctic Siberian ostracod $\delta^{18}O$ records ranging from −18 to −11‰ (Wetterich et al. 2008a), the data presented here show more evaporation influence by more positive (heavier) values ranging from about −15 to −9‰ (Figure 3-9). This general tendency in the $\delta^{18}O$ records of ostracod calcite reflects cooler conditions and lower evaporation (higher P/E ratios) in the North as compared to the South, and is consistent with southwards-decreasing continentality as estimated by the stable isotope record of the host waters. Furthermore, the influence of evaporation is obvious when comparing $\delta^{18}O$ of waters or ostracod calcite and electrical conductivity as an expression of ionic concentration (salinity).

Even though Central Yakutia and NE Yakutia are geographically and hydrologically different regions, they may be used to illustrate the Rayleigh distillation process during evaporation of lakes. We found a logarithmic correlation ($R^2 = 0.69$, n = 55; Figure 3-13a) between $\delta^{18}O$ of lake water and EC when both regions are plotted in one diagram. The observed relationship is controlled by Rayleigh distillation processes, wherein light isotopes evaporate faster than heavy ones leading to nonequilibrium enrichment of the residual water (Clark and Fritz 1997). Depending upon relative humidity this relation leads to an asymptotic increase in $\delta^{18}O$ values under high evaporation conditions to a steady-state value which is strongly influenced by the salinity of the residual water (e.g. Gat 1979, 1981). As shown in Figure 3-13a a steady-state value of about −6‰ is reached in

evaporated residual waters at conductivities of about 4 mS/cm and more. However, this interpretation is likely based only on few data, but may be a reliable explanation of the scatter observed. The correlation between $\delta^{18}O$ of ostracod calcite and conductivity is weak (R^2 = 0.39, n = 34; Figure 3-13b) and more data and sampling of time-series during the ice-free season are required to assess this relationship. Nevertheless, it seems that these first results should be taken into account for interpreting stable isotope data from fossil ostracods of East Siberia, where lakes occurred during the Quaternary past under high continental conditions and climate-driven lake level changes up to desiccation took place (Bosikov 2005).

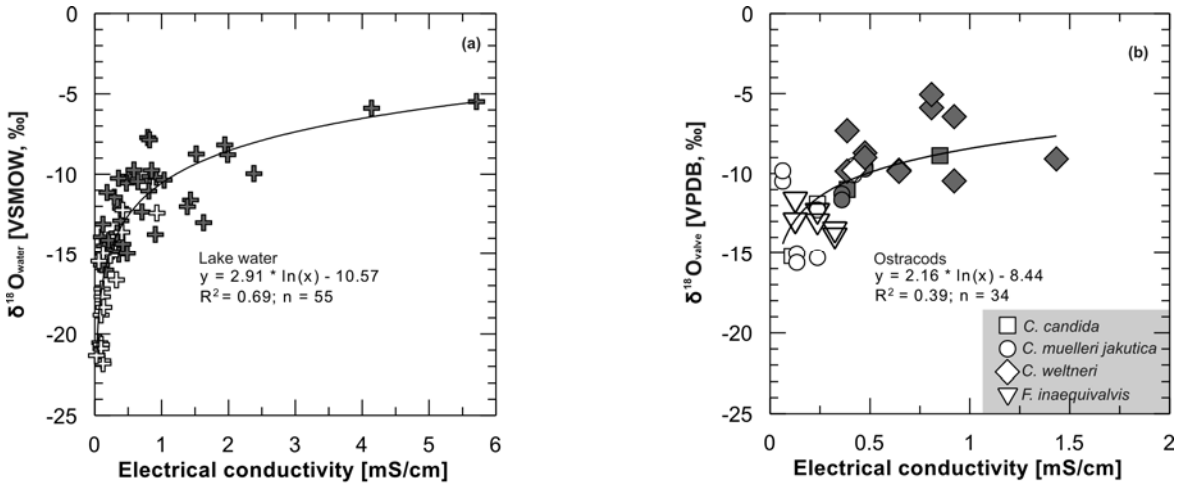

Figure 3-13 Plot of electrical conductivity and oxygen stable isotopes in (a) host waters and (b) ostracod calcite. Data from Central Yakutia are shown by grey symbols and those from NE Yakutia by white symbols

The $\delta^{13}C$ composition of TDIC in waters is controlled by fractionation during several carbon cycles; the most important influences are the isotopic composition of inflows, CO_2 exchange between air and lake water, and photosynthesis/respiration of aquatic plants (Leng and Marshall 2004). The last two controls are characterised by high seasonal and even daily variability; thus it is more difficult to interpret these data since periodic sampling during the open-water season is required to register carbon cycle dynamics. The $\delta^{13}C$ records from both host waters and ostracod calcite reflect a positive trend over great ranges of about 9‰ for $\delta^{13}C$ in waters and about 14‰ for $\delta^{13}C$ in ostracod calcite (Figure 3-10). For *C. muelleri jakutica* from six lakes we found a correlation between $\delta^{13}C$ in host waters and valves (R^2 = 0.82, n = 12; Figure 3-10a). However, as explained above any interpretation of this relationship is complicated.

3.6.4 Element ratios in ostracod calcite

The relationship between element ratios (Sr/Ca, Mg/Ca) in host waters and in ostracod calcite has been investigated in (palaeo-) limnological studies (e.g. Palacios-Fest and Dettman 2001; Palacios-Fest et al. 2002; Xia et al., 1997c). The partitioning is usually expressed as the species-dependent coefficient *D*(M):

$$D(M) = (M/Ca)_{valve} / (M/Ca)_{water} \quad (1)$$

where M can either be Mg or Sr, and M/Ca ratios are molar ratios (e.g. Chivas et al. 1986). The strong dependency on temperature of Mg uptake into the valves at the time of valve secretion must also be taken into account (Engstrom and Nelson 1991; De Deckker et al. 1999). Furthermore, Xia et al. (1997c) showed in field experiments that the uptake of both Sr and Mg is influenced by Mg/Ca ratios of the host water whereas physiological costs of calcification becomes substantial at high Mg/Ca waters.

Both proxies have been used to indicate changes in salinity due to evaporation leading to increasing Sr/Ca and/or Mg/Ca ratios in both host water and ostracod calcite (e.g. Chivas et al. 1993; Xia et al. 1997a; Ingram et al. 1998). However, the correlation between M/Ca of host water and measured EC as an expression of ionic concentration (salinity) is not clear, as has been shown by several authors in studies of modern environments. Engstrom and Nelson (1991) explained the weakness of the correlation between salinity and the Sr/Ca ratio of Devils Lake, North Dakota, USA by postulating continuous Sr removal via mineral precipitation of both calcite and inorganic aragonite. Keatings et al. (2006a) suggested that the lacking of correlation between water salinity and M/Ca ratios in the arid Faiyum Depression, Egypt was caused by regional characteristics of groundwater input and precipitation/dissolution of evaporative minerals.

In the Yakutian dataset, correlations between Sr/Ca ratios in waters and valves are obvious for the most common species *C. muelleri jakutica* (R^2 = 0.92, n = 12; Figure 3-11a) and *C. weltneri* (R^2 = 0.74, n = 12; Figure 3-11b) over a Sr/Ca range from about 2 to 6.5 ($\times 10^{-3}$) in host waters. It has to be mentioned that the database is actually poor since the ostracod calcite analyses for *C. muelleri jakutica* were performed on two single-valve samples per lake and only six lakes were taken into account. For the same approach ostracod calcite of *C. weltneri* from seven lakes was measured. Two single-valve samples could be applied to five lakes and one single-valve samples each to two lakes.

According to Eq. 1, average partition coefficients were calculated for live-caught *C. muelleri jakutica* with *D*(Sr) = 0.32 ± 0.03 (1σ) and *C. weltneri* with *D*(Sr) = 0.38 ± 0.05 (1σ). Similar results from field collections were obtained for *Fabaeformiscandona pedata* from Arctic Siberia (*D*(Sr) = 0.33 ± 0.06 (1σ); Wetterich et al. 2008a) and for *Fabaeformiscandona rawsoni* in laboratory cultures (*D*(Sr) = 0.406; Engstrom and Nelson 1991).

A clear correlation of lake water Sr/Ca ratio to conductivity has not been obtained especially because the Sr/Ca ratios in waters at low conductivities below 0.5 mS/cm are highly variable ranging from about 1.8 to 7.6 ($\times 10^{-3}$) (Figure 3-14a). However, higher conductivities in the waters where ostracods have been caught lead to higher Sr/Ca ratios in ostracod calcite, though the relation between host water and ostracod calcite data (Figure 3-14b) suffers by time lag between sampling and calcification, and a general poor database of mostly two single-valve samples per lake.

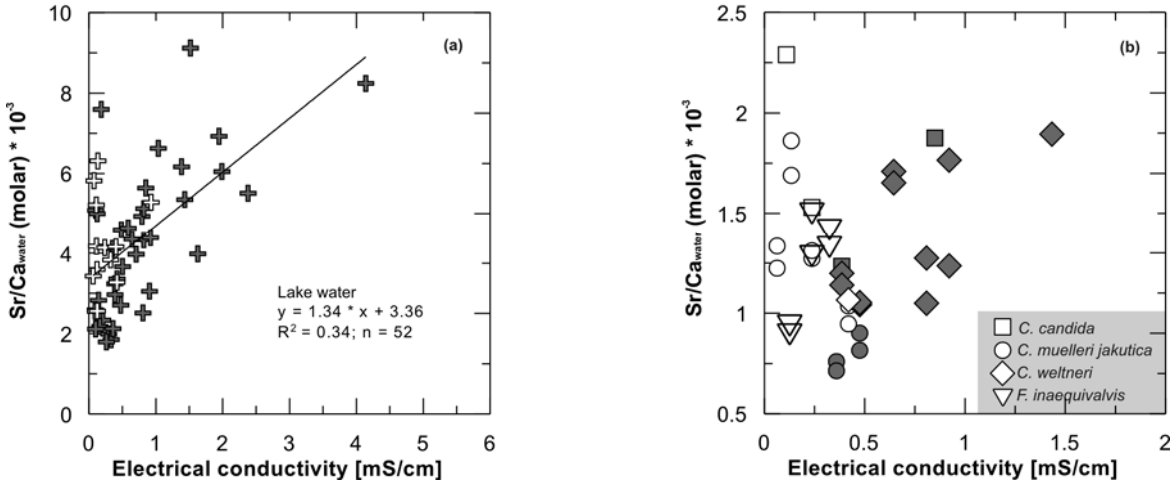

Figure 3-14 Plot of electrical conductivity and molar strontium/calcium (Sr/Ca) ratios in (a) host waters and (b) ostracod calcite. Data from Central Yakutia are shown by grey symbols and those from NE Yakutia by white symbols

The Mg/Ca ratios in the studied Yakutian waters and in ostracod calcite are correlated for *C. weltneri* (R^2 = 0.66, n = 12; Figure 3-12b) over an Mg/Ca range in waters between 0.4 and 7; the other species studied occurred in restricted ranges with low Mg/Ca ratios of about 2 or less. The uptake of Mg by ostracods and the resulting Mg/Ca ratios of ostracod calcite are controlled by temperature (Engstrom and Nelson 1991; De Deckker et al. 1999). However, the temperature effect is small in comparison to the dependence on Mg/Ca of water at higher ranges. For the species *C. candida*, *C. muelleri jakutica* and *F. inaequivalvis* that were found in a narrow (and low) range of Mg/Ca waters, temperature effect became relatively large, and consequently no correlation between Mg/Ca of water and Mg/Ca of ostracod calcite is seen (Figure 3-12a). For *C. weltneri*, the range of Mg/Ca of water was large enough that a positive trend became apparent (Figure 3-12b), but with a large scatter that is caused by different sampling time in relation to the time of calcification which leads in our data based mostly on two single-valve samples per lake to clear shifts in ostracod calcite chemistry from individual lakes. This effect is clearly seen in *C. weltneri* data from lakes Yak-12, Yak-20 and Yak-27 (Appendix III-5) and should be avoided in future studies by applying more measurements on

ostracod calcite per lake in order to improve the database for more robust statistic evidence of the data obtained. However, our results give a first base on geochemical properties of Yakutian ostracods in relation to their host waters.

The partition coefficient *D*(Mg) has not been calculated, since the temperature dependence of Mg uptake cannot be quantified in our dataset based on field collections. Due to generally higher ionic concentrations (i.e. electrical conductivities) as compared to Arctic environments in the Lena Delta (Wetterich et al. 2008a), Mg/Ca records of both waters and ostracod calcite reflect increasing salinity by increasing ratios under low Mg/Ca conditions in the host waters.

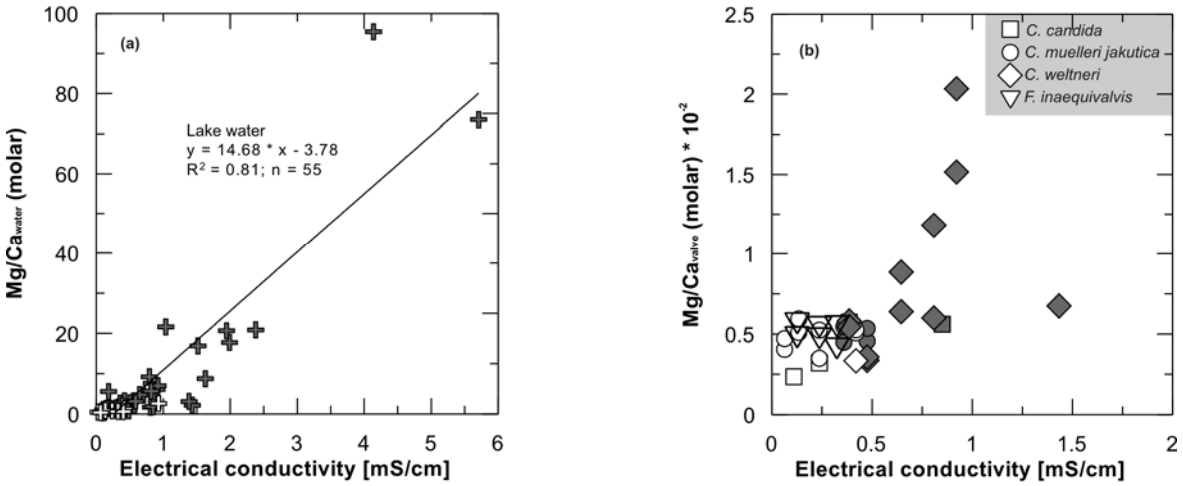

Figure 3-15 Plot of electrical conductivity and molar magnesium/calcium (Mg/Ca) ratios in (a) host waters and (b) ostracod calcite. Data from Central Yakutia are shown by grey symbols and those from NE Yakutia by white symbols

As compared to EC, Mg/Ca ratios in waters show covariance (R^2 = 0.81, n = 55; Figure 3-15a), but the conductivity gradient is mostly covered by values below 2.5 mS/cm. The Mg/Ca ratio in *Candona* species in relation to Mg/Ca ratios in host waters shows a different scatter (Figure 3-15b). The relatively low Mg/Ca values in the Na + K and HCO_3 dominated waters Yak-31 with 1.43 mS/cm and Yak-33 with 0.85 mS/cm are probably caused by different hydrological setting. Both waters are exposed on the floodplain of the Lena River in Central Yakutia and the river water control on the hydrochemical setting might explain the probably different relationship in Mg uptake into ostracod calcite. However, these assumptions are currently based on two single-valve samples from two old branches and surely need additional sampling of such waters.

3.7 Conclusions

Siberian freshwater ostracods and their geochemical properties have so far been poorly studied; this paper presents adequate data for further expansion of the database as

prerequisite for the use of ostracods in palaeoenvironmental reconstruction from East Siberian records. The following conclusions can be drawn from this paper:

(1) The species *C. muelleri jakutica* seems to be common in East Siberia in modern habitats and also in fossil records. Due to its distribution over significant environmental gradients, this species should be subjected to further studies on geochemistry and palaeoenvironments since the species was already recorded in Quaternary lake sediments, and permafrost deposits.

(2) The stable isotope ratios ($\delta^{18}O$, $\delta^{13}C$) and the element ratios (Sr/Ca, Mg/Ca) in ostracod calcite are correlated to the composition of host lake waters, if the studied species were found in higher frequencies and over significant ranges in the respective environmental proxies. Thus, geochemical proxies of ostracod calcite can provide environmental information for further studies of fossil assemblages in East Siberia.

(3) The relation between electrical conductivity as evaporation proxy and geochemical properties of ostracod calcite ($\delta^{18}O$, $\delta^{13}C$, Sr/Ca, Mg/Ca) is not apparent due to the general low database and several controls on the uptake of the respective isotopes and elements into ostracod calcite such as temperature effects and physiological costs which could not been quantified in the presented field study.

(4) Synchronic sampling of waters and ostracods at calcification time in course of monitoring approaches would be desirable for better understanding of complex biomineralisation processes and biogeochemical cycles in lakes.

4 Eemian and Late Glacial/Holocene palaeoenvironmental records from permafrost sequences at the Dimitri Laptev Strait (NE Siberia, Russia)

Sebastian Wetterich[1], Lutz Schirrmeister[1], Andrei A. Andreev[1], Michael Pudenz[2], Birgit Plessen[3], Hanno Meyer[1] and Viktor V. Kunitsky[4]

(1) Alfred Wegener Institute for Polar and Marine Research, Telegrafenberg A43, 14473 Potsdam, Germany; (2) Institute of Geological Sciences, Palaeontology Branch, Free University Berlin, Malteserstrasse 74-100, 12249 Berlin, Germany; (3) Deutsches GeoForschungsZentrum Potsdam, Section 3.3, Telegrafenberg, 14473 Potsdam, Germany; (4) Permafrost Institute, Siberian Branch of the Russian Academy of Sciences, ul. Merzlotnaya, 36, 677010 Yakutsk, Russia

In preparation for Palaeogeography Palaeoclimatology Palaeoecology

4.1 Abstract

Terrestrial permafrost sections from the southern and northern coasts of Dimitri Laptev Strait have preserved records of landscape transition from glacial to interglacial periods. They allow geomorphologic and environmental changes to be traced from pre-Eemian time to the Eemian, and from the Late Glacial to the Holocene. The transition from one period to another induced extensive thawing of permafrost (thermokarst). Evolving thermokarst depressions transformed formerly frozen ground into taberal (unfrozen) deposits with accumulating overlying lacustrine deposits. Lacustrine horizons rich in palaeontological remains retain evidence of changes in environmental conditions. The pollen records reflect changes from grass-sedge dominated vegetation during the Early Eemian to shrub dominated spectra during the Middle Eemian thermal optimum followed by Late Eemian grass-sedge dominated tundra vegetation. Abundant *Larix* pollen have been found in Middle Eemian deposits from the south coast of the Dimitri Laptev Strait (Oyogos Yar), but are absent in similar deposits from the north coast (Bol'shoy Lyakhovsky Island), likely indicating that the northern tree line was located near the Oyogos Yar region during the Eemian thermal optimum. Grass-sedge dominated tundra vegetation occurred during the Late Glacial/Holocene transition which was replaced by shrub tundra during the early Holocene. Rich fossil ostracod records from Eemian and Late Glacial/Holocene lacustrine deposits could be correlated with the Eemian thermal optimum and the Late Glacial Allerød warm period. For both periods, the stable oxygen isotope data from the fossil ostracods indicate an approximate mean summer water temperature range between 10 and 19 °C in the palaeo-lakes.

4.2 Introduction

Climate and subsequent environmental changes occurred in northern Eurasia during the Quaternary. Glacial-interglacial cycles certainly exerted an enormous influence on Eurasian periglacial landscapes and ecosystems. The study of palaeoindicators from interglacial periods that are preserved in different palaeoarchives allow to reconstruct ancient environments; such reconstructions are useful for understanding the controls on, interactions between, and effects of climate change and ecosystem response (e.g. Lozhkin and Anderson 1995; Velichko and Nechaev 2005; Sirocko et al. 2007). However, although Arctic Eurasia is especially sensitive to current and future climate warming (ACIA 2005), interglacial palaeoenvironmental records from this region are less studied than are those from lower latitudes.

Huge areas of the Eurasian landmass are underlain by permafrost. Permafrost occurrence depends on climate (temperature) conditions, and both past and present climate dynamics influence the state, stability, and distribution of permafrost. One of the most common reactions of periglacial landscapes during interglacial warm periods is extensive thawing of ground ice; this permafrost-degrading process is known as thermokarst. Thermokarst progressively leads to the formation of large-scale, often lake-filled depressions (alases) in the landscape surface and also to the formation of ice wedge casts (pseudomorphs) which are small-scale, secondary sediment-filled depressions (French 2007).

Both alases and pseudomorphs can be regarded as interglacial palaeoarchives in Northeast Siberia because they contain well-preserved remains such as plant macrofossils (e.g. Kienast et al. 2008), pollen, rhizopods, and chironomids (e.g. Andreev et al. 2004, 2008; Ilyashuk et al. 2006); these remains are useful for palaeoenvironmental reconstructions. In this context, fossil freshwater ostracods are a newly-introduced palaeoindicator for the permafrost archive (Wetterich et al. 2005); their taxonomical-ecological relationships and their geochemistry (stable isotopes) are the primary useful measurements.

The study presented here deals with cryolithological as well as palaeoecological pollen and ostracod records from two Eemian and two Late Glacial/Holocene permafrost sequences exposed on the coasts of the Dimitri Laptev Strait. These records were obtained during the summer 2007 by a joint Russian-German Lena-New Siberian Islands expedition.

4.3 Regional setting

The Dimitri Laptev Strait connects the Laptev and East Siberian Seas (Figure 4-1); its coasts have long been of geographical and geological interest. The coastal outcrops

along the Dimitri Laptev Strait are characterised by frozen Quaternary sediments of different ages and accumulation types which are exposed on steep bluffs of thermokarst depressions, thermo-erosional valleys and Yedoma hills which are remnants of late Pleistocene accumulation plains in Northeast Siberian lowlands (Figure 4-2).

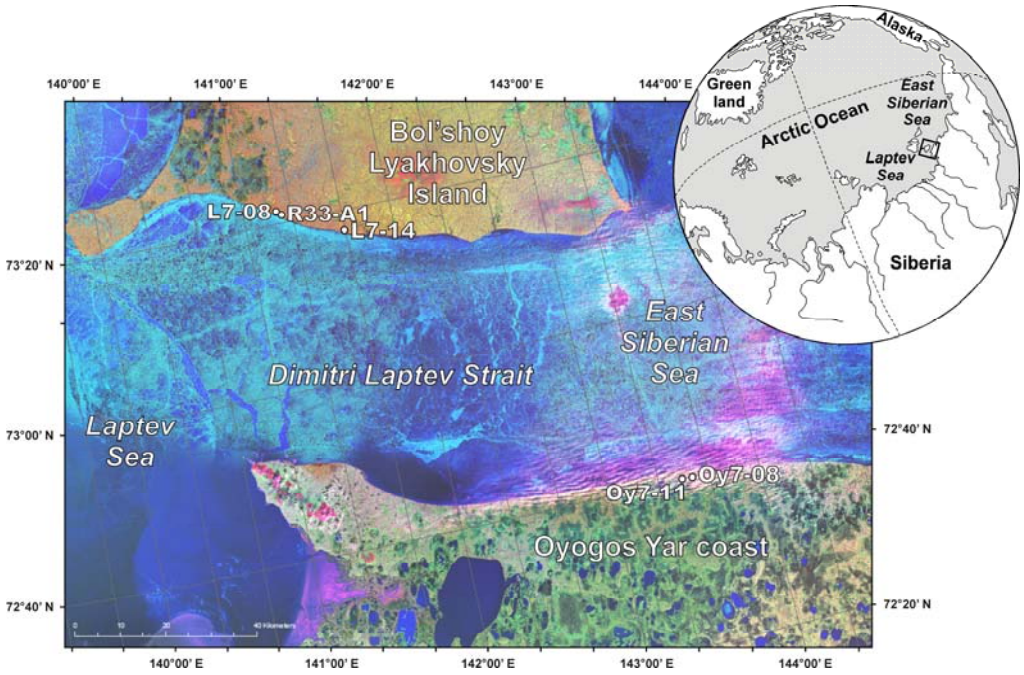

Figure 4-1 The coasts of the Dimitri Laptev Strait with exposure positions. Map compiled by H. Lantuit (AWI Potsdam) using a satellite image (LANDSAT 7 ETM+ 29.06.2001)

Figure 4-2 South coast of the Bol'shoy Lyakhovsky Island west of the Zimov'e River mouth at the Dimitri Laptev Strait

Since its discovery in the 18th century, Bol'shoy Lyakhovsky Island, north of the Dimitri Laptev Strait, has been well-known for the presence of fossil mammal bones; it has become one of the most important Pleistocene mammal sites in Siberia (Chersky 1891). Permafrost sequences exposed on the south coast of Bol'shoy Lyakhovsky Island were

first studied in the 19th century (Bunge 1887; von Toll 1897). However, detailed geocryological and palaeoenvironmental studies began much later on both Bol'shoy Lyakhovsky Island (Romanovskii 1958a-c; Pirumova 1968; Igarashi et al. 1995; Nagaoka et al. 1995; Arkhangelov et al. 1996; Kunitsky 1996, 1998; Kunitsky and Grigoriev 2000) and on the coast of Oyogos Yar, south of Dimitri Laptev Strait (Kayalaynen and Kulakov 1966; Ivanov 1972; Gravis 1978; Konishchev and Kolesnikov 1981; Vereshchagin 1982). The general stratigraphic situation of Quaternary sediments exposed on both coasts of the Dimitri Laptev Strait is similar (Table 4-1), but the stratigraphy is complicated because absolute age determinations are rare and single stratigraphic units possess different local definitions.

Table 4-1 Synopsis of the stratigraphic units exposed on the Dimitri Laptev Strait. The stratigraphical position of the Bychchagy Suite (grey highlighted) is still unclear

№	Period*	Characteristics	Name	Selected references
8	Holocene	Lacustrine and boggy deposits	Alas Sequence	Andreev et al. (2008)
7	Late (Sartan*), middle (Kargin), and early (Zyryan) Weichselian	Ice Complex deposits	Yedoma Suite	Nagaoka et al.(1995), Andreev et al. (2004, 2008), Nikolsky and Basilyan (2004)
6	Eemian (Kazantsevo)	Lacustrine and boggy deposits	Krest Yuryakh Suite	Andreev et al. (2004), Nikolsky and Basilyan (2004), Ilyashuk et al. (2006), Kienast et al. (2008)
5	Pre- or post-Eemian	Ice-rich deposits of controversial stratigraphic position	Bychchagy Suite	Tumskoy and Basilyan (2006)
4	Late Saalian (Taz)	Well-sorted flood plain deposits	Kuchchugui Suite	Andreev et al. (2004)
3	Middle Saalian (Shirta)	Palaeo active layer	Zimov'e Strata	Tumskoy and Basilyan (2006)
2	Middle Saalian (Shirta)	Ice Complex deposits	Yukagirsky Suite	Arkhangelov et al. (1996), Schirrmeister et al. (2002c), Andreev et al. (2004), Tumskoy and Basilyan (2006)
1	(?)	Late Cretaceous to Palaeocene periglacial reworked weathering crust	Cryogenic eluvium	Romanovskii and Hubberten (2001), Andreev et al. (2004)

* Local stratigraphic terms are given in parentheses according to Velichko et al. (2005)

However, such archives including Eemian deposits are generally low studied in the Siberian Arctic (e.g. Allaikha River, Indigirka River lowland, Kaplina et al. 1980; Duvanny Yar, Kolyma River lowland, Kaplina et al. 1978; El'gygytgyn Lake, Chukotka, Lozhkin et al.

2007) and the coastal exposures of the Dimitri Laptev Strait are regarded as the longest and most comprehensive Arctic permafrost archive; it contains records of two to three glacial-interglacial cycles from the middle Pleistocene to the Holocene. Past studies by Russian scientists (e.g. Romanovskii 1958a-c; Arkhangelov et al. 1996; Kunitsky 1998; Romanovskii et al. 2000) and joint Russian-German projects (Meyer et al. 2002b; Schirrmeister et al. 2002c; Andreev et al. 2004, 2008) have described and partly dated different stratigraphic units of middle and late Quaternary age. Tertiary deposits and weathering crusts, middle Pleistocene ice-rich deposits, and well-sorted loess-like sequences have been found. The permafrost coast along both sides of the Dimitri Laptev Strait is composed of Eemian horizons of lacustrine deposits containing ice wedge casts and late Pleistocene ice-rich deposits of the Yedoma Suite as well as Holocene thermokarst sequences (Table 4-1).

4.4 Material and methods

4.4.1 Field methods and cryolithology

After conducting a survey along the sea coasts, permafrost exposures in coastal bluffs were selected for detailed studies. In general, field studies were difficult due to limited accessibility of the steep permafrost outcrops and extensive mudflows on the slopes. Therefore, composite profiles were obtained which consist of several sub-profiles. Such subprofiles were dug by spades and cleaned with hatchets. The exposed sequences were surveyed, described, photographed, and sketched according to sediment colour, composition, and structures as well as ice structures (cryostructures). Distances, altitudes above sea level (a.s.l.), and depths below surface (b.s.) were gauged using measuring tape. Afterwards, the frozen deposits were taken for further analyses using hammers and small axes and packed in plastic bags. While still in the field, subsamples were placed in sealed aluminium boxes in order to determine the gravimetric (grav.) ice content which is defined as the ratio of ice mass in a sample to the total dry sample mass, expressed as a weight percentage (wt%) (van Everdingen 1998).

4.4.2 Geochronology

Sediment samples were obtained from Eemian sequences (Figures 4-3 and 4-5 on pages 72 and 75) for Optically Stimulated Luminescence (OSL) dating by horizontally drilling with an electric drill (Hilti) and were protected from daylight during sampling. These samples are currently being processed at the Quaternary Geochronology Section, Saxon Academy of Science (Freiberg, Germany).

Selected plant fragments from Late Glacial/Holocene sequences (Figures 4-6 and 4-8 on pages 77 and 79) were radiocarbon-dated at the Accelerator Mass Spectrometry (AMS)

facilities at the Leibniz Laboratory for Radiometric Dating and Stable Isotope Research (Kiel University, Germany). Conventional ^{14}C ages were calculated according to Stuiver and Polach (1977), with a $\delta^{13}C$ correction for isotopic fractionation based on the $^{13}C/^{12}C$ ratio measured by the AMS system simultaneously with the $^{14}C/^{12}C$ ratio. Calibrated ages were calculated using "CALIB rev 5.01" (Data set: IntCal04; Reimer et al. 2004). The Leibniz Laboratory reduces the background inherent to the spectrometer, which results in low background count rates of the detector, equivalent to an apparent age of 75 kyr (gated background) (Nadeau et al. 1997). Details of the Leibniz Laboratory AMS procedures are given by Nadeau et al. (1997, 1998).

4.4.3 Sedimentology and stable isotopes

Moist sediment samples were freeze-dried (Christ ALPHA 1-4) in the laboratory, gently manually homogenised, and split into equal parts for the various analyses. In total, 102 samples have been analysed using different methods. A laser particle analyser (Coulter LS 200) was used to measure grain size distribution. Samples were treated with hydrogen peroxide before analysis to successively dissolve organic particles. The mass-specific mineral magnetic susceptibility (MS) was determined using a Bartington MS2 MS meter equipped with an MS2B sensor. The values of mass specific magnetic susceptibility are expressed in SI units (10^{-8} m³/kg). The contents of total organic carbon (TOC), total carbon (TC), and nitrogen (N) were measured with a Carbon-Nitrogen-Sulphur CNS analyser (Elementar Vario EL III). Stable carbon isotope ratios ($\delta^{13}C$) in TOC were measured with a Finnigan DELTA S coupled to a FLASH element analyser and a CONFLO III gas mix system after removal of carbonate with 10% HCl in Ag-cups and combustion to CO_2. Due to technical difficulties, samples from the Oy7-11 profile were analysed for their $\delta^{13}C$ in TOC using a Finnigan DELTAplusXL mass spectrometer coupled with a Carlo-Erba CN2500 elemental analyser. Accuracy of the methods was determined by parallel analysis of international and internal standard reference materials. The analyses were accurate to ±0.2‰. The $\delta^{13}C$ values are expressed in delta per mil notation (δ, ‰) relative to the Vienna Pee Dee Belemnite (VPDB) Standard.

Ice wedges from two sections on Bol'shoy Lyakhovsky Island were sampled for stable oxygen ($\delta^{18}O$) and hydrogen (δD) isotopes; the first section was located above an Eemian sequence, and the second section within a Late Glacial/Holocene sequence. Ice screws were used to drill transects across the exposed ice, keeping a distance of 0.1 m between the drill-holes. The ice samples were stored cool and afterwards analysed by equilibration technique with a mass spectrometer (Finnigan MAT Delta-S). The reproducibility derived from long-term standard measurements is established with 1σ better than ±0.1‰ (Meyer et al. 2000). All samples were run at least in duplicate. The values are expressed in delta

per mil notation (δ, ‰) relative to the Vienna Standard Mean Ocean Water (VSMOW) Standard.

4.4.4 Palaeoecological proxies

Pollen

In total, 102 samples were studied for pollen and palynomorphs. A standard hydrofluoric acid HF technique was applied for pollen preparation (Berglund and Ralska-Jasiewiczowa 1986). Pollen and spores were identified using a microscope (Zeiss Axioskop 2) with 400 x magnification. At least 200 pollen grains were counted in every sample. The relative frequencies of pollen taxa were calculated from the sum of the terrestrial pollen taxa. Spore percentages are based on the sum of pollen and spores. The relative abundances of reworked taxa (Tertiary spores and redeposited Quaternary pollen) are based on the sum of pollen and redeposited taxa, and the percentages of algae are based on the sum of pollen and algae. The Tilia/TiliaGraph/TGView software programs (Grimm 1991, 2004) were used to calculate percentages and to draw diagrams. Diagrams were zoned by visual inspection.

Freshwater ostracods

For ostracod analyses, sediment samples (ca. 200 g each) were wet-sieved through a 0.25 mm mesh screen, and then air-dried. In total, 102 sediment samples were screened for ostracods. Ostracod valves were found in 47 sediment samples and identified under a stereo-microscope (Zeiss Stemi SV11 Apo). The ostracod taxonomy was based on relevant species descriptions (Alm 1914; Pietrzeniuk 1977; Meisch 2000) following the nomenclature in Meisch (2000).

The common species *Candona candida* and *Cytherissa lacustris* from 11 sediment samples in total were prepared for stable isotope analyses. In order to create sufficient material (ca. 50 µg) for isotope analyses for each species we combined three valves of *C. candida* or two valves of *C. lacustris* into one subsample. Altogether, 58 ostracod subsamples were analysed for stable oxygen ($\delta^{18}O$) and carbon ($\delta^{13}C$) isotopes. Usually three subsamples per sediment sample were analysed and afterwards averaged. Following Keatings et al. (2006a) the ostracod valves were manually cleaned by removing adhered particles under the binocular microscope using fine brushes and needles. Only clean valves from adult specimens were used for analysis. The prepared valves were dissolved with 103% phosphoric acid and analysed for $\delta^{18}O$ and $\delta^{13}C$ by a mass-spectrometer (Finnigan MAT 253) directly coupled to an automated carbonate preparation device (Kiel IV). The analytical precision as determined by standard measurements (NBS

19) is better than ±0.06‰ (1σ) for $\delta^{18}O$ and ±0.04‰ (1σ) for $\delta^{13}C$. The stable isotope data are expressed in delta per mil notation (δ, ‰) relative to the VPDB standard.

4.5 Results

4.5.1 Geochronology, lithostratigraphy, sedimentology, and cryolithology

4.5.1.1 Eemian sequences

Geochronology

Eemian deposits were stratigraphically classified according to previously dated and palaeo-ecologically determined interglacial horizons of similar structure and composition in comparable stratigraphic positions (Andreev et al. 2004, 2008; Ilyashuk et al. 2005; Kienast et al. 2008). The most essential lithostratigraphic evidence besides the geochronological and biostratigraphical records is the large-scale coverage of the assumed Eemian deposits by Ice Complex sequences of the late Pleistocene Yedoma Suite.

Eemian exposure on the south coast of Bol'shoy Lyakhovsky Island (L7-14)

On Bol'shoy Lyakhovsky Island a section within an ice wedge cast, filled with alternating beds of peaty brownish plant detritus layers and grey clayish silt layers, was studied (subprofiles B and C; Figure 4-3a, b, e). Ripple bedding (ripples 1-2 cm high, 2-5 cm spacing), fine laminated layers (each lamination 5-10 mm thick), and small-scale synsedimentary slumping structures were common (Figure 4-3e). Several layers contained mollusc shells, about 5 mm in diameter. Larger twig fragments and peat inclusions of 2-3 cm in diameter were also observed. The cryostructure was predominantly massive. Only single thin ice veins (< 1 mm thick) were visible parallel to the bedding).

The ice wedge cast was underlain by grey silt (subprofile A; Figure 4-3a, b, e) with irregular fine single white laminations (< 1 mm thick). No plant remains were observed, but numerous small, dark-grey round spots, probably decomposed plant remains, were visible. The cryostructure was massive. This material represents thawed and refrozen (taberal) deposits.

The alternate bedding structures of the ice wedge cast were discordantly covered by ice-rich deposits (subprofile D, E and F; Figure 4-3a, b, d). This sequence exposed the transition between laminated lacustrine and weakly-bedded ice-rich boggy deposits. The latter were characterised by lens-like cryostructures, ice bands (Figure 4-3d), and the occurrence of single twig fragments. The ice-rich sequence of silty sand transformed gradually into a thick peat horizon.

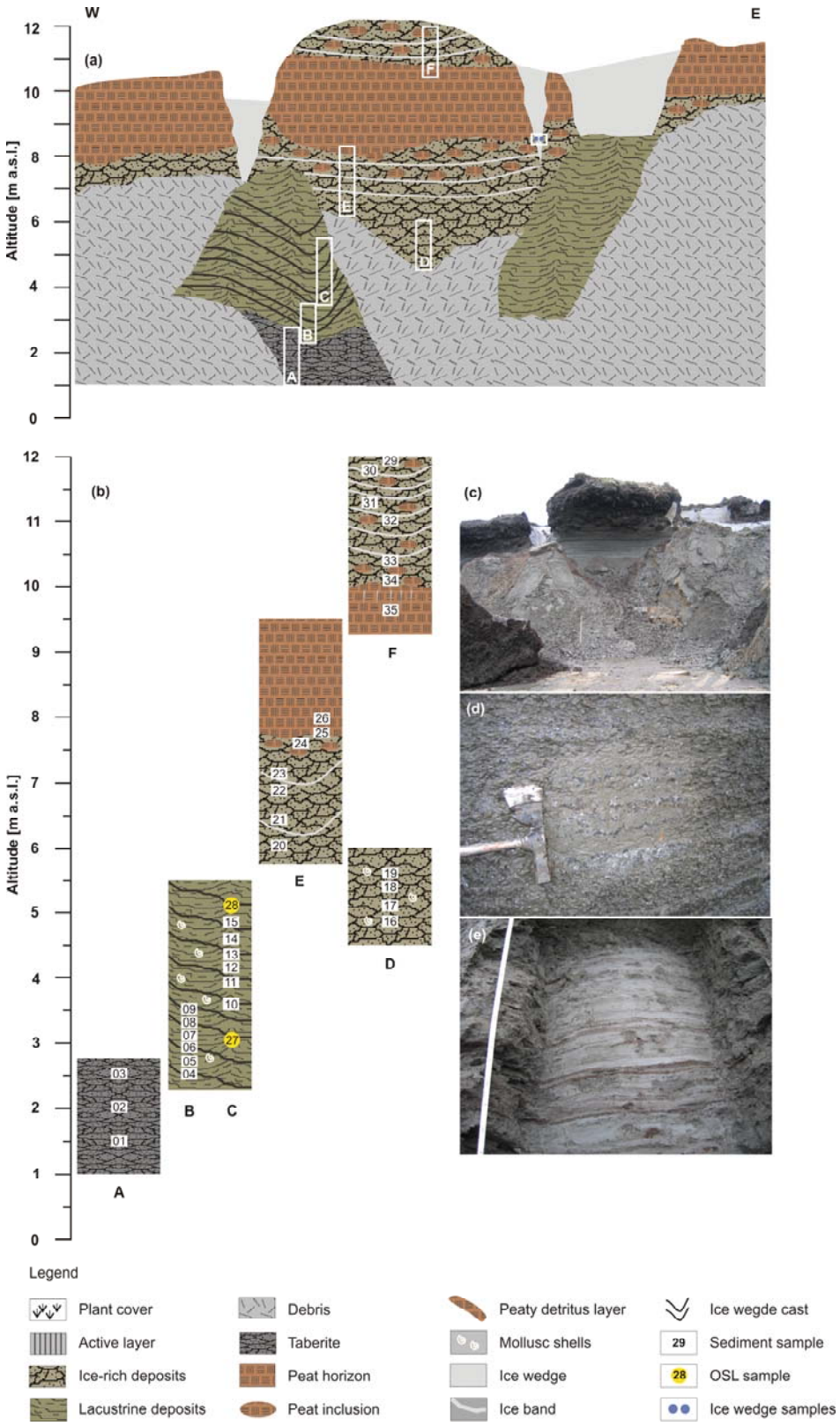

Figure 4-3 Composite Eemian to post-Eemian sequence L7-14 at the south coast of Bol'shoy Lyakhovsky Island (73.28770 °N; 141.69097 °E): (a) Exposure scheme with position of the studied subprofiles A to F; (b) Positions of the sediment samples and samples for OSL-dating (in yellow); (c) Overview picture of the studied sequence; (d) Ice-rich deposits covering the Eemian sequence; (e) Well-bedded Eemian lake deposits in an ice wedge pseudomorph

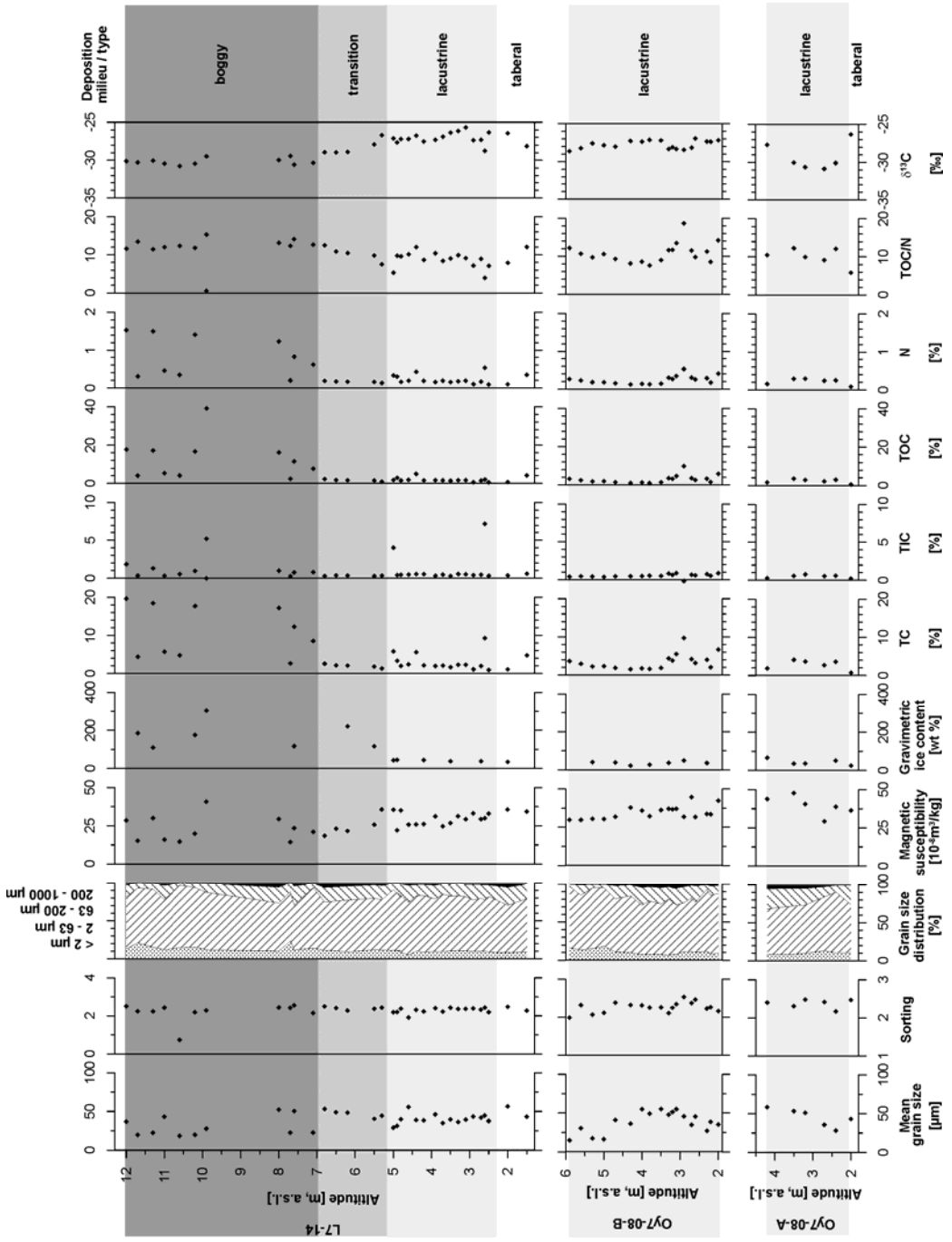

Figure 4-4 Comparison of sedimentological, biogeochemical, and cryolithological records of the composite Eemian profiles L7-14 and Oy7-08

The transition horizon contained several large peat inclusions ≈30 cm in diameter. The cryostructure was banded (2-5 cm thick bands) with coarse lens-like reticulations between ice bands, reflecting conditions of ice supersaturation. Several vertical ice veins (1 to 1.5 cm broad, 20 cm long) were observed in 20 cm distance to each other in the upper part of the peat horizon. The entire sequence was framed by ≈1 m wide ice wedges to the left and to the right, and is considered to be polygon filling (Figures 4-3a, c). The peat horizon consisted of numerous large peat lenses embedded in greyish sandy silt. Similar thick

peaty horizons were observed several other places on the coast. Therefore, it can be concluded that the sequence of interglacial finely-laminated lake deposits covered by ice-rich silty sands and a peat layer is of stratigraphic importance. Further upwards to the surface the coastal section consisted of a ≈20 m thick Ice Complex sequence. According to grain size analysis, the studied deposits are poorly sorted clayish sandy silts (Figure 4-4). The silt fraction is dominant, but the changing content of fine-grained and middle-grained sand reflects the alternating beds of lacustrine Eemian deposits. The sedimentological records of the well-bedded part and the adjacent underlying and covering layers are similar. Therefore, both the underlying and overlying layers seem to have been transformed by thawing and freezing or by refreezing only after accumulation. In general, two horizons could be distinguished. The lower horizon containing less ice and organic carbon corresponds to the Eemian lacustrine sequence. The upper horizon of higher ice (100-300 wt%) and TOC contents is considered to be a boggy formation. The $\delta^{13}C$ record probably reflects changes in plant associations which would result from a gradual transition from aquatic to boggy environmental conditions (Figure 4-4).

Eemian exposure on the coast of Oyogos Yar (Oy7-08)

A second ice wedge cast profile studied on the Oyogos Yar coast was part of a 28 m long coastal section mostly composed of late Pleistocene Ice Complex deposits (Schirrmeister et al. in press). For this paper, we selected the lower two subprofiles A and B underlying the Ice Complex deposits (Figure 4-5a). Subprofiles A and B were exposed between 2 and 6 m a.s.l. at the cliff wall of the thermo-terrace to the sea and in a small thermo-erosional gully cutting the thermo-terrace (Figure 4-5b).

The lowest horizon (sample Oy7-08-01 of subprofile A) underlying the ice wedge cast contained grey taberal deposits with black spots and several plant remains. The cryostructure was massive. These deposits were covered by light-brown peat lenses (2 x 5 to 10 x 15 cm) in a grey sandy silt matrix with lens-like reticulated cryostructure and higher ice content. In addition, single ice lenses 5 mm thick were visible. Disturbed layering and white lines of thaw structures between the layers were observed. The lowermost layer of the exposed ice wedge cast consisted of finely-laminated 1-2 to 5-10 mm thick alternating layers of brownish plant detritus layers and grey sandy silt layers (Figure 4-5a). The cryostructure was fine lens-like reticulated.

The centre of the ice wedge cast and the overlying deposits were studied in the second subprofile B (Figure 4-5a). This subprofile was composed of numerous 5-10 cm thick alternating plant detritus layers and sandy silt layers (Figure 4-5c). Ripple bedding, synsedimentary slumping structures, and separate peat lenses were observable in some layers. The cryostructure was lens-like layered. Ice lenses were oriented parallel to the

bedding. Further upwards the bedding was disturbed and the plant detritus content decreased. Grey silty sand dominated this horizon, which contained numerous mollusc shells. The cryostructure changed upward from lens-like layered to lens-like reticulated. Because of overlapping sample heights the analytical records of subprofile A were presented separately in Figure 4-4. The entire sequence consisted of less-sorted clayish sandy silt. Small-scale changes of mean grain size and of sand fraction reflect the alternating bedding of the lacustrine deposits. The horizon below the ice wedge cast is characterised by $\delta^{13}C$ values lighter than those of the ice wedge cast sediments (Figure 4-4).

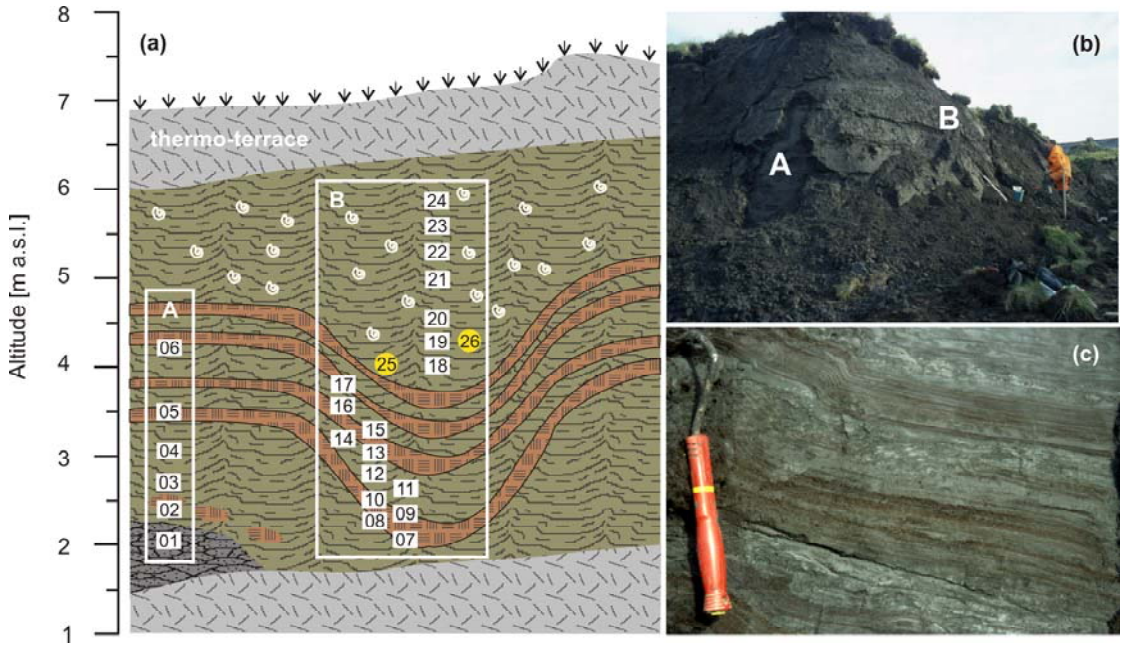

Figure 4-5 Composite Eemian sequence Oy7-08 at the north coast of Oyogos Yar (72.68002 °N; 143.53181 °E): (a) Exposure scheme with positions of the studied subprofiles A and B, sediment samples, and samples for OSL-dating (in yellow); (b) Photograph of the positions of subprofiles A and B which occur close together; (c) Detail of the well-bedded sediment structure within the ice wedge cast. For legend see Figure 4-3

4.5.1.2 Late Glacial/Holocene sequences

Geochronology

In total, the plant remains and detritus in twenty sediment samples from both Late Glacial/Holocene sequences have been radiocarbon dated (Table 4-2).

The age-height relationship is not consistent, probably due to pre-sedimentary relocation and post-sedimentary cryogenic processes. Furthermore, the interpretation of the stratification is complicated by the sampling of subprofiles at different positions. However, the general picture is similar at both study sites on the northern and southern coasts of the Dimitri Laptev Strait. Late Pleistocene taberal deposits dated between about 46.6 and

36.6 kyr BP are discordantly overlain by lake deposits dated from about 11.8 to 7.1 kyr BP at the Bol'shoy Lyakhovsky section (profile L7-08) and from about 14.8 to 10.7 kyr BP at the Oyogos Yar section (profile Oy7-11). The overlying boggy deposits accumulated from about 7.5 to 4.0 kyr BP at the Bol'shoy Lyakhovsky section and between about 10.0 and 3.3 kyr BP at the Oyogos Yar section. The late Holocene deposits discordantly cover the underlying older Holocene sediments.

Table 4-2 AMS-measured radiocarbon ages of plant remains in samples of the Alas sequences from Bol'shoy Lyakhovsky (L7-08) and Oyogos Yar (Oy7-11)

Sample №	Lab №	Altitude [m, a.s.l.]	Uncal. AMS ages [yr BP]		Cal. AMS ages* [yr BP], maximum	Cal. AMS ages* [yr BP], minimum
L7-08-25	KIA 36692	10.7	3960	±140	4830	4083
L7-08-22	KIA 35227	10.0	7525	±40	8309	8293
L7-08-19	KIA 35226	9.0	11610	+690/-640	15497	11755
L7-08-18	KIA 36691	8.4	10090	±150	12184	11223
L7-08-16	KIA 35225	7.9	9220	+190/-180	10890	9894
L7-08-14	KIA 36690	7.5	7095	±60	8020	7794
L7-08-12	KIA 35224	6.8	11210	+880/-800	15378	10650
L7-08-08	KIA 35223	5.7	11860	±160	14050	13362
L7-08-05	KIA 35222	5.0	46620	+1750/-1440		
L7-08-02	KIA 36689	4.2	44030	+820/-750		
Oy7-11-14	KIA 35234	11.1	3325	±35	3635	3477
Oy7-11-12	KIA 35233	10.1	8335	±45	9472	9247
Oy7-11-10	KIA 35232	8.8	8260	±40	9408	9092
Oy7-11-09	KIA 36687	8.6	9985	±35	11616	11271
Oy7-11-08	KIA 36686	8.3	11145	±40	13141	12943
Oy7-11-07	KIA 35231	8.0	14830	+70/-60	18500	17731
Oy7-11-06	KIA 36688	7.7	10720	+40/-35	12839	12700
Oy7-11-04	KIA 35230	7.1	11995	±50	13984	13748
Oy7-11-03	KIA 35229	6.8	41290	+2370/-1830		
Oy7-11-01	KIA 35228	6.0	36580	+1090/-960		

*Calibrated ages were calculated using the software program „ CALIB rev 5.01" (Data set: IntCal04; Reimer et al. 2004)

Alas exposures on the south coast of Bol'shoy Lyakhovsky Island (L7-08, R33-A1)

An 8 m thick sediment sequence in the centre of a thermokarst depression, cut by the coastal cliff, was studied about 4.1 km west of the Zimov'e River mouth (Figure 4-1).

The lowermost exposed horizon consisted of greenish grey sandy silt, the thawed and refrozen (taberal) remains of Ice Complex deposits (Yedoma Suite), containing peat lenses of 5-10 cm length (Figure 4-6).

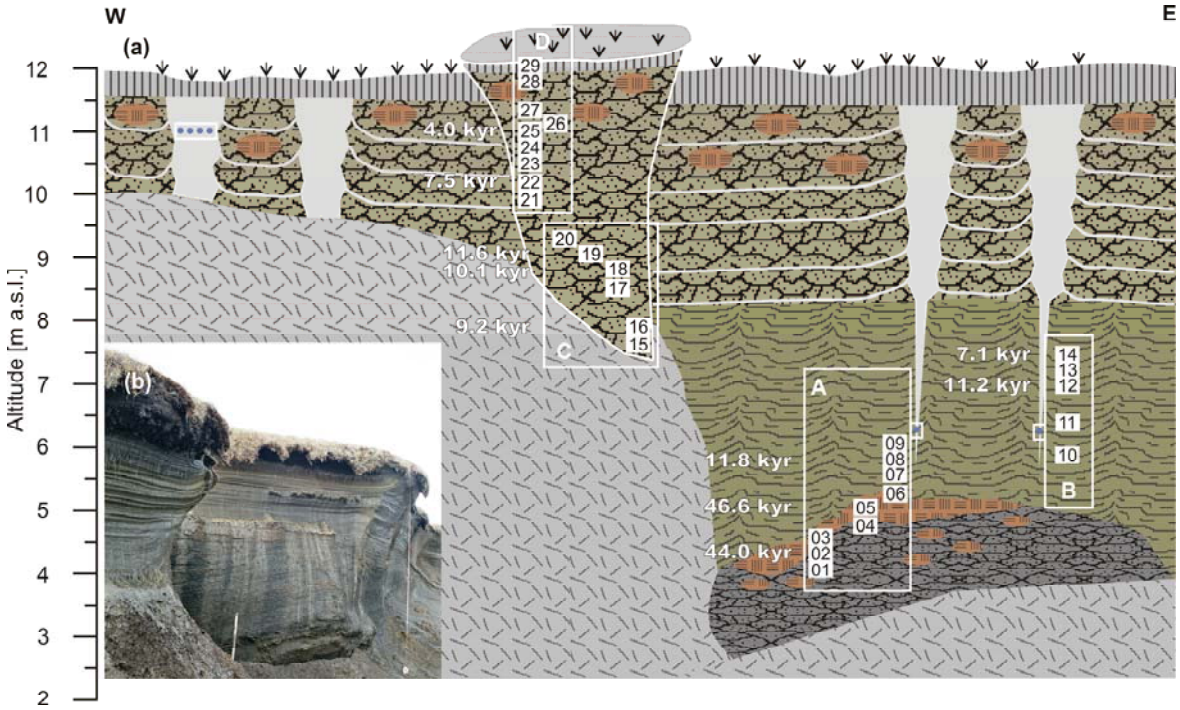

Figure 4-6 Composite Late Glacial/Holocene thermokarst sequence L7-08 on the south coast of Bol'shoy Lyakhovsky Island (73.28161 °N; 141.83794 °E); (a) Exposure scheme with positions of the studied subprofiles A to D, sediment samples, and AMS-measured dates (kyr BP); (b) Overview photograph of the studied sequence. For legend see Figure 4-3

The cryostructure was coarse lens-like reticulated. The gravimetric ice content was relatively low. Above this horizon, a 0.5 m thick layer of cryoturbated peaty palaeosol containing less-decomposed, light-brown peat moss and a dark-brown peat layer with wood fragments in a sandy silt matrix was exposed. The cryostructure was net-like to lens-like, with 4-5 cm long ice lenses, and an ice content of 38 to 46 wt%. This segment was covered by 4 m of lacustrine deposits altogether, consisting of alternating beds of dark-grey clayish silt and 2 mm thick dark-grey layers of plant detritus. The cryostructure was lattice-like with distances between separate ice veins of 5-10 cm. This part was additionally marked by 2 to 3 cm thick brownish zones of iron oxide impregnations along cracks. The uppermost 3 m of the alas sequence were characterised by light-brown, 10 to 15 cm long peat inclusions in light-grey sandy silt matrix reflecting subaerial accumulation conditions. The cryostructure was banded and lens-like between ice bands. Between 1.1 to 0.3 m below the surface grass roots and peat layers occurred. The cryostructure consisted of diagonally-ordered, partly-broken ice veins and lenses, or of lattice-like structures. The studied deposits from the L7-08 sequence are predominantly composed of less-sorted fine-grained sand. Three horizons (taberal, lacustrine, boggy) were separated according to sedimentological, biogeochemical, and cryolithological results (Figure 4-7).

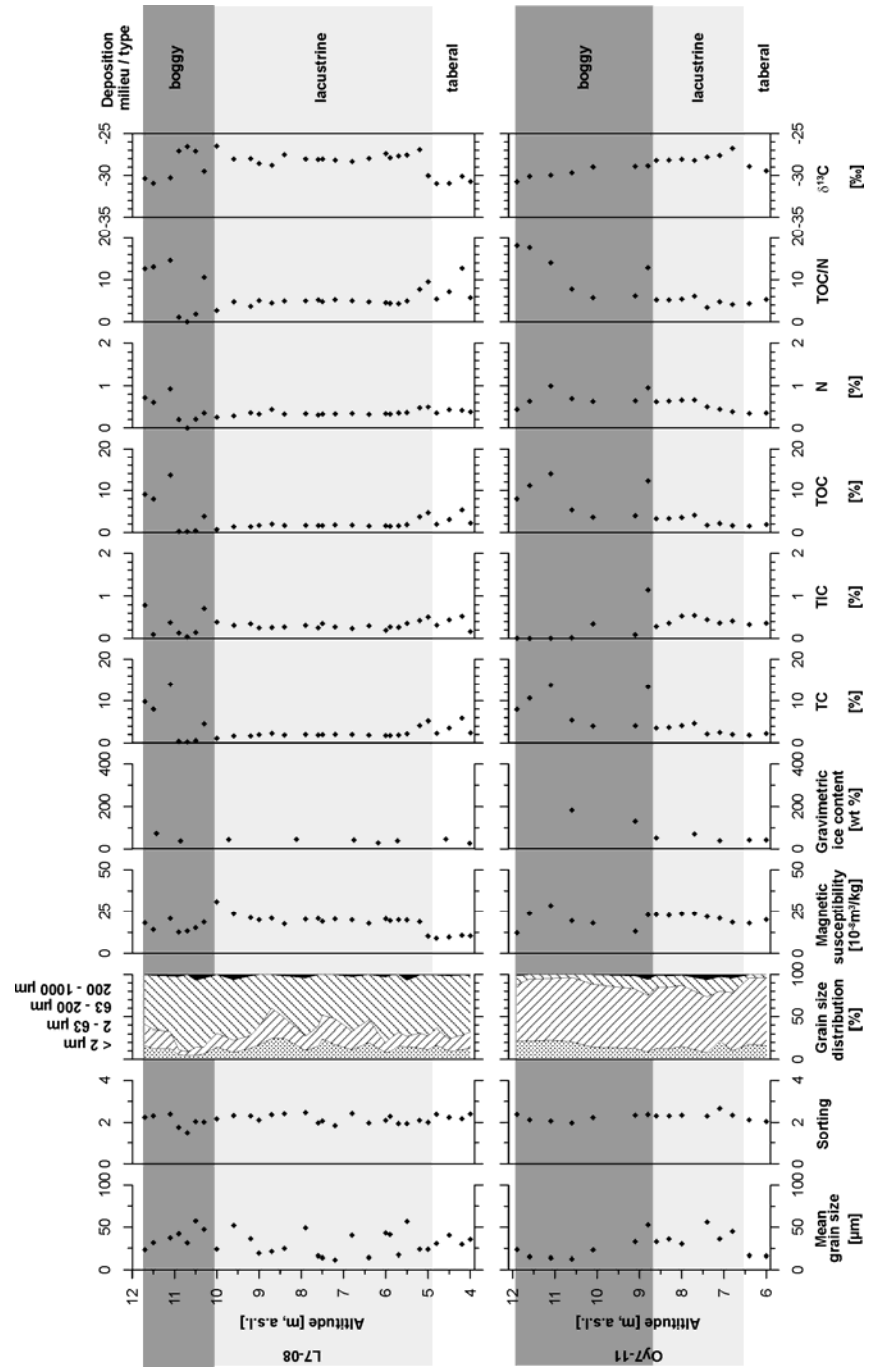

Figure 4-7 Comparison of sedimentological, biogeochemical, and cryolithological records of the composite Holocene alas profiles and underlying taberal deposits L7-08 and Oy7-11

The bedding of the lacustrine segment is reflected in changing mean grain size values and variations in the silt and sand fractions. The less variable magnetic susceptibility reflects the homogenous mineral composition of these deposits. Taberal Ice Complex deposits below and boggy deposits above the lacustrine horizon are clearly separated by lighter $\delta^{13}C$ values (< −30‰), higher TOC contents, and low values of magnetic susceptibility.

An additional alas section (R33) already described by Andreev et al. (2008) exposed on the eastern slope of the same thermokarst depression was additionally used for ostracod studies. The cryolithological and stratigraphic situation was generally similar to that of the above-mentioned section. According to radiocarbon data, the lower horizon was formed during the Middle Weichselian. The upper subaquatic and the subaerial sediments containing molluscs, snails, and thin layers with leaves, accumulated between 12 and 8 ^{14}C kyr BP. The sequence was covered by boggy deposits that are 3.7 kyr BP old. Woody remains were radiocarbon dated between 8.4 and 8.9 kyr BP and found in a near-surface ice wedge cast (Andreev et al. 2008).

Alas exposure on the coast of Oyogos Yar (Oy7-11)

This exposure consists of two subprofiles that were studied at the coast on both sides of an erosional crack (Figure 4-8a).

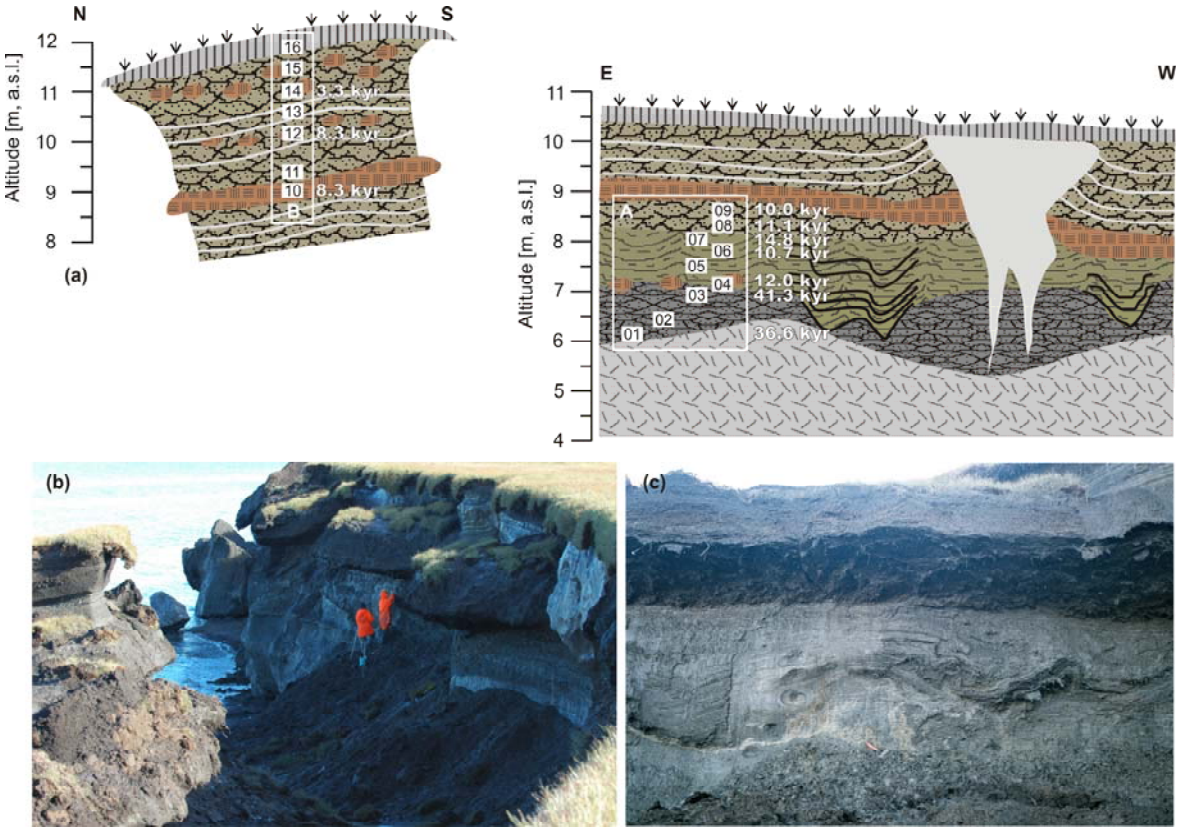

Figure 4-8 Composite Late Glacial/Holocene thermokarst sequence Oy7-11 on the north coast of Oyogos Yar (72.68347 °N; 143.47526 °E): (a) Exposure scheme with position of the studied subprofiles A and B, sediment samples, and AMS-measured dates (kyr BP); (b) Overview photograph showing both walls of an erosional crack; (c) Subprofile A with taberal Ice Complex deposits, lacustrine deposits and ice wedge casts, and the covering peat layer. For legend see Figure 4-3

The sediment sequence was exposed at an ≈ 10 m high wall, where subprofile A was studied, and at a fallen block opposite to the wall, where subprofile B was accessible. The lower subprofile A (Figure 4-8a) consists of taberal Ice Complex deposits of the Yedoma Suite.

The light-grey silty sand contained no or rare visible plant detritus. The cryostructure was lens-like layered. One mm thick, 5-15 cm long ice lenses occurred 1-2 cm apart. Irregular white lines were also observed and were interpreted as thaw structures. These whitish structures occurred with increasing frequency closer to the overlaying peaty soil. This palaeosol layer contained twigs and peat inclusions. Above this buried soil, lacustrine deposits were indicated by alternating layers of silty fine sand and plant detritus. Ripple marks, small faults, wood fragments, and mollusc shells were observed. The cryostructure was lens-like layered. Similar lacustrine sediments were found in a flanking ice wedge cast (Figure 4-8c). Small epigenetic ice wedges became a broad syngenetic ice wedge crossing the sediment sequence, similar to the above-described section on Bol'shoy Lyakhovsky Island.

The lake sequence was covered by a peat horizon which was not accessible in subprofile A. Therefore, the upper part of the alas sequence was studied in a seperate block directly in front of the wall (Figure 4-8b). The 20 to 30 cm thick peat horizon was dense and platy and contained wood fragments (2-3 cm in diameter) and 1-2 mm thick silt layers. Further upward, greyish silty sand and light-brown peat lenses were found. The cryostructure was banded and coarse lens-like reticulated. Ice lenses up to 1 cm thickness were composed of vertical ice needles.

Field observations indicated that the alas sequence was subdivided into three different parts; this conclusion was confirmed by analytical records (Figure 4-7). The entire sequence predominantly consists of poorly sorted silt. The lowermost taberal Ice Complex deposits are characterised by fine-grained clayish silt. The covering lacustrine segment contains more sand. The magnetic susceptibility of both parts was similar (about 20 x 10^{-8} m^3/kg) reflecting a similar sediment source. The observed bedding of lacustrine sediments is shown by variations in mean grain size. Finally, the uppermost boggy segment is characterised by higher ice content, lower mean grain size, and variations in magnetic susceptibility and TOC values.

4.5.2 Stable isotope ground ice records

Stable isotope data from ice wedges presented here were obtained on Bol'shoy Lyakhovsky Island. Corresponding samples were taken on Oyogos Yar; those analyses are still in progress and the subject of an upcoming paper by Opel et al. (in preparation).

We obtained four samples at 8.5 m a.s.l. from a syngenetic ice wedge exposed at section L7-14 above the Eemian lacustrine sediments (Figure 4-3).

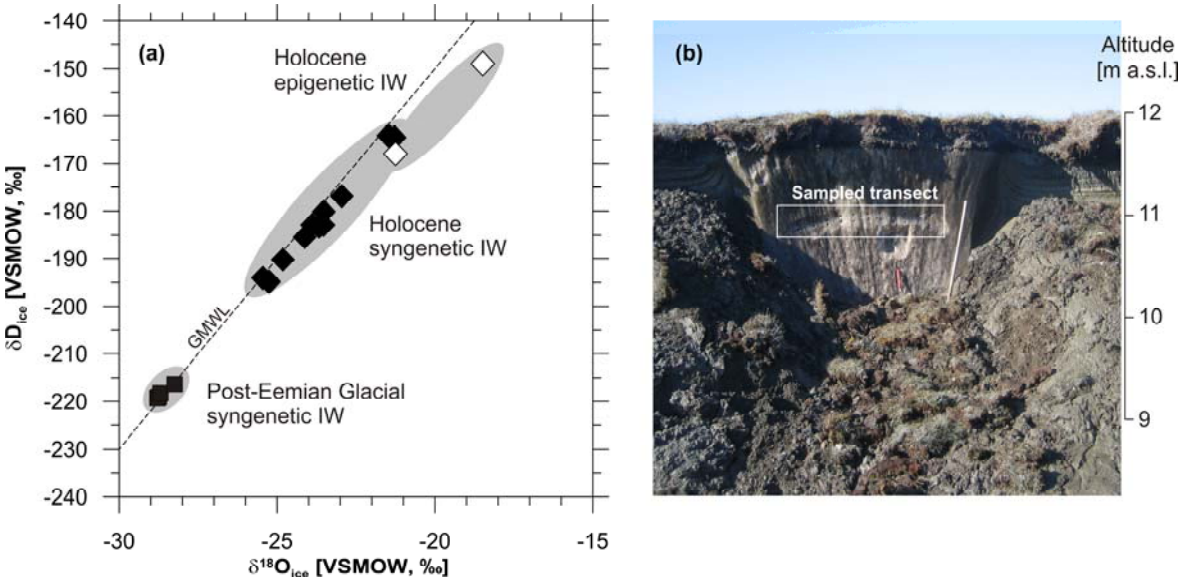

Figure 4-9 (a) $\delta^{18}O$–δD plot of post-Eemian Glacial syngenetic ice wedges (Section L7-14) and Holocene syngenetic and epigenetic ice wedges (Section L7-08) with respect to the Global Meteoric Water Line (GMWL), which correlates fresh surface waters on a global scale (Craig 1961); (b) Overview photograph of the sampled Holocene syngenetic ice wedge in the upper part of section L7-08 at 11 m a.s.l.

Syngenetic ground ice formed concurrently with sediment accumulation. The isotopic record shows values of ≈ −29‰ for $\delta^{18}O$ and −218‰ for δD, which are relatively light isotopically when compared to the Holocene records of section L7-08. The deuterium (*d*) excess averages about 10.7 (Figure 4-9, Table 4-3).

The Holocene stable isotope ground ice record comes from two samples taken at 6.3 m a.s.l. from the epigenetic part and 11 samples at 11 m a.s.l. from the syngenetic part of the Holocene ice wedges exposed at section L7-08 (Figure 4-6). The epigenetic part formed after sedimentation in the underlying lacustrine deposits, and the syngenetic part formed approximately simultaneously during sediment accumulation in the boggy deposits (Figure 4-6). The isotopic records of the Holocene syngenetic ice wedge show heavier values of around −24‰ for $\delta^{18}O$ and −182‰ for δD than the post-Eemian Glacial records of section L7-14. The d excess averages about 7.3 (Figure 4-9, Table 4-3). The $\delta^{18}O$ and δD values of the sampled epigenetic parts of the Holocene ice wedges were heavier than those of the syngenetic parts; about −20‰ for $\delta^{18}O$ and −158‰ for δD, an a deuterium excess of around 0.5 (Figure 4-9, Table 4-3). The latter value points to interactions between the thin epigenetic parts of ice wedges and the surrounding frozen sediments, altering the primary meteoric precipitation signal.

Table 4-3 Oxygen and hydrogen stable isotope signatures (mean values and standard deviations) of post-Eemian Glacial and Holocene ice wedges (IWs)

Type of ground ice	Sub-samples	Altitude	$\delta^{18}O$ mean	$\delta^{18}O$ σ	δD mean	δD σ	*d* mean	*d* σ
		[m a.s.l.]	[‰]	[‰]	[‰]	[‰]	[‰]	[‰]
Holocene IW (syngenetic)	11	11	−23.63	1.35	−181.8	10.2	7.3	1.2
Holocene IW (epigenetic)	2	6.5	−19.87	1.96	−158.4	13.4	0.5	2.2
Post-Eemian IW (syngenetic)	8	8.5	−28.62	0.25	−218.3	1.3	10.7	0.8

4.5.3 Pollen studies

4.5.3.1 Eemian sequences

Eemian pollen record from Bol'shoy Lyakhovsky Island

The lowermost spectra (pollen zone I: PZ I) in profile L7-14 (Figure 4-10) are dominated by pollen of Poaceae and Cyperaceae with some *Betula* sect. *Nanae* and *Alnus fruticosa*. The pollen concentration is low. PZ I contains high numbers of *Glomus* spores (indicative of denudated soils) and reworked ancient (mineralised) Pinaceae. It is also likely that *Pinus* and *Picea* pollen found in PZ I have been reworked as well. Therefore, the pollen spectra of PZ I should be considered carefully. Poaceae and Cyperaceae pollen and *Glomus* spores were probably mostly produced by local vegetation during sedimentation, while numerous coniferous pollen were reworked from older sediments. *Betula* and *Alnus* pollen might also be of reworked or contaminated origin. Taking this into consideration, we should exclude the PZ I spectra from palaeoecological interpretation.

Pollen spectra from PZ II are dominated by pollen from Poaceae, Cyperaceae, *Betula* sect. *Nanae*, and *Alnus fruticosa*. These spectra also contain rather high amounts of *Salix* and *Artemisia* pollen, spores of fungi (dung-inhabiting Sordariales and *Glomus*), and remains of green algae colonies (*Pediastrum* and *Botryoccous*). According to pollen spectra the area around a supposed initial thermokarst lake was dominated by shrubby tundra vegetation. Climate conditions were relatively moderate (warm and moist).

Pollen spectra from PZ III are mainly composed of pollen from Poaceae, Cyperaceae, *Betula* sect. *Nanae*, and *Alnus fruticosa*. This zone can be subdivided into two subzones. The contents of shrub pollen are the highest in PZ IIIa, reflecting the warmest interval. The remains of green algae colonies and fungal spores are completely absent in the PZ IIIb zone, reflecting dryer local environmental conditions. Lower contents of shrub pollen in the upper subzone also point to a slight cooling.

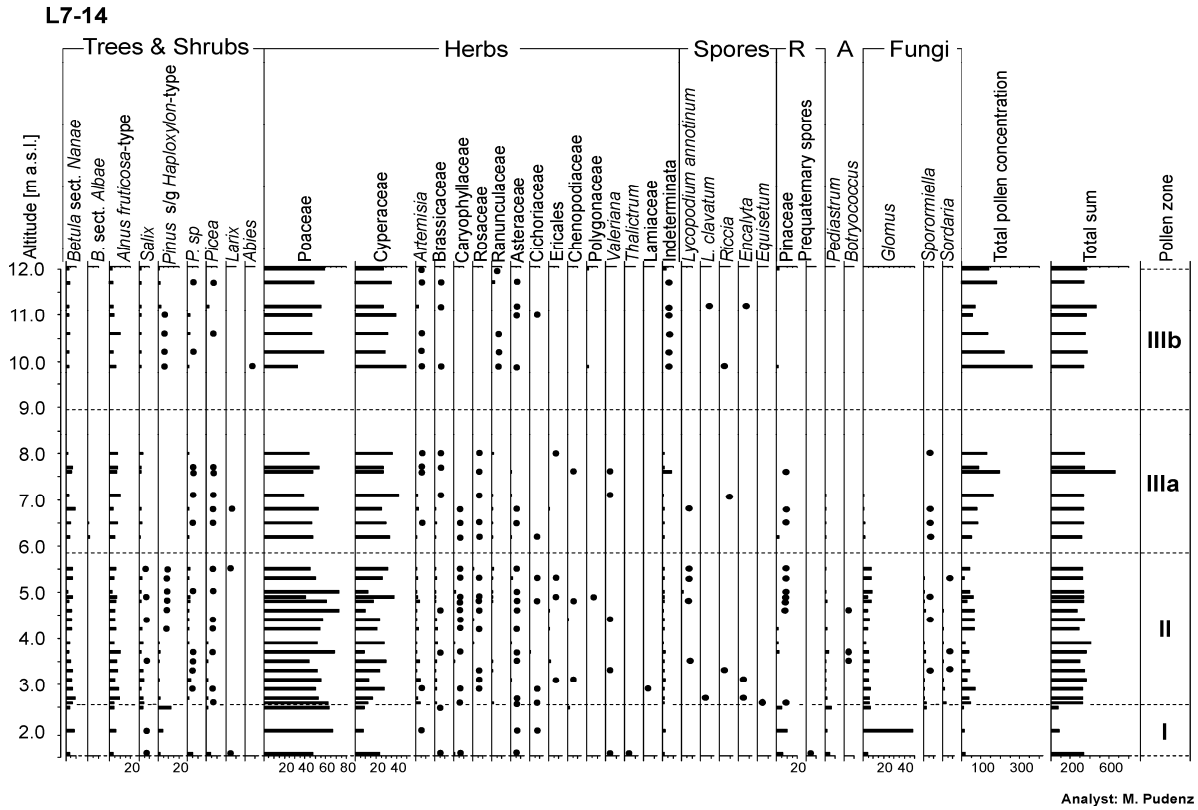

Figure 4-10 Eemian pollen record from Bol'shoy Lyakhovsky Island (Section L7-14)

Eemian pollen record from Oyogos Yar

The pollen concentration of the lowermost sample (PZ I of section Oy7-08) is low (Figure 4-11). As in the samples from PZ I of section L7-14, it contains relatively high amounts of reworked ancient (mineralised) coniferous pollen (*Larix*, *Pinus*, *Picea*), and is therefore of minor relevance for palaeoecological interpretation. However, some taxa from PZ I can be used to characterise environmental conditions in the area during sedimentation. For example, rather high amounts of Cichoriaceae pollen and *Riccia* spores are notable in the spectrum. Both taxa are indicative of denuded soils and may reflect an unstable environment connected with melting Saalian ice wedges and initial formation of Eemian thermokarst depressions. It is also notable that the Poaceae, Cyperaceae, and *Betula* sect. *Nanae* pollen in PZ I are very similar to pollen types in the lower part of PZ II, and probably reflect similar vegetation around the site. Pollen spectra of PZ II dominated by Poaceae, Cyperaceae, *Larix* and *Betula* sect. *Nanae* pollen (Figure 4-11) can be subdivided into two subzones. PZ IIa contains higher amounts of *Salix* and *Artemisia* pollen and spores of dung-inhabiting Sordariales fungi (*Sporormiella*, *Podospora*, *Sordaria*), while PZ IIb contains more pollen of *Betula* sect. *Nanae*, *B.* sect. *Albae*, and *Alnus fruticosa*. Rather high amounts of *Larix* pollen in PZ II indicate that larch grew around the study site. Shrub alder and dwarf birch stands were also common. Very high amounts of *Salix* pollen in the lowermost sample of PZ II may reflect a predominance of

willow shrubs in the pioneer vegetation around the site. Relatively high amounts of dung-inhabiting fungal spores in the PZ IIa subzone indirectly point to the presence of grazing herds in the area during the interval between PZ 11a and PZ 11b.

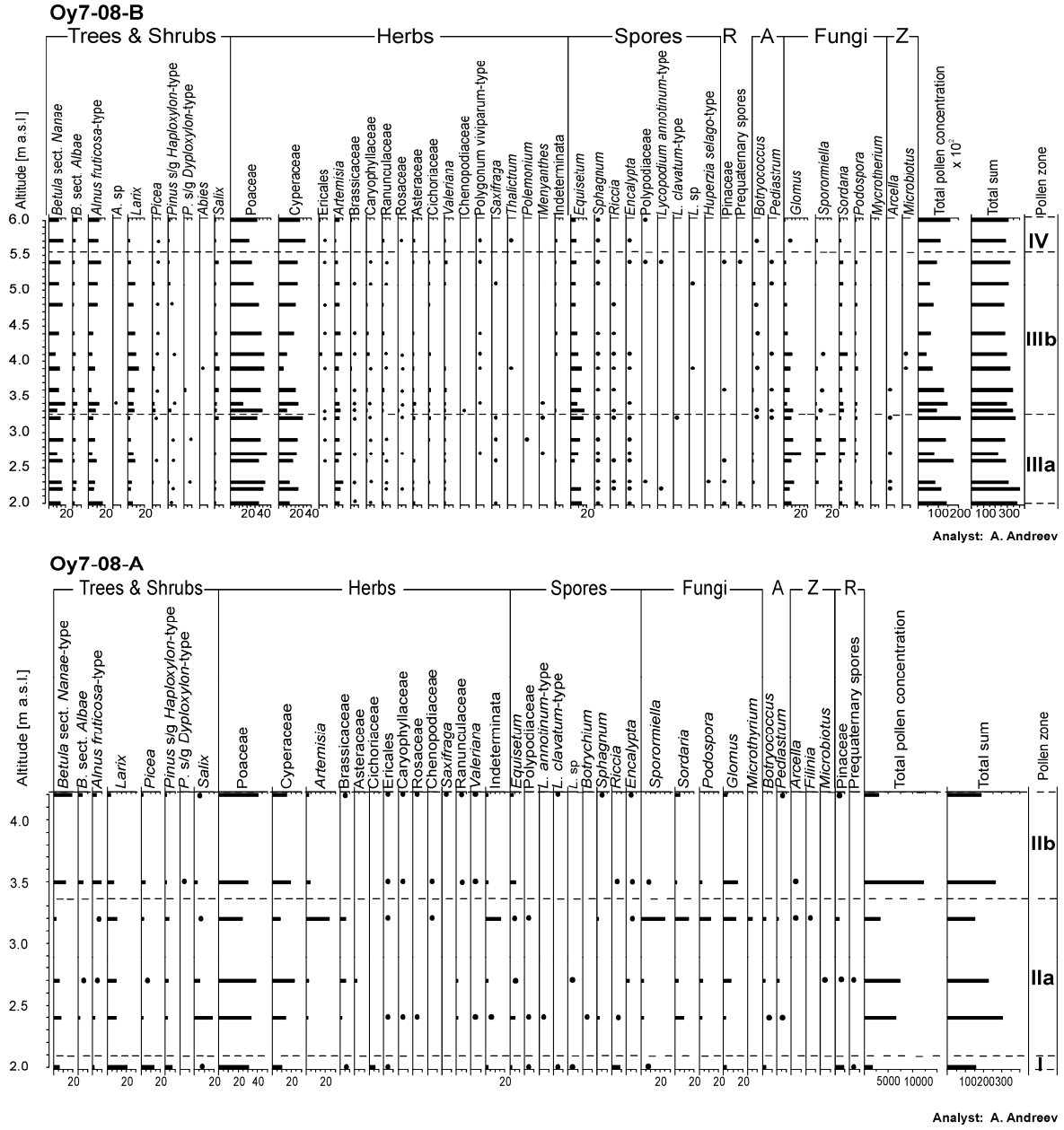

Figure 4-11 Eemian pollen record from Oyogos Yar (Section Oy7-08)

The PZ IIb Oy7-08-05 and -06 samples from subprofile Oy7-08-A correlate with the samples Oy7-08-07 and -17 from the subprofile Oy7-08-B that was sampled in detail; at Oy7-08-B the record continues as PZ III of subprofile Oy7-08-B (Figure 4-11).

PZ III is dominated by pollen of Poaceae, Cyperaceae, *Betula* sect. *Nanae*, *Alnus fruticosa*, *Larix*, and spores of *Equisetum* and fungi. The pollen spectra of PZ III can be subdivided into two subzones (Figure 4-11). PZ IIIa differ from PZ IIIb because higher amounts of fungal spores (dung-inhabiting Sordariaceae and *Glomus*) are present in PZ

IIIa, while the numbers of *Larix*, *Salix,* and *Picea* pollen are higher in PZ IIIb. PZ III pollen assemblages reveal a larch forest, with alder shrub and dwarf birch stands dominating the vegetation (Figure 4-13). The content of *Glomus* spores, which indicate disturbed soils, shows a trend similar to that of the Sordariaceae (especially with *Sporormiella*) and likely indicate the presence of numerous grazing animals during this interval. The highest presence of larch and spruce pollen occurs in PZ IIIb, indicating the most favourable conditions during the Eemian, i.e. the Middle Eemian thermal optimum. Slightly higher numbers of *Salix* pollen and remains of green algae colonies (*Botryococcus* and *Pediastrum*) point to a wetter environment than during the PZ IIIa interval. Numbers of *Larix*, *Salix,* and *Picea* pollen are significantly lower in PZ IV, indicating climate deterioration. Disappearance of dung-inhabiting fungi spores indirectly shows that the number of grazing animals in the area was significantly reduced.

4.5.3.2 Late Glacial/Holocene sequences

Late Glacial/Holocene pollen record from Bol'shoy Lyakhovsky Island (L7-08)

The pollen spectra of PZ I are mostly dominated by Poaceae and Cyperaceae with few Asteraceae and *Artemisia* (Figure 4-12).

Two radiocarbon dates within PZ I of about 46.6 and 44.0 kyr BP show that the sediments were accumulated during the Middle Weichselian. Similar pollen spectra reflecting open steppe- and tundra-like vegetation are known from the area (Andreev et al. 2008). The presence of shrub pollen (especially *Salix*) might reflect a growth of shrub communities in the area.

PZ II is dominated by Poaceae and Cyperaceae, but also contains rather large numbers of *Betula* sect. *Nanae*, *B.* sect. *Albae,* and *Alnus fruticosa* (Figure 4-12). According to the radiocarbon dates (Table 4-2) the sediments were accumulated during the Allerød and the early Holocene. Comparing the studied spectra with other local records (Andreev et al. 2008) shows that these spectra are typical of early Holocene records, but they also contain organic material of different origins due to reworking by thawing and refreezing, and therefore should be interpreted very carefully.

The pollen spectra of PZ III are also dominated by Poaceae and Cyperaceae and contain relatively high amounts of *Betula* sect. *Nanae*, *B.* sect. *Albae* and *Alnus fruticosa* (Figure 4-12). However, radiocarbon dates from the low part of the section (Table 4-2) show that sediment is contaminated by older organic matter. The upper part of the sediments (PZ IIIb pollen subzone) was accumulated in under wetter conditions as evident by higher amounts of Cyperaceae and green algae colonies remains.

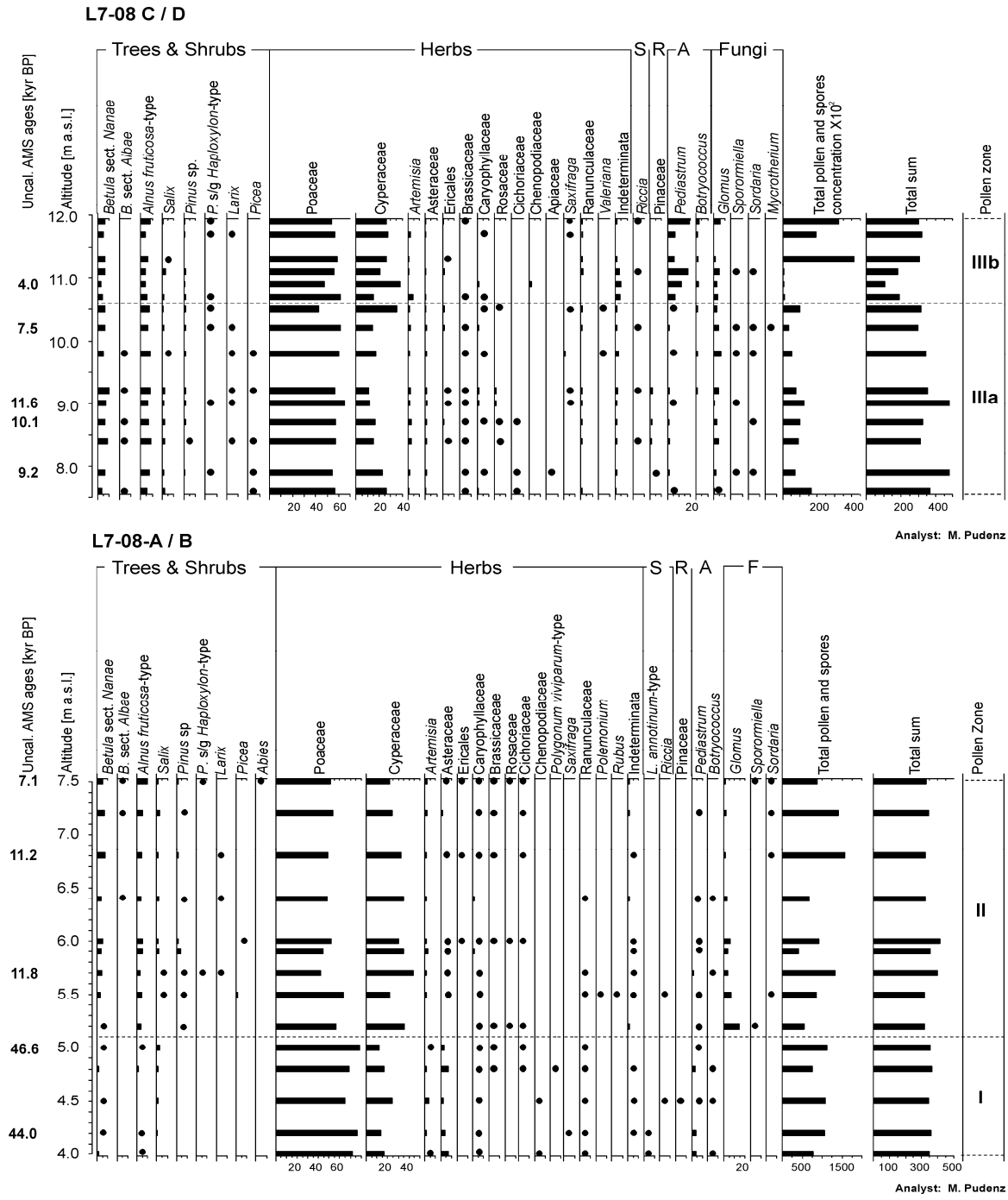

Figure 4-12 Late Glacial/Holocene pollen record from Bol'shoy Lyakhovsky Island (Section L7-08)

Late Glacial/Holocene pollen record from Oyogos Yar (Oy7-11)

The lowermost PZ I is dominated by Poaceae and Cyperaceae, but also contains large numbers of *Betula* sect. *Nanae*, *B.* sect. *Albae,* and *Alnus fruticosa* (Figure 4-13).

In addition, the uppermost pollen spectra of PZ I (sample Oy7-11-03) contain a large amount of Sordariaceae fungi spores. Two radiocarbon dates within PZ I of about 41.3 and 36.6 kyr BP (Table 4-2) show that the sediments accumulated during the Middle Weichselian period. However, the taberal sediments representing PZ I could have been

contaminated by organic material of a different origin due to reworking by thawing and refreezing, and therefore should be interpreted carefully.

The pollen spectra of PZ II are mostly dominated by Poaceae pollen with some pollen from Cyperaceae, *Artemisia*, *Betula* sect. *Nanae,* and a few other taxa. PZ II can be subdivided into two subzones (Figure 4-13). PZ IIa contains higher numbers of shrub and tree pollen, while PZ IIb shows higher numbers of Asteraceae and spores of fungi. According to the radiocarbon dates (Table 4-2) PZ IIa spectra indicate a relatively warm interval which might be correlated with the Allerød. PZ IIb spectra indicate some climate deterioration which occurred during the Younger Dryas.

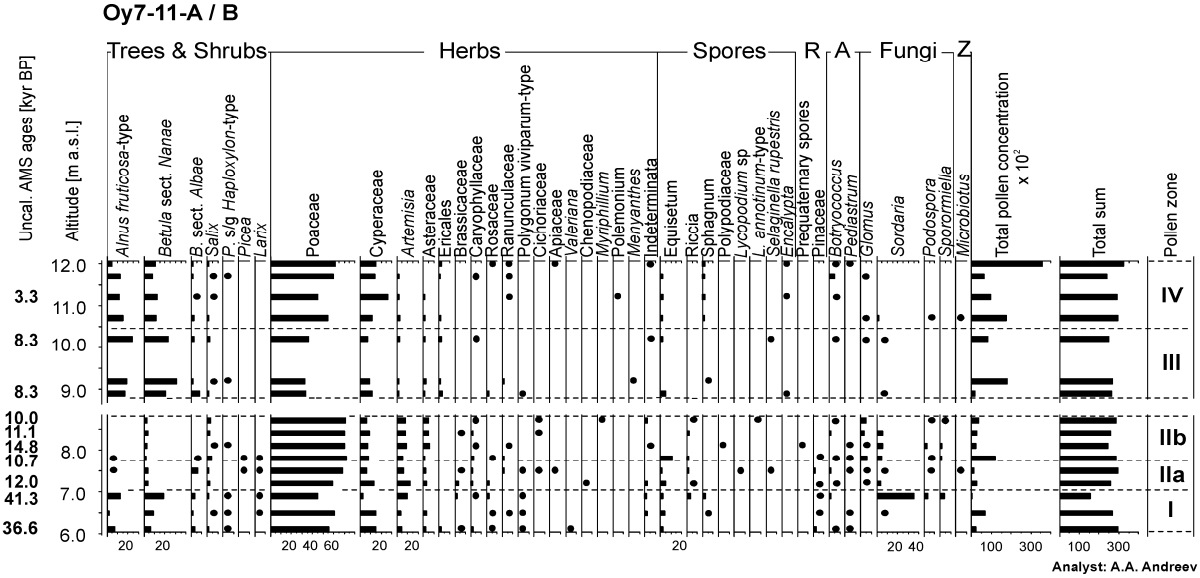

Figure 4-13 Late Glacial/Holocene pollen record from Oyogos Yar (Section Oy7-11)

PZ III is characterised by large numbers of shrub and tree pollen reflecting the shrubby tundra vegetation around the site (Figure 4-13). The radiocarbon dates (Table 4-2) show the early Holocene age of the sediments. The environmental conditions were warmer than today, corresponding to the Holocene thermal optimum.

PZ IV spectra reflect some climate deterioration that occurred during the late Holocene at about 3.3 kyr BP. However, the climate was still warmer than today and shrubs (*Betula* sect. *Nanae* and *Alnus fruticosa*) grew at a location where no shrubs grow today. The uppermost pollen spectrum is dominated by Poaceae with some Cyperaceae and *Betula* sect. *Nanae,* reflecting a further deterioration. However, the climate was still warmer than today as evidenced by high pollen numbers of *B.* sect. *Nanae* which is not present in the area nowadays.

4.5.4 Ostracod studies

4.5.4.1 Eemian sequences

Taxonomy

Remains of ostracods have been found in most of the lacustrine sediment samples of Eemian sequences. Taberal deposits situated below the lacustrine sediments generally lack ostracods, but in the overlying zone of section L7-14 which represents a transition from a lacustrine to a boggy milieu a rich ostracod fauna has been observed.

Changing abundances of ostracods are obvious for several time slices within the record. Especially at the bottom of the lacustrine sediments, ostracods are found rarely or not at all in sediment samples, most likely due to unstable conditions during the early stages of thermokarst lake formation. However, also within the lacustrine sediments but further upwards, the ostracod record is inconsistent, probably indicating periods of desiccation or other changes in the aquatic regime. A total of 14 Eemian ostracod species was identified (Figure 4-14). The species composition differs between the deposits from Bol'shoy Lyakhovsky Island and Oyogos Yar coast since the abundance of each species differs between the sites. For example, *Limnocythere falcata* is very common in deposits from Oyogos Yar, but rare on Bol'shoy Lyakhovsky Island while *L. suessenbornensis* and *Cypria exsculpta* are generally lacking on Bol'shoy Lyakhovsky Island. The three species *L. falcata*, *L. suessenbornensis,* and *Eucypris dulcifons* from the Eemian sequences are not reported from modern environments, but are known from Eemian deposits in Germany (Diebel 1968; Diebel and Pietrzeniuk 1969). Common species from both coastal exposure sites are *Candona candida*, *Fabaeformiscandona levanderi*, *F. rawsoni*, *Limnocytherina sanctipatricii* and *Ilyocypris lacustris*. The modern ecological requirements of these species are not very specific since these species are tolerant to temperature and salinity variations. *C. candida* and *F. rawsoni* are known from modern thermokarst lakes in Central Yakutia (Wetterich et al. 2008b) and *L. sanctipatricii* from polygon ponds in North Yakutia (Wetterich et al. 2008a).

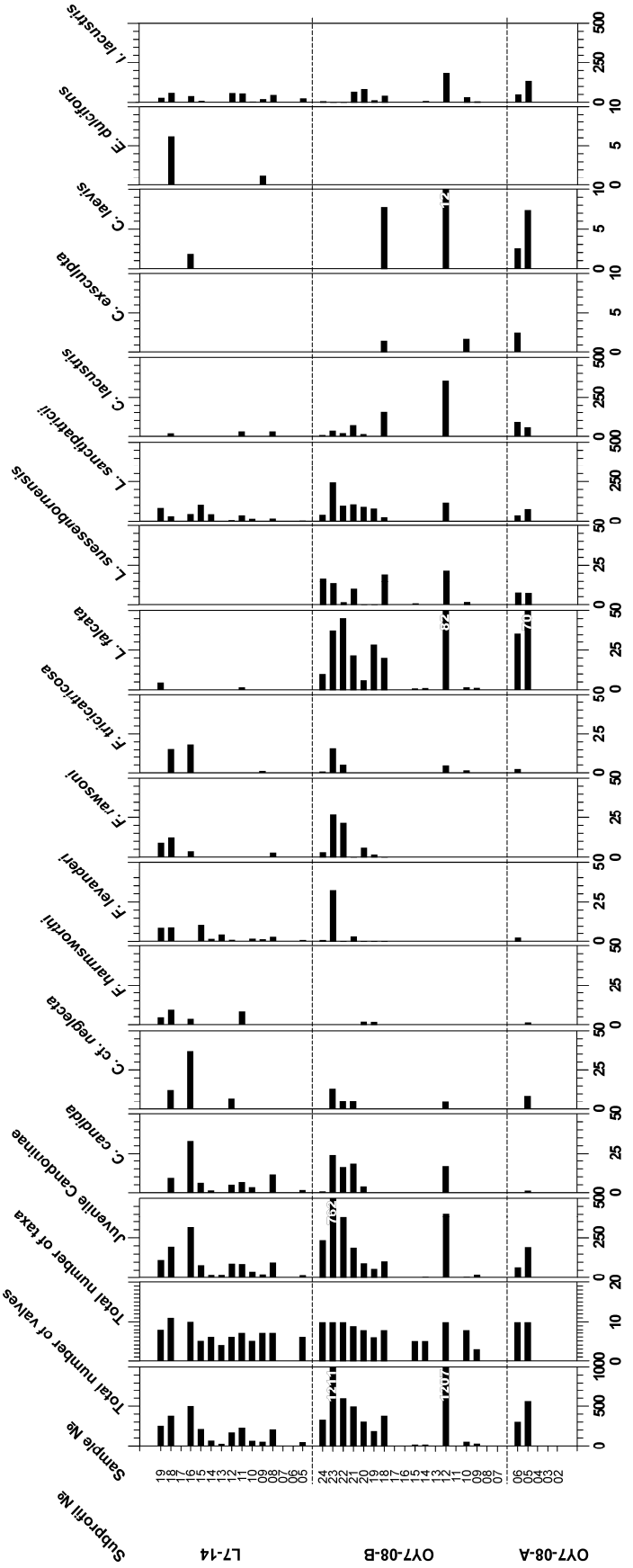

Figure 4-14 Ostracod species assemblages from Eemian deposits of Bol'shoy Lyakhovsky Island and Oyogos Yar. Note varying scales.

Stable isotopes

The stable isotope record of ostracod calcite from the Eemian period was analysed in samples from section Oy7-08 (Table 4-4). The mean $\delta^{18}O$ record of *C. candida* during this period ranges from −11.3 to −12.6‰, while the record of species *C. lacustris* varies from −12.2 to −14.5‰ (Table 4-4).

Table 4-4 Oxygen and carbon stable isotope signatures (mean values, maxima and minima) of ostracod calcite from different periods

Site	Uncal. ages [kyr BP]	№ of sub-samples	Species	$\delta^{18}O$ mean [‰]	$\delta^{18}O$ max [‰]	$\delta^{18}O$ min [‰]	$\delta^{13}C$ mean [‰]	$\delta^{13}C$ max [‰]	$\delta^{13}C$ min [‰]
North Yakutia*	modern	1	*C. candida*	−14.97	--	--	−6.91	--	--
Central Yakutia**	modern	6	*C. candida* / *C. muelleri-jakutica*	−10.34	−8.88	−11.64	−1.96	0.24	−5.75
L7-08	11.6 to 10.1	8	*C. candida*	−13.37	−12.34	−15.12	−5.62	−4.23	−7.40
		10	*C. lacustris*	−14.10	−13.03	−14.89	−7.54	−6.28	−9.93
R33 A1***	12.5	21	*C. candida*	−12.99	−12.21	−13.93	−6.13	−5.29	−6.77
		19	*C. lacustris*	−14.01	−12.82	−14.86	−7.82	−6.04	−9.77
Oy7-08	Eemian	5	*C. candida*	−11.70	−11.25	−12.59	−5.05	−4.70	−5.50
		8	*C. lacustris*	−13.08	−12.15	−14.48	−8.53	−7.28	−10.2

*Wetterich et al. (2008a); **Wetterich et al. (2008b); ***Andreev et al. (2008)

The difference of > 1‰ between the mean values of the two species is probably due to species-dependent metabolic (vital) offsets. Such an effect leads to ^{18}O-enrichment, compared to the precipitation of calcite when organismal isotopes are in equilibrium with the lake water (Hammarlund et al. 1999). The vital offset of *Candona candida* was quantified as 2.1 ± 0.2‰ by von Grafenstein et al. (1999) and as +2.5 to +3‰ by Keatings et al. (2002), whereas the vital offset of *Cytherissa lacustris* is lower at 1.2 ± 0.3‰ (von Grafenstein et al. 1999). The $\delta^{13}C$ values range from −4.7 to −5.5‰ for *C. candida* and from −7.3 to −10.2‰ for *C. lacustris* (Table 4-4).

4.5.4.2 Late Glacial/Holocene sequences

Taxonomy

In sediments from the Late Glacial/Holocene L7-08 and R33 A1 sections on Bol'shoy Lyakhovsky Island, ostracods were found in the lacustrine horizon and in the lower part of the boggy horizon. In total, 11 species have been identified of which *Candona candida*,

Fabaeformiscandona levanderi, *Cytherissa lacustris,* and *Cypria exsculpta* were the most abundant (Figure 4-15).

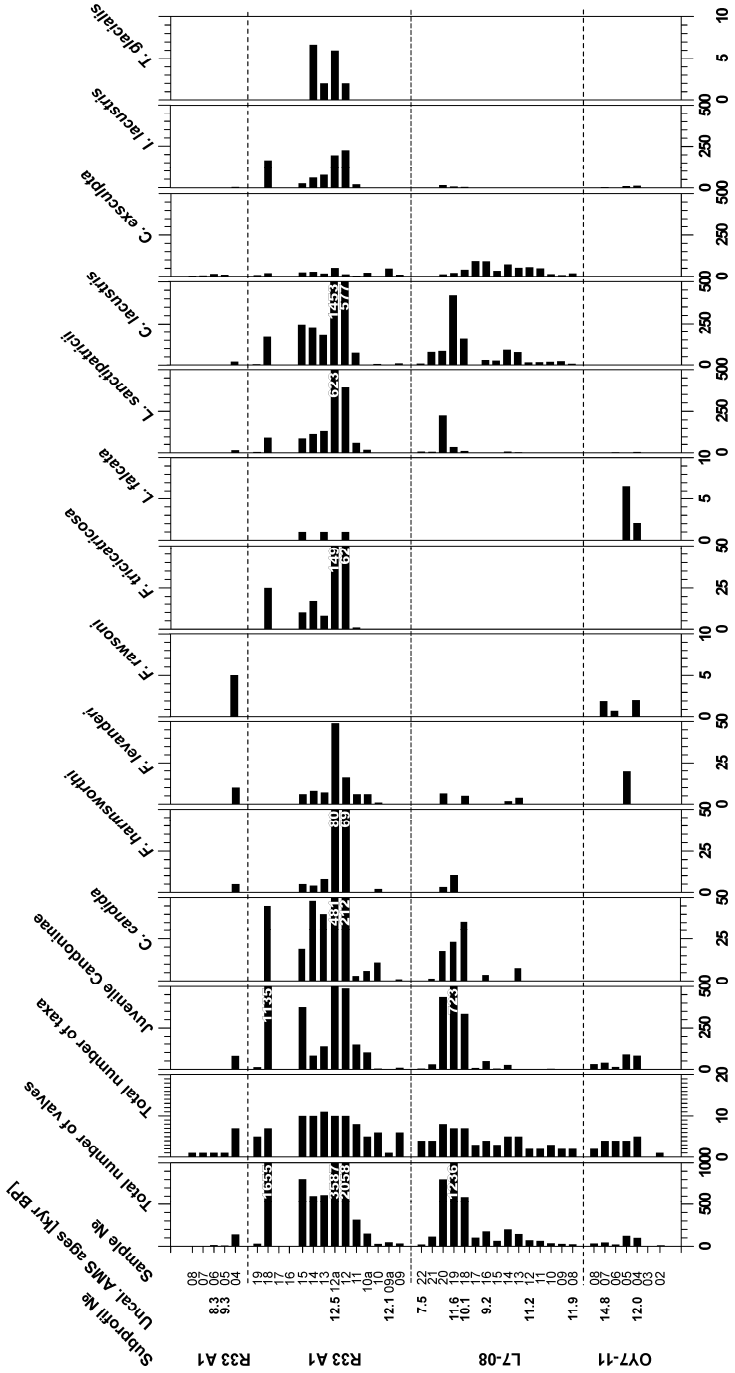

Figure 4-15 Ostracod species assemblages from Late Glacial/Holocene deposits of Bol'shoy Lyakhovsky Island and Oyogos Yar. Note varying scales.

In contrast, the Oyogos Yar Oy7-11 section provided a very poor ostracod record; it included a single valve of juvenile Candoninae in the lowermost taberal deposits, and low numbers of *F. levanderi*, *F. rawsoni,* and *L. falcata* in the overlying lacustrine sediments from the Late Glacial age (Figure 4-15). As in the Eemian records, changing abundances

of ostracods are obvious in several time slices. During the transition from the Late Glacial to the early Holocene, the highest numbers of ostracod remains are seen at about 12.5 kyr BP (samples R33 A1-12 to -15) and at about 11.6 to 10.1 kyr BP (samples L7-08-18 to -20). Such data point to the occurrence of well-developed thermokarst lakes and stable aquatic conditions even before the beginning of the Holocene. Compared to the Eemian records, the modern ecological demands of the most common species in the Late Glacial/Holocene records do not allow differentiation of aquatic conditions; these species are generalists, preferring cold water and tolerating slightly salty conditions. However, except for *Candona candida* the dominant species from the Late Glacial/Holocene record are absent from modern Central Yakutian thermokarst environments (Pietrzeniuk 1977; Wetterich et al. 2008b) probably due to generally warmer water temperatures today.

Stable isotopes

A stable isotope record of ostracod calcite from the Late Glacial/Holocene period was obtained from samples of sections L7-08 and R33 A1, and dated from 12.5 to 10.1 kyr BP (Table 4-4). The $\delta^{18}O$ record of *C. candida* during this period ranges from −12.2 to −15.1‰, and the record of *C. lacustris* ranges from to −12.8 to −14.9‰ (Table 4-4). As in the Eemian stable isotope record, a general shift of about 1‰ between the mean values of the two species has been observed, likely resulting from different species-dependent vital offsets. The $\delta^{13}C$ values range from −4.2 to −7.4‰ for *C. candida* and from −6.0 to −9.9‰ for *C. lacustris* (Table 4-4).

4.6 Discussion and interpretation

4.6.1 Local palaeoenvironmental changes during the Eemian

The lithostratigraphical structure of the Eemian sections at the northern and southern coast of Dimitri Laptev Strait show a similar general pattern of three different horizons which accumulated under different environmental conditions.

The lowermost sequences of taberal deposits represent thawed and subsequently refrozen material which likely accumulated in pre-Eemian times and underwent thawing during the Eemian Interglacial when thermokarst processes led to the formation of lakes and thawed deposits (taliks) below the lakes.

The sedimentological and cryolithological features of the pre-Eemian taberal horizons show single whitish laminations which are interpreted as thaw signs, numerous small dark-grey spots representing strongly decomposed organic matter, and a massive cryostructure. The pollen records (lowermost PZ I of L7-14 and Oy7-08) reveal relatively high amounts of reworked ancient (mineralised) coniferous pollen, and ostracod remains

are absent. Similar results were obtained in formerly described pre-Eemian deposits of Bol'shoy Lyakhovsky Island (Andreev et al. 2004).

The refreezing of the taberal horizons took place in post-Eemian time and the deposits remained frozen until today. Such taberal deposits are covered by the Eemian lacustrine sequence that formed due to warmer conditions during the Interglacial when thermokarst lakes occurred. Under such conditions pre-Eemian ice wedges thawed; at their positions small thermokarst lake basins formed and lacustrine sediments began to accumulate. Distinctive features of the lacustrine sediments are the alternating beds of finely laminated brownish plant detritus and grey sandy silt layers.

The Eemian pollen records (PZ II and III) from both locations show similarities reflecting comparable vegetation. The main difference between the Bol'shoy Lyakhovsky and Oyogos Yar Eemian pollen records is the absence of *Larix* at the northern location. The northern tree line likely reached the Oyogos Yar region during the Middle Eemian, but not the Bol'shoy Lyakhovsky region. Basing on correlation of the studied pollen assemblages with previously studied records (Andreev et al. 2004; Ilyashuk et al. 2006; Kienast et al. 2008) we may assume that the PZ II of L7-14 and Oy7-08 represents the Early to Middle Eemian period. High numbers of *Glomus* spores indicate that vegetation and soils were significantly disturbed, probably due to active erosion processes connected with the melting of Saalian ice wedges and thermokarst lake formation. Rather high numbers of *Artemisia* and the presence of herb pollen taxa such as Brassicaceae, Caryophyllaceae, and Asteraceae show that open plant associations were also common. Dung-inhabiting fungi spores in the pollen spectra indirectly point to the presence of grazing animals around the lake. PZ IIIa (Oy7-08-B) was formed during the Middle Eemian thermal optimum. Climate conditions in the Eemian were warmer than today in northern Yakutia as has already been discussed on the basis of pollen and plant macrofossil data from exposures on Bol'shoy Lyakhovsky Island. Andreev et al. (2004) provided a quantitative climate reconstruction based on a pollen-climate reference data set from northern Eurasia (Tarasov et al. 2005). Mean air temperatures of the warmest month (MTWA) vary from 7.8 to 9.6 °C for the Eemian thermal optimum (modern MTWA at Cape Shalaurova, Bol'shoy Lyakhovsky Island: 2.8 °C; Rivas-Martínez 2007). Using Eemian plant macrofossil records from Bol'shoy Lyakhovsky Island, Kienast et al. (2008) concluded a MTWA of about 12.5 °C for the Eemian optimum. The pollen spectra of PZ IIIb (Oy7-08-B) indicate gradual climate deterioration during the Late Eemian.

The occurrence of numerous well-preserved ostracod remains in the lacustrine horizons points to stable aquatic conditions due to extensive thawing of pre-Eemian permafrost deposits and the widespread occurrence of thermokarst lakes caused by generally warmer climate conditions. The Eemian ostracod assemblages are dominated by species

which tolerate the considerable changes in temperature and salinity regimes that are typical of modern habitats like thermokarst lakes and polygon ponds in the periglacial landscapes of East Siberia.

The Eemian lacustrine deposits are discordantly covered by thick Ice Complex deposits (Yedoma Suite) of late Pleistocene age.

4.6.2 Local palaeoenvironmental changes during the Late Glacial/Holocene

As already described for the Eemian sequences, the Late Glacial/Holocene sedimentological records are also subdivided into taberal, lacustrine, and boggy deposits. The accumulation record of this period based on available radiocarbon dates is not consistent (Table 4-2). Middle Holocene deposits from about 7.5 to 4.0 kyr BP have not been found in the Dimitri Laptev Strait exposure. Similar situations are known from other key regional Quaternary sections of permafrost deposits (Schirrmeister et al. 2002a, b, 2003, 2008a; Sher et al. 2005; Andreev et al. 2008). Thermokarst-related landscape dynamics during interglacial or interstadial warm periods led to extensive melting and reworking of underlying ice-rich deposits, and such processes are likely responsible for the lack of sediment preservation. Low sedimentation rates during the middle Holocene are another possible explanation that to date remains unsubstantiated. Generally, Late Glacial and Holocene deposits mostly appear in the permafrost region of northern Yakutia as filling of thermokarst depressions or as a thin horizon above late Pleistocene sequences. The studied sequences exhibit a sedimentation history in which late Pleistocene Ice Complex deposits dated from about 46.6 to 36.6 kyr BP are discordantly overlain by Late Glacial deposits dated to 14.8 kyr BP and younger. The boundary between the two sequences is visually obvious due to exposure characteristics, and is also distinguished by differences in sedimentological and cryolithological properties. The lowermost sequence is built up of taberal deposits of the former Ice Complex, composed of sandy silt containing peat lenses and thaw signs (whitish laminations) and lens-like reticulated or layered cryostructures with generally low ice content. The pollen data from the taberal horizons point to a Middle Weichselian interstadial vegetation. Due to reworking during thawing and refreezing of the deposits, the possibility of pollen contamination cannot be excluded and therefore the taberal horizon is of minor relevance for the palaeoenvironmental interpretation. Ostracods have very rarely been observed in the taberal deposits, but their occurrence in undisturbed Middle Weichselian Ice Complex sequences has been reported by Wetterich et al. (2005, 2008c).

The taberal horizon is discordantly covered by a lacustrine horizon of Late Glacial/Holocene age. Its lowermost part is composed of cryoturbated peaty palaeosols in both sections on the northern and southern coasts of the Dimitri Laptev Strait. The

overlying lacustrine horizons of alternating beds of clayish silts and plant detritus layers are of lens-like or lens-like layered cryostructure and contain mollusc shells, ostracods, and wood fragments.

Radiocarbon dates of single samples and a comparison with previously studied regional records (Grosse et al. 2007; Andreev et al. 2008) confirm Allerød (PZ IIa of Oy7-11) and Younger Dryas (PZ IIb of Oy7-11) ages of the Late Glacial pollen records. Warmer conditions (MTWA: 8-12 °C) than today have already been reconstructed for the Allerød and the early Holocene, using pollen records from Bol'shoy Lyakhovsky Island (Andreev et al. 2008).

The ostracod records point to stable aquatic conditions during the last period of the Late Glacial. The highest numbers and rich assemblages of ostracod remains were found in such sediments. Obviously, thermokarst development started some time before the Holocene.

The uppermost sequence accumulated under subaerial conditions in a boggy polygonal tundra environment. Ice wedges syngenetic to the boggy deposits are present. Their stable isotope record clearly differs from those of Glacial ice wedges of post-Eemian age, pointing to warmer conditions during the Holocene. Numerous peat inclusions or single peat layers were found in a sandy silt matrix with ice bands and a lens-like cryostructure between single bands which indicate simultaneous (syngenetic) freezing of the sediments at the time of accumulation. An early Holocene shrubby tundra vegetation is reconstructed from the pollen spectra, whereas the pollen spectra indicate late Holocene cooling and a shift to modern tundra vegetation. The ostracod assemblages from the early Holocene are sparse and generally low diverse. As in the Eemian record, the prevailing species are tolerant to changes in the temperature and salinity regimes. The up-filling (aggradation) of the Late Glacial lake environment and its successive transformation into polygonal tundra may be deduced from the ostracod record. Moreover, the preservation of ostracod calcite in an organic-rich milieu such as the boggy horizon is generally poor (Wetterich et al. 2005). Therefore, ostracods likely occurred in Holocene polygonal ponds, but were not preserved due to acidic conditions in peaty deposits.

4.6.3 Palaeoenvironmental interpretation of ostracod calcite $\delta^{18}O$ data

The stable oxygen isotope ($\delta^{18}O$) data from ostracod calcite reflect the stable isotope composition of the host water (at the time of shell formation) which itself mostly depends on temperature regime and evaporation effects (e.g. Wetterich et al. 2008a, 2008b). The stable isotope composition of thermokarst lakes in the permafrost zone is mostly influenced by precipitation waters and, to a lesser degree, by the melt water from the surrounding and underlying permafrost. Available $\delta^{18}O$ annual precipitation data from

Central Yakutia (Station Yakutsk: 1997 to 2006) average about −23.1‰ and from North Yakutia (Station Tiksi: 2003 to 2007) about −24.4‰ (Kloss 2008). These values are fairly similar considering the latitudal distance of about 1500 km between them. Assuming a similar precipitation input, the lake water $\delta^{18}O$ is also influenced by local temperature and resulting evaporation effects which are stronger in Central Yakutia due to higher temperatures (Wetterich et al. 2008b). Consequently, the $\delta^{18}O$ in lake waters is controlled by the climatic setting. The $\delta^{18}O$ ostracod calcite data reflect the lake water composition and can therefore be assumed to indicate the water temperature and evaporation regime of lakes.

Comparing the fossil data to the very scarce modern reference data of ostracod $\delta^{18}O$ and water temperatures where those ostracods are found, some preliminary conclusions for the palaeo-temperature regime of waters can be drawn. As shown in Figure 4-16, heavier stable $\delta^{18}O$ values are obtained from specimens of the Eemian and Late Glacial ostracod *Candona candida* than from the same modern species found today, suggesting conditions of warmer mean water temperatures and/or higher evaporation during the ancient as compared to the modern North Yakutia. Furthermore, when a second modern data set from continental Central Yakutia is compared with the fossil $\delta^{18}O$ records, the fossil records are lighter; this can likely be interpreted as colder and/or lower evaporation conditions for the ancient as compared to the modern Central Yakutia. The rare water temperature data from the North Yakutian site for the months of June and July (relevant for ostracod growth) show averages of T_{June} = 8.4 °C and T_{July} = 11.1 °C (measured in 2007/08, 0.24 m below the water surface; unpublished data from Samoylov Island, Lena Delta; kindly provided by Julia Boike, SPARC group, AWI Potsdam). Distinctly warmer conditions were documented in continental Central Yakutian thermokarst lakes where T_{June} = 19.1 °C and T_{July} = 19.2 °C (measured in 2005, 0.4 m below the water surface; Wetterich et al. 2008b).

Considering the sparse database, a quantitative palaeo-temperature estimation is actually impossible since continuous temperature data are rare and ostracod monitoring in northern regions and accompanying stable isotope analyses are still lacking. However, because the fossil $\delta^{18}O$ values from the Eemian and also from the Late Glacial clearly fall between modern reference $\delta^{18}O$ values of about −15‰ and −10‰ (reflecting mean summer water temperatures of about 10 °C and 19 °C, respectively), an approximate palaeo-temperature range can be assumed for the palaeo-lakes during both periods. Such fairly accurate estimation is also supported by the above mentioned MTWA temperature reconstruction of 7.8 to 9.6 °C (by pollen data) and ≈12.5°C (by plant macrofossil data) for the Eemian thermal optimum, and 8-12 °C (by pollen data) for the Late Glacial/Holocene period.

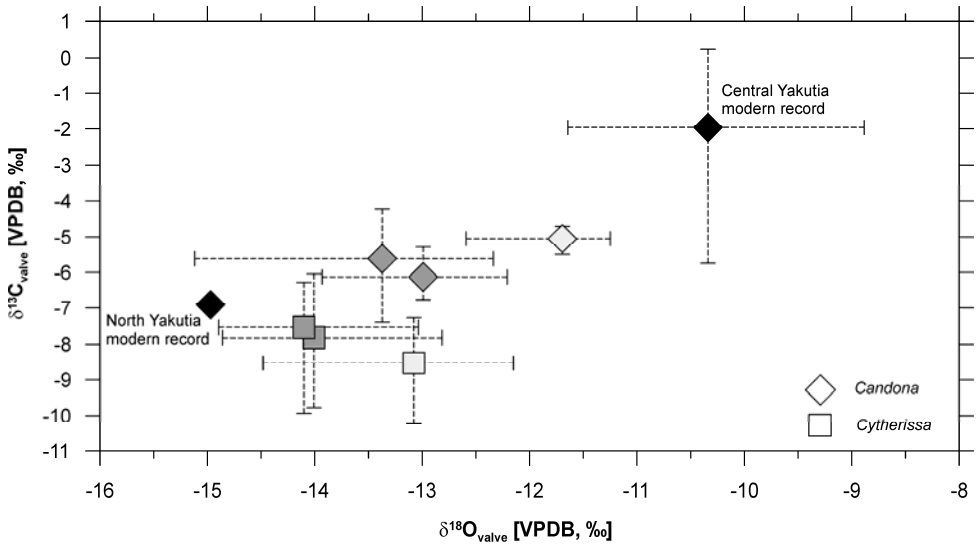

Figure 4-16 Oxygen and carbon stable isotope signatures (mean values, maxima and minima) of ostracod calcite from different periods. Eemian records are given by light grey symbols, Late Glacial records by dark grey symbols and modern reference records from thermokarst lakes in North Yakutia (Lena Delta; Wetterich et al. 2008a) and Central Yakutia (Wetterich et al. 2008b) by black symbols. Diamonds indicate data from the species *Candona candida* (and *Candona muelleri-jakutica* for the modern record from Central Yakutia) and squares indicate data from the species *Cytherissa lacustris*

4.7 Conclusions

The studied permafrost exposures on the northern and southern coasts of the Dimitri Laptev Strait contain warm-stage Eemian Interglacial and Holocene deposits as well as underlying deposits reflecting the glacial-interglacial transitions. The multi-proxy palaeoenvironmental record from both periods constructed using sedimentological, cryolithological, and palaeontological methods indicates a general pattern of landscape development according to changes in the climatic setting. The transition from glacial to interglacial conditions is accompanied by extensive thawing of permafrost (thermokarst), which leads to the formation of basins, or so-called thermokarst depressions. Thawing ice wedges of the former glacial period are transformed into ice wedge pseudomorphs and preserve well-bedded deposits of the thermokarst lakes developing above. Underlying deposits transform into taberal deposits due to thawing. Lacustrine sequences above the taberal horizons contain rich palaeontological records. Further climate change leading to colder and drier conditions in the case of the Eemian/Early Weichselian boundary results in disappearing thermokarst lakes and the development of a polygonal tundra landscape which is reflected in thick sequences of late Pleistocene Ice Complex. In the case of the Late Glacial/Holocene boundary, lakes which had already formed during the Late Glacial warming period at ≈12 kyr BP (Allerød) underwent succession stages and were

transformed into boggy polygonal tundra with considerable peat accumulation. Evidence of the three landscape development stages, including (1) thermokarst-induced formation of basins, (2) accumulation of lacustrine sequences, and (3) transformation of lake-dominated areas into polygonal tundra, was obtained and studied for both time slices, and these stages are therefore considered to be of stratigraphical significance (Figure 4-17).

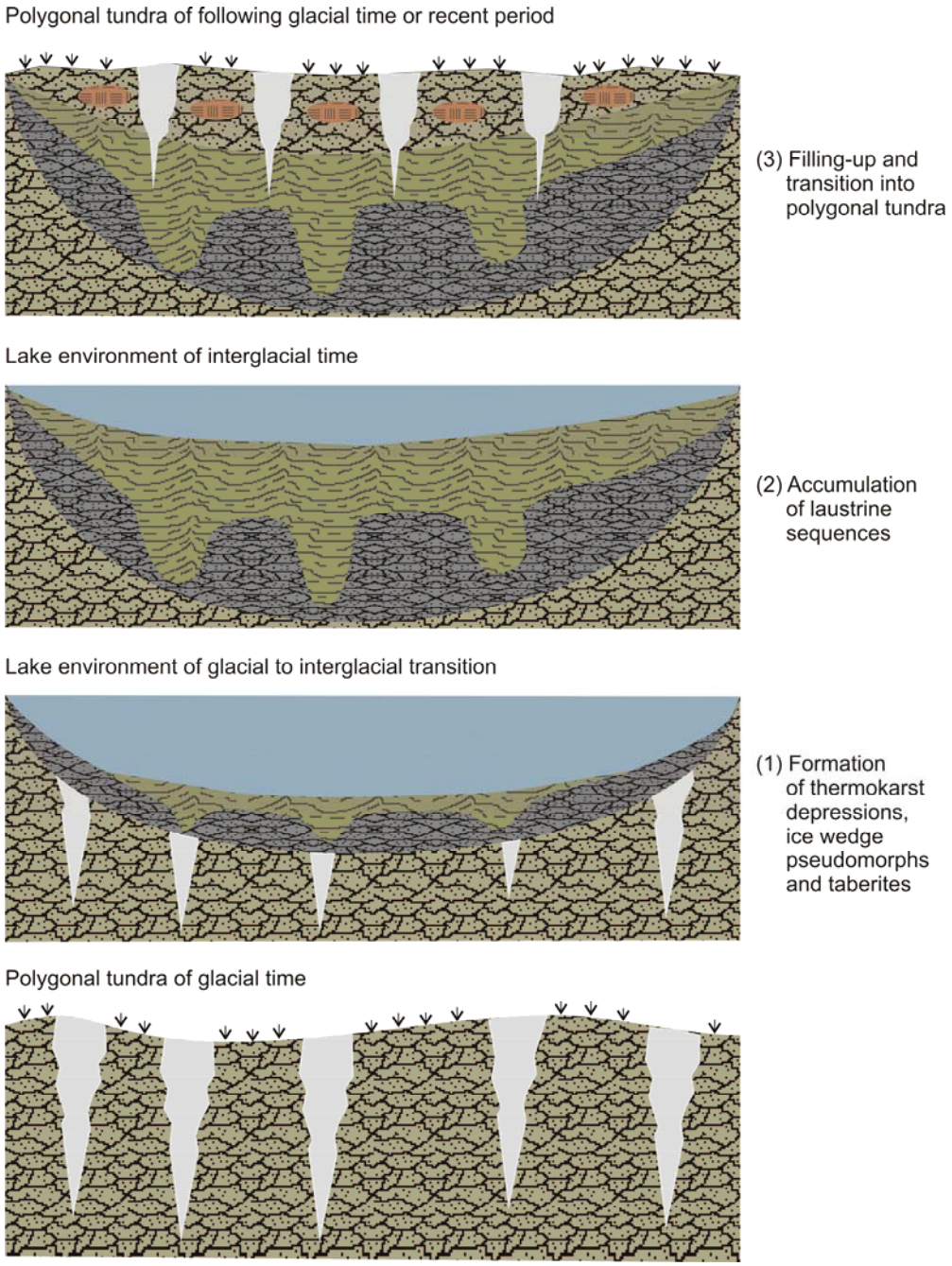

Figure 4-17 General scheme of glacial-interglacial landscape dynamics controlled by thermokarst processes

The Eemian record presented here is to be one of the northernmost terrestrial records in existence from the last Interglacial. Abundant *Larix* pollen have been found in Middle

Eemian deposits from Oyogos Yar, but are absent from the northerly Middle Eemian records from Bol'shoy Lyakhovsky Island (Andreev et al. 2004; Ilyashuk et al. 2006), likely indicating that the northern tree line was located near the Oyogos Yar region during the Eemian thermal optimum. The Late Glacial/Holocene records correlate very well with data from the Laptev Sea coastal lowland concerning the onset of permafrost degradation during the Allerød and the general vegetation dynamics (Grosse et al. 2007; Andreev et al. 2008).

In the course of ostracod studies depositional records like those described above can be used for taxonomical and geochemical studies. The Eemian associations contain more taxa than the Late Glacial/Holocene. However, apart from three species (*C.* cf. *neglecta, L. suessenbornensis, L. laevis*) in the Eemian and one species (*T. glacialis*) in the Late Glacial/Holocene sequences the ostracod associations are similar. Comparable habitats in thermokarst lakes are therefore assumed for both periods. Increasing occurrence of ostracods in lacustrine deposits could be correlated with the Eemian thermal optimum and the Allerød warm period. Only six of the species presented here also occurred in the Late Weichselian association studied at Bykovsky Peninsula and in the Lena River Delta (Wetterich et al. 2005, 2008c). This first presentation of interglacial freshwater ostracod associations from Arctic periglacial environments can be used as a reference for understanding similar Quaternary periglacial records in Europe.

The application of ostracods as a palaeo-proxy in permafrost sediments by comparing ancient data to modern reference data is a relative new approach to understanding palaeo-archive permafrost; expanding the modern database of species ecology, the modern geochemical reference data of host waters, and the database of stable isotope data from ostracod calcite would improve the accuracy of this method. However, initial assumptions that can be made from comparing Eemian and Late Glacial fossil ostracods to modern reference assemblages were presented here. The $\delta^{18}O$ data from the fossil ostracods indicate an approximate mean summer water temperature range between 10 and 19 °C in the palaeo-lakes during both periods. Future monitoring of modern associations in thermokarst lakes and polygonal ponds in connection with continuous climate and hydrological observations will expand the database and improve our ability to utilize ostracods as a palaeoenvironmental indicator.

5 Synthesis

5.1 Taxonomy and ecology of ostracods

One goal of the studies presented here is to inventory and compare modern and fossil freshwater ostracod assemblages from high-latitude Siberian regions, and to estimate current ostracod-relevant environmental parameters (Table 5-1). Since reliable and complete modern ostracod and limnological data from Arctic Siberia are very rare, studies of modern ostracod taxonomy and ecology have been performed at representative sites in North, Northeast, and Central Yakutia in order to obtain reference data for fossil applications. Because modern ostracod records are sparse, every study site revealed original data of ostracod species distribution and environmental conditions in Siberian periglacial waters comprising polygonal ponds, thaw lakes, and thermokarst lakes.

Table 5-1 Selected hydrochemical characteristics from modern Yakutian study sites

Study region	№ of sites	Prevailing ostracod habitats	EC mean [mS/cm]	pH mean
North Yakutia* (Lena River Delta)	23	Polygonal waters	0.10	7.39
Northeast Yakutia** (Moma region)	7	Lowland depressions	0.25	7.24
Central Yakutia** (Lena-Amga interfluve, Yakutsk)	8	Thermokarst-affected waters	0.74	8.35

* Wetterich et al. (2008a); ** Wetterich et al. (2008b)

The ostracod taxa have mostly been identified to the species level by valve and soft body characteristics, but due to the rarity of reference collections several taxa were only determinable to genus level (Table 5-2 on page 103). One taxon is represented only by unidentified juvenile Candoninae. The taxonomical records include 14 taxa from 23 North Yakutian sites (71-72 °N, 126-127 °E), mainly polygonal ponds and thaw lakes, on islands of the Lena River Delta (Chapter 2). Seven Northeast Yakutian sites (66 °N, 143 °E) in the Moma River region produced specimens from 11 taxa only, thus exhibiting the lowest diversity, whereas eight Central Yakutian sites (61-62 °N, 129-132 °E) near the town of Yakutsk and on the Lena-Amga interfluve are the most diverse, with 16 taxa identified (Chapter 3). The records reveal regional differences in the environmental conditions that influence species distribution. As we move from North to South, decreasing latitude means increasing mean monthly and yearly temperatures, decreasing precipitation, and increasing continentality, i.e. influence of evaporation on water characteristics (Figure 1-4 on page 11, Table 1-2 on page 12); habitat-specific parameters differ as well between the three regions studied (Chapters 2 and 3, Table 5-1).

The tundra landscapes of North Yakutia are characterised by shallow polygonal waters in different stages of development which serve as primary habitat for ostracods. These waters are mainly precipitation-fed and are therefore very low in ionic content (measured as electrical conductivity, EC); in addition, the open water period that defines the period of active growth for ostracods is only about three months long. Therefore, living conditions for ostracods in the northernmost sites are fairly extreme. Thermokarst-affected waters in the taiga landscapes of Central and Northeast Yakutia offer more favourable conditions since these waters are, in general, warmer and ice-free for a longer period of time. As compared to the northern sites, the ionic content of Central Yakutian waters is higher due to higher evaporation rates and greater meltwater supply from frozen deposits around the lakes caused by higher ground temperatures and a thicker unfrozen active layer during summer. Consequently, the variability in the environmental setting is higher and the ostracod species diversity is therefore greater (Figure 3-7 on page 51).

The same species may occur in temperate regions of Europe or elsewhere, and also at higher latitudes; the higher-latitude populations must tolerate extremely short periods of time in which to complete their life cycle, large water temperature variations, and the ionic and nutrient contents that are generally characteristic of arctic and subarctic waters. Therefore, the ecological ranges in which these species could occur at mid-latitudes is expanded when we consider data from northern environments (Figure 2-7 on page 26, Figure 3-8 on page 51).

Concerning the modern distribution of ostracods, the species *Candona candida* (O.F. MÜLLER, 1776) and *C. muelleri jakutica* PIETRZENIUK, 1977 are present in all three study regions in Yakutia, whereas the dominant species from North Yakutia, *Fabaeformis-candona pedata* (ALM, 1914), was not found in more southerly sites, where *Candona weltneri* HARTWIG, 1899 was one of the most common species.

The taxonomic position of several species could be adapted to modern nomenclature. In particular the species *Fabaeformiscandona pedata* and *Fabaeformiscandona inaequivalvis* (SARS, 1889) formerly belonging to the genus *Candona* have been re-evaluated according to their soft body characteristics. According to Meisch (2000) the species *Physocypria kraepelini* G.W. MÜLLER, 1903 found in Central Yakutia most likely corresponds to the species *Physocypria fadeewi* DUBOWSKY, 1927 formerly described by Pietrzeniuk (1977).

The fossil ostracod records obtained from permafrost exposures at the Laptev and East Siberian seacoasts include particularly rich assemblages from several periods of the late Quaternary. The oldest records have been obtained from Eemian interglacial deposits. Generally, permafrost deposits can be regarded as an informative ostracod archive since ostracod shells are preserved by freezing and can be identified under the microscope

after standard preparation. However, ostracod shells are poorly preserved under pre-sedimentary acidic conditions that existed in, for instance, the peaty deposits of early Holocene tundra environments. Normally, large numbers of fossil ostracods are found in deposits from all warm stages and temperate periods of the late Quaternary such as the Eemian Interglacial, the Middle Weichselian Interstadial, the transition from the Late Weichselian to the early Holocene (including the Allerød period), and the late Holocene. As many as 15 taxa were identified in Eemian thermokarst lake deposits, and as many as 14 in Middle Weichselian polygonal pond deposits (Table 5-2). Fossil ostracods could only rarely be found in deposits from cold stages like the Early and the Late Weichselian Glacials. During these glacial periods the climate was generally dry, and cold and water bodies were unstable; because these conditions are unfavourable for aquatic organisms like ostracods, poor records of not more than six taxa are unsurprising (Table 5-2).

Two deposits types within Quaternary permafrost sequences have been found to be promising for ostracod studies: (1) filled areas of formerly low-centred polygons where intrapolygonal shallow ponds occurred, and (2) thermokarst lake deposits. The first type was chiefly found in Late Pleistocene Ice Complex sequences; the second type, in which formation is controlled by thermokarst processes, prevails in sequences from warm stages. Several species could be found as numerous and common fossils in permafrost sequences from different periods. In particular, the species *Candona muelleri jakutica,* which is numerous in modern records, could be indentified in deposits from the Early and Middle Weichselian, and also in late Holocene. All lacustrine records, except for those from the Early and Late Weichselian, contain shells of *Fabaeformiscandona harmsworthi* (SCOTT 1899), a species likely endemic to the Arctic that nowadays occurs in North Yakutia. Fossils of the species *Fabaeformiscandona rawsoni* (TRESSLER, 1957), present in modern Central Yakutia, have also been obtained from warm-stage deposits. Other common fossil ostracods belong to the species *Limnocytherina sanctipatricii* (BRADY & ROBERTSON, 1869) and *Ilyocypris lacustris* KAUFMANN, 1900 which are rare or lacking in the modern environments studied. Four species without a modern record (*Limnocythere falcata,* DIEBEL, 1968; *L. goersbachensis,* DIEBEL, 1968; *L. suessenbornensis,* DIEBEL, 1968; and *Eucypris dulcifons,* DIEBEL & PIETRZENIUK, 1969), but described from Quaternary lacustrine deposits in Germany (e.g. Diebel 1968; Diebel and Pietrzeniuk 1969, 1975, 1978a) were also frequently found in the warm stage sediments studied.

Taking into account the generally sparse database and comparing the total of 42 identified taxa in modern and fossil records, ten taxa could be found in both the modern and the fossil periglacial environments studied, whereas 18 taxa only occur today and 14 taxa, including some extinct species, have only been described from fossil records (Table 5-2).

Table 5-2 Overview of modern and fossil ostracod species. Detailed information about specific localities given in Chapter 2 (a), Chapter 3 (b), Annex I (c), Chapter 4 (d), Annex II (e). Very rare occurrences (in one or two samples): one cross; rare occurrences (in more than two samples): two crosses; common occurrences (in more than 50 % of all samples of one dataset): three crosses

	Period	Modern environments			Late Holocene	Late Weichselian / Early Holocene		Late Weichselian (Sartan)	Middle Weichselian (Kargin)		Early Weichselian (Zyrian)	Eemian (Kazantsevo)
	Radiocarbon ages [kyr BP]				3	14-7.5	15-7.5	34-14	48-34	41	58-53	
	Locality	Lena Delta[a]	Moma Region[b]	Amga / Yakutsk[b]	Bykovsky[c]	Bykovsky[c]	Laptev Strait[d]	Bykovsky[c]	Bykovsky[c]	Lena Delta[e]	Bykovsky[c]	Laptev Strait[d]
	Region	North Yakutia	NE Yakutia	Central Yakutia	North Yakutia							
	№ of samples	23	7	8	4	2	38	2	12	1	3	26
	№ of taxa	14	11	16	9	11	12	2	14	4	6	15
1	Juvenile Candoninae	xxx	xxx	xxx	xxx	x	xxx	x	xxx		xx	xxx
2	*Candona* cf. *acutula*				x	x			x			
3	*C. candida*	x	x	xx			xx					xxx
4	*C. combibo*								xx			
5	*C. muelleri jakutica*	xx	xxx	xxx	x				xxx	x	xx	
6	*C. cf. neglecta*											xx
7	*C. weltneri*		x	xxx								
8	*Pseudocandona compressa*			xx								
9	*Fabaeformiscandona acuminata*		x	x								
10	*F. fabaeformis*		x	x								
11	*F. harmsworthi*	xxx			xxx	x	xx		xxx	x		xx
12	*F. hyalina*	x		xx		x						
13	*F. inaequivalvis*		xx									
14	*F. lapponica* var. *arctica*									x		
15	F. levanderi				x	x	xx	x	xxx		x	xxx
16	*F. pedata*	xxx										
17	*F. protzi*	xx										
18	*F. rawsoni*			x		x	xx		xx			xx
19	*F. tricicatricosa*	x					xx					xx
20	*F.* sp. 1	x										
21	*F.* sp. 2	x										

Table 5-1 Continuation

Period		Modern environments			Late Holocene	Late Weichselian / Early Holocene		Late Weichselian (Sartan)	Middle Weichselian (Kargin)		Early Weichselian (Zyrian)	Eemian (Kazantsevo)
Radiocarbon ages [kyr BP]					3	14-7.5	15-7.5	34-14	48-34	41	58-53	
Locality		Lena Delta[a]	Moma Region[b]	Amga / Yakutsk[b]	Bykovsky[c]	Bykovsky[c]	Laptev Strait[d]	Bykovsky[c]	Bykovsky[c]	Lena Delta[e]	Bykovsky[c]	Laptev Strait[d]
Region		North Yakutia	NE Yakutia	Central Yakutia	North Yakutia							
№ of samples		23	7	8	4	2	38	2	12	1	3	26
№ of taxa		14	11	16	9	11	12	2	14	4	6	15
22	*Bradleystrandesia reticulata*	x	x							x		
23	*Limnocythere inopinata*			x								
24	*L. falcata*				xxx	x	xx		xxx		x	xxx
25	*L. goersbachensis*					x			xx			
26	*L. suessenbornensis*											xx
27	*Limnocytherina sanctipatricii*	x			x	x	xx		x		x	xxx
28	*Cytherissa lacustris*						xxx					xx
29	*Cypris pubera*			x								
30	*Eucypris dulcifons*				xxx	x			xx		x	x
31	*Tonnacypris glacialis*	x					xx		x			
32	*Cypria exsculpta*						xxx					xx
33	*C. ophtalmica*	x										
34	*Physocypria kraepelini*		x	xx								
35	*Cyclocypris* sp.			x								
36	*C. laevis*											xx
37	*C. ovum*		xxx	xx								
38	*Dolerocypris fasciata*		x	x								
39	*Ilyocypris* sp.											
40	*I. decipens*			x								
41	*I. lacustris*				xxx	x	xx		xxx			xxx
42	*Trajancypris* sp.								x			

Along with climatic and environmental variability through space and time, the dominance of modern taxa without fossil analogues is likely explainable by selective preservation of several species in fossil records and higher sampling resolution in modern studies.

5.2 Geochemistry of ostracods

Element ratios (Sr/Ca and Mg/Ca)

The geochemical properties of the ostracod calcite that precipitates from the host water at the time of shell secretion are commonly regarded as a spatially- and temporally-restricted reflection of the host water composition (Griffiths and Holmes 2000). In particular, stable isotopes of oxygen and carbon ($\delta^{18}O$, $\delta^{13}C$) as well as molar element ratios of strontium and magnesium to calcium (Sr/Ca, Mg/Ca) in ostracod calcite have already been studied and applied in palaeoenvironmental reconstructions (Chivas et al. 1986; Engstrom and Nelson 1991; Xia et al. 1997a, b, c; Keatings et al. 2002, 2006a, b). Modern data describing the geochemical properties of high-latitude ostracod calcite and fossil applications of these data are widely lacking in the literature, and are first presented in this thesis.

Concerning Sr/Ca and Mg/Ca element ratios, the relationship between the element content in ostracod calcite and in the host water which controls the uptake of these elements is usually expressed as the partition coefficient $D(M) = (M/Ca)_{valve} / (M/Ca)_{water}$, where M can either be Mg or Sr, and M/Ca ratios are molar ratios. In this context the Sr/Ca element ratio of water is regarded as indicative of salinity, whereas the Mg/Ca ratio of water depends on the temperature and salinity regimes (e.g. Boomer et al. 2003). However, other factors also control the elemental composition of ostracod calcite, such as the biological effect of temperature-dependent metabolic rates and ionic uptake (e.g. Dettmann et al. 2002); the relationship between the elemental composition of host waters and of ostracod calcite is as yet not fully understood (Ito et al. 2003).

In the North Yakutian study sites in the Lena River Delta (Chapter 2) the generally very low ionic content of the waters (EC_{mean} = 0.1 mS/cm; Table 5-1) is reflected in narrow arrays of element ratios in water and consequently in ostracod calcite. Therefore, the elemental geochemistry data represent the lower endmember on a scale of such proxy data. The correlation between element ratios in host waters and in the calcite of *Fabaeformiscandona pedata,* the most common ostracod species in this data set, is weak or lacking (Figures 2-11 and 2-12 on page 31) because there is no corresponding gradient in host water element ratios. The average partition coefficients *D*(Sr) for live-caught specimens of *F. pedata* were calculated: *D*(Sr) = 0.33 ± 0.06 (1σ) for female adults and *D*(Sr) = 0.32 ± 0.06 (1σ) for male adults. The Mg/Ca ratios in host waters and in the calcite of *F. pedata* are not correlated due to the temperature dependence of Mg partitioning and to the very low Mg/Ca ratios in waters. At the opposite end of the spectrum, host waters studied at the Northeast and Central Yakutian sites (Chapter 3) were generally higher in ionic content (EC_{mean} = 0.25 mS/cm, EC_{mean} = 0.74 mS/cm; Table 5-1) than those at the northernmost sites because of higher evaporation rates and greater meltwater supply.

Thus, the host water element ratio gradients are larger, resulting in better correlations between Sr/Ca and Mg/Ca ratios in the host waters and in the calcite of the common ostracod species *Candona muelleri jakutica* and *Candona weltneri* (Figures 3-11 and 3-12 on page 54). Average partition coefficients were calculated: D(Sr) = 0.32 ± 0.03 (1σ) for live-caught *C. muelleri jakutica*, and D(Sr) = 0.38 ± 0.05 (1σ) for live-caught *C. weltneri*. Generally, the element ratios in ostracod calcite are correlated with the composition of host waters, if the species studied are found in higher frequencies and over significant ranges in the host water proxies. No correlation was found between EC measurements, which express ionic content (i.e. salinity), and either lake water or ostracod calcite Sr/Ca ratios due to the very broad scatter in Sr/Ca values at low EC values below 0.5 mS/cm (Figure 3-14 on page 61). Such effects could not be explained by the field data collected during this study; an explanation likely requires research in a laboratory setting under conditions of fixed salinities and temperatures in order to understand metabolic controls on the ionic uptake from host water into ostracod calcite. Consequently, the element ratios of fossil ostracod calcite were not studied as part of the work presented in this thesis.

Stable isotopes ($\delta^{18}O$, $\delta^{13}C$)

In (palaeo-) limnological studies, the stable oxygen ($\delta^{18}O$) and carbon ($\delta^{13}C$) isotope records of ostracod calcite are considered to provide a restricted reflection of the isotopic composition of host water and total dissolved inorganic carbon (TDIC) at the time of shell secretion (e.g. Griffiths and Holmes 2000).

Lake water $\delta^{18}O$ is mainly controlled by precipitation, drainage basin hydrology, groundwater input, the precipitation/evaporation ratio, the residence time of water, the size of the water body, and the hydrochemical properties and temperature of the lake water (e.g. Kelts and Talbot 1990; Schwalb 2003; Leng and Marshall 2004). The $\delta^{18}O$ of ostracod calcite is commonly used as a proxy for temperature of the lake water (e.g. Chivas et al. 1993; Xia et al. 1997b; von Grafenstein et al. 1999).

When stable isotope compositions of host waters and ostracod calcite are compared, interspecific and intraspecific variations are obvious. The timing of shell calcification in different seasons and at different temperatures, species-dependent preferences for different microhabitats, and species-dependent metabolic effects on isotope fractionation likely control the ostracod calcite composition (e.g. Heaton et al. 1995; von Grafenstein et al. 1999). Metabolic (vital) effects lead to ^{18}O enrichment relative to the ^{18}O content of inorganic calcite precipitated in isotopic equilibrium with the lake water (Hammarlund et al. 1999); these effects must be quantified using modern datasets if stable isotope data from fossil ostracods are to be reliably interpreted.

The $\delta^{18}O$ - δD plots of host waters reveal evaporation effects at all study sites (Figures 2-4 and 3-4 on pages 23 and 48). The waters are mainly affected by the general climatic setting, the water source (precipitation or river water), and the influence of meltwater from the frozen ground, and the $\delta^{18}O$ in host waters and ostracod valves are correlated if the species studied were found in high frequencies and over large gradients in the host water proxies (Figures 2-13 and 3-9 on pages 33 and 52).

Because of temperature and vital effects, the $\delta^{18}O$ is shifted to heavier values in ostracod calcite than in the host water in all study regions. The near 1:1 relationship of $\delta^{18}O$ found in waters and valves in the North Yakutian data set (Chapter 2) could be quantified as a mean shift of Δ_{mean} = 2.2‰ ± 0.5 (1σ) for modern *F. pedata* ($\Delta = \delta^{18}O_{valve} - \delta^{18}O_{water}$ [‰]; Xia et al. 1997b). The shift is not dependent on $\delta^{18}O$ of the host waters and its temperature dependence is reflected in the variations of the shift (between Δ_{min} = +1.1‰ and Δ_{max} = +3.2‰). When the minima and maxima in the shift and in the water temperature (T_{min} = 5.9 °C and T_{max} = 15.3 °C) are compared, a temperature-dependent $\delta^{18}O$ fractionation can be shown for *F. pedata;* increasing temperature leads to smaller shifts (Figure 2-14 on page 34). Such insights are useful for a reliable interpretation of stable isotope data from fossil ostracod calcite. The temperature-independent vital effect on $\delta^{18}O$ fractionation as compared to the $\delta^{18}O$ fractionation of inorganic calcite in equilibrium was quantified as 1.4‰ for the species *F. pedata*.

The relationship between EC and $\delta^{18}O$ of lake waters as a likely evaporation-controlled expression of ionic concentration (salinity) was studied in the Central and Northeast Yakutian sites where the data showed the existence of an EC gradient from about 0 to 6 mS/cm (Chapter 3).

A logarithmic correlation between $\delta^{18}O$ of lake water and water EC has been found (Figure 3-13 on page 59) which is controlled by Rayleigh distillation processes, wherein light isotopes evaporate faster than heavy ones leading to nonequilibrium enrichment of the residual water (Clark and Fritz 1997). Depending upon relative humidity, this process leads to an asymptotic increase in $\delta^{18}O$ values under high evaporation conditions; a steady-state value is reached which is strongly influenced by the salinity of the residual water (e.g. Gat 1979, 1981). However, because this interpretation is based on few data, it must be considered a provisional explanation for the observed scatter. The correlation between EC and $\delta^{18}O$ of ostracod calcite is weak (Figure 3-13 on page 59) due to the sparse database and the numerous controls on ostracod isotope uptake. More data and sampling of time-series during the ice-free season are required to elucidate this relationship.

The $\delta^{13}C$ in TDIC reflects changes in carbon quality and sources and bioproductivity within a lake and is controlled by fractionation during several carbon cycles; the most

important influences are the isotopic composition of inflows, organic decay, bacterial processes, CO_2 exchange between air and lake water, and photosynthesis/respiration of aquatic plants. (e.g. von Grafenstein et al. 1999; Schwalb 2003; Leng and Marshall 2004). The last two controls are characterised by high seasonal and even daily variability; thus it is more difficult to interpret these data, since periodic sampling during the open-water season is required to register carbon cycle dynamics. Therefore, reliable correlations between the $\delta^{13}C$ data from host waters and from ostracod calcite have not been found. The $\delta^{13}C$ records from all study sites scatter over great ranges (Figures 2-15 and 3-10 on pages 37 and 53) and any interpretation of such relationships is complicated.

Geochemical analyses of modern and fossil ostracod calcite require sufficient material in order to ensure reliable multiple measurements according to rigorous analytical procedures. Furthermore, the dominant species with greatest numbers of valves differ between modern and fossil records. Therefore, the comparison of fossil ostracod data and modern analogues suffers because data were obtained from different species and the elemental and stable isotope uptake from the ambient water into the ostracod shell is obviously controlled by species-specific metabolic (vital) effects. Such problems are apparent in this thesis, and they are intensified by the generally sparse data base for both modern and fossil ostracods. Dominant modern species such as *Fabaeformiscandona pedata* from North Yakutia or *Candona weltneri* from Central Yakutia were not detected in fossil assemblages, and their geochemical records are therefore not regarded as an informative modern analogue. Less available geochemical data from *Candona candida* and *Candona muelleri jakutica*, species which are common in both modern and fossil assemblages, were therefore used for the first use of stable oxygen isotopes in ostracod calcite from Siberian permafrost deposits of the Eemian and Late Glacial/Holocene periods (Chapter 4). The average $\delta^{18}O$ value of *Candona candida* from both fossil assemblages was located between the modern reference data mean maximum and minimum of about –15‰ and –10‰ (reflecting mean summer water temperatures of about 10 °C and 19 °C, respectively) from North and Central Yakutia (Figure 4-16 on page 97). Such a fairly accurate estimation indicates warmer mean water temperatures and/or higher evaporation rates as compared to modern conditions in North Yakutia, and consequently colder mean water temperatures and/or lower evaporation rates than in modern Central Yakutia. Supporting palaeo-temperature reconstructions of air temperatures of the warmest month (MTWA) from regional pollen and plant macrofossil data, however, calculated an MTWA of 7.8-9.6 °C (by pollen data) and of about 12.5°C (by plant macrofossil data) for the Eemian thermal optimum, and an MTWA of 8-12 °C (by pollen data) for the Late Glacial and early Holocene periods (Andreev et al. 2004; Kienast et al. 2008).

5.3 Indicator potential of freshwater ostracods in late Quaternary permafrost deposits

In conclusion, the presence of ostracods in permafrost deposits clearly points to the existence of aquatic habitats in the palaeo-environment. Ostracod remains can be regarded as *in-situ* preserved fossils because their thin valves are likely destroyed by intensive re-deposition processes. Since the species assemblages commonly consist of generalists, i.e. species with broad tolerance to environmental parameters like temperature regime or ionic content, and cold-adapted species or species endemic to the Arctic, further deductions from taxonomic records of fossil ostracods are complicated. Surely, the interpretation of fossil ostracod assemblages requires comparison with modern analogues and their current ecological controls. However, shallow ponds in low-centred ice wedge polygons and shallow, less-disturbed shore zones of thermokarst lakes were habitats for freshwater ostracods in the periglacial lowlands of Arctic Siberia during the late Quaternary.

Permafrost deposits from interglacial and interstadial periods are particularly rich in ostracod fossils. On the other hand, the lack or very sparse occurrence of ostracods during glacial or stadial times reflects the corresponding unfavourable harsh environmental conditions. In addition to other palaeontological data from pollen, plant macrofossils, and testate amoebae (rhizopods), ostracod fossil data support the reconstruction of stable shallow aquatic conditions in regional palaeoenvironmental records and complete reconstructions of landscapes such as polygonal tundra plains or thermokarst-affected landscapes. Fossil freshwater ostracods also have the potential to mirror the palaeo-hydrological and palaeo-hydrochemical regimes of periglacial inland waters. Cryolithological and sedimentological records pointing to refreezing of bedded and plant-detritus-rich lacustrine warm-stage deposits can also be confirmed by the occurrence of ostracod fossils. In addition, syncryogenic ice structures in deposits of polygonal ponds reflect the long seasonal freezing period of the entire water and sediment body, as well as the short period during which ostracods live.

However, the indicator potential of freshwater ostracods in Quaternary permafrost deposits is still limited by an uncompleted database which complicates (1) the application of modern reference data to fossil records, and (2) the interpretation of fossil assemblages in multiproxy palaeoenvironmental reconstructions.

In particular, the positive identification of Arctic species according to modern taxonomic nomenclature is complicated by different classifications used in the past by American, Russian, and European researchers. Reference collections, especially for the Russian Arctic, are rare, and probable species synonyms have not yet been ruled out. Because of the dominance of generalists and the lack of specialists, indicator species (e.g. for

temperature, salinity, or water depth) could not be identified in the modern data set. In addition, modern reference data are not available for many fossil species. Synchronous sampling of waters and ostracods at the time of shell calcification would be a desirable monitoring approach for bettering our understanding of complex biogeochemical cycles in waters and biomineralisation processes in ostracod calcite.

Ostracods have up to now been largely unstudied in Arctic periglacial regions; the knowledge of environmental conditions and interactions affecting modern ostracods has been improved and, for the first time, applied to fossil ostracods from Quaternary permafrost deposits. The applicability of common geochemical proxies, i.e. stable isotopes and element ratios in ostracod studies, for further interpretations of environmental parameters was examined and critically evaluated using modern reference data. Furthermore, the species inventory revealed for the first time an ostracod presence in modern periglacial environments and Quaternary sequences in Northeast Siberia. The taxonomical and environmental data provide reference data for related studies. Established preparatory and analytical methods for performing field and laboratory studies on ostracods were adapted for material from Arctic environments. Finally, the research presented in this thesis, including methodology and data sets, will be useful for future ostracod studies in the Arctic.

5.4 Outlook

Any application of bioindicators in palaeoecological research needs as much reference data as possible of species distribution and habitat requirements under modern environmental conditions. The more modern reference data is known, the better any interpretation from ancient environmental archives can be deduced. In this context, freshwater ostracods from Arctic periglacial regions in Siberia are largely unstudied. This thesis presents the first steps taken towards using them in palaeoenvironmental reconstruction. Both modern and fossil aspects of this research require further comprehensive study if ostracods are to be used as reliable bioindicators in Arctic Siberia. These first studies conducted in different regions of Northeast Siberia profile diverse species occurrences over climatic and aquatic gradients. However, due to the spotty character of the studies performed in modern environments, clear dependencies of species distribution on environmental factors remain to be elucidated. For these reasons, the inventory of ostracod species in the Arctic continued during the 2007/2008 field seasons on the Dimitri Laptev Strait coast (Wetterich and Schirrmeister 2009), in the Kolyma River lowland (Wetterich and Schirrmeister in prep.) in Siberia, and in 2008 on Alaska's Seward Peninsula. For the first time, host waters and ostracods were repeatedly sampled and continuous temperature measurements were performed at single sites in

order to detect seasonal changes in hydrochemical parameters, ostracod species, and shell calcite composition. Results of these studies will be prepared for publication in 2009. The further development of this monitoring approach is planned within the framework of a submitted joint German-Russian research project, which is focused on polygonal tundra wetlands; several developmental stages of polygonal habitats will be studied in a gradient transect comprising three representative sites across the Northeast Siberian lowlands between the Lena and the Kolyma rivers. Using an interdisciplinary approach, modern, sub-recent, and fossil environments will be characterised and compared in order to understand temporal and spatial environmental dynamics in relation to climate change. Cryological, limnological, pedological, and ecological features will be combined to link past, present, and future environmental dynamics in Polar regions. Present day environmental conditions and their main forcing parameters will be thoroughly assessed, faunal and floral communities in ponds, mires, and cryosols, which make up the major part of the polygonally-patterned ground, will be described, and cryogenic processes affecting these structured landscape units will be observed and evaluated. Species and assemblages that are indicative of modern ecosystem conditions will be identified and used as indicators to reconstruct Quaternary climate variations and ecosystem reactions. The results obtained will be used to explain and forecast future environmental dynamics in permafrost regions.

Arctic ostracod species have already been reported to the Non-marine Ostracod Database of Europe (NODE; Horne 1998) as a prerequisite for using a mutual temperature-range method for Quaternary palaeoclimatic analysis; this is a nonanalogue approach based on the presence/absence of species in a fossil assemblage (Horne 2007). Further extension of the Arctic dataset and possible application of this method to fossil ostracod assemblages from Arctic Siberia will greatly advance the relevance of fossil ostracods in quantitative palaeo-temperature reconstructions. Samples are already available from late Quaternary permafrost sequences in Arctic Siberia, Alaska, and Canada; they will be studied for ostracods with the same combined analytical approach as presented in the thesis.

In pursuit of quantified palaeoenvironmental reconstructions which are essential to estimate the impact of future climate changes on ecosystems, ecological training sets are also a progressive modern approach. Such work is based on faunistic data from regional multireference sites and limnological surveys, and can be used to build transfer functions to infer major environmental variables (e.g. temperature, conductivity and pH values). Freshwater ostracods from Arctic environments can potentially be used to hindcast glacial/interglacial and stadial/interstadial palaeoclimate variations. Various methods can be applied to fossil assemblages including an indicator species approach, modern

analogue techniques, and transfer functions based on ecological training sets. In this context, the first steps have already been taken to combine modern ostracod data from the Canadian and the Siberian high latitudes in cooperation with Finn Viehberg (Technical University Braunschweig, Institute of Environmental Geology, Germany). The current dataset, which already includes 75 locations in Canada and Siberia, was presented during the European Geophysical Union General Assembly 2008 (Wetterich et al. 2008e); further extension of the database and development of ostracod transfer functions is intended for 2009.

Several new or rediscovered ostracod taxa have been found during the identification of modern species. Hopefully, a detailed taxonomical examination of Arctic freshwater ostracod assemblages and an extensive description of the modern species using soft body features will take place in cooperation with Claude Meisch (National Museum of Natural History Luxembourg).

I Freshwater ostracodes in Quaternary permafrost deposits in the Siberian Arctic

Sebastian Wetterich[1], Lutz Schirrmeister[1] and Erika Pietrzeniuk[2]

(1) Alfred Wegener Institute for Polar and Marine Research, Research Unit Potsdam, 14473 Potsdam, Germany; (2) Almstadtstr. 11, 10119 Berlin, Germany (formerly Museum of Natural History Berlin)

Journal of Paleolimnology 34: 363-376 (DOI 10.1007/s10933-005-5801-y)

I.1 Abstract

Ostracode analysis was carried out on samples from ice-rich permafrost deposits obtained on the Bykovsky Peninsula (Laptev Sea). A composite profile was investigated that covers most of a 38 m thick permafrost sequence and corresponds to the last ca. 60 kyr of the late Quaternary. The ostracode assemblages are similar to those known from European Quaternary lake deposits during cold stages. The ostracode habitats were small, shallow, cold, oligotrophic pools located in low centred ice wedge polygons or in small thermokarst depressions. In total, fifteen taxa, representing seven genera, were identified from 65 samples. The studied section is subdivided into six ostracode zones that correspond to late Quaternary climatic and environmental stadial-interstadial variations established by other paleoenvironmental proxies: (1) cold and dry Zyrianian Stadial (58 – 53 kyr BP); (2) warm and dry Karginian Interstadial (48 – 34 kyr BP); (3) transition from the Karginian Interstadial to the cold and dry Sartanian Stadial (34 – 21 kyr BP); (4) transition from the Sartanian Stadial to the warm and dry late Pleistocene period, the Allerød (21 – 14 kyr BP); (5) transition from the Allerød to the warm and wet middle Holocene (14 – 7 kyr BP); and (6) cool and wet late Holocene (ca. 3 kyr BP). The abundance and diversity of the ostracodes will be used as an additional bioindicator for paleoenvironmental reconstructions of the Siberian Arctic.

I.2 Introduction

Fossil freshwater ostracodes have been used as bioindicators for the reconstruction of late Quaternary environments in Europe for about sixty years (e.g. Triebel 1941; Lüttig 1955, 1959; Kempf 1967; Diebel 1968; Diebel and Pietrzeniuk 1969, 1975, 1978a, 1978b; Fuhrmann and Pietrzeniuk 1990a, 1990b; Meisch 2000; Schwalb 2003). Ostracodes have also been used as paleoindicators in many other regions, such as North America (e.g. Curry and Delorme 2003) and Africa (e.g. Park et al. 2003), as well as in other regions. Whereas fossil and modern ostracode fauna and their ecology in Europe are relatively

well known due to numerous investigations, there are only a few records concerning freshwater ostracodes in Siberia, particularly from periglacial permafrost regions. Recent ostracodes were summarised by Bronshtein (1947) and Kurashov (1995) for the area covering the former USSR. The occurrence of Arctic freshwater ostracodes is only briefly mentioned. In addition, recent freshwater ostracodes from Siberia are described for Lake Baikal (Mazepova 2001), Central Yakutia (Pietrzeniuk 1977), and Arctic Siberia (Alm 1914; Neale 1969). Only a few freshwater ostracodes studies have been published for the Arctic regions of Alaska (e.g. Swain 1963) and Canada (e.g. Delorme 1970c; Delorme et al. 1977). Detailed studies of fossil ostracodes occurring in permafrost deposits are lacking.

A diverse ostracode fauna was observed during multidisciplinary investigations of late Pleistocene, ice-rich Arctic permafrost sequences on the Bykovsky Peninsula, Russia (Figure I-1). The occurrence of ostracode valves in these permafrost sequences was previously mentioned by Kunitsky (1989) and Slagoda (1993). However, up to now, detailed taxonomic and quantitative analysis of these freshwater Arctic ostracodes has not been carried out. The aim of this paper is to describe freshwater ostracodes as bioindicators within a paleoenvironmental permafrost archive. This study was carried out in a geochronologically, sedimentologically and paleoecologically well-studied permafrost sequence located at Mamontovy Khayata ("Mammoth hill"), on the Bykovsky Peninsula. In the future, freshwater ostracode studies in periglacial environments will be supported by studies of the modern Arctic assemblages, as well as by stable isotope studies on ostracode valves.

I.3 Study area and geological background

The permafrost sequence in this study is an exposure located on the east coast of the Bykovsky Peninsula (71°40'-72° N and 129°-129°30' E) in the southern Laptev Sea (Figure 1). Initial paleoecological studies were carried out at the beginning of the 19th century when the first complete mammoth carcass was recovered (Adams 1807). Subsequently, the Mamontovy Khayata profile has become one of the most extensively paleoecologically studied permafrost sequences in the Siberian Arctic. Geomorphological, geocryological, and sedimentological studies were conducted by Kunitsky (1989), Slagoda (1993), and Grigoriev (1993). Mamontovy Khayata was also mentioned in reviews of Ice Complex deposits in Siberia by Tomirdiaro and Chernenky (1987), and Fartyshev (1993).

Under the framework of the Russian-German science cooperation "SYSTEM LAPTEV SEA", the Bykovsky Peninsula has been studied by expeditions every year since 1998. The results include several publications concerning geocryology, sedimentology, and geochronology (Schirrmeister et al. 2002a; Siegert et al. 2002), stable isotope ratio and

hydrochemistry of ground ice (Meyer et al. 2000, 2002a), and bioindicators such as fossil pollen (Andreev et al. 2002), plant macrofossil remains (Kienast et al. 2005), and rhizopods (Bobrov et al. 2004). A comprehensive paleoenvironmental reconstruction is presented in Schirrmeister et al. (2002b).

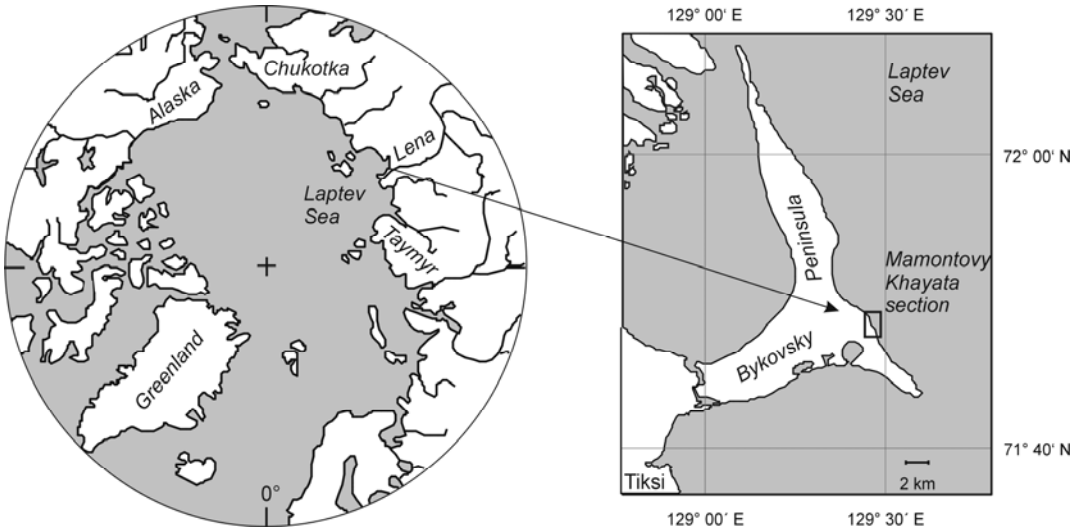

Figure I-1 Location of the Mamontovy Khayata study section

The ice-rich permafrost sequence of Mamontovy Khayata covers the last ca. 60 kyr of the Quaternary. The profile was divided into four units (A, B, C, D), which include the late Pleistocene Ice Complex units and its overlying Holocene cover (Figure 2). This division is based on changes in biogeochemical parameters, such as total organic carbon content (TOC), carbon/nitrogen ratio (C/N), isosope values of organic carbon ($\delta^{13}C_{org}$) and carbonate content, as well as cryolithological and grain size parameters, and mass-specific magnetic susceptibility (Schirrmeister et al. 2002a). The units reflect several stages of the late Quaternary landscape history in the Laptev Sea region.

Ice Complex deposits were formed on the accumulation plains of the dry Siberian shelf areas during the late Pleistocene. These Arctic accumulation plains were characterised by widely distributed ice wedge polygon systems. The studied coastal outcrops are dominated by giant ice wedges reaching approximately 40 m long and 5-6 m wide, which were formed continuously and syngenetically during periods of sedimentation on these plains. The studied permafrost sequence consists of numerous cryoturbated peaty cryosol horizons with silty to fine-grained sandy interbeds, which are mostly supersaturated with ice. Numerous well preserved micro- and macrofossils are found in the frozen deposits. Thus, the syngenetically formed permafrost sequences are excellent terrestrial paleoenvironmental archives. Most of the samples belong to the Ice Complex deposits (units A-C) and their Holocene cover (unit D). Two additional deposit types (Figure I-2) were classified as thermoerosional valley deposits (unit E) and thermokarst depression

deposits (unit F). Both were formed during the late Holocene, when thawing of ground ice reduced the extent of Ice Complex deposits due to thermo-erosional and thermokarst processes. This resulted in a strong transformation of the Arctic landscape by changing the hydrological regime, as well sediment accumulation conditions.

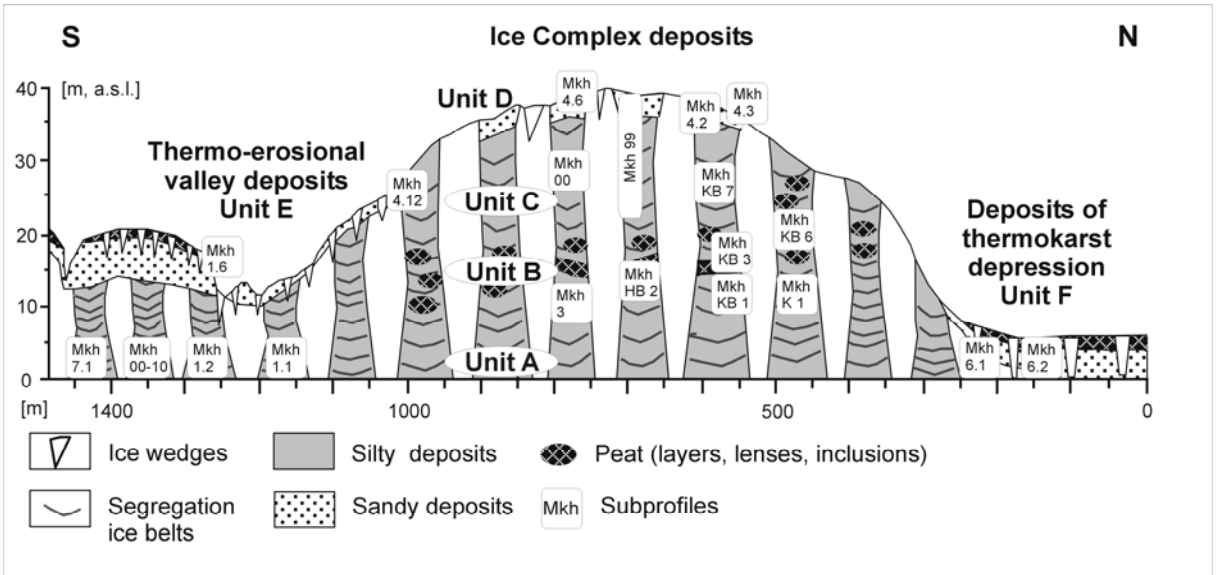

Figure I-2 Schematic profile of the study section on the east coast of Bykovsky Peninsula with subdivided cryolithological units (A-F) and the position of the analysed subprofiles

I.4 Materials and methods

Frozen samples weighing approximately 0.5 kg each were collected from several overlapping thermokarst mound subprofiles (Figure I-2). Thermokarst mounds represent intra-polygon sediment blocks that surround the perimeter of ice wedges that have melted (Figure I-3). A composite profile was studied covering most of the 38 m thick permafrost sequence. Ostracode valves were obtained from the deposits of the Ice Complex (units A-C), the Holocene cover (unit D), and the thermokarst depression (unit F). The thermo-erosional valley deposits (unit E) generally lacked ostracodes.

Samples were freeze-dried, wet sieved through a 0.250 mm mesh screen, and then air-dried. About 0.2 kg of each sample was used for ostracode analysis. If less material was available, the numbers of valves counted were normalised to a 0.2 kg sediment weight. Ostracode valves were analysed under a binocular microscope (Zeiss SV 11) and their structure was studied by light microscopy, as well as by scanning electron microscopy (Phillips CM 20 ATEM). Broken fragments of valves were also used for ostracode analysis if they could be identified. The species identification was based on Diebel and Pietrzeniuk (1969, 1975, 1978a, b) and Pietrzeniuk (1977), as well as on the reference collection of ostracodes at the Museum of Natural History in Berlin, Germany.

Figure I-3 Photograph of some analysed subprofiles on thermokarst mounds showing the structure and composition of the exposed permafrost deposits

The age control of the Mamontovy Khayata section was provided by 70 radiocarbon AMS-dates and 20 conventional radiocarbon dates. The geochronological results are presented in detail by Schirrmeister et al. (2002a). The age-height correlation of *in-situ* organic remains is in good agreement. This age model takes into account the rising uncertainties of older radiocarbon AMS-dates. Nevertheless the high accuracy of the dates provided by Leibniz Laboratory Kiel, Germany (Nadeau et al. 1997, 1998) and the corresponding geological observations allow an estimation of the chronology back to 60 kyr BP. Therefore, continuous accumulation during the last 60 kyr BP is assumed for the Ice Complex units (units A-C) and its younger cover (unit D). Additionally, the thermo-erosional valley deposits (unit E) were dated between 2 and 1 kyr BP. The sediments of the thermokarst depression (unit F) accumulated at about 3 kyr BP.

I.5 Results and interpretations

Ostracode valves occurred in the silty, fine-grained sandy Ice Complex deposits and its Holocene cover, as well as in the sandy sediments of the thermokarst depression (Figure I-2, Plates I-1 – I-3). Peaty permafrost deposits from all sections generally lacked ostracode valves because of the acidic environment present during peat accumulation (Figure 2). The thermokarst deposit profile (unit F) includes a 0.1 m thick layer of eroded Ice Complex material dated to 13560±80 yr BP, which do not correspond with the Holocene sequence dated between 2910±30 yr BP and 2925±30 yr BP. This layer is a

result of slope processes depositing material within the thermokarst deposits and consequently will have to be considered separately (Figure I-5).

In general, the ostracode taxa presented in this paper are similar to late Pleistocene assemblages from the Lena Delta (Pietrzeniuk 1986), as well as to a modern assemblage from Central Yakutia (Pietrzeniuk 1977). There are no evident distinctions between ostracode assemblages identified in the deposits of the thermokarst depression and the Ice Complex. However, the exact number of taxa is different. In total, fifteen taxa were identified and counted. Fourteen taxa were found in the Ice Complex sequence, while eleven taxa were observed in the Ice Complex material layer within the thermokarst depression deposits, and nine taxa within the true thermokarst depression deposits. The study section can be subdivided into six ostracode zones based on the ostracode distribution in the profile (Table I-1, Figures I-4 and I-5). These zones correspond to the profile zones established using sedimentological, geochemical, and paleoecological proxies (Schirrmeister et al. 2002b).

Table I-1 Ostracode zones of the Mamontovy Khayata sequence

Ostracode zones	Unit	Altitude [m, a.s.l.]	^{14}C Age [kyr BP]	Number of samples	Number of valves Mean (min-max)	Number of taxa
Zone VI	F	0.4- 1.5	ca. 3	4	77 (54 - 103)	3 - 7
Zone V	D	34.5 - 37.6	14 - 7	10	< 1 (0 - 7)	0 - 2
Zone IV	C	30.0 - 34.5	21 - 14	11	32 (0- 124)	0 - 6
Zone III	C	22.0 - 30.0	34 - 21	13	< 1 (0 - 9)	0 - 2
Zone II	B	8.8 - 22.0	48 - 34	20	410 (0 - 3710)	0 - 11
Zone I	A	1.3 - 3.5	58 - 53	6	71 (0 - 298)	0- 6

I.5.1 Ostracode zone I (58 to 53 kyr BP, 1.3 – 3.4 m, a.s.l.)

Six of the eight samples in ostracode zone I contained ostracodes with up to 300 valves per sample. Ostracodes were not found in two of the zone's samples. Six taxa are present in this zone, with juvenile *Candoninae* and *Limnocytherina sanctipatricii* being the most abundant taxa (Figure 4). According to Meisch (2000), *Limnocytherina sanctipatricii* (Plate I-3; 9-12) are found from the shallow littoral to the profundal zone in lakes, as well as in permanent small water bodies. They have been reported in fossil records in Europe ranging from the Pleistocene to recent times. Their habitats range from oligotrophic, cold waters to brackish waters with up to 3 ‰ salinity in the Baltic Sea (Frenzel 1991). Their presence in this zone suggests arid climatic conditions with higher evaporation rates than the present. The low species diversity and abundance of the identified assemblage reflect unfavourable (cold and dry) life conditions for ostracodes. Ostracode zone I corresponds

to unit A of the sedimentological data (Zyrianian Stadial), which is, according to grain size distributions, considered to be a shallow, fluvial environment with graded bedding (Siegert et al. 2002). The pollen data suggest an open treeless landscape with scarce vegetation cover, dominated by cold and dry summers (Andreev et al. 2002). Strong climatic conditions are also reported by the analysis of plant macrofossils, which are represented primarily by the remains of kryoxerophytic pioneer plants (Kienast et al. 2005). The Permafrost sequence between 3.4 and 8.8 m, a.s.l. was buried by modern deposits that were deposited by coastal erosion and, therefore, could not be studied.

I.5.2 Ostracode zone II (48 to 34 kyr BP, 8.8 – 22.0 m, a.s.l.)

Zone II is characterised by the profile's highest valve abundance and diversity (Figure I-4). Altogether twenty samples from this zone were studied. Two samples did not contain any ostracodes. The faunal association of zone II is characterised by the dominance of juvenile *Candoninae* and *Ilyocypris lacustris*. The arctic summers were probably too short to complete their life cycle and allow sufficient growth for the *Candoninae* to develop into their adult stage. Six species of the genera *Candona* and *Fabaeformiscandona* were identified. Only one valve of *Candona* cf. *acutula* was found in single sample (Plate I-2; 1), suggesting that it may have been misidentified. *Candona acutula* has previously been found in Holocene lake sediments (Porter et al. 1999) and presently occurs in shallow water with abundant vegetation in Canada (Delorme 1970c). *Candona* cf. *combibo* was identified in five samples (Plate I-1; 1). The ecological characteristics of *Candona combibo* are not well understood. Fossil records of *Candona combibo* are reported in Russia from the middle Pliocene to the middle Pleistocene periods (Kaz'mina 1975).

Candona harmsworthi were found in eight samples of zone II with up to sixteen valves being found in a single sample (Plate I-1; 5-6). *Candona harmsworthi* has been found in the modern Arctic environments of Novaya Zemlya and Franz-Josef-Land (Neale 1969) and as cold stage fossils in both Europe and northern Siberia (Lena Delta) (Pietrzeniuk 1986). Only female *C. harmsworthi* valves have been found. Males are not known.

Candona muelleri ssp. *jakutica* was present in eight samples, with up to fourteen female and male valves being found in a single sample (Plate I-1; 2-4). This species was first described by Pietrzeniuk (1977) in thermokarst lakes from Central Yakutia, as subspecies of *Candona muelleri*. It has been frequently recorded and the records point to a wide general distribution in Siberia (Meisch 2000). Further findings of *Candona muelleri* ssp. *jakutica* are reported for late Pleistocene thermokarst deposits in Central Yakutia (Pietrzeniuk 1984).

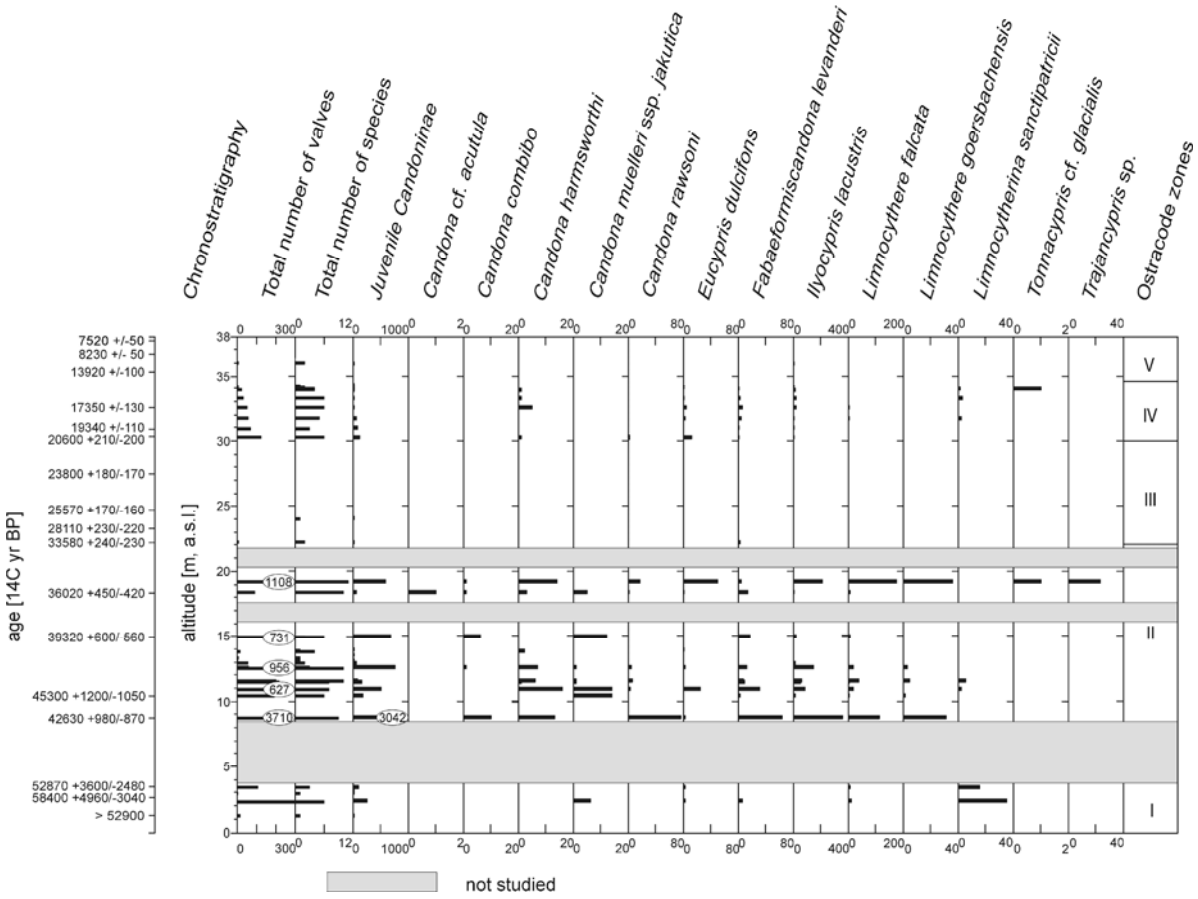

Figure I-4 Chronostratigraphy, and stratigraphic variation in two ostracode indices (total numbers of valves and species) as well as in number of each ostracode species of the Ice Complex sequence and the Holocene cover (units A-D). Counts are based on 0.2 kg sediment

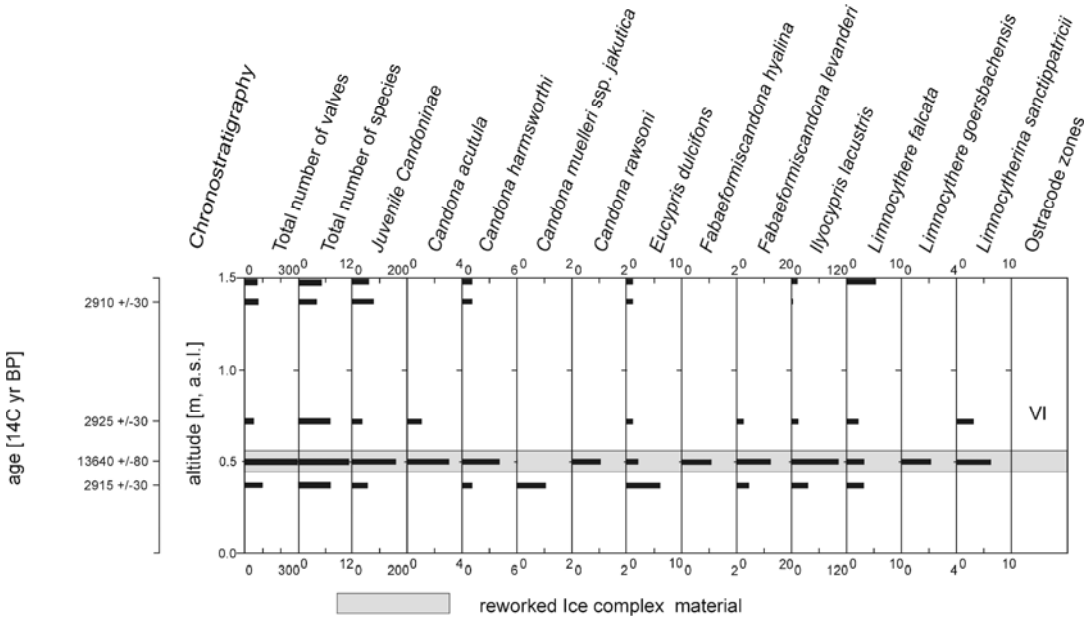

Figure I-5 Chronostratigraphy, and stratigraphic variation in two ostracode indices (total numbers of valves and species) as well as in number of each ostracode species of the thermokarst depression (unit F). Counts are based on 0.2 kg sediment

Plate I-1 Species of the genus *Candona*. *Candona* cf. *combibo*: (1) female, carapace; *Candona muelleri* ssp. *jakutica*: (2) male, RV; (3) female, LV; (4) female, RV; *Candona harmworthi*: (5) female, LV; (6) female, RV; *Candona rawsoni*: (7) male, LV; (8) male, RV; (9) female, LV; (10) female, RV

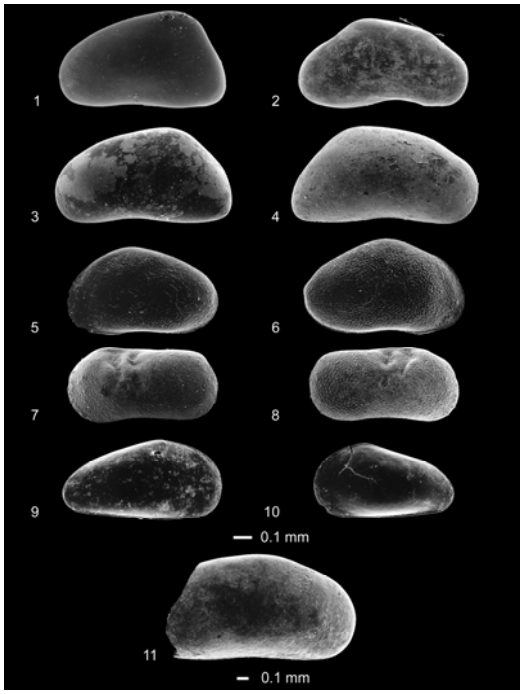

Plate I-2 Species and taxa of the genera *Candona*, *Fabaeformiscandona*, *Eucypris*, *Ilyocypris*, *Trajancypris* and *Tonnacypris*. *Candona* cf. *acutula*: (1) female, LV; *Candona* sp. *hyalina*: (2) male, RV; *Fabaeformiscandona levanderi:* (3) female, LV; (4) female, RV; *Eucypris dulcifons*: (5) female, LV; (6) female, RV; *Ilyocypris lacustris*: (7) female, LV; (8) female, RV; *Trajancypris* sp. juv.: (9) LV; (10) RV; *Tonnacypris* cf. *glacialis*: (11) LV

Candona muelleri is Holarctic and oligothermophilic (Meisch 2000), and has been observed in Europe in sediments ranging from Pleistocene cold stage deposits up to recent times (Fuhrmann et al. 1997).

A high abundance of female and male *Candona rawsoni* was recorded in only one sample at 8.8 m, a.s.l. (Plate I-1; 7-10). *Candona rawsoni* occurs in cold, oligotrophic lakes, and small temporary water bodies (Delorme 1969). Smith (1997) describes the species as eurytopic (tolerant to a wide range of physical and chemical conditions). Fossil records are reported for both cold and warm Pleistocene stages in Middle Europe (Diebel and Pietrzeniuk 1975, 1978a, 1978b), through the Holocene to recent times in North America (Delorme 1968, 1970c; Smith 1997) and Siberia (Bronshtein, 1947; Pietrzeniuk 1983).

The highest abundance of *Fabaeformiscandona levanderi* was found in the lower part of zone II (Plate I-2; 3-4). *F. levanderi* has been observed in the littoral and profundal zones of lakes, even those with a higher salinity (1–6 ‰). It has been described as oligothermophilic, likely titanoeuryplastic (occuring in different calcium-ranges from 0 mg/L up to >72 mg/L), oligorheophilic, (Hiller 1972), and mesohalophilic (Meisch 2000). Its presence in the fossil record ranges from the lower Pleistocene to recent times with a Holarctic distribution (Meisch 2000).

The species *Ilyocypris lacustris* (Plate I-2; 7-8) occurs in most samples of ostracode zone II**.** It is has been reported in Pleistocene cold stage sediments in Germany (Diebel and Pietrzeniuk 1969) and in Central Yakutia (Pietrzeniuk 1983, 1985), and has recently been reported in Europe in Switzerland and in Lake Constance (Meisch 2000). Its ecology and life history are unknown.

Eucypris dulcifons (Plate I-2; 5-6), *Limnocythere falcata* (Plate 3; 1-4), and *Limnocythere goersbachensis* (Plate I-3; 5-8) are numerous in two samples within ostracode zone II, as well as being less frequently found in other samples. *Limnocythere falcata* valves were found up to 0.85 mm in length (Plate I-3; 1-2). The environmental preferences of these species are not known. Fossil records are reported from Pleistocene cold stages in Europe (Fuhrmann et al. 1997; Diebel and Pietrzeniuk 1969, 1975, 1978a) and Northern Yakutia (Pietrzeniuk 1986), as well as from Holocene lake sediments in north-west China (Mischke 2001).

Broken fragments of *Tonnacypris* cf. *glacialis* were found in only two samples (Plate I-2; 11). *Tonnacypris glacialis* inhabits Arctic freshwaters and is also found as a Pleistocene cold stage fossil in Europe (Griffith et al. 1998). *Tonnacypris glacialis* is characterised as a Holarctic, circumpolar species, which occurs at mean summer temperatures of 5.9 (± 3.2) °C (Griffith et al. 1998). Valves of the genus *Trajancypris* sp. (Plate I-2; 9-10) were mostly juvenile and similar to those of *Trajancypris clavata* and *Trajancypris laevis*. Adults were

only represented as broken fragments. Both species have been found as fossils spanning from Pleistocene to recent times (Meisch 2000).

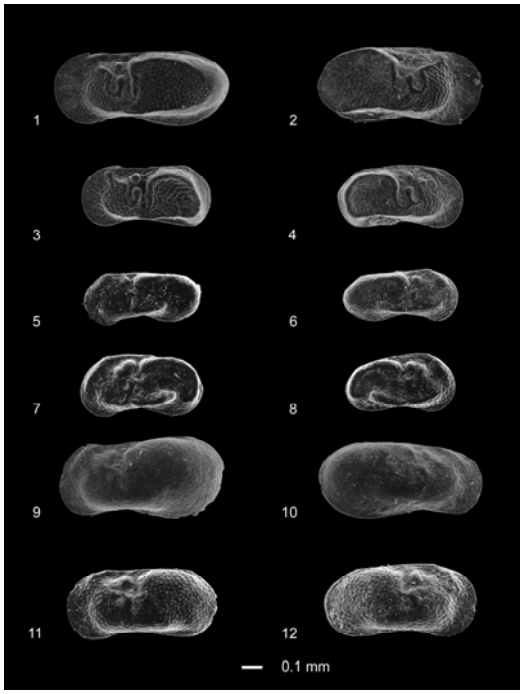

Plate I-3 Species of the genera *Limnocythere* and *Limnocytherina*. *Limnocythere falcata*: (1) female LV; (2) female RV; (3) female LV; (4) female RV; *Limnocythere goersbachensis*: (5) male LV; (6) male RV; (7) female LV; (8) female RV; *Limnocytherina sanctipatricii*: (9) male, LV; (10) male, RV; (11) female, LV; (12) female, RV

Ostracode zone II presents the most favourable environmental conditions for ostracodes preferring a stable shallow water environment. This is reflected in the high diversity of the ostracode fauna and high abundances of several species. The ostracode assemblages are characterised by the occurrence of Arctic species (e.g. *Candona harmsworthi* and *Tonnacypris glacialis*), typical cold stage species (e.g. *Eucypris dulcifons*, *Limnocythere falcata* and *Limnocythere goersbachensis*), and cosmopolitans with a preference for cold conditions (e.g. *Candona rawsoni* and *Fabaeformiscandona levanderi*). According to paleoecological and geochronological data, zone II belongs to the Karginian Interstadial (unit B). The pollen record of this period is represented by the shrubby vegetation of steppe-like and tundra environments that correspond to dry and relative warm summers (Andreev et al. 2002). In addition, the frequent occurrence of kryoxerophitic pioneer and tundra bog plants, as well as hydrophytes is reported by plant macro fossil remains (Kienast et al. 2005).

I.5.3 Ostracode zone III (34 to 21 kyr BP, 22.0 – 30.0 m, a.s.l.)

In Zone III, only two of the thirteen samples yielded a total of nine juvenile *Candoninae* and *Fabaeformiscandona levanderi* valves (Figure I-4). The lack of ostracodes in zone III suggests extremely unfavourable life conditions and corresponds to the transition to the coldest and driest period known as the Sartanian Stadial (unit C). Because of the dry conditions, polygon ponds were not continuously formed and habitats for ostracodes therefore did not exist. This climatic and environmental situation is supported by testate amoebae data that note the absence of hydrophillic, hygrophillic, and sphagnophillic species (Bobrov et al. 2004) as well as by paleobotanical data which contain a large number of xerophytes and species characteristic to a scarce steppe-like environment (Andreev et al. 2002; Kienast et al. 2005).

I.5.4 Ostracode zone IV (21 to 14 kyr BP, 30.0 – 34.5 m, a.s.l.)

Zone IV contains ostracode valves in ten out of twelve studied samples, but not as many valves as in zone I (Figure I-4). The ostracode species richness per sample ranges up to six taxa. The *Candoninae* group of this zone includes juvenile *Candoninae*, *Candona harmsworthi,* and *Fabaeformiscandona levanderi*. In addition, a few valves of *Eucypris dulcifons*, *Limnocytherina sanctipatricii,* and *Ilyocypris lacustris*, as well as one fragment of *Tonnacypris* cf. *glacialis*, were found. Zone IV indicates a warming trend at the end of the Sartanian Stadial (unit C), which improved the life conditions for ostracodes. However the zone IV assemblages are dominated by *Candona harmsworthi* and *Eucypris dulcifons*, which still imply cold conditions. In this period, the effective moisture gradually increased and consequently the hydrological conditions allowed for the formation of small polygon ponds. This interpretation of climate amelioration at the end of the Sartanian Stadial (~15 kyr BP) is supported by several paleoecological indicators including pollen (Andreev et al. 2002), testate amoebae (Bobrov et al. 2004), and insect records (Schirrmeister et al. 2000b). These data suggest an increase of herb communities, wet and warm soil conditions, and the occurrence of tundra-steppe insects.

I.5.5 Ostracode zone V (14 to 7 kyr BP, 34.5 – 37.6 m, a.s.l.)

Only one of the ten samples in zone V contained ostracodes, yielding three valves of juvenile *Candoninae* and four valves of *Ilyocypris lacustris* (Figure I-4). The sediment in this zone consists mainly of peat, which is not a favourable environment for ostracodes and the preservation of their carbonatic valves. Zone V corresponds to the Holocene optimum (unit D) when climatic conditions were at both their warmest and wettest climate according to the data of pollen (Andreev et al. 2002) and macrofossil plant remains (Kienast et al. 2005).

I.5.6 Ostracode zone VI (about 3 kyr BP, 0.4 – 1.5 m, a.s.l.)

Ostracodes from the late Holocene sandy deposits of the thermokarst depression were delineated as ostracode zone VI (unit F). The species assemblage and diversity seem to be quite similar to those of zone IV (Figure I-5). The ostracode data suggest cool and wet climatic conditions, as well as the stable persistence of ostracode habitats. The occurrence of the species *Eucypris dulcifons* and *Limnocythere falcata* in late Holocene deposits, mostly known from Pleistocene cold stage deposits in Europe (Fuhrmann et al. 1997; Diebel and Pietrzeniuk 1969, 1975, 1978b) are noteworthy. Zone VI reflects the recent conditions of the Arctic tundra (Andreev et al. 2002).

I.6 Conclusions

Ostracode valves from permafrost deposits on the Bykovsky Peninsula reflect the existence of stable aquatic habitats in the Siberian Arctic coastal lowlands during different paleoecological periods of the late Quaternary (Table I-2). Their occurrence in permafrost deposits depends mainly on climatic changes such as the stadial-interstadial variations of the late Quaternary. During the Zyrianian Stadial (58 to 53 kyr BP), the Karginian Interstadial (48 to 34 kyr BP), the end of the Sartanian Stadial (21 to 14 kyr BP), and the late Holocene (about 3 kyr BP), the climatic and environmental conditions allowed for the formation of polygon ponds and thermokarst lakes that were inhabited by ostracodes. Whereas, during most of the Sartanian Stadial (34 to 21 kyr BP) the climatic conditions for were too cold and dry to ensure the persistence of stable ostracode habitats. The lack of ostracodes in the early and middle Holocene (14 to 7 kyr BP) is likely caused by the poor preservation conditions of the acidic peaty sediments of this time period, even if the existence of ponds and lakes can be assumed.

Ostracode-bearing samples are characterised by a dominance of *Ilyocypris lacustris* and juvenile *Candoninae*. Other taxa occur in substantially less numbers. Some general ecological conditions could be concluded despite the wide ecological spectrum that characterise the identified ostracode taxa.

The ostracode zones correspond with the zones established by sedimentological, geochemical, and other paleoecological proxies (Schirrmeister et al. 2002b).

The profile was subdivided into six ostracode zones representing stadial-interstadial variations in late Quaternary climate change: (1) cold and dry Zyrianian Stadial (58 – 53 kyr BP); (2) warm and dry Karginian Interstadial (48 – 34 kyr BP); (3) transition from the Karginian Interstadial to the cold and dry Sartanian Stadial (34 – 21 kyr BP); (4) transition from the Sartanian Stadial to the warm and dry Allerød (late Pleistocene) period; (5) transition from the Allerød to the warm and wet middle Holocene (14 – 7 kyr BP); and (6) cool and wet late Holocene (ca. 3 kyr BP). The ostracode data suggest that the main

habitats were small, shallow, cold, oligotrophic pools located in either low centred ice wedge polygons or in small thermokarst depressions that warmed during the summer season. The presence of *Fabaeformiscandona levanderi* and *Limnocytherina sanctipatricii* suggest arid climatic conditions with higher evaporation rates than the present. Our study shows that ostracode fauna preserved in permafrost deposits provides considerable potential for paleoenvironmental reconstructions in aquatic habitats of the Siberian Arctic.

Table I-2 Characteristics and stratigraphy of the Ostracode zones in the Mamontovy Khayata section

Ostracode zones (^{14}C kyr BP)	**Units**	**Ecological characteristics**	**Typical species**	**Stratigraphy**
Zone VI (ca. 3)	F	low diversity and abundances cool and wet conditions stable shallow water environment	*C. harmsworthi* *E. dulcifons* *L. falcata* *I. lacustris*	Late Holocene
Zone V (14 – 7)	D	lack of ostracodes warm and wet conditions stable peat environment	*I. lacustris*	Middle Holocene Allerød
Zone IV (21 – 14)	C	low diversity and abundances climate amelioration unstable shallow water environment	*C. harmsworthi* *E. dulcifons* *L. sanctipatricii* *I. lacustris*	Sartanian Stadial
Zone III (34 – 21)	C	lack of ostracodes coldest and driest conditions unstable shallow water environment	*F. levanderi*	
Zone II (48 – 34)	B	high diversity and abundances warm and dry conditions stable shallow water environment	*C. harmsworthi* *C. muelleri-jakutica* *C. rawsoni* *F. levanderi* *L. falcata* *L. goersbachensis* *I. lacustris*	Karginian Interstadial
Zone I (58 – 53)	A	low diversity and abundances cold and dry conditions shallow, fluvial environment	*F. levanderi* *E. dulcifons* *L. falcata* *L. sanctipatricii*	Zyrianian Stadial

II Palaeoenvironmental dynamics inferred from late Quaternary permafrost deposits on Kurungnakh Island, Lena Delta, Northeast Siberia, Russia

Sebastian Wetterich[1], Svetlana Kuzmina[2], Andrei A. Andreev[1], Frank Kienast[3], Hanno Meyer[1], Lutz Schirrmeister[1], Tatyana Kuznetsova[4] and Melanie Sierralta[5]

(1) Alfred Wegener Institute for Polar and Marine Research, Research Unit Potsdam, Telegrafenberg A43, 14473 Potsdam, Germany; (2) Department of Earth and Atmospheric Sciences, University of Alberta, Edmonton, Canada T6G 2E3; (3) Research Institute and Museum for Natural History Senckenberg, Research Station for Quaternary Palaeontology Weimar, Am Jakobskirchhof 4, 99423 Weimar, Germany; (4) Department of Palaeontology, Moscow State University, Leninskie Gory, 11992 Moscow, Russia; (5) Leibniz Institute for Applied Geosciences, Stilleweg 2, 30655 Hannover, Germany

Quaternary Science Reviews 27: 1523-1540 (DOI 10.1016/j.quascirev.2008.04.007)

II.1 Abstract

Late Quaternary palaeoenvironments of the Siberian Arctic were reconstructed by combining data from several fossil bioindicators (pollen, plant macrofossils, ostracods, insects, and mammal bones) with sedimentological and cryolithological data from permafrost deposits. The record mirrors the environmental history of Beringia and covers glacial/interglacial and stadial/interstadial climate variations with a focus on the Middle Weichselian Interstadial (50–32 kyr BP). The late Pleistocene to Holocene sequence on Kurungnakh Island reflects the development of periglacial landscapes under changing sedimentation regimes which were meandering fluvial during the Early Weichselian, colluvial or proluvial on gently inclined plaines during the Middle and Late Weichselian, and thermokarst-affected during the Holocene. Palaeoecological records indicate the existence of tundra–steppe vegetation under cold continental climate conditions during the Middle Weichselian Interstadial. Due to sedimentation gaps in the sequence between 32 and 17 kyr BP and 17 and 8 kyr BP, the Late Weichselian Stadial is incompletely represented in the studied outcrops. Nevertheless, by several palaeoecological indications arctic tundra–steppe vegetation under extremely cold-arid conditions prevailed during the late Pleistocene. The tundra–steppe disappeared completely due to lasting paludification during the Holocene. Initially subarctic shrub tundra formed, which later retreated in course of the late Holocene cooling.

II.2 Introduction

The complex composition and structure of late Quaternary ice-rich permafrost deposits in the Siberian Arctic has been investigated by a number of studies in the last decades (e.g. Lungersgauzen 1961; Tomirdiaro 1982; Galabala 1987; Sher et al. 1987; Kunitsky 1989; Grigoriev 1993), but the origin of these sediments and their exact stratigraphical classification still remain unclear. Special problems concern the position and characteristic of the so-called Kargin Interstadial between 50 and 25 kyr BP according to the regular stratigraphic order in Russia. Despite of legitimate criticism on the stratigraphic position of the stratotyp at Cape Karginsky on the lower Yenissei, which belongs to the Eemian (Kazantsevo) Interglacial (Astakhov 2001, 2006; Astakhov and Mangerud 2005) as well as the already revised interglacial environmental interpretation in Northeast Siberia (Kind 1974) the term Kargin is not substituted yet by the Russian Interdepartmental Stratigraphic Commission on the Quaternary. Therefore, we have to use this term further on as long as no other name is established describing this special late Pleistocene period.
Palaeoenvironmental records from the continental part of the Laptev Sea region link the West Siberian Arctic and Alaska (Figure II-1) and reveal the arctic palaeoenvironments of Beringia - the landmass that connected both regions during the late Pleistocene.

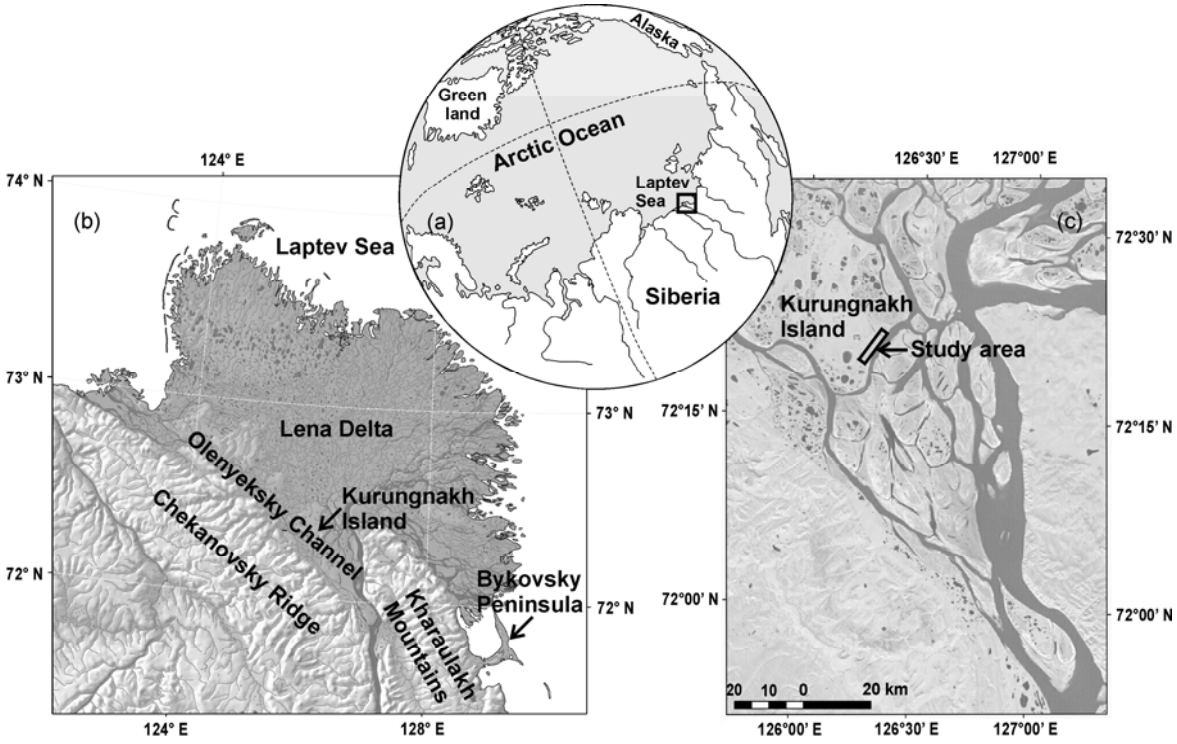

Figure II-1 Position of the study site (a) in Northeast Siberia at the Laptev Sea coast; (b) in the southern part of the Lena Delta; and (c) on Kurungnakh Island

Numerous multidisciplinary publications have already focused on permafrost deposits as late Quaternary palaeoclimate archives in the Siberian Arctic (e.g. Schirrmeister et al.

2002a, b, 2003; Hubberten et al. 2004; Pitulko et al. 2004; Sher et al. 2005; Grosse et al. 2007), especially since other long-term Quaternary records such as lake sediments are rare in this region.

The generally high content of well-preserved fossil remains in late Quaternary permafrost deposits in combination with sedimentological, geocryological, and stratigraphical descriptions allow detailed reconstructions of environmental and climatic dynamics. Various palaeoproxies in frozen deposits such as pollen (Andreev et al. 2002), plant macrofossils (Kienast et al. 2005), rhizopods (Bobrov et al. 2004), chironomids (Ilyashuk et al. 2006), freshwater ostracods (Wetterich et al. 2005), insects (Kuzmina and Sher 2006), and mammal bones (Kuznetsova et al. 2003) as well as stable isotope records of ground ice (Meyer et al. 2002a, b) have been used for reconstructions of late Quaternary palaeoenvironments and palaeoclimate in the Laptev Sea region (Northeast Siberia).

The goal of this study is to describe palaeoecological features and landscape development in the Siberian Arctic in comparison to other palaeorecords from this region. Different regional settings such as the change from an inland to a coastal position due to the late Quaternary marine transgression may alter the information preserved in permafrost deposits.

The study is focused on the Middle Weichselian (Kargin) period, which correlates with the Marine Isotope Stage 3 (MIS-3) when thick ice-rich permafrost deposits (so-called Ice Complex) accumulated. Regional climatic variations within this period are well documented by detailed records of plant macrofossils and insect remains. Pollen records were interpreted as a supra-regional record.

During three joint Russian–German expeditions in 1998, 2000, and 2002, fieldwork was conducted on outcrops of Kurungnakh Island (Rachold 1999; Rachold and Grigoriev 2001; Grigoriev et al. 2003). The results of the expeditions in 1998 and 2000 were summarised by Schwamborn et al. (2002) and Schirrmeister et al. (2003), whereas the results of the work done in 2002 are presented here for the first time. In 2002 we returned to Kurungnakh Island in order to supplement previous studies by sampling the site in more detail and in higher resolution. We aimed to make additional age determinations of the sediments, and receive additional bioindicator data from pollen, plant macrofossils, freshwater ostracods, insect remains, and mammal bones.

II.3 Regional setting

The fieldwork was performed in the Lena Delta that is located at the Laptev Sea coast (Figure II-1) in Northeast Siberia. The studied permafrost outcrops were obtained on Kurungnakh Island (72°20′N; 126°18′E) in the southern part of the delta beside the Olenyeksky Channel, which is the major western outlet of the Lena River within the delta.

In this part of the delta several islands remain as fragments of a broad foreland plain north of the Chekanovsky Ridge (Figure II-1). The foreland plain is dissected by several distributaries (outlets) of the lower Lena River and a number of small rivers and brooks that drain the slope of the Chekanovsky Ridge (Schirrmeister et al. 2003).

Kurungnakh Island is mainly composed of late Quaternary sediments that belong to the third Lena River terrace (Grigoriev 1993) with altitudes up to 40 m above the river level (m a.r.l.). The sediments consist of two main formations (Figure II-2). The first formation is described as sandy deposits that are covered by the second formation that built up by ice-rich peaty and silty Ice Complex deposits (Yedoma Suite). In addition, Holocene deposits are widely distributed on top of the third Lena River terrace in small-scale thermokarst depressions and in fillings of large thermokarst depressions called “alases”. Alases are an important landscape-forming feature of the ice-rich permafrost zone, which is mainly caused by extensive melting of ground ice in the underlying permafrost (van Everdingen 1998). Such sequences of sandy deposits overlain by Ice Complex deposits and frequently interrupted by thermokarst depressions are exposed along the entire Olenyeksky Channel.

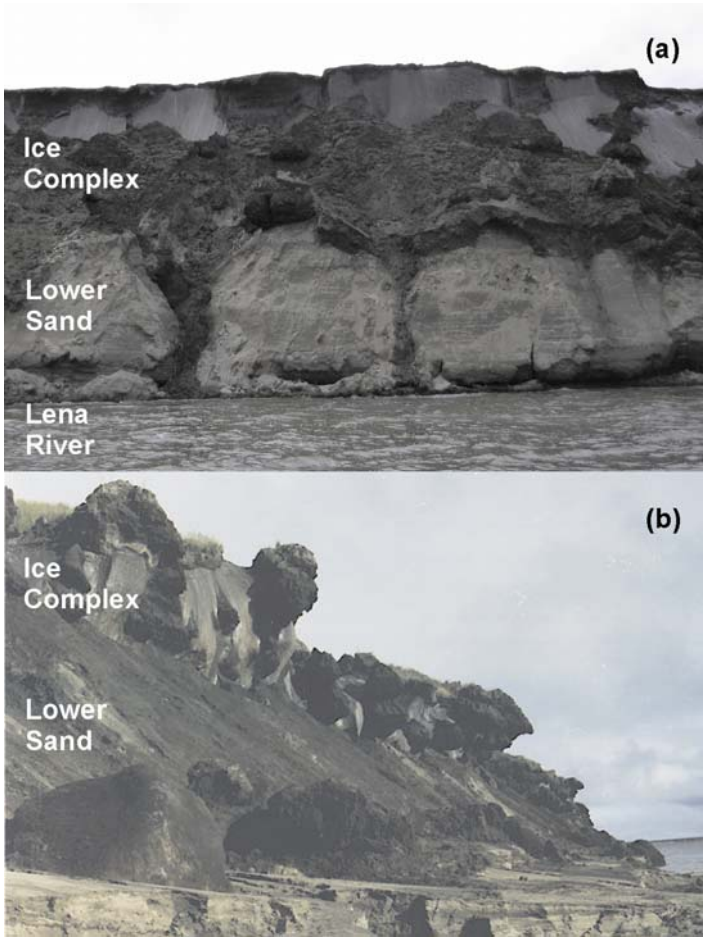

Figure II-2 Exposure situation at Kurungnakh Island: (a) overview of the general stratigraphic configuration along the coast of the Olenyeksky Channel (photograph taken in summer 2000); (b) exposure situation at the sampling sites in 2002

II.4 Material and methods

II.4.1 Sedimentology and cryolithology

Sedimentological and cryolithological features of permafrost deposits from two sections were studied by describing and sampling several subprofiles on coastal exposures of frozen deposits (Figure II-3) in August 2002 by S. Kuzmina and S. Wetterich. The upper section was sampled at 72°20′41″N and 126°18′33″E top down from the island's surface, whereas the lower section was sampled at 72°20′35″N and 126°18′20″E bottom up from the Lena River bank. In total, 53 samples were studied for sedimentological and cryolithological characteristics.

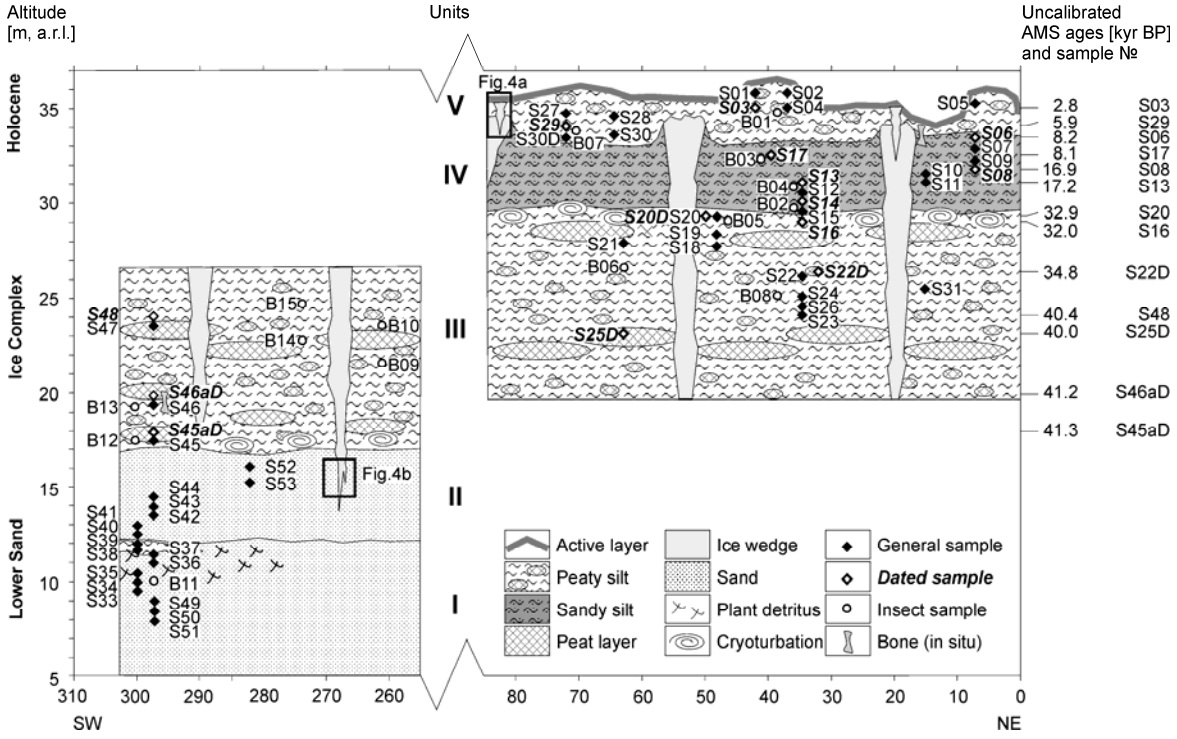

Figure II-3 Scheme of the studied permafrost sequence with sample positions and radiocarbon ages. The position of the additional sampled ice wedges are marked by black frames (see Figure II-4). Note distance of about 150 m between the sections

The frozen sediment samples were taken by knife or axe. In the upper part of the section we collected samples along a stratigraphic vertical sequence of thermokarst mounds (baydzherakhs) with overlapping tops and bottoms (Figure II-3). The lower section was sampled at excavations. Various methods were used to characterise the permafrost deposits. While still in the field, the ice content was gravimetrically determined on a dry-weight basis, as the ratio of the mass of ice in a frozen sample to the mass of the dry sample, expressed as a percentage (van Everdingen 1998). For these purposes we used an electric balance (Kern) for weight determination before and after sample-drying on metal field-oven. Before laboratory analyses all samples were freeze-dried and afterwards

prepared for different sedimentological, geochronological, and palaeoecological analyses. The grain-size distribution was measured by Laser Particle Analyser (Beckmann Coulter LS 200). Mass-specific magnetic susceptibility was determined using Bartington MS2 and MS2B instruments. Analyses of nitrogen, total carbon, and total organic carbon contents were carried out by CNS-Analyser (Elementar Vario EL III).

II.4.2 Geochronology

In order to understand the age sequence of the late Quaternary deposits exposed on Kurungnakh Island we used different dating methods for several sediment units. Two samples taken in 2000 (Schirrmeister et al. 2001) from two frozen peat layers within the lower sand horizon were dated by isochron uranium–thorium disequilibria technique with a thermal ionisation mass spectrometer (TIMS, Finnigan MAT 262+RPQ) at the Leibniz Institute for Applied Geosciences (GGA, Hannover, Germany). Analytical procedures are described in detail by Schirrmeister et al. (2002c) and Frechen et al. (2007). The external reproducibility was determined by measurements of standard solution of NBL-112A (New Brunswick Laboratories Certified Reference Material) and yields a value of 0.3% (1σ SD).
The radiocarbon dating of handpicked plant remains from a total of 14 sediment samples was performed at the Leibniz Laboratory for Radiometric Dating and Stable Isotope Research, University of Kiel (Germany) using accelerator mass spectrometry (AMS). Details of the AMS procedures at the Leibniz Laboratory are given by Nadeau et al. (1997) and Nadeau et al. (1998). Calibrated ages were calculated using the software “CALIB rev 4.3” (Stuiver et al.1998).

II.4.3 Stable isotopes

Ice wedges are common features of periglacial landscapes in non-glaciated regions of Northeast Siberia (Figure II-2). Palaeoclimate studies in polar regions often provide reconstructions of palaeotemperatures and moisture sources using the composition of hydrogen (δD) and oxygen (δ^{18}O) stable isotopes of ice as well as the deuterium excess (d=δD−8δ^{18}O). In this context, ice wedges reflects a winter temperature signal (e.g. Vasil’chuk 1992; Meyer et al. 2002a, b).
The stable carbon isotope (δ^{13}C) content of TOC was analysed by mass spectrometry (Finnigan Delta S) after removal of carbonate with 10% HCl in Ag-cups and combustion to CO_2 in a Heraeus elemental analyser (Fry et al. 1992). Accuracy of the methods was determined by parallel analysis of international standard reference material. The analyses were accurate to ±0.2‰. The values are expressed in delta per mil notation (δ, ‰) relative to the Vienna Pee Dee Belemnite (VPDB) Standard.

Ice wedges were sampled for oxygen and hydrogen stable isotope analysis (δD, δ^{18}O) at two sites of the section; the first site (Bkh IW I) within in the upper sequence of the outcrop at 34–35 m a.r.l., and the second site (Bkh IW II) at 16 m a.r.l. (Figure II-3). We used ice screws to drill transects across the exposed ice, keeping a distance of 0.1 m between the drill-holes. Altogether we obtained 14 samples in one transect for stable isotope analysis from the lower site and 15 samples in three levels from the upper sites (Figure II-4). The ice samples were stored cool and afterwards analysed by equilibration technique (Meyer et al. 2000) with a mass spectrometer (Finnigan MAT Delta-S). The reproducibility derived from long-term standard measurements is established with 1σ better than ±0.1‰ (Meyer et al. 2000). All samples were run at least in duplicate. The values are expressed in delta per mil notation (δ, ‰) relative to the Vienna Standard Mean Ocean Water (VSMOW) Standard.

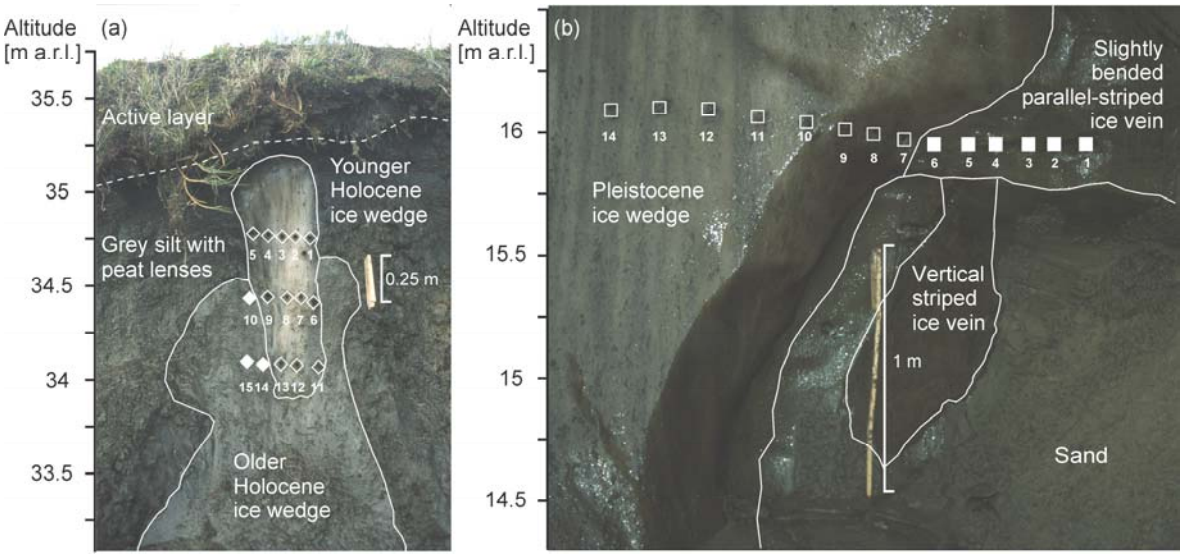

Figure II-4 Sample transects across the studied ice wedges: (a) exposure of two Holocene ice wedge generations (Bkh IW I); (b) Pleistocene ice wedge exposure (Bkh IW II). Filled and open symbols correspond to Figure II-7

II.4.4 Palaeoecological proxies

The palaeoecological reconstruction is based on the remains of several bioindicators preserved in the frozen deposits such as pollen, plant macrofossils, ostracods, insect remains, and mammal bones. These proxies were determined by A. Andreev (pollen), F. Kienast (plant macrofossils), S. Wetterich (ostracods), S. Kuzmina (insect remains), and T. Kuznetsova (mammal bones).

In total, 18 samples from the radiocarbon-dated units were used for analyses of pollen and palynomorphs. Pollen and spores were identified using a microscope with 400× magnification. Pollen percentages were calculated based on the tree and herbs pollen

sum. Pollen zonation was determined by visual inspection. The TILIAGRAPH programme (Grimm 1991) was used for graphing the pollen data.

For the identification of plant macro-remains and ostracods in the sediments, samples were wet-sieved through a 0.25 mm mesh screen, and then air-dried. About 0.2 kg of each sample was used. If less material was available, the counted numbers of remains were normalised to a 0.2 kg sediment weight. In total, 66 (sub-)-samples were screened for these purposes. Plant macro-remains and ostracod valves were analysed under a stereo-microscope. The species identification of plant remains was based on a carpological reference collection, whereas the ostracod taxa were determined using taxonomical keys (Alm 1914; Pietrzeniuk 1977; Meisch 2000) as well as the reference collection of freshwater ostracods at the Museum of Natural History (Berlin, Germany). For scanning electron microscopy (SEM) photographs of ostracod valves we used a Zeiss DSM 962 at the GeoForschungsZentrum (Research Centre for Geosciences, Potsdam, Germany).

In total, 15 samples of about 50 kg each, mostly taken from thawed sediment, were screened for insect remains. One sample was collected from the lower sequence and 10 samples were taken from the upper sequence. In addition, four samples were screened from two freshly fallen frozen blocks of Ice Complex sediments, which could be assigned to their original position. We used a 0.4 mm mesh sieve for field screening. After drying, the concentrated plant detritus with insect remains was separated using a set of small soil sieves with meshes from 0.25 to 5 mm. The large fraction (2–5 mm) was studied visually; the smaller fractions were analysed under a stereo-microscope. The species identification is based on etalon collections of modern insects from the Zoological Institute of the Russian Academy of Science (RAS), St. Petersburg and the Palaeontological Institute RAS, Moscow, Russia. Photographs of fossil insects were taken at the Otto Schmidt Laboratory, St. Petersburg, Russia. For palaeoenvironmental reconstruction based on fossil insects, we used the Ecological Group Analysis (EGA), which was described in detail in previous works (Sher et al. 2005; Kuzmina and Sher 2006).

During our fieldwork we also collected mammal bones and their fragments. Afterwards, these fossil remains of the Mammoth Fauna were identified. The bones were obtained: (a) in situ, i.e. within the frozen sediment, (b) in thermo-erosional cirques, where the original position within the sediments can be determined, (c) within the thawed debris of the outcrop, and (d) on the Lena River bank. Two of these bones were used for radiocarbon dating at the Geological Institute (GIN) of the RAS in Moscow and at the Oxford Radiocarbon Accelerator Unit Research Laboratory (OxA).

II.5 Results

II.5.1 Lithostratigraphy, sedimentology, and cryolithology

In general the cliffs along the Olenyeksky Channel consist dominantly of a lower, sandy and ice-poor formation (units I and II) and an upper ice-rich, fine-grained, peaty formation (Ice Complex), which contains numerous large ice wedges (units III and IV), and which are overlain by thermokarst depression fillings (unit V). Because of quite similar cryostructures in upper ice-rich formation and partly problematic exposure conditions (steep, slippery muddy, many debris) boundaries between the separate units were not always very well visible during the field observation. Nevertheless, our sedimentological data from the deposits of Kurungnakh Island confirm the stratigraphical division of the exposure into five main units (Figure II-5; Table II-1), which was made during the field work. The deposits of the lower sand sequence are well exposed along the whole section. The sands reach altitudes up to 17 m a.r.l. and delineate a division by sedimentological parameters into two units (Figure II-5).

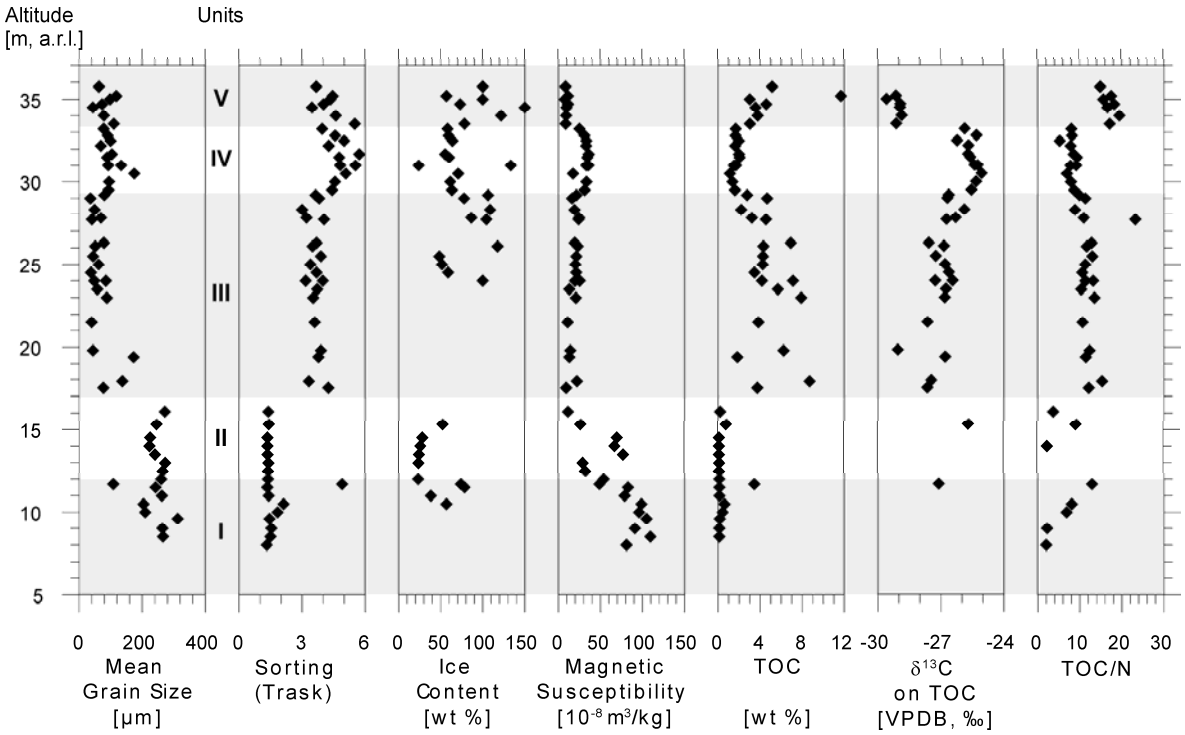

Figure II-5 Stratigraphic differentiation of the permafrost sequence into units I–V according to sedimentological records

II.5.1.1 Unit I (up to 12 m a.r.l.)

Unit I consists of interbedded yellow medium-grained sand (1–5 cm thick) and grey silty sand (1–2 cm thick) with plant detritus, roots, and single silt layers (Supplementary data A). In some layers of unit I, the sands contain abundant grass roots and stems. Well-sorted medium-grained sands with low TOC and TOC/N ratios alternate with poorly sorted

silty sands with higher TOC and TOC/N ratios. This interbedding reflects frequent changes in the current velocity under shallow water conditions. The ice content is generally lower in coarser sediments (about 25 wt%). No ice wedges were observed within unit I. The cryostructure is massive, i.e. no distinct small-scale segregated ice lenses or veins were visible. The magnetic susceptibility decreases from more than 100×10^{-8} m^3/kg at about 9 m a.r.l. to less than 50×10^{-8} m^3/kg at the transition to unit II.

Table II-1 Stratigraphic composition of the studied permafrost sequence and sediment characteristics of individual sediment units

Unit	Altitude [m a.r.l.]	AMS ages [kyr BP]	Stratigraphy	Sediments
V	33.5 – 37	6 – 3	Middle and late Holocene	Grey peaty silt with peat lenses and the uppermost modern active layer
IVb	32 – 33.5	about 8	Early Holocene	Grey sandy silt with rare plant detritus
			Gap	
IVa	29.5 – 32	about 17	Late Weichselian Stadial (Sartan)	Grey sandy silt with rare plant detritus
			Gap	
III	17 – 29.5	42 – 32	Middle Weichselian Interstadial (Kargin)	Grey peaty silt as continuous Ice Complex deposits with peat lenses and layers, including cryoturbated palaeosol horizons
II	12 – 17	> 50	Early Weichselian Stadial (Zyryan)	Yellow medium grained homogeneous finely-laminated pure sand
I	Up to 12	> 50	Early Weichselian Stadial (Zyryan)	Interbedded yellow medium grained sand and grey silty sand with plant detritus, roots and single silt layers

II.5.1.2 Unit II (12–17 m a.r.l.)

Above the alternation of sand, silt and plant detritus layers in unit I the upper part of the sand formation was characterised by homogeneous finely laminated pure sand (Supplementary data A). Single laminae of grey, greyish, and light-brown colour are 0.2–2 cm thick partly with graded bedding structures. The boundary between units I and II was not very sharp and hardly identifiable. Deposits of unit II are well-sorted medium-grained sands and contain only very little organic material (TOC 0.12–0.19 wt%) (Figure II-5). Thin layers of fine plant detritus were only observed in some places. The fine lamination was synsedimentarily disturbed at the mm-scale (load casts). Sediment features reflect that fluvial accumulation conditions changed to more continuous transport in rather shallow

water. The general trend of decreasing magnetic susceptibility continues in unit II. The ice content varies between 23 and 26 wt%. The cryostructure is massive without any small-scale structures of segregated ice. No syngenetic ice wedges were formed. But epigenetic thin ice wedges, which form the “roots” of the large ice wedges in unit III penetrate the upper part of unit II.

II.5.1.3 Unit III (17–29.2 m a.r.l.)

The upper sand sequence of unit II is covered by the Ice Complex sequence. The boundary between the lower sand and the Ice Complex is sharp and visible along the whole section (Figure II-2). At this boundary an approximately 1-m-thick horizon of a cryoturbated palaeosol occurred. Ice Complex ice wedges sharply narrow near the boundary with the lower sand sequence, and their long and thin tails penetrate about 1–2 m into the sand unit II. The Ice Complex is often exposed in the form of an ice wall along the river bank (Figure II-2). This wall, up to 1 km long, is likely the longitudinal part of a polygonal ice wedge system. The ice wall is covered by overhanging frozen blocks of peat and silt (Figure II-2). In less steep parts of the outcrop numerous thermokarst mounds reflect the transversal cut through a polygonal ice wedge system (Supplementary data A). The thickest peat layers are observed in the lower part of the Ice Complex sequence (unit III). At least two such layers are clearly observed along the section. In addition, cryoturbated greyish-brown palaeosols of about 0.5 m thickness with peat inclusions and twig fragments occurred repeatedly within unit III. The described characteristics reflect the subaerial accumulation of these sediments.

Unit III is composed of ice-rich poorly sorted, cryoturbated greyish sandy silt with 0.5–0.7 m thick peat horizons, single sand and peat lenses (0.2–0.5 m in diameter), and large ice wedges (Figure II-3 and Figure II-5). The ice wedges are 2–4 m wide and 15–20 m high. They have symmetrical shoulders, which merge to ice bands (segregation ice). Such ice wedges are vertically striped, consist of numerous 1–2 cm thick elementary ice veins, and contain numerous small gas bubbles. The ice content in sediments of unit III varies from 50 to 133 wt%. Ice bands of 1–3 cm thickness as well as reticulate nets of mm-thin ice veins and lenses between the ice bands characterise the cryostructure. The shape of the large wedges and their connection to the bands of segregated ice band as well as the ice supersaturation are signs of syngenetic (i.e. contemporary) ice wedge growth and accumulation. The magnetic susceptibility shows a stable signal of about 20×10^{-8} m^3/kg. The TOC content of these organic-rich sediments ranges from about 2 to 7 wt%, and the TOC/N ratio varies from about 9 to 23. The $\delta^{13}C$ averages about −27‰.

In the upper part of the Ice Complex sequence the peat layers are rare and less thick. The boundary to the overlain unit IV is again formed by a cryoturbated palaeosol of 0.5–1.5 m

thickness. There, sandy layers or lenses are often observed near the contact between ice wedges and the surrounding sediments.

II.5.1.4 Unit IV (29.5–33.5 m a.r.l.)

According to field observations unit IV could be separated from the underlain unit III because of yellowish grey to greenish-grey colour, higher sand content, a lack of peat inclusions, and the lesser content of plant remains (only few thin grass roots; Supplementary data A). Unit IV is composed of very poorly sorted sandy silt with low organic content. The TOC is significant lower than in unit III (1.7–2 wt%). The $\delta^{13}C$ composition of unit IV is clearly shifted to more positive values averaging about −25.5‰ and reaching at its most positive (heaviest) a value of −25.1‰. The TOC/N ratio in unit IV does not clearly differ from that of unit III. As far as observable the large ice wedges of unit III seemed to continue in unit IV without any interruption. The cryostructure is similar to those of unit III and the ice content is variable (24–150 wt%). The magnetic susceptibility is higher as compared to the overlying unit V and the underlying unit III with values of 17.4–36×10^{-8} m^3/kg.

II.5.1.5 Unit V (33.5–37 m a.r.l.)

The uppermost part of the outcrop below the active layer consists of sandy silt with peat lenses 0.1–0.2 m in diameter (Supplementary data A). This deposits form separate, several decametres wide bodies of thermokarst depressions fillings on top of the underlain ice-rich deposits. The contact next to the thick Pleistocene ice wedges between the surrounding sediments of units V and IV is turned up (Figure II-3) indicating the particular erosion (thermokarst) of the upper part of unit IV sediments. Ice wedges of 0.5–1.5 m width and up to 5 m height often penetrate into the much larger ice wedges of unit IV (Figure II-4a) forming larger composite ground ice bodies, which consist of several separate ice wedges. The cryostructure is similar to the ice-rich units below. The ice content of frozen sediments ranges from 48 to 117 wt%. The TOC content is similar to that of unit III and varies between about 3 and 12 wt%. The $\delta^{13}C$ signal of unit V clearly differs from all other units and reaches at its most negative (lightest) a value of about −29‰. The TOC/N ratio of about 17 in unit V is significant higher than in the other units. The mass-specific magnetic susceptibility reaches only 8.4–11.5×10^{-8} m^3/kg.

II.5.2 Geochronology

New ^{230}Th/U data from peat layers of unit I show isochron derived mean ages of 107±3 and 95±4 kyr at 3.2–3.8 m a.r.l. (Table II-2). Peat layers in similar position in the western Lena Delta exposed about 5 m a.r.l. at the Anrynsky Channel were ^{230}Th/U dated at

113±14 kyr (Schirrmeister et al. 2003). Krbetschek et al. (2002) provided three age determinations between 4.3 and 8.8 m a.r.l. by Infrared Optical Simulated Luminescence (IR-OSL) from 88±14 to 65±8 kyr.

Table II-2 Data of ^{230}Th/U age determinations of two samples (three subsamples each) from two peat horizon within unit I taken in 2000 (Schirrmeister et al. 2001)

Sample № TIMS №	**Altitude [m, a.r.l.]**	**^{234}U/^{238}U ± 2σ**	**^{230}Th/^{232}Th ± 2σ**	**U conc. [ppm]**	**Th conc. [ppm]**	**^{230}Th/U age 10^3 yr ± 2σ**	**^{230}Th/U age 10^3 yr ± 2σ Isochrone-corr.**
Bkh2 U/Th-1	**3.2-3.4**						**107 ±3**
700		1.181 ±0.003	0.566 ±0.003	0.83	5.19	315 ±10	104 ±5
701		1.241 ±0.005	0.7726 ± 0.004	1.50	6.37	194 ±3	105 ±3
702		1.194 ±0.005	0.608 ±0.005	0.66	3.98	343 ±21	114 ± 6
Bkh2 U/Th-2	**3.6-3.8**						**95 ±4**
704		1.141 ±0.003	0.550 ±0.004	0.66	4.30	457 ±60	94 ±8
705		1.241 ±0.002	0.651 ±0.004	1.08	5.79	234 ±4	94 ±6
706		0.98 ±0.005	0.546 ±0.005	0.62	3.52	>650	99 ±9

The radiocarbon ages (Table II-3) of unit III range between 41.3 +2.0/−1.6 kyr BP at 17.9 m a.r.l. and 32.9±0.3 kyr BP at 29.2 m a.r.l. One dating from this unit (Bkh2002 S14; 665±30 yr BP at 30 m a.r.l.) was excluded from further interpretation, because it comes from relocated material of late Holocene age. In unit IV two ages of about 17 kyr BP were determined at 31 and 31.7 m a.r.l., and two early Holocene ages of about 8 kyr BP at 32.5 and 33.2 m a.r.l. According to these results unit IV should be divided into two subunits IVa and IVb (Table II-1). The uppermost unit V was formed during the middle Holocene between about 6 and 3 kyr BP.

In order to understand the complete radiocarbon geochronology of the studied section we combined our new results with previous radiocarbon data from Schirrmeister et al. (2003) (Figure II-6a); the good agreement of these two studied outcrops on Kurungnakh Island is apparent. Considering the total data set of 28 radiocarbon ages it has to be mentioned

that two gaps in the chronology are present between approximately 32 and 17 kyr BP and between 17 and 8 kyr BP. The continuous sedimentation between about 50 and 32 kyr BP (during the Middle Weichselian/Kargin/MIS-3 Interstadial) allows us to estimate an age–height correlation (R^2_{mean}=0.87) based on 11 dates for this period (Figure II-6b). This good correlation was also used in palaeoecological studies for age estimations of non-dated samples.

Table II-3 Radiocarbon AMS ages of plant remains in samples of the Kurungnakh study site collected in 2002

Sample №	Lab №	Material dated	Altitude [m, a.r.l.]	uncalibrated AMS ages [yr BP]	cal AMS ages* [yr BP] Max	cal AMS ages* [yr BP] Min
Bkh02 S03	KIA31046	plants	35	2795 ±30	2954	2841
Bkh02 S29	KIA31047	plant detritus	34	5860 ±35	6756	6593
Bkh02 S06	KIA31048	plants	33.2	8155 ±45	9155	9,010
Bkh02 S17	KIA31049	plants	32.5	8075 ±30	9034	8980
Bkh02 S08	KIA30235	wood	31.7	16 860 ±70	20 195	19 855
Bkh02 S13	KIA31050	plants	31	17 200 ±80	21 138	19 849
Bkh02 S14	KIA31051	plants (relocated)	30	665 ±30	602	558
Bkh02 S20	KIA30236	wood	29.2	32 920 +330/-310		
Bkh02 S16	KIA30237	wood	29	31 960 +380/-360		
Bkh02 S22D	KIA30238	wood, leaves	26.3	34 830 +390/-370		
Bkh02 S48	KIA30240	wood	24	40 410 +610/-560		
Bkh02 S25D	KIA30239	wood, moss, coarse leaves	23	40 020 +660/-610		
Bkh02 S46aD	KIA30241	moss, leaf fragments	19.8	41 220 +1260/-1090		
Bkh02 S45aD	KIA31052	plants	17.9	41 330 +2000/-1600		

* Calibrated ages were calculated using the software „CALIB rev 4.3" (Stuiver et al.1998)

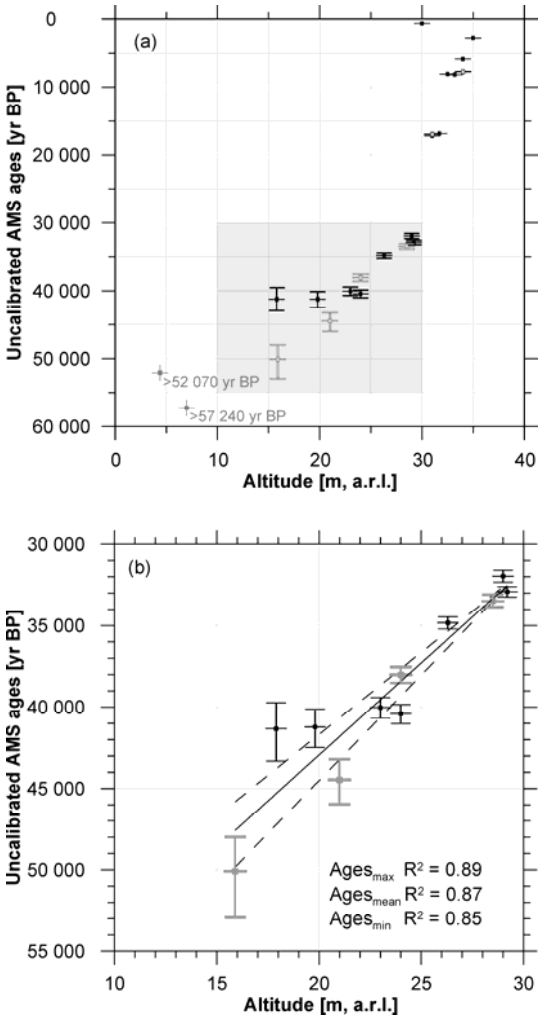

Figure II-6 Results of radiocarbon AMS age determination from Kurungnakh Island: (a) age-model of the entire radiocarbon-dated permafrost sequence; (b) age–altitude-correlation of the continuously accumulated Kargin period between 50 and 31 kyr BP. Previous dates from Schirrmeister et al. (2003) are marked as grey symbols

II.5.3 Oxygen and hydrogen stable isotopes of ground ice

The studied late Pleistocene ice wedge is about 2 m wide at the sample site and penetrates another 2 m further into unit II. The sampled transect covers the right side of a large ice wedge (samples Bkh-II 7–14) and a smaller, slightly bended parallel-striped ice vein (samples BKh IW II 1–6), which merges oblique into the ice wedge (Figure II-4b). Such kind of small “daughter ice wedges” was often observed in the lowermost part of large ice wedges. They mirror changing frost crack orientation during epigenetic ice wedge formation if stress relations during frost cracking were not yet clear. The apparently horizontal orientation of such ice wedge is caused by angular cutting orientation of the inclined oriented ice body. Two small Holocene ice wedges that nest one into another (Bkh IW I) were sampled at the top of the section (Figure II-4a).

The stable isotope signature of late Pleistocene ice lies in a more negative (lighter) range of about −32‰ for $\delta^{18}O$ and −248‰ for δD, whereas the *d* excess averages 6‰ (Table II-4). The horizontally striped ice vein next to this ice wedge is slightly shifted to heavier values of −31‰ for $\delta^{18}O$ and −241‰ for δD ($d \approx 4‰$).

Table II-4 Oxygen and hydrogen table isotope signatures of late Pleistocene and Holocene ice wedges

Type of ground ice	Sub-samples	Altitude	$\delta^{18}O$ mean	$\delta^{18}O$ std. dev.	δD mean	δD std. dev.	*d* mean	*d* std. dev.
		[m a.r.l.]	[‰]	[‰]	[‰]	[‰]	[‰]	[‰]
Younger Holocene ice wedge	12	34 - 35	−24.6	0.8	−185.1	6.1	11.6	1.0
Older Holocene ice wedge	3	34 - 35	−25.4	1.1	−198.6	7.0	4.2	1.7
Late Pleistocene ice wedge	8	16	−31.8	0.5	−248.3	3.2	5.8	0.4
Horizontal striped ice vein	6	16	−30.6	0.5	−240.7	3.4	4.0	0.7

The younger Holocene ice wedge shows relatively heavy values of around −25‰ for $\delta^{18}O$ and −185‰ for δD. The *d* excess averages about 12‰ (Table II-4). This is clearly different from the surrounding older Holocene ice in which the younger ice wedge grew, with values of about −25‰ for $\delta^{18}O$, −199‰ for δD, and 4‰ for the *d* excess (Table II-4). The $\delta^{18}O$-δD signature of the older Holocene ice wedge lies below the Global Meteoric Water Line (GMWL; Figure II-7).

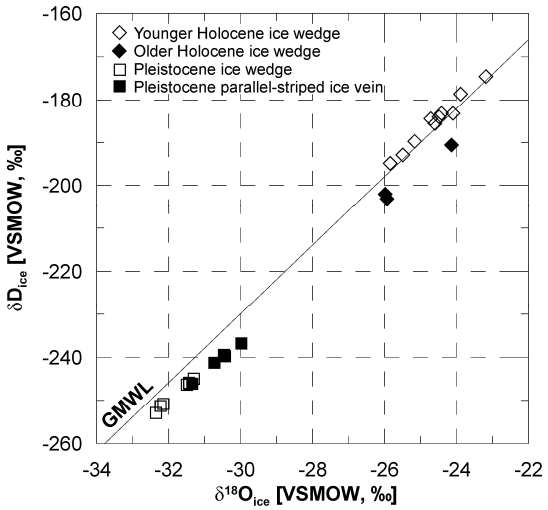

Figure II-7 $\delta^{18}O$–δD plot of Pleistocene and Holocene ground ice as with respect to the Global Meteoric Water Line (GMWL), which correlates fresh surface waters on a global scale (Craig 1961)

The relatively low *d* excess is not typical for Holocene ice wedges and might indicate that this generation of ice wedges formed not only under the influence of winter snow, but also were fed by additional water supply. However, these samples are less suitable for climate interpretation.

In summary, late Pleistocene and Holocene ground ice are clearly differentiated by their stable isotopic signals. Similar results have been obtained from other outcrops in the Laptev Sea region (Meyer et al. 2002a, b; Schirrmeister et al. 2003). The interpretation of

the stable isotope data allows us to conclude that winter temperatures were warmer during the late Holocene than in the late Pleistocene when the Ice Complex formed.

II.5.4 Palynological studies

Sediments of units I and II contain almost no pollen. Five pollen zones (PZ 1–5) can be distinguished in units III–V (Figure II-8). The dominance of Cyperaceae and Poaceae pollen with some *Artemisia* and *Salix* is typical for pollen zone 1 (PZ 1) corresponding to the lower part of unit III (ca 45–40 kyr BP). The pollen spectra reflect the domination of open tundra- and steppe-like associations in the area at that time, although willow shrublets were probably present in the vegetation as well. A relatively high content of green algae colonies (*Pediastrum*) indicates the existence of shallow water bodies (e.g. centres of ice wedge polygons). The interval corresponds well with the beginning of the Kargin Interstadial when climate amelioration took place.

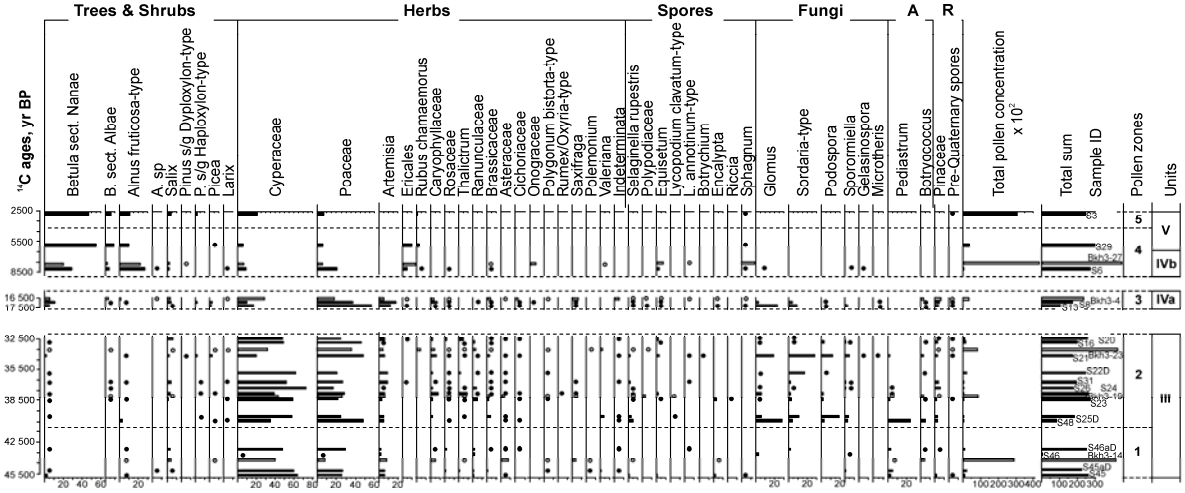

Figure II-8 Pollen and spore diagram of Kargin, late Sartan and Holocene sediments (A—algae remains, R—re-deposited taxa). Pollen and spore data from Schirrmeister et al. (2003) are marked as grey bars and dots

The dominance of Poaceae, Cyperaceae, *Artemisia*, and Caryophyllaceae pollen with some Asteraceae, *Thalictrum*, and Brassicaceae is typical for PZ 2 corresponding to the upper part of unit III (ca 40 and 32 kyr BP). This interval corresponds well with the climatic optimum of the Kargin Interstadial. The pollen spectra reflect the domination of open steppe-like and tundra-like associations in the area at that time. Relatively high contents of *Pediastrum* and *Botryococcus* colonies and *Salix* pollen indicate relatively moist local conditions during this interval. A similar environment was reconstructed for this time for the Bykovsky Peninsula, Laptev Sea (72°N, 129°E; Figure II-1) as well (Andreev et al. 2002; Schirrmeister et al. 2002a). Large amounts of spores from dung-inhabiting Sordariales fungi (*Sporormiella*, *Podospora*, and *Sordaria*) are also characteristic for the

spectra, and can be seen as an indication of grazing mammals in the area during that time.

Very low pollen concentrations characterise PZ 3 (unit IVa) dated at around 17 kyr BP. This feature may indicate scarce vegetation around the site, or more likely very low pollination during the Sartan stage. Pollen spectra are dominated by Poaceae, Cyperaceae, *Artemisia*, and Caryophyllaceae. They also contain reworked indeterminable Pinaceae pollen grains and rather numerous dung-inhabiting fungi spores. The latter most likely indicate the presence of grazing herds in the area. It can be assumed that scarce steppe-like grass-sedge-*Artemisia* communities dominated the study area. The climate was probably extremely cold and dry. However, relative high contents of *Betula* sect. *Nanae* and *Salix* pollen may reflect the beginning of slight climate amelioration after the Last Glacial Maximum (LGM).

An increase in *Alnus fruticosa*, *Betula* sect. *Nanae*, *B*. sect. *Albae*, and Ericales pollen contents and the presence of *Rubus chamaemorus* in PZ 4 reflect the early Holocene warming (unit IVb). Such changes suggest that shrubby tundra was widely distributed around the site ca 8 kyr BP. Previous studies at the area confirm this conclusion (Schirrmeister et al. 2003). The second spectrum of PZ 4 (unit V) radiocarbon dated to 5.9 kyr BP is characterised by a strong decrease in *A. fruticosa* and increase in *Betula nana* and Ericales pollen. These changes reflect some climatic deterioration resulting in the disappearance of shrub alder from the vegetation.

The uppermost spectrum of PZ 5 (unit V) radiocarbon dated to ca 2.5 kyr BP is characterised by a disappearance of Ericales and *R. chamaemorus* pollen, and an increase in *Salix*, Cyperaceae, and long-distance transported pollen (*Pinus*). The spectrum reflects vegetation and climate conditions similar to modern.

II.5.5 Plant macrofossils

In general, the studied sequence is poor in plant macrofossils. Altogether 66 samples were studied of which only 42 contained identifiable material (Supplementary data B).

In the lowermost units I and II, plant macro-remains were especially rare. Both units are similar in their fossil plant composition. The macrofossil spectra include beside *Salix* sp., and *Carex* sp. mainly tundra–steppe representatives like *Potentilla* sp., *Kobresia myosuroides*, *Puccinellia* sp. but also wetland species such as *Carex* sect. *Phacocystis*, *Saxifraga hirculus*, and *Eriophorum angustifolium* (Figure II-9). They reflect a tundra–steppe-like vegetation, thus cold and dry conditions and the presence of wet localities. The scarcity of plant remains is likely the result of taphonomical conditions and is not regarded as being due to climatic conditions. Well-sorted sand is deposited by wind or

running water, implicating the removal of lightweight fractions of the sediment load including small grain sizes and plant detritus.

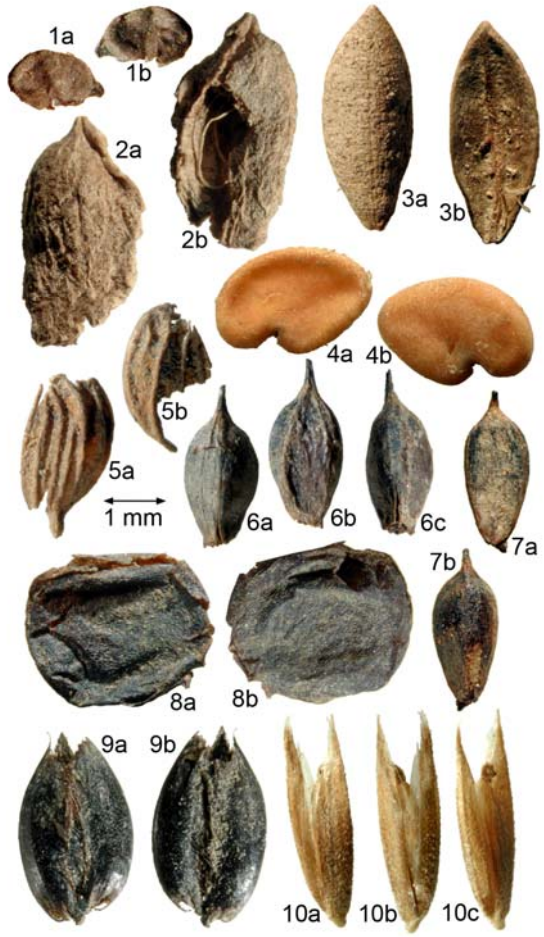

Figure II-9 Fossil plant macro-remains from Kurungnakh Island: (1) *Alyssum obovatum*, both sides of a seed fragment; (2) *Lagotis minor*, fragment of the fruit, two sides; (3) *Phlox sibirica*, valve of the capsule, two-sided; (4) *Astragalus* sp., both sides of the seed; (5) *Thalictrum alpinum*, fragments of two individual pericarps; (6) *Kobresia myosuroides*, three sides of a nutlet; (7) *Kobresia myosuroides*, two sides of another nutlet; (8) cf. *Lesquerella arctica*, seed, two-sided; (9) *Hierochloë* cf. *odorata*, spikelet with two visible staminate florets enclosing one pistillate floret, two sides; (10) *Arctagrostis latifolia*, caryopsis, (a) and (b) lateral, (c) obliquely ventral view showing that the peduncle is lacking (evidence that spikelets are uniflorous)

Unit III consists mainly of organic-rich silty and peaty deposits, which inherently contain more identifiable plant remains. Consistently, the diversity and abundance of plant macro-remains in unit III are the highest within the recorded sequence. The spectra are mainly dominated by artic upland plants characteristic of *Kobresia* meadows and by steppe plants (Supplementary data B), reflecting the presence of a tundra–steppe under dry conditions. Remains of *Carex* sect. *Phacocystis* were also abundant, indicating the existence of constantly wet habitats possibly connected with periodic flooding in the proximity of a riverbed. The nearby existence of a river bed might also explain the scarcity of *Puccinellia* sp., a plant species that is actually very abundant in Pleistocene deposits of Arctic Siberia (Kienast et al. 2005, 2008). This grass occurs inland only under dry climate conditions in closed depressions, which lack drainage, where groundwater level and salt concentration fluctuate seasonally due to high evaporation. The high drainage that exists close to a river bed probably hampered salt accumulation in the top soil.

In unit IVa, the composition of the macrofossil assemblages does not change significantly from that of unit III, but the abundance and diversity of plant remains decrease (Supplementary data B). This might be the result of a higher accumulation rate or of poor macrofossil preservation. Since all palaeoecological records indicate a drastic decrease in diversity and abundance and a dominance of cold-tolerant taxa, a strong temperature decrease has to be assumed.

Interestingly, the floral composition does not change notably towards the early Holocene warming (unit IVb). Plants typical of the Pleistocene tundra–steppe such as *K. myosuroides* and *Potentilla* cf. *stipularis* continue to exist in the study area beyond the Weichselian/Holocene border. Their existence together with the low number of wetland plants during the early Holocene might be an indication of a continuing continental climate as a result of delayed Laptev Sea transgression. Plant remains indicating a temperature increase towards the early Holocene are largely absent except for a single Betulaceae fruit in the Bkh2002 S30D sample. This result is in contrast to palynological results, which clearly show a drastic increase in *A. fruticosa*, *Betula* sect. *Nanae*, *B.* sect. *Albae*, and Ericales pollen.

Unit V corresponds largely to the late Holocene and is characterised by a further floral impoverishment connected with increasing oceanic climate influence due to the Laptev Sea transgression. Among the few macrofossils that were found, remains of wetland sedges (*Carex* sect. *Phacocystis*) and willow shrubs dominate. Single remains of *Betula* cf. *fruticosa* and *Ledum palustre* indicate subarctic temperature conditions. Steppe, meadow, and cryo-arid elements are completely absent from the late Holocene record.

II.5.6 Ostracod remains

In total, 54 samples from the site studied in 2002 and 15 samples from the outcrop sampled in 2000 were checked for ostracod remains. However, only five samples from the 2000 and 2002 sample sets contained any ostracod remains, mostly rare valve fragments or single valves of juvenile Candoninae and *Candona muelleri jakutica*. The only sample with sufficiently high valve numbers (in total 2485 valves) for further interpretation was found at an altitude of 19.8 m a.r.l. (sample Bkh2002 S46aD) in the lower part of unit III. This sample was dated to 41 220+1260/−1090 yr BP. The species composition comprises five taxa. Four species were identified by valves of adult specimens and one taxon comprises juvenile Candoninae, which represents more than 50% of the total amount of ostracod valves. The abundance of the four species is shown in Figure II-10. Due to finding only four species represented by adults the species diversity is low. Nevertheless, some interpretation can be undertaken. All observed species are already described for modern (sub-)arctic shallow water habitats (e.g. Alm 1914; Semenova, 2003, 2005;

Wetterich et al. 2008a). The good preservation of the valves which even contain, in some cases, soft body parts, and also the occurrence of closed carapaces indicate in situ conditions (Figure II-11).

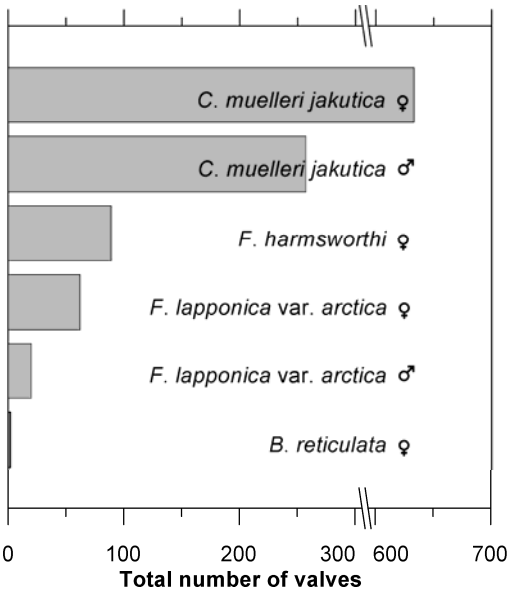

Figure II-10 Ostracod species spectra of sample Bkh2002 S 46 aD (19.8 m a.s.l.) in the lower part of unit III dated to 41 kyr BP

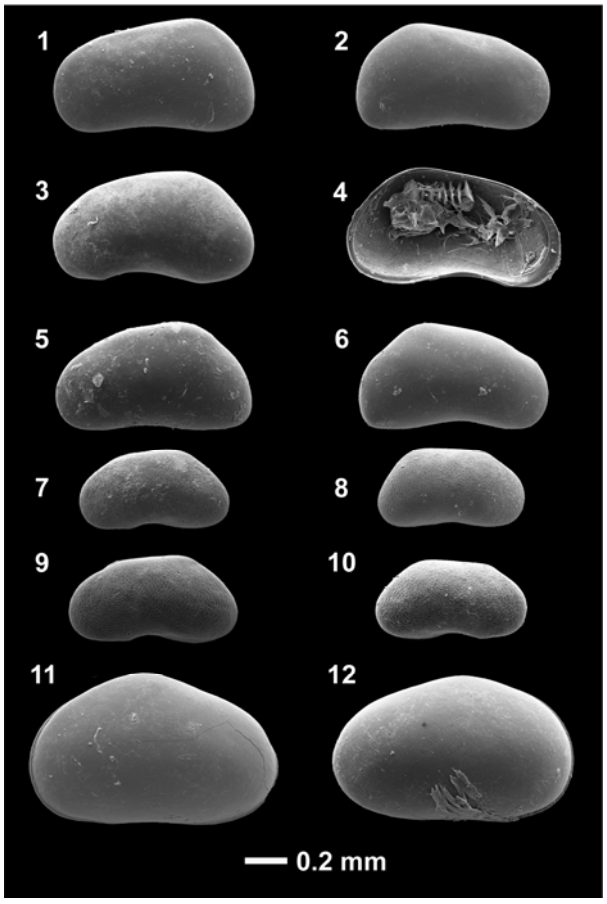

Figure II-11 SEM photography of freshwater ostracod valves (left valve-LV, right valve-RV). *Candona muelleri jakutica*: (1) female LV, (2) female RV, (3) male LV, (4) male LV (internal view with preserved soft body parts); *Fabaeformiscandona harmsworthi*: (5) female LV, (6) female RV; *Fabaeformiscandona lapponica* var. *arctica*: (7) female LV, (8) female RV, (9) male LV, (10) male RV; *Bradleystrandesia reticulata*: (11) female LV, and (12) female RV.

The most common species in the record here presented is *C. muelleri jakutica* PIETRZENIUK, 1977 (Figure II-11, 1–4) which was first observed in Central Yakutian

thermokarst lakes (Pietrzeniuk 1977) and has also been found in arctic polygonal ponds in the Lena Delta (Wetterich et al. 2008a) under very low electrical conductivities (salinities) and water temperatures between about 5 and 15°C. Fossils of *C. muelleri jakutica* are already known from Kargin Interstadial deposits from Bykovsky Peninsula, Laptev Sea, Northeast Siberia (Wetterich et al. 2005). Modern and fossil assemblages of *C. muelleri jakutica* are commonly represented by female and male specimen.

The species *Fabaeformiscandona harmsworthi* (SCOTT, 1899) (Figure II-11, 5–6) has been found in the modern arctic environments of Novaya Zemlya and Franz Josef Land (Neale 1969) and also in the Lena Delta under the same environmental conditions as *C. muelleri jakutica* (Wetterich et al. 2008a). Fossil valves were obtained in Kargin interstadial deposits in Northeast Siberia (Wetterich et al. 2005). Only female *F. harmsworthi* valves have been found. Males are not known.

Fabaeformiscandona lapponica var. *arctica* (ALM, 1914) (Figure II-11, 7–10) was first described from ponds on Novaya Zemlya Archipelago, Russian Arctic (Alm 1914). Semenova (2003) classified this species as a high-arctic form also common on Spitsbergen and in other regions in the Arctic. The female and male valves presented here are very similar to *F. lapponica* var. *arctica* in size and outline. Nevertheless, it has to be mentioned that the valve surface is covered by a pitted pattern (Figure II-11, 7–10), which was originally not described by Alm (1914). Males of *F. lapponica* var. *arctica* have not been previously observed in modern records (Semenova 2003). For several ostracod species populations of both sexes are known to indicate more favourable living conditions, whereas the parthenogenetic reproduction takes place when the environmental setting of habitats changes. The identification of *F. lapponica* var. *arctica* males is doubtless due to preserved Zenker organs (typical male reproduction organ) in some specimens. Males of *F. lapponica* var. *arctica* in unit III may indicate more favourable conditions for this species than exist today for the regions where this species has been found. To verify this argument, male specimens should be observed under modern conditions.

The species *Bradleystrandesia reticulata* (ZADDACH, 1844) (Figure II-11, 11–12) is broadly distributed in mid-latitudes as well as in high-latitude regions and has broad tolerance to such environmental factors (Meisch 2000). Populations of both sexes are known from northern habitats, but probably due to the rareness of *B. reticulata* valves in our record we observed only female valves. The species has been found in East Siberia (Pietrzeniuk 1977; Semenova 2005), and also in Greenland and in the Siberian Arctic (Alm 1914; Wetterich et al. 2008a). Fossil records of this species were obtained in European Quaternary deposits (Griffiths 1995), but have not been found in Siberia to date.

The fossil ostracod assemblage can be interpreted as typical for shallow water conditions with moderate water temperature variations. The habitat was most likely a pond, as these

organisms are typical in today's polygonal tundra landscapes. The great rarity of ostracod findings in the studied sequence contradicts the former studies of Wetterich et al. (2005) on the Bykovsky Peninsula. The occurrence and preservation of ostracod shells in syngenetic frozen deposits of ponds in low-centred ice wedge polygon systems depends on numerous hydrological, pedological, and cryological factors. Nevertheless, the high abundance of shells in even one sample confirms that freshwater ostracods could appear in such a periglacial environment.

II.5.7 Insect remains

The samples for insect remains analysis were mostly taken in equal volume, but contain different numbers of individuals. The poorest sample with 43 insect remains (Bkh2002 B11, 10 m a.r.l.) comes from unit I, and the richest sample with 463 insect remains comes from the upper part of the unit IVa (Bkh 2002 B04, 31.7 m a.r.l.). The fossil insect fauna is mostly represented by beetles (order Coleoptera) whose hard chitin parts allow good preservation in non-consolidated deposits (Supplementary data C and Figure II-12). We also found some unidentified remains from other orders such as Hymenoptera, Diptera, Trichoptera, and Hemiptera, which have not been included in the species list.

The insect association in unit I (Bkh2002 B11) consists predominantly of representatives of the typical arctic tundra group and the mesic tundra group. Insects of the steppe groups as well as the shrub, meadows, and forest groups are only secondarily represented. This spectrum does not show that there are differences between insect assemblages of the lower sand units I and II, and the Ice Complex units III and IVa (Figure II-13). Fossil insect assemblages from the Ice Complex units III and IVa show a rather consistent composition of species representative of different ecological spectra (Figure II-13). There are almost equal abundances of xerophilous groups, mostly tundra xerophilous (ks), meso-hygrophilous tundra insects (mt), and arctic insects (tt). An increase of steppe insects is evident at about 40 kyr BP (Bkh2002 B10), but later the species composition returns to the previous one.

In the Ice Complex units III and IVa (Figure II-13) insect remains are present at an unusually high level for an arctic group, with an average of 20–30% and a maximum of up to 86% of all remains. Insects of typical and arctic tundra (tt) are represented here mostly by the willows weevil *Isochnus arcticus*. The steppe group (ss) which normally plays an important role in most late Pleistocene entomofauna records from Northeast Siberia (Kiselyov 1981; Sher and Kuzmina 2007) is not very abundant in the section, except for one single assemblage. Nevertheless, the character of the late Pleistocene insect fauna from Kurungnakh Island is evidently steppe–tundra. The assemblage includes such typical Pleistocene steppe–tundra species as the pill beetle *Morychus viridis*, the leaf beetles

Chrysolina brunnicornis and *Ch. arctica*, the weevils *Coniocleonus cinerascens*, *Coniocleonus astragali*, *Coniocleonus ferrugineus*, and *Stephanocleonus fossulatus* in association with some xerophilous species, which were widespread in the Pleistocene steppe–tundra landscape and have become relatively rare recently, as well as the weevils *Mesotrichapion wrangelianum*, *Hemitrichapion tschernovi*, *Sitona borealis*, *Hypera ornate*, and others. The most typical member of the steppe-tundra insect community, the weevil *Stephanocleonus eruditus*, was not found in the Kurungnakh assemblages, but was present in most samples of neighbouring outcrops (Kuzmina, unpublished data; Sher et al. 2005). Although this weevil is a significant local feature of this section, it seems to be not characteristic of the entire region.

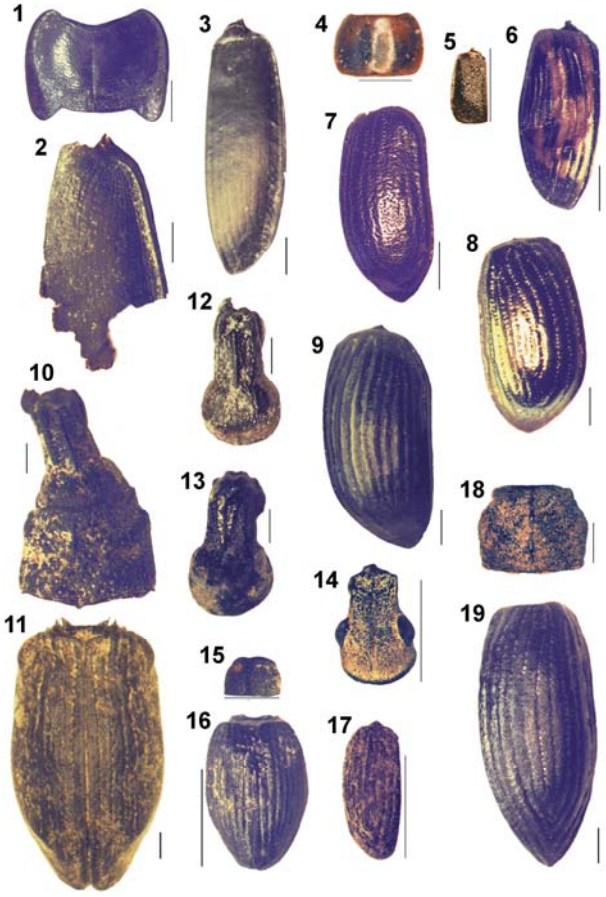

Figure II-12 Fossil insect remains from Kurungnakh Island: (1) Ground beetle *Carabus kolymensis*, pronotum; (2) Ground beetle *Carabus kolymensis*, elytron; (3) Ground beetle *Pterostichus tundrae*, elytron; (4) Rove beetle *Tachinus brevipennis*, pronotum; (5) Rove beetle *Eucnecosum* cf. *tenue*, elytron; (6) Dung beetle *Aphodius* sp., elytron; (7) Leaf beetle *Chrysomela blaisdelli*, elytron; (8) Leaf beetle *Chrysolina brunnicornis wrangeliana*, elytron; (9) Leaf beetle *Chrysolina subsulcata*, elytron; (10) Weevil *Coniocleonus cinerascens*, head and pronotum; (11) Weevil *Coniocleonus* sp., connected elytrons; (12) Weevil *Coniocleonus astragali*, head; (13) Weevil *Stephanocleonus fossulatus*, head; (14) Weevil *Sitona borealis*, head; (15) Weevil *Isochnus arcticus*, pronotum; (16) Weevil *Isochnus arcticus*, connected elytrons; (17) Weevil *Isochnus flagellum*, elytron; (18) Weevil *Lepyrus nordenskioeldi*, pronotum; and (19) Weevil *Lepyrus nordenskioeldi*, elytron. Note varying scales which correspond to 1 mm length each

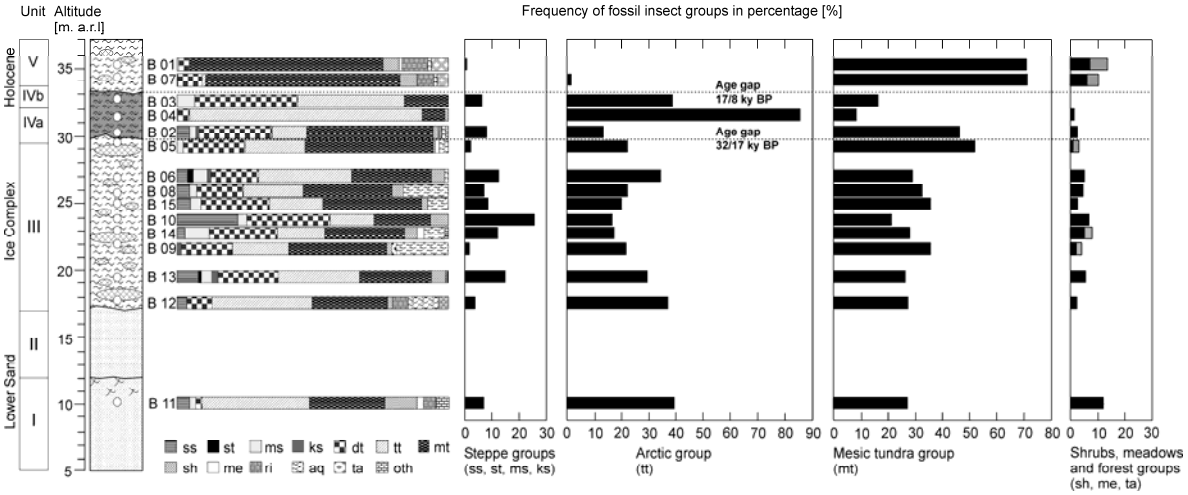

Figure II-13 Distribution of the fossil insect groups from Kurungnakh Island: (ss) insects of hemicryophytic steppe; (st) insects of thermophilic steppe; (ms) insects of meadow-steppe and steppe-like habitats in the tundra zone; (ks) xerophilic insects of different habitats; (dt) insects of dry tundra habitats; (tt) insects from typical and arctic tundra; (mt) insects of mesic tundra habitats; (sh) insects associated with shrubs; (me) insects living in meadows, mostly in the forest zone; (ri) riparian insects; (aq) aquatic insects; (ta) dendrophagous and insects restricted to the taiga zone; and (oth) other insects

In unit IVa the appearance of the insect assemblage changed at about 17 kyr BP (Bkh2002 B04). There is a distinct domination of arctic species with up to 86%, which have not been described in Siberian fossil insect records yet. Even the “coldest” insect assemblages (LGM) from Bykovsky Peninsula (Sher et al. 2005) contain less percent of arctic species. In general, the species diversity of this sample is low. This sample contains no true steppe insects, except for the quite cold-resistant meadow-steppe leaf beetle *Chrysolina arctica*, recently known only from Wrangel Island, East Siberian Sea. The overlying sample (Bkh2002 B03) at 33.3 m a.r.l. belongs to the early Holocene unit IVb and has lost the overwhelmingly arctic species assemblage, but it still contains more than 30% arctic insects.

The observed pattern seems to be similar to the well-studied Ice Complex sequence of Bykovsky Peninsula, Laptev Sea (Sher et al. 2005), where one stage in the section (ca 46–34 kyr BP) with mostly low occurrences of the steppe insect group and a remarkable number of arctic insects was also discovered. Nevertheless, some short intervals of slightly increasing steppe insects are present also. The Bykovsky Peninsula sediments, dated between 24 and 15 kyr BP, which corresponds to the coldest time of the LGM, is characterised by 20–67% of arctic insects.

Two samples (Bkh2002 B01 and B07) were studied from the Holocene unit V. An additional sample taken in 2000 from nearby thermokarst deposits (profile Bkh 4, Figure 4 in Schirrmeister et al. 2003) was also analysed (Supplementary data C). All Holocene

insect assemblages are significantly different from those found in both the lower sand and the Ice Complex deposits. The Holocene entemofauna is dominated by species of wet tundra (mt) at up to 72%. The wet tundra group includes species such as the ground beetles *Diacheila polita*, *Pterostichus brevicornis*, *P. pinguedineus*, *P. vermiculosus*, and *P. agonus* as well as the rove beetles *Olophrum consimile* and *Tachinus brevipennis*.

The ground beetle *Pterostichus (Cryobius) brevicornis* is the most abundant beetle in the Holocene sediments. This is one of the most common beetles in modern tundra and forest-tundra regions. The rove beetle *O. consimile* was dominant in the thermokarst unit V. This is not surprising, since the rove beetles of *Olophrum* genus prefer boggy habitats, which are typical of succession stages of thermokarst depressions. There are also a number of other hygrophilous insects in all Holocene assemblages from Kurungnakh: the ground beetles *Dyschiriodes nigricornis*, *Agonum* sp., the rove beetle *Holoboreaphilus nordenskioeldi*, the leaf beetle *Hydrothassa hannoverana*, and the weevil *Tournotaris bimaculatus*. In addition, some forest species have been found: the ground beetle *Notiophilus sylvaticus*, the rove beetle *Phyllodrepa angustata*, and the bark beetle *Polygraphus* sp. The species diversity of shrub insects in the Holocene unit V is higher than in the Pleistocene insect assemblages. The shrub group (sh) includes the leaf beetles *Chrysomela blaisdelli* and *Phratora vulgatissima* and the weevils *Dorytomus imbecillus*, *D. rufulus amplipennis*, and *Lepyrus nordenskjoeldi*.

According to the insect studies we can discern three stages of the developing environment. During the first stage (>50–32 kyr BP), there existed a cold variant of steppe–tundra that comprises the formation of the lower sand units I and II as well as the Ice Complex unit III. The second stage (about 17 kyr BP) was characterised by dry and cold tundra conditions (unit IVa). During the Holocene (<8 kyr BP) an open tundra-like landscape occurred, probably with weakly developed forest vegetation (units IVb and V).

II.5.8 Mammal remains

The mammal bone collection consists of 118 bones sampled by different scientists in 2000–2002, 2005, and 2007 on the outcrops of Kurungnakh Island. Palaeontological findings from the island are also stored in the Museum of the Lena Delta Reservation, Tiksi, Russia.

According to the finding's location the bones were divided into four groups. Group A comprises eight strictly in situ-found bones, probably of one individual horse (*Equus caballus*) from the Ice Complex deposits. Additionally, another in situ horse bone was found with copulas and marrow in a state of excellent preservation. The second group B includes 37 samples from thermo-erosional cirques. Knowing the altitude of these findings (i.e. the minimum level of their original position), we can define the approximate altitude

from which these bones come. Therefore, both groups A and B have direct importance for the geological interpretation of the deposits. A third group C of mammal remains were collected within the debris of the exposure. They also belong to the section. Group D includes the biggest part of the collection from Kurungnakh Island, which comes from the shore and sandbank. Such bones were probably relocated from distant outcrops by river current or ice flow. Nevertheless, such findings also reflect the association of large fossil mammals.

The composition of the studied bone collection is typical for the late Pleistocene "Mammoth Fauna" of the Siberian Arctic. Fossil remains of woolly mammoths (*Mammuthus primigenius* BLUMENBACH, 1799), horses (*Equus caballus* LINNAEUS, 1758), reindeer (*Rangifer tarandus* LINNAEUS, 1758), bison (*Bison priscus* BOJANUS, 1827), muskox (*Ovibos moschatus* ZIMMERMANN, 1780), and hares (*Lepus* sp.) are found (Figure II-14). The lower horizon of the Ice Complex (unit III) contains rather abundant bone material. The bones that were found there belonged to separate individuals, e.g. several ribs and leg bones from two mammoth individuals, as well as several leg bones from one horse individual.

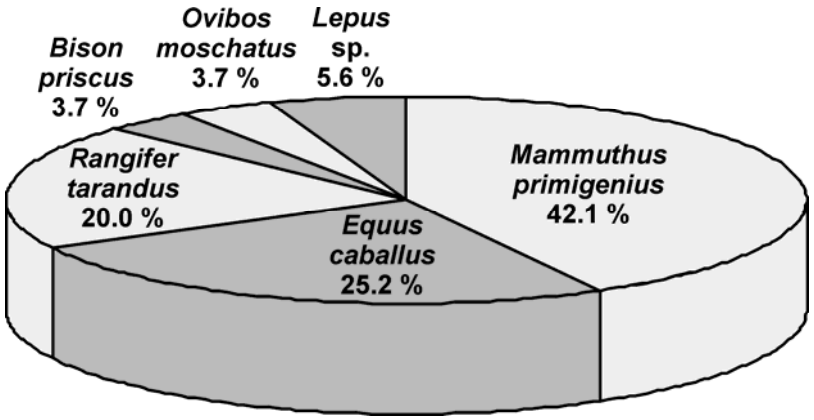

Figure 14 Taxonomic composition of mammal bones collected from Kurungnakh Island (total number - 107 samples)

The taxonomical study was completed by radiocarbon dates obtained from bone collagen. In unit III several horse bones were found in situ. Large hind leg bones from one horse individual were collected from the frozen silt sediments between two peat layers at a height near 20 m a.r.l. From the same level a foreleg bone from a horse was collected and radiocarbon dated at 34 200±500 yr BP (GIN 110883, BKh–O65, Schirrmeister et al. 2003). Another radiocarbon date on bone material of 31 220±180 yr BP (OxA-13675, BKh–O42) also indicates the age of the Ice Complex deposits.

Palaeontological material from the thermo-erosional cirques of Kurungnakh Island is characterised by good preservation and completeness. Often different parts of a skeleton

lay not far from each other. Of particular interest is the find of a woolly mammoth skeleton fragments (23 bones: vertebrae, ribs, foreleg, and hind leg bones) from the highest layers of the Ice Complex at 32–35 m a.r.l.

The species diversity of the Kurungnakh collection agrees with other records from Arctic Siberia (e.g. Kuznetsova et al. 2003; Sher et al. 2005). The large number of bones from grazing mammals mostly originating from deposits of the Kargin interstadial period (unit III) is evidence for the high bioproductivity of the tundra–steppe (mammoth steppe) vegetation during this period. This conclusion is also supported by large amounts of spores from dung-inhabiting Sordariales fungi, which were determined by palynological studies.

II.6 Discussion

II.6.1 Local stratigraphic and palaeoenvironmental interpretation

The multidisciplinary palaeo-proxy dataset allows several stages of the late Quaternary history of the study area to be distinguished (Table II-5).

Table II-5 Summary of stratigraphy, facies, and palaeecology deduced from multiproxy records

Stratigraphy	Age	Palaeoenvironment						
	[kyr BP]	Sediment	Ice	Pollen	Seeds	Ostracods	Insects	Mammals
Middle / Late Holocene	6-3	*Unit V* Modern landscape of the 3rd Lena terrace	Small syngenetic ice wedges, warmer winter temperature	*PZ 5* Modern vegetation and climate conditions	Wet tundra with willow shrubs		Wet shrub tundra	
Early Holocene	≈ 8	*Unit IVb* Thermokarst	Small syngenetic ice wedges, warmer winter temperature	*PZ 4* Shrub tundra, climate optimum	Dry tundra or tundra steppe, no climate change recorded		Open shrub tundra	
Hiatus	17 - 8	No records						
Late Weichselian (Sartan) stadial	≈ 17	*Unit IVa* Ice complex	Huge syngenetic ice wedges, cold winter temperature	*PZ 3* Scarce arctic tundra steppe, cold and dry	Dry tundra or tundra steppe, cold and dry		Arctic tundra, cold and dry	
Hiatus	32 - 17	No records						
Middle Weichselian (Kargin) interstadial	50 - 32	*Unit III* Pediment plain in front of the Chekanovsky Ridge, Ice complex	Huge syngenetic ice wedges, cold winter temperature	*PZ 2* Arctic tundra steppe, climate optimum *PZ 1* Arctic tundra steppe, climate	Tundra steppe, generally dry, wet habitats existing	Shallow ponds with moderate temperature variations	Arctic tundra steppe, cold and dry	Optimum of the "Mammoth Fauna"
Early Weichselian (Zyryan) stadial	100 - 50	*Unit I to II* Meandering river branch	No syngenetic ice wedges due to unstable conditions		Sparse data. Arctic tundra-steppe, cold and dry		Arctic tundra steppe, cold and dry	

The lower sand formation of the section (units I and II) accumulated under changing shallow water conditions probably in a meandering fluvial milieu of the Palaeo-Lena River between 100 and 50 kyr before. This is evident by IR-OSL dating (Schwamborn et al. 2002), ^{230}Th/U dates, and a lot of indefinite radiocarbon ages >50 kyr BP (Schirrmeister et al. 2003). According to our new data, which coincide with previous datings of these widely

exposed sands in the western Lena Delta, an Early Weichselian (Zyryan) Stadial river landscape existed there. Changing transport and accumulation conditions can be deduced from the sedimentological data from units I and II. While in unit I, small-scale interbedding, poor sorting, and repeated peat layer accumulation reflect frequently varying water runoff in a quiet, shallow river branch or near-shore area, unit II is distinguished by fine lamination, less organic material, more continuous grain sizes, and a higher degree of sorting. Such properties give evidence for stable fluvial current conditions. Probably because of meandering the course of the river branch shifted between the sedimentation of units I and II. These sediments were epigenetically frozen after their accumulation. The fluvial sedimentation conditions were unfavourable for the deposition and preservation of pollen, plant macrofossils, insect remains, and ostracod shells in units I and II. The concentration of these fossils is therefore too low for detailed environmental interpretations. The bioindicators merely reflect the existence of a tundra–steppe environment during the time of deposition, which correspond to previous regional multiproxy records (Schirrmeister et al. 2002a, b, c, 2003; Sher et al. 2005).

Great change in all environmental conditions is evident with the beginning of the Middle Weichselian (Kargin) Interstadial in connection with the formation of the Ice Complex unit III. Large syngenetic ice wedges, ice-supersaturated deposits, segregated ice veins, and thick cryoturbated peaty palaeosol horizons, which are characteristic for the late Pleistocene Yedoma Suite reflect the different landscape that existed between 50 and 32 kyr BP. Subaerial accumulation within a polygonal ice wedge net, which formed on a badly-drained plain in front of the Chekanovsky Ridge, is assumed for this period, with an estimated mean accumulation rate of about 12.5 cm per 100 years. In addition, decreasing values of magnetic susceptibility reveal a change of the sediment source. According to heavy mineral analysis the sediments source was the neighbouring Chekanovsky Ridge (Schwamborn et al. 2002; Schirrmeister et al. 2003). The formation of large syngenetic ice wedges clearly indicates long-term stable landscape conditions during this interval. We doubt interpretations of the Yedoma Suite as pure Arctic loess and the primarily aeolian origin (Tomirdiaro 1982) because of poorly sorting, multimodal grain-size distribution, ice-supersaturated cryolithology, and local sediment sources (Schirrmeister et al. 2008b).

Palynological spectra from unit III reflect relatively warm summer conditions for the earlier part of the Kargin Interstadial about 42 kyr BP (PZ 1) and climate amelioration during the Kargin climate optimum between 40 and 32 kyr BP (PZ 2). Abundant *Pediastrum* and *Botryococcus* colonies indicate the presence of small ponds in the surrounding area and wet places may have existed in the floodplain itself during that time as is indicated by the presence of *Carex* sect. *Phacocystis* macrofossils during most of the period. The variation

of dominating insect groups is probably indicative of short-term environmental fluctuations during the entire interstadial period.

An age gap of 15 kyr between 32 kyr (units III) and 17 kyr BP (unit IVa) spans long periods of the Sartan glacial. This gap could be explained by local erosion most of the Sartan deposits. A rather similar gap between 28.5 and 12 kyr BP was recorded from Bol'shoy Lyakhovsky Island (73°N, 141°E), eastern Laptev Sea (Andreev et al. 2008). Nevertheless, in other Ice Complex sequences e.g. from Bykovsky Peninsula southeast of the Lena Delta (Andreev et al. 2002; Schirrmeister et al. 2002a, b) and at Cape Mamontov Klyk (73°N, 117°E), western Laptev Sea (Schirrmeister et al. 2008b) complete Sartan sequences were proven. Unit IV, which is sedimentologically and cryolithologically uniform, consists of the late Sartan part (unit IVa) and the Holocene part (unit IVb). This subdivision in a scarce tundra environment (PZ 3) and more moderate shrubby tundra (PZ 4) is also clearly evident according to pollen and insect data. Therefore, unit IV probably could be considered as deposits that buried an erosional surface of the Ice Complex sequence, where late Sartan deposits were preserved between small Holocene thermokarst depressions. Layers of poorly sorted sand with low organic content indicate occasionally stronger transport energy due to sporadic surface runoff events during the late Sartan and the partial reworking of unit IVa deposits during the early Holocene. The age hiatus of almost 10 kyr between units IVa and IVb was probably caused by Holocene thermokarst processes. Nevertheless, a polygonal ice wedge system persisted for the entire time as is indicated by the continuous growth of large syngenetic ice wedges. Pollen and plant macro-remains indicate that a tundra–steppe, typical for extremely continental arctic climate, persisted during the late Sartan (unit IVa) period even though this ecosystem was probably much scarcer than before due to a temperature drop. The fossil insect records also point to very cold conditions before termination of the last glacial period.

Large changes in nearly all sedimentological parameters and palaeoecological records are evident for the uppermost middle to late Holocene part (unit V) of the sequence, which discordantly covers the frozen deposits below. This part of the sequence was accumulated from the middle Holocene on. Modern environmental conditions appeared after 5 kyr BP. Warmer winter temperatures during the late Holocene in comparison to the Kargin Interstadial are deduced from the stable isotope signature of the ice wedges. The size of the polygonal ice wedge systems decreased because of warmer winter conditions as well as the newly formed small-scale thermokarst relief. All bioindicators reflect a sharp shift of environmental conditions in the Holocene. Paludification and a complete disappearance of dry habitats are the most sustained effects, indicated by plant and insect

remains. The pollen record indicates a rapid warming during the early Holocene and successive cooling towards modern climate conditions in the course of the Holocene.

II.6.2 Beringian palaeoenvironmental context

The local records that are presented from Kurungnakh Island in the southern Lena Delta are additional pieces required to reconstruct the puzzle that is the late Pleistocene environment and the climate dynamics of Western Beringia.

The lower sand horizon was part of a meandering fluvial system that ran parallel to the Chekanovsky Ridge. Early Weichselian fluvial deposits are widely distributed in the Laptev Sea region. Similar horizons of fluvial sands below Ice Complex deposits were also observed on Cape Mamontov Klyk in front of the Pronchishchev Ridge at the western Laptev Sea coast (Schirrmeister 2004; Schirrmeister et al. 2008b) and on the Bykovsky Peninsula in front of the Kharaulakh Ridge southeast of the study site (). The formation of such deposits was explained by Galabala (1987) as accumulation of a huge alluvial fan of the Lena River within a closed non-marine basin. This interpretation is similar to our opinion. According to Schwamborn et al. (2002) and Schirrmeister et al. (2003) the sandy units were formed on a flood plain of the Early Weichselian Lena River and intensified fluvial activities are assumed for the Early Weichselian (Zyryan) period. The landscape-forming processes in the study region probably pertained to a more comprehensive reorganisation of the hydrological systems in northern Eurasia. For example, Mangerud et al. (2004) have reported on the rerouting of the drainage in northern Eurasia during this period connected with changing orientation of glacial meltwater runoff.

The Ice Complex horizon on Kurungnakh Island belongs to the Yedoma Suite of the Northeast Siberian Quaternary stratigraphy (Sher et al. 1987). The studied horizon contains primarily middle Weichselian (Kargin) interstadial records and a part of Late Weichselian (Sartan) Stadial. Sedimentological, cryolithological, pollen, plant macrofossil, and insect data sets are similar to those of the Kargin sequence on Bykovsky Peninsula (Andreev et al. 2002; Kienast et al. 2005; Sher et al. 2005). For most of the sedimentation time (>50 to about 32 kyr BP), the palaeoecological records from Kurungnakh Island indicate the existence of tundra–steppe vegetation under a cold continental climate. In contrast to the Ice Complex sequence on the Bykovsky Peninsula (Andreev et al. 2002; Kienast et al. 2005; Sher et al. 2005), the Kargin interstadial climate was possibly somewhat cooler during the summer periods. The Bykovsky Peninsula was most likely climatically favoured by the proximity of the Kharaulakh Mountain range, which hampered cloud formation, trapped rainfall coming from the west, and caused warm southerly winds (foehn). According to Arkhipov et al. (2005) the Kargin Interstadial in West Siberia lasted from 55–50 to 23 kyr BP and consisted of three warming periods separated by two cooling

periods (44–42 and 35–30 kyr BP). In Central Yakutia the duration of the Kargin period is given between 42–43 and 25–26 kyr BP (Fradkina et al. 2005a). In the Yana-Indigirka lowland the Kargin Interstadial between 50 and 26 kyr BP was also characterised by three warming and two cooling phases (Fradkina et al. 2005b). The younger Kargin sediments were not preserved in the studied sequence. Therefore, our palaeoecological records reflect at least some weak environmental fluctuations during approximately 42–32 kyr BP, which probably correspond to the end of the first cooling and the next warming period. Interstadial records were evident also in the eastern region of the Beringian landmass during the Kargin period. In Alaska the Middle Wisconsin was also characterised by stronger soil formation and accumulation of detritic organic beds (Hopkins 1982) as well as downward thawing of permafrost and ice wedges in the Fairbanks area about >38 kyr BP, which was connected with a warmer period during the Middle Wisconsin time (Péwé 1975). In addition, Berger (2003) refers several papers about a MIS warming between 40 and 30 kyr BP in northwest and Central Alaska as well as in the Canadian Yukon Territory. Finally, Anderson and Lozhkin (2001) summarise most of the Beringian MIS 3 records available ten years before. Between 30–26 and 39–33 kyr BP the climate was as warm or nearly as warm as present whereas cool and dry intervals occurred between 33–30 and 45–39 kyr BP. That also corresponds with our local interpretation from Kurungnakh Island of climate variations during the studied MIS3 time frame.

The sharp cut of the sequence at about 32 kyr BP and the absence of about 15 kyr of sedimentation are probably connected with strong erosional processes due to neotectonic seismic events on the seismically highly active rift region at the northeastern border of the Eurasian continental plate (Drachev et al. 1998; Franke et al. 2000). Similar explanations are given for the lack of the Sartan stage in Ice Complex deposits on Bol'shoy Lyakhovsky Island (Andreev et al. 2008).

The degradation of permafrost by thermokarst processes and the transgression of the arctic shelf seas due to global warming were the most radical environmental impacts on the entire arctic and subarctic Siberian lowlands during the late Pleistocene–Holocene transition period. Ice-rich permafrost sequences in Siberia are therefore often not complete on the top because of thermokarst processes and discontinued accumulation. A strong reorganisation of hydrological systems and the entire periglacial landscape is evident during this highly dynamic transition period (e.g. Grosse et al. 2007).

The Holocene climate optimum in Arctic Siberia was characterised by the spreading of warmth-loving species associations, especially of shrubby tundra and trees. This is also reported by some other studies in the Siberian Arctic.

II.7 Conclusions

The sedimentation regimes in the periglacial palaeo-landscapes changed repeatedly during the late Quaternary (meandering fluvial, proluvial or colluvial, and thermokarst-affected). Erosional events occurred as a consequence of permafrost degradation and likely neotectonic seismic activity.

The studied sequence covers a time of various glacial/interglacial and stadial/interstadial climate variations. The corresponding stratigraphic configuration of the late Pleistocene to Holocene sequence on Kurungnakh Island correlates well with the regional stratigraphy in northeastern Siberia and with Eurasian equivalents (Early, Middle, and Late Weichselian, Holocene) as well as global analogues (MIS 4–1).

Between >50 and 32 kyr BP, the palaeoecological records indicate the existence of tundra–steppe vegetation under a cold continental climate. After a sedimentation gap at the termination of the Late Weichselian cold stage, extremely cold-arid conditions prevailed in the study area according to bioindicators. At the beginning of the Holocene, the tundra–steppe disappeared completely due to lasting paludification. A shrub tundra formed with boreal elements like *A. fruticosa*, which later retreated in response to the late Holocene cooling.

Supplementary data A, B and C

Supplementary data A Selected photographs of the studied sediment units I–V of late Quaternary permafrost outcrops from Kurungnakh Island

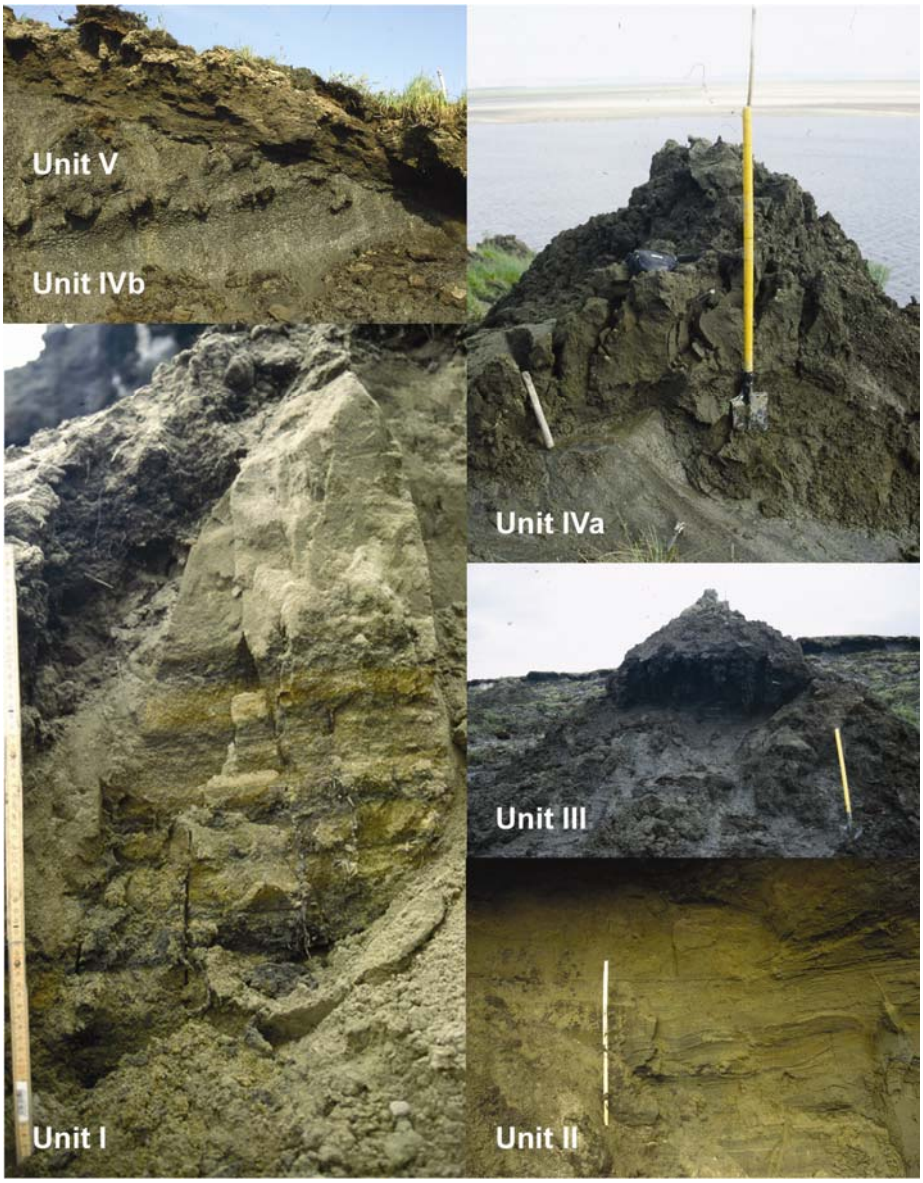

Supplementary data B Taxonomic composition of plant macrofossils from Kurungnakh Island

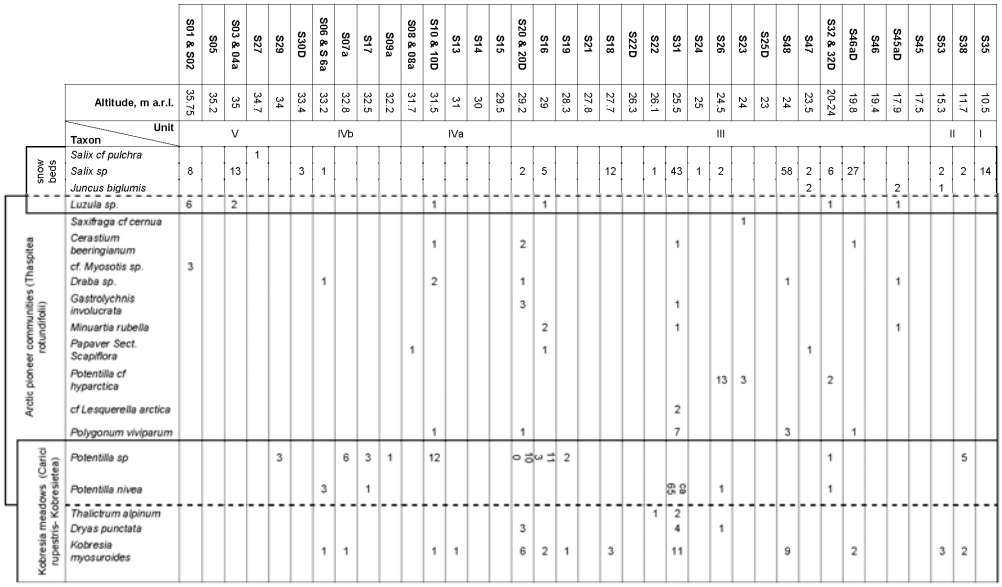

		S01 & S02	S05	S03 & 04a	S27	S29	S30D	S06 & S 6a	S07a	S17	S09a	S08 & 08a	S10 & 10D	S13	S14	S15	S20 & 20D	S16	S19	S21	S18	S22D	S22	S31	S24	S26	S23	S25D	S48	S47	S32 & 32D	S46aD	S46	S45aD	S45	S53	S38	S35
	Altitude, m a.r.l.	35.75	35.2	35	34.7	34	33.4	33.2	32.8	32.5	32.2	31.7	31.5	31	30	29.5	29.2	29	28.3	27.8	27.7	26.3	26.1	25.5	25	24.5	24	23	23	24	23.5	20-24	19.8	19.4	17.9	17.5	15.3	11.7	10.5
	Unit			V				IVb					IVa											III													II		–
	Taxon																																					
snow beds	*Salix cf pulchra*				1																																	
	Salix sp	8		13			3	1									2	5			12		1	43	1	2			58	2	6	27				2	2	14
	Juncus biglumis																													2				2		1		
	Luzula sp.	6		2									1					1													1		1					
Arctic pioneer communities (Thaspitea rotundifolii)	*Saxifraga cf cernua*																									1											
	Cerastium beeringianum												1				2							1								1						
	cf. Myosotis sp.	3																																				
	Draba sp.							1					2				1												1				1					
	Gastrolychnis involucrata																3							1														
	Minuartia rubella																	2						1														
	Papaver Sect. Scapiflora											1						1												1								
	Potentilla cf hyparctica																									13	3					2						
	cf Lesquerella arctica																							2														
	Polygonum viviparum												1				1							7					3			1						
Kobresia meadows (Caricirupestris-Kobresietea)	*Potentilla sp*					3			6	3	1		12				10	11	2					ca 65							1					5	
	Potentilla nivea							3		1																1					1							
	Thalictrum alpinum																						1	2														
	Dryas punctata																3							4		1												
	Kobresia myosuroides							1	1				1	1			6	2	1		3			11					9			2				3	2	

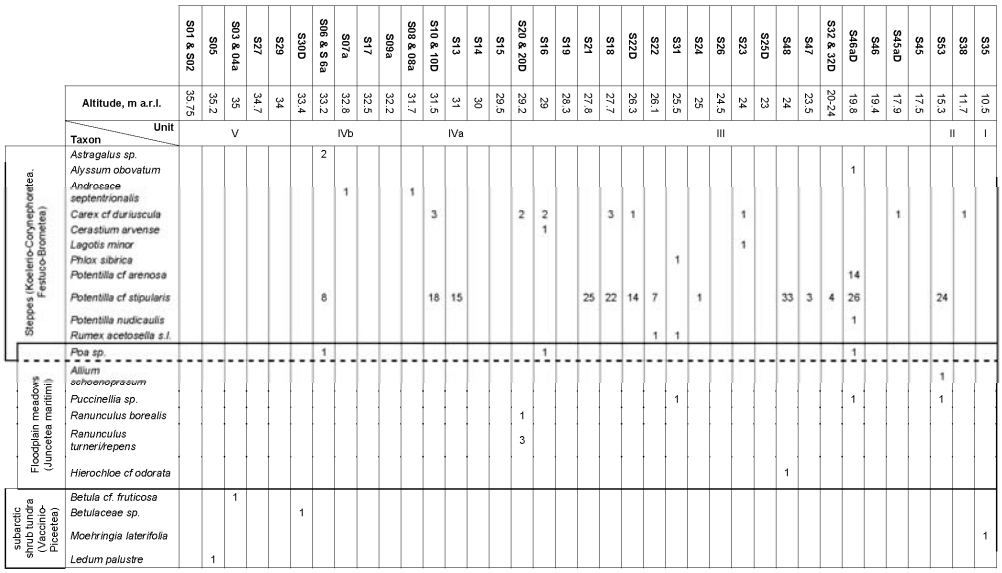

		S01 & S02	S05	S03 & 04a	S27	S29	S30D	S06 & S 6a	S07a	S17	S09a	S08 & 08a	S10 & 10D	S13	S14	S15	S20 & 20D	S16	S19	S21	S18	S22D	S22	S31	S24	S26	S23	S25D	S48	S47	S32 & 32D	S46aD	S46	S45aD	S45	S53	S38	S35
	Altitude, m a.r.l.	35.75	35.2	35	34.7	34	33.4	33.2	32.8	32.5	32.2	31.7	31.5	31	30	29.5	29.2	29	28.3	27.8	27.7	26.3	26.1	25.5	25	24.5	24	23	23	24	23.5	20-24	19.8	19.4	17.9	17.5	15.3	11.7	10.5
	Unit			V				IVb					IVa											III													II		–
	Taxon																																					
Steppes (Koelerio-Corynephoretea. Festuco-Brometea)	*Astragalus sp.*							2																														
	Alyssum obovatum																															1						
	Androsace septentrionalis								1			1																											
	Carex cf duriuscula												3				2	2			3	1					1							1			1		
	Cerastium arvense																	1																					
	Lagotis minor																										1											
	Phlox sibirica																							1														
	Potentilla cf arenosa																															14						
	Potentilla cf stipularis							8					18	15						25	22	14	7		1				33	3	4	26				24		
	Potentilla nudicaulis																															1						
	Rumex acetosella s.l.																						1	1														
	Poa sp.							1										1														1						
Floodplain meadows (Juncetea maritimi)	*Allium schoenoprasum*																																			1		
	Puccinellia sp.																							1								1				1		
	Ranunculus borealis																1																					
	Ranunculus turneri/repens																3																					
	Hierochloe cf odorata																												1									
subarctic shrub tundra (Vaccinio-Piceetea)	*Betula cf. fruticosa*			1																																	
	Betulaceae sp.						1																															1
	Moehringia laterifolia																																					
	Ledum palustre		1																																			

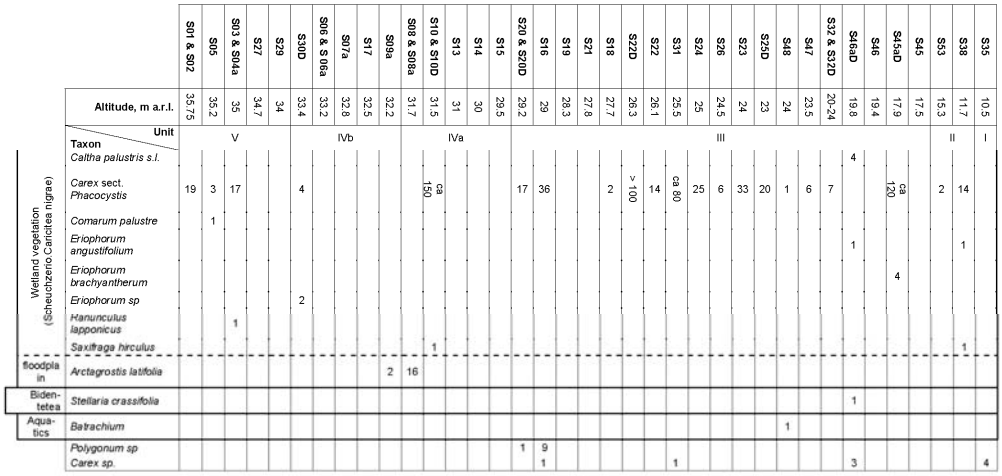

		S01 & S02	S05	S03 & S04a	S27	S29	S30D	S06 & S 06a	S07a	S17	S09a	S08 & S08a	S10 & S10D	S13	S14	S15	S20 & S20D	S16	S19	S21	S18	S22D	S22	S31	S24	S26	S23	S25D	S48	S47	S32 & S32D	S46aD	S46	S45aD	S45	S53	S38	S35
	Altitude, m a.r.l.	35.75	35.2	35	34.7	34	33.4	33.2	32.8	32.5	32.2	31.7	31.5	31	30	29.5	29.2	29	28.3	27.8	27.7	26.3	26.1	25.5	25	24.5	24	23	23	24	23.5	20-24	19.8	19.4	17.9	17.5	15.3	11.7	10.5
	Unit			V				IVb					IVa											III													II		–
	Taxon																																					
Wetland vegetation (Scheuchzerio Caricitea nigrae)	*Caltha palustris s.l.*																															4						
	Carex sect. Phacocystis	19	3	17			4						ca 150				17	36			2	> 100	14	ca 80	25	6	33	20	1	6	7		ca 120		2	14	
	Comarum palustre		1																																			
	Eriophorum angustifolium																															1					1	
	Eriophorum brachyantherum																																	4				
	Eriophorum sp						2																															
	Hanunculus lapponicus			1																																	
	Saxifraga hirculus												1																								1	
floodplain	*Arctagrostis latifolia*										2	16																										
Biden-tetea	*Stellaria crassifolia*																															1						
Aqua-tics	*Batrachium*																												1									
	Polygonum sp																1	9																				
	Carex sp.																	1						1								3						4

Supplementary data C Taxonomic composition of insect associations from Kurungnakh Island. For ecological index (EcoCode) see Figure II-13

TAXON		MNI															
		Bkh-02															Bkh-00
Sample №	EcoCode	B11	B12	B13	B9	B14	B10	B15	B08	B06	B05	B02	B04	B03	B07	B01	B-4
Altitude [m a.r.l.]		10	17.5	19.2	21.5	22.7	23.5	24.7	26	27.5	30	30.7	31.7	33.3	34.7	35.7	34
Unit		I	III								IVa		IVb	V			
Order Coleoptera																	
Family Carabidae																	
Carabus (Morphocarabus) odoratus Motsch.	dt	—	—	—	—	—	—	—	—	—	1	—	—	—	—	—	—
C. (Aulonocarabus) truncaticollis Esch.	mt	—	—	—	1	1	—	1	1	—	1	—	—	—	—	—	—
C. (Aulonocarabus) kolymensis Kryzh.et Bud.	ms	—	—	1	—	—	—	—	—	—	—	—	—	—	—	—	—
Carabus sp.	oth	1	1	—	—	—	—	—	—	—	—	1	—	—	—	—	—
Notiophilus aquaticus L.	ks	—	—	—	—	—	—	—	—	—	—	1	—	—	—	—	1
N. sylvaticus Esch.	ta	—	—	—	—	—	—	—	—	—	—	—	—	—	8	9	—
Diacheila polita Fald.	mt	—	—	—	—	—	—	—	—	—	—	—	—	—	11	7	5
Dyschiriodes nigricornis Motsch.	na	1	—	—	—	—	—	—	—	—	—	—	—	—	1	—	—
Dyschiriodes sp.	na	—	—	—	—	—	—	—	—	—	—	1	—	—	—	—	—
Bembidion (Peryphanes) dauricum Motsch.	dt	—	—	—	—	—	—	—	—	1	—	—	—	—	—	—	—
B. (Peryphanes) sp.	na	—	—	—	1	—	—	—	—	—	—	—	—	—	—	—	1
B. (Plataphus) sp.	na	1	—	—	—	—	—	—	—	—	—	—	—	—	—	—	—
Bembidion sp.	oth	—	—	—	—	1	—	—	—	—	—	—	—	—	—	—	—
Stereocerus haematopus (Dej.)	dt	—	—	1	—	—	—	—	—	—	—	—	—	—	—	—	1
Pterostichus (Cryobius) ventricosus Esch.	mt	—	—	—	—	1	—	—	—	—	1	—	—	—	—	—	1
P. (Cryobius) pinguedineus Esch.	mt	—	—	2	—	—	3	—	—	1	3	—	1	1	—	3	—
P. (Cryobius) brevicornis (Kirby)	mt	2	—	—	—	1	—	13	18	—	2	3	—	—	55	46	3
P. (Cryobius) sp.	mt	2	1	19	5	6	—	5	2	22	8	3	4	3	7	10	8
Family Carabidae																	
P. (Lenapterus) costatus Men.	mt	—	7	1	8	2	—	2	3	1	8	1	—	—	—	—	—

TAXON		MNI															
		Bkh-02															Bkh-00
Sample №	EcoCode	B11	B12	B13	B9	B14	B10	B15	B08	B06	B05	B02	B04	B03	B07	B01	B-4
Altitude [m a.r.l.]		10	17.5	19.2	21.5	22.7	23.5	24.7	26	27.5	30	30.7	31.7	33.3	34.7	35.7	34
Unit		I	III								IVa		IVb	V			
P. (Lenapterus) vermiculosus Men.	mt	—	—	—	—	—	—	—	—	—	—	—	—	—	3	3	4
P. (Lenapterus) agonus Horn.	mt	—	—	—	—	—	—	—	—	—	—	—	—	—	—	—	1
P. (Petrophilus) abnormis Sahlb.	dt	—		9	1	—	2	6	2	3	—	—	—	—	—	3	—
P. (Petrophilus) tundrae Tschitsch.	dt	—	—	—	—	—	—	—	—	—	—	1	—	—	2	—	—
P. (Tundraphilus) sublaevis Sahlb.	dt	1	—	3	—	2	—	4	1	4	4	—	2	3	—	1	—
Agonum sp.	na	—	—	—	—	—	—	—	—	—	—	—	—	—	2	—	1
Curtonotus alpinus (Payk.)	dt	—	2	32	7	3	14	12	12	12	11	19	18	25	5	3	2
Harpalus sp.	ms	1	—	—	—	—	—	—	—	—	—	—	—	—	—	—	—
Family Dytiscidae																	
Hydroporus lapponum (Gyll.)	aq	—	—	—	—	1	—	—	—	—	—	—	—	—	—	—	—
H. acutangulus ? Thoms.	aq	—	4	—	7	2	—	4	—	2	3	1	—	—	—	1	2
Hydroporus sp.	aq	—	—	—	—	—	—	—	1	—	—	—	—	—	—	—	—
Agabus moestus (Curt.)	aq	—	2	—	2	—	—	3	—	—	—	—	—	—	—	—	1
Agabus sp.	aq	—	—	—	—	2	—	—	1	—	1	—	—	—	—	—	—
Family Hydrophilidae																	
Helophorus splendidus Sahlb.	aq	—	—	—	1	—	—	3	22	—	—	—	—	—	—	—	1
Helophorus sp.	aq	—	—	—	—	—	—	—	—	—	—	—	—	—	1	—	—
Hydrobius fuscipes F.	aq	—	—	—	—	—	—	—	—	—	—	—	—	—	—	—	1
Family Leiodidae																	
Cholevinus sibiricus (Jean.)	mt	—	—	27	—	2	2	4	3	3	7	21	5	3	—	—	—
Family Staphylinidae																	
Phyllodrepa angustata Maekl.	ta	—	—	—	—	—	—	—	—	—	—	—	—	—	1	—	—

TAXON		MNI															
		Bkh-02															Bkh-00
Sample №	EcoCode	B11	B12	B13	B9	B14	B10	B15	B08	B06	B05	B02	B04	B03	B07	B01	B-4
Altitude [m a.r.l.]		10	17.5	19.2	21.5	22.7	23.5	24.7	26	27.5	30	30.7	31.7	33.3	34.7	35.7	34
Unit		I	III								IVa		IVb	V			
P. (Lenapterus) vermiculosus Men.	mt	—	—	—	—	—	—	—	—	—	—	—	—	—	3	3	4
P. (Lenapterus) agonus Horn.	mt	—	—	—	—	—	—	—	—	—	—	—	—	—	—	—	1
P. (Petrophilus) abnormis Sahlb.	dt	—		9	1	—	2	6	2	3	—	—	—	—	—	3	—
P. (Petrophilus) tundrae Tschitsch.	dt	—	—	—	—	—	—	—	—	—	—	1	—	—	2	—	—
P. (Tundraphilus) sublaevis Sahlb.	dt	1	—	3	—	2	—	4	1	4	4	—	2	3	—	1	—
Agonum sp.	na	—	—	—	—	—	—	—	—	—	—	—	—	—	2	—	1
Curtonotus alpinus (Payk.)	dt	—	2	32	7	3	14	12	12	12	11	19	18	25	5	3	2
Harpalus sp.	ms	1	—	—	—	—	—	—	—	—	—	—	—	—	—	—	—
Family Dytiscidae																	
Hydroporus lapponum (Gyll.)	aq	—	—	—	—	1	—	—	—	—	—	—	—	—	—	—	—
H. acutangulus ? Thoms.	aq	—	4	—	7	2	—	4	—	2	3	1	—	—	—	1	2
Hydroporus sp.	aq	—	—	—	—	—	—	—	1	—	—	—	—	—	—	—	—
Agabus moestus (Curt.)	aq	—	2	—	2	—	—	3	—	—	—	—	—	—	—	—	1
Agabus sp.	aq	—	—	—	—	2	—	—	1	—	1	—	—	—	—	—	—
Family Hydrophilidae																	
Helophorus splendidus Sahlb.	aq	—	—	—	1	—	—	3	22	—	—	—	—	—	—	—	1
Helophorus sp.	aq	—	—	—	—	—	—	—	—	—	—	—	—	—	1	—	—
Hydrobius fuscipes F.	aq	—	—	—	—	—	—	—	—	—	—	—	—	—	—	—	1
Family Leiodidae																	
Cholevinus sibiricus (Jean.)	mt	—	—	27	—	2	2	4	3	3	7	21	5	3	—	—	—
Family Staphylinidae																	
Phyllodrepa angustata Maekl.	ta	—	—	—	—	—	—	—	—	—	—	—	—	—	1	—	—

Supplementary data C Continuation

TAXON		MNI															
		Bkh-02															Bkh-00
Sample №	**EcoCode**	**B11**	**B12**	**B13**	**B9**	**B14**	**B10**	**B15**	**B08**	**B06**	**B05**	**B02**	**B04**	**B03**	**B07**	**B01**	**B-4**
Altitude [m a.r.l.]		**10**	**17.5**	**19.2**	**21.5**	**22.7**	**23.5**	**24.7**	**26**	**27.5**	**30**	**30.7**	**31.7**	**33.3**	**34.7**	**35.7**	**34**
Unit		**I**				**III**						**IVa**		**IVb**		**V**	
Ch. septentrionalis Men.	mt	2	—	—	—	—	—	1	—	2	2	—	2	—	—	2	—
Ch. brunnicornis wrangeliana Vor.	ms	—	—	—	—	2	—	—	—	—	2	1	—	3	—	—	—
Chrysomela blaisdelli Van Dyke	sh	—	—	1	—	2	—	—	—	—	—	—	—	—	—	—	1
Phratora vulgatissima L.	sh	—	—	—	—	—	—	—	—	—	—	—	—	—	—	—	1
Hydrothassa hannoverana F.	na	—	1	—	2	—	—	—	—	—	—	—	—	—	1	1	1
H. glabra Hbst.	na	—	—	1	—	—	—	—	—	—	—	—	—	—	—	—	—
Phaedon concinnus Steph.	me	—	—	—	1	—	—	—	—	—	2	—	—	—	—	—	—
Family Apionidae																	
Pseudoprotapion cf. *astragali* Payk.	ms	—	—	1	—	—	—	4	1	2	—	—	—	—	—	—	—
Hemitrichapion tschernovi T.-M.	dt	—	—	8	1	12	1	8	3	3	5	1	—	—	2	—	—
Mesotrichapion wrangelianum Kor.	dt	—	1	—	—	—	—	—	1	—	3	2	—	—	—	—	—
Apionidae gen. indet.	dt?	—	—	—	—	—	—	—	—	—	—	—	—	—	2	—	—
Family Curculionidae																	
Sitona lineellus Bonsd.	me	—	—	—	—	2	—	—	—	—	—	—	—	—	—	—	—
Family Curculionidae																	
S. borealis Kor.	dt	—	—	8	1	—	2	2	3	3	5	—	—	—	1	—	—
Coniocleonus cinerascens Hochh.	ms	—	—	6	—	—	—	—	—	—	—	—	—	—	—	—	—
C. astragali T.-M.et Kor.	ms	—	—	2	—	—	2	—	—	—	—	—	—	—	—	—	—
C. ferrugineus Fahr.	ms	—	—	—	—	—	—	—	2	—	—	—	—	—	—	—	—
Coniocleonus sp.	ms	—	—	3	—	2	—	1	—	5	1	—	—	2	—	1	—
Stephanocleonus fossulatus F-W.	st	—	—	1	—	—	—	—	—	1	—	—	—	—	—	—	—
Stephanocleonus sp.	st	—	—	—	—	—	—	—	—	2	—	—	—	—	—	—	—

TAXON		MNI															
		Bkh-02															Bkh-00
Sample №	**EcoCode**	**B11**	**B12**	**B13**	**B9**	**B14**	**B10**	**B15**	**B08**	**B06**	**B05**	**B02**	**B04**	**B03**	**B07**	**B01**	**B-4**
Altitude [m a.r.l.]		**10**	**17.5**	**19.2**	**21.5**	**22.7**	**23.5**	**24.7**	**26**	**27.5**	**30**	**30.7**	**31.7**	**33.3**	**34.7**	**35.7**	**34**
Unit		**I**				**III**						**IVa**		**IVb**		**V**	
Ch. septentrionalis Men.	mt	2	—	—	—	—	—	1	—	2	2	—	2	—	—	2	—
Ch. brunnicornis wrangeliana Vor.	ms	—	—	—	—	2	—	—	—	—	2	1	—	3	—	—	—
Chrysomela blaisdelli Van Dyke	sh	—	—	1	—	2	—	—	—	—	—	—	—	—	—	—	1
Phratora vulgatissima L.	sh	—	—	—	—	—	—	—	—	—	—	—	—	—	—	—	1
Hydrothassa hannoverana F.	na	—	1	—	2	—	—	—	—	—	—	—	—	—	1	1	1
H. glabra Hbst.	na	—	—	1	—	—	—	—	—	—	—	—	—	—	—	—	—
Phaedon concinnus Steph.	me	—	—	—	1	—	—	—	—	—	2	—	—	—	—	—	—
Family Apionidae																	
Pseudoprotapion cf. *astragali* Payk.	ms	—	—	1	—	—	—	4	1	2	—	—	—	—	—	—	—
Hemitrichapion tschernovi T.-M.	dt	—	—	8	1	12	1	8	3	3	5	1	—	—	2	—	—
Mesotrichapion wrangelianum Kor.	dt	—	1	—	—	—	—	—	1	—	3	2	—	—	—	—	—
Apionidae gen. indet.	dt?	—	—	—	—	—	—	—	—	—	—	—	—	—	2	—	—
Family Curculionidae																	
Sitona lineellus Bonsd.	me	—	—	—	—	2	—	—	—	—	—	—	—	—	—	—	—
Family Curculionidae																	
S. borealis Kor.	dt	—	—	8	1	—	2	2	3	3	5	—	—	—	1	—	—
Coniocleonus cinerascens Hochh.	ms	—	—	6	—	—	—	—	—	—	—	—	—	—	—	—	—
C. astragali T.-M.et Kor.	ms	—	—	2	—	—	2	—	—	—	—	—	—	—	—	—	—
C. ferrugineus Fahr.	ms	—	—	—	—	—	—	—	2	—	—	—	—	—	—	—	—
Coniocleonus sp.	ms	—	—	3	—	2	—	1	—	5	1	—	—	2	—	1	—
Stephanocleonus fossulatus F-W.	st	—	—	1	—	—	—	—	—	1	—	—	—	—	—	—	—
Stephanocleonus sp.	st	—	—	—	—	—	—	—	—	2	—	—	—	—	—	—	—

III Data tables from Chapters 2 and 3

Appendix III-1 (Chapter 2) Location, type and hydrochemical characteristics of the studied lakes and ponds. The sample sites are arranged by water types as in Figure 2-6. The water type identification follows the key: intrapolygon pond → intrapolygon; interpolygon pond → interpolygon; thaw lake → thaw lake; thermokarst lake shore → thermokarst and river branch of the Lena River → river branch

Sample №	Locality	Date yy-mm-dd	Water type	Sample depth [m]	Cond* [µS/cm]	pH	O_2 [mg/l]	T_{Air} [°C]	T_{Water} [°C]
SAM-13	Kurungnakh	02-08-15	intrapolygon	0.5	27.0	6.5	5.9	13.3	13.6
SAM-21	Samoylov	02-08-21	intrapolygon	0.5	105.6	7.5	9.0	11.9	11.4
SAM-23	Samoylov	02-08-21	interpolygon	0.5	98.8	7.5	8.3	15.8	13.9
SAM-25	Samoylov	02-08-25	interpolygon	0.5	94.3	7.5	9.4	6.1	6.2
SAM-30	Samoylov	02-08-27	intrapolygon	0.5	106.6	7.5	10.6	10.5	8.0
SAM-37	Samoylov	02-08-30	interpolygon	0.5	93.3	7.2	11.3	7.9	9.3
SAM-44	Samoylov	02-09-03	intrapolygon	0.5	70.8	7.5	9.0	7.6	7.0
SAM-01	Samoylov	02-08-02	thaw lake	0.5	90.4	7.1	9.8	10.4	11.4
SAM-17	Samoylov	02-08-19	thaw lake	0.5	64.9	7.5	8.4	11.1	12.0
SAM-19	Samoylov	02-08-20	thaw lake	0.5	53.1	7.5	8.8	13.5	12.5
SAM-24	Samoylov	02-08-21	thaw lake	0.5	254.0	7.0	5.3	16.5	15.3
SAM-26	Samoylov	02-08-25	thaw lake	0.5	78.5	7.5	10.6	8.6	7.7
SAM-27	Samoylov	02-08-25	thaw lake	0.5	109.4	7.5	10.0	8.5	8.3
SAM-28	Samoylov	02-08-26	thaw lake	0.5	122.6	7.6	8.8	9.8	7.8
SAM-29	Samoylov	02-08-26	thaw lake	0.5	110.8	7.5	11.0	17.0	10.3
SAM-32	Samoylov	02-08-27	thaw lake	0.5	113.2	7.5	10.8	14.2	9.8
SAM-33	Samoylov	02-08-29	thaw lake	0.5	96.9	7.5	9.7	8.0	6.7
SAM-34	Samoylov	02-08-29	thaw lake	0.5	107.7	7.5	9.5	6.7	6.1
SAM-40	Samoylov	02-09-01	thaw lake	0.5	77.8	7.5	11.2	8.7	5.9
SAM-41	Samoylov	02-09-01	thaw lake	0.5	79.6	7.3	9.4	6.3	6.6
SAM-12	Kurungnakh	02-08-15	thermokarst	0.5	28.0	7.2	7.7	11.6	13.4
SAM-38	Kurungnakh	02-08-31	thermokarst	0.5	109.2	7.5	9.8	6.1	7.8
SAM-14	Samoylov	02-08-18	river branch	0.5	86.6	7.5	8.8	13.0	12.6

*Electrical conductivity

Appendix III-1 (Chapter 2) Continuation

Sample №	Locality	Water type	Mg ppm	Sr ppm	Ca ppm	HCO_3 ppm	Na ppm	Cl ppm	K ppm	SO_4 ppm
SAM-13	Kurungnakh	intrapolygon	1.39	0.03	2.68	13.4	1.04	1.90	< 0.3	< 0.1
SAM-21	Samoylov	intrapolygon	4.31	0.03	5.25	67.5	0.81	2.22	0.46	< 0.1
SAM-23	Samoylov	interpolygon	7.09	0.06	11.22	60.8	1.68	2.50	0.56	< 0.1
SAM-25	Samoylov	interpolygon	7.01	0.06	10.86	65.5	1.79	1.86	0.32	< 0.1
SAM-30	Samoylov	intrapolygon	7.23	0.06	8.87	66.4	1.37	2.21	0.76	< 0.1
SAM-37	Samoylov	interpolygon	6.88	0.06	11.07	61.4	1.68	2.61	0.43	< 0.1
SAM-44	Samoylov	intrapolygon	4.22	0.04	6.43	39.3	1.20	1.86	0.59	< 0.1
SAM-01	Samoylov	thaw lake	4.68	0.05	7.62	50.3	2.17	3.45	0.60	0.91
SAM-17	Samoylov	thaw lake	3.80	0.04	8.07	38.3	0.88	1.20	0.56	< 0.1
SAM-19	Samoylov	thaw lake	2.84	0.04	6.31	31.8	1.53	2.35	0.47	0.73
SAM-24	Samoylov	thaw lake	14.51	0.25	36.63	148	2.29	1.98	1.83	< 0.1
SAM-26	Samoylov	thaw lake	5.48	0.05	8.19	52.1	1.57	2.16	0.99	< 0.1
SAM-27	Samoylov	thaw lake	7.85	0.08	12.30	66.4	1.77	2.74	0.79	< 0.1
SAM-28	Samoylov	thaw lake	8.21	0.08	14.53	77.5	1.87	2.81	1.00	< 0.1
SAM-29	Samoylov	thaw lake	7.19	0.08	13.86	70.6	1.55	2.31	0.96	< 0.1
SAM-32	Samoylov	thaw lake	8.29	0.08	13.74	78.6	1.55	2.20	0.91	< 0.1
SAM-33	Samoylov	thaw lake	6.68	0.06	10.83	56.7	1.34	1.79	0.79	< 0.1
SAM-34	Samoylov	thaw lake	8.48	0.07	11.80	71.5	1.67	2.63	0.78	< 0.1
SAM-40	Samoylov	thaw lake	5.26	0.05	8.64	48.6	1.46	2.73	0.76	< 0.1
SAM-41	Samoylov	thaw lake	5.34	0.05	8.83	50.4	1.45	2.09	0.48	< 0.1
SAM-12	Kurungnakh	thermokarst	1.50	0.02	3.18	16.7	0.66	0.92	0.37	< 0.1
SAM-38	Kurungnakh	thermokarst	2.80	0.06	8.73	66.9	0.80	2.44	0.39	0.28
SAM-14	Samoylov	river branch	3.29	0.08	10.77	41.6	4.26	6.39	0.59	3.96

Appendix III-2 (Chapter 2) Stable isotopes ($\delta^{18}O$, $\delta^{13}C$) and element ratios (Mg/Ca, Sr/Ca) of ostracod calcite and ambient water. The species identification follows the key: species (e.g. pedata → *F. pedata*), sex (f → female or m → male) and state (rec → recent or sub → subfossil)

Sample №	Species identification	Valve $\delta^{18}O$ ‰ PDB	Water $\delta^{18}O$ ‰ SMOW	Valve $\delta^{13}C$ ‰ PDB	Water $\delta^{13}C$ ‰ PDB
SAM-01	pedata_f_rec	-13.55	-16.65	-3.75	-2.11
SAM-01	pedata_m_rec	-13.83	-16.65	-3.95	-2.11
SAM-12	pedata_f_rec	-15.92	-17.64	-8.44	-8.14
SAM-12	pedata_m_rec	-16.16	-17.64	-5.89	-8.14
SAM-12	pedata_f_sub	-15.47	-17.64	-7.15	-8.14
SAM-12	pedata_m_sub	-15.72	-17.64	-6.89	-8.14
SAM-13	pedata_f_rec	-11.38	-13.34	-11.01	-14.40
SAM-13	pedata_f_sub	-11.49	-13.34	-10.81	-14.40
SAM-13	pedata_m_sub	-10.81	-13.34	-11.10	-14.40
SAM-14	candida_f_rec	-17.69	-20.38	-7.74	-6.85
SAM-14	harmsworthi_f_rec	-18.46	-20.38	-6.47	-6.85
SAM-17	hyalina_f_rec	-14.21	-15.87	-2.76	-3.89
SAM-17	hyalina_m_rec	-14.12	-15.87	-2.85	-3.89
SAM-17	hyalina_f_sub	-13.97	-15.87	-2.98	-3.89
SAM-17	hyalina_m_sub	no data	-15.87	no data	-3.89
SAM-19	harmsworthi_f_rec	-15.14	-16.39	-3.40	-10.01
SAM-21	pedata_f_rec	-10.93	-13.29	-3.17	-0.22
SAM-21	pedata_m_rec	-11.00	-13.29	-3.50	-0.22
SAM-21	sanctipatricii_f_sub	no data	-13.29	no data	-0.22
SAM-23	pedata_f_rec	-12.66	-14.57	-2.38	-5.61
SAM-23	pedata_m_rec	-12.82	-14.57	-1.94	-5.61
SAM-23	species2_f_rec	-12.71	-14.57	-3.35	-5.61
SAM-23	species2_m_rec	no data	-14.57	no data	-5.61
SAM-23	harmsworthi_f_rec	-13.53	-14.57	-1.58	-5.61
SAM-23	harmsworthi_m_rec	-14.07	-14.57	-1.94	-5.61
SAM-24	pedata_f_rec	-10.94	-17.59	-4.19	-4.88
SAM-24	pedata_m_rec	-11.51	-17.59	-4.16	-4.88
SAM-24	pedata_f_sub	-10.80	-17.59	-4.19	-4.88
SAM-24	pedata_m_sub	-11.65	-17.59	-4.14	-4.88
SAM-25	pedata_f_rec	-13.31	-14.41	-3.72	-2.50
SAM-25	pedata_f_sub	-13.21	-14.41	-3.79	-2.50
SAM-25	pedata_m_sub	no data	-14.41	no data	-2.50
SAM-25	jakutica_f_sub	no data	-14.41	no data	-2.50
SAM-26	pedata_f_rec	-11.37	-13.46	-2.54	-9.12
SAM-26	pedata_m_rec	-11.78	-13.46	-3.44	-9.12
SAM-27	pedata_f_rec	-12.19	-14.11	-2.42	-1.39
SAM-27	pedata_m_rec	-12.45	-14.11	-1.84	-1.39
SAM-27	pedata_f_sub	-12.51	-14.11	-2.52	-1.39
SAM-28	pedata_f_rec	-11.71	-13.35	-2.48	0.05
SAM-28	pedata_m_rec	-11.52	-13.35	-2.84	0.05
SAM-29	pedata_f_rec	-12.56	-14.17	-4.16	-3.45
SAM-29	pedata_m_rec	-12.13	-14.17	-4.41	-3.45
SAM-30	pedata_f_rec	-10.69	-13.16	-1.82	-0.19
SAM-30	pedata_m_rec	-10.94	-13.16	-2.50	-0.19
SAM-32	pedata_f_rec	-11.80	-14.26	-2.55	-3.71
SAM-32	pedata_m_rec	-12.12	-14.26	-2.45	-3.71
SAM-32	pedata_f_sub	-11.55	-14.26	-2.11	-3.71
SAM-33	pedata_f_rec	-11.83	-14.01	-4.13	-1.13
SAM-33	pedata_m_rec	-12.20	-14.01	-4.89	-1.13
SAM-34	pedata_f_rec	-10.84	-13.80	-2.18	-1.95
SAM-34	pedata_m_rec	-11.76	-13.80	-2.53	-1.95
SAM-37	harmsworthi_f_rec	-13.32	-15.41	-3.89	-4.60
SAM-38	pedata_f_rec	-15.46	-17.39	-6.99	-3.49
SAM-38	pedata_m_rec	-15.17	-17.39	-6.75	-3.49
SAM-38	pedata_f_sub	-15.36	-17.39	-7.25	-3.49
SAM-38	pedata_m_sub	-14.95	-17.39	-6.82	-3.49
SAM-38	candida_f_rec	-14.97	-17.39	-6.91	-3.49
SAM-38	candida_f_sub	-14.74	-17.39	-6.57	-3.49
SAM-40	pedata_f_rec	-12.46	-15.37	-3.59	-4.00

Appendix III-2 (Chapter 2) Continuation

Sample №	Species identification	Valve Mg/Ca ($\times 10^{-2}$) molar	Water Mg/Ca molar	Valve Sr/Ca ($\times 10^{-3}$) molar	Water Sr/Ca ($\times 10^{-3}$) molar
SAM-01	pedata_f_rec	0.51	1.07	1.01	3.02
SAM-01	pedata_m_rec	0.37	1.07	1.06	3.02
SAM-12	pedata_f_rec	0.53	0.81	1.07	3.33
SAM-12	pedata_m_rec	0.48	0.81	0.98	3.33
SAM-12	pedata_f_sub	0.44	0.81	1.36	3.33
SAM-12	pedata_m_sub	0.20	0.81	1.52	3.33
SAM-13	pedata_f_rec	0.38	0.90	1.94	4.83
SAM-13	pedata_f_sub	0.21	0.90	1.67	4.83
SAM-13	pedata_m_sub	0.31	0.90	1.40	4.83
SAM-14	candida_f_rec	0.13	0.53	1.43	3.37
SAM-14	harmsworthi_f_rec	0.35	0.53	0.96	3.37
SAM-17	hyalina_f_rec	0.37	0.81	0.95	2.65
SAM-17	hyalina_m_rec	0.39	0.81	0.95	2.65
SAM-17	hyalina_f_sub	0.32	0.81	0.92	2.65
SAM-17	hyalina_m_sub	0.45	0.81	0.97	2.65
SAM-19	harmsworthi_f_rec	0.45	0.78	0.85	2.69
SAM-21	pedata_f_rec	0.41	1.39	0.93	3.09
SAM-21	pedata_m_rec	0.58	1.39	0.80	3.09
SAM-21	sanctipatricii_f_sub	1.00	1.39	1.18	3.09
SAM-23	pedata_f_rec	0.38	1.08	0.73	2.74
SAM-23	pedata_m_rec	0.57	1.08	0.69	2.74
SAM-23	species2_f_rec	1.08	1.08	0.89	2.74
SAM-23	species2_m_rec	0.62	1.08	0.85	2.74
SAM-23	harmsworthi_f_rec	0.87	1.08	0.69	2.74
SAM-23	harmsworthi_m_rec	0.84	1.08	0.75	2.74
SAM-24	pedata_f_rec	0.61	0.66	0.92	3.18
SAM-24	pedata_m_rec	0.46	0.66	0.92	3.18
SAM-24	pedata_f_sub	0.24	0.66	0.97	3.18
SAM-24	pedata_m_sub	0.47	0.66	0.96	3.18
SAM-25	pedata_f_rec	0.47	1.11	1.14	2.76
SAM-25	pedata_f_sub	0.39	1.11	0.73	2.76
SAM-25	pedata_m_sub	0.39	1.11	0.71	2.76
SAM-25	jakutica_f_sub	0.57	1.11	0.70	2.76
SAM-26	pedata_f_rec	0.29	1.15	1.06	3.00
SAM-26	pedata_m_rec	0.47	1.15	0.89	3.00
SAM-27	pedata_f_rec	0.41	1.11	0.77	2.94
SAM-27	pedata_m_rec	0.57	1.11	0.84	2.94
SAM-27	pedata_f_sub	0.51	1.11	0.80	2.94
SAM-28	pedata_f_rec	0.37	0.98	0.85	2.77
SAM-28	pedata_m_rec	0.52	0.98	1.10	2.77
SAM-29	pedata_f_rec	0.42	0.89	1.36	2.64
SAM-29	pedata_m_rec	0.46	0.89	1.23	2.64
SAM-30	pedata_f_rec	0.52	1.40	0.87	3.07
SAM-30	pedata_m_rec	0.67	1.40	0.92	3.07
SAM-32	pedata_f_rec	0.51	1.03	0.83	2.73
SAM-32	pedata_m_rec	0.32	1.03	0.81	2.73
SAM-32	pedata_f_sub	0.53	1.03	0.92	2.73
SAM-33	pedata_f_rec	0.54	1.06	1.13	2.75
SAM-33	pedata_m_rec	0.80	1.06	1.21	2.75
SAM-34	pedata_f_rec	0.39	1.24	0.81	2.78
SAM-34	pedata_m_rec	0.44	1.24	0.78	2.78
SAM-37	harmsworthi_f_rec	0.97	1.09	0.66	2.64
SAM-38	pedata_f_rec	0.77	0.55	0.92	3.22
SAM-38	pedata_m_rec	0.54	0.55	0.84	3.22
SAM-38	pedata_f_sub	0.25	0.55	0.84	3.22
SAM-38	pedata_m_sub	0.42	0.55	0.86	3.22
SAM-38	candida_f_rec	0.68	0.55	1.18	3.22
SAM-38	candida_f_sub	0.26	0.55	1.18	3.22
SAM-40	pedata_f_rec	0.59	1.07	1.04	2.96

Appendix III-3 (Chapter 3) Location, type, and general characteristics of the studied lakes and ponds

Lake №	Date*	Region**	Latitude °N	Longitude °E	Elevation [m, a.s.l.]	Lake type***	Size [m x m]	Depth [m]
Yak-01	10.07.05	Lena	61°45'39,6"	130°28'15,6"	213	D	20 x 30	1.8
Yak-02	10.07.05	Lena	61°45'36,0"	130°28'19,2"	213	D	60 x 100	3.5
Yak-03	10.07.05	Lena	61°45'39,6"	130°28'26,4"	233	D	80 x 80	4.6
Yak-04	11.07.05	Lena	61°45'54,0"	130°27'55,9"	209	Alas	40 x 250	1.8
Yak-05	11.07.05	Lena	61°46'11,1"	130°28'07,4"	215	T	100 x 300	4.6
Yak-06	13.07.05	Lena	62°06'13,3"	130°13'21,6"	130	L-D	300 x 400	1.3
Yak-07	13.07.05	Lena	62°01'00,1"	130°03'57,1"	138	L-D	400 x 700	1.0
Yak-08	15.07.05	Yakutsk	62°03'60,5"	129°03'23,4"	228	Alas	400 x 800	1.5
Yak-09	15.07.05	Yakutsk	62°03'28,9"	129°03'13,9"	228	Alas	200 x 300	2.2
Yak-10	17.07.05	Lena	61°42'11,4"	129°22'11,1"	160	Alas	80 x 150	5.2
Yak-11	17.07.05	Lena	61°36'50,4"	130°42'12,6"	182	Alas	200 x 350	5.2
Yak-12	17.07.05	Lena	61°37'06,6"	130°42'28,1"	172	Alas	no data	3.0
Yak-13	18.07.05	Lena	61°33'26,0"	130°32'48,3"	219	Th-E	200 x 600	3.9
Yak-14	18.07.05	Lena	61°34'06,0"	130°33'59,2"	203	Th-E	100 x 300	1.9
Yak-15	18.07.05	Lena	61°34'20,7"	130°36'42,7"	198	Th-E	80 x 300	1.6
Yak-16	19.07.05	Lena	61°24'13,4"	130°33'10,8"	224	Alas	150 x 400	1.5
Yak-17	19.07.05	Lena	61°33'09,3"	130°51'34,0"	234	Alas	40 x 350	1.6
Yak-18	20.07.05	Lena	61°33'01,5"	130°53'11,7"	211	Th-E	no data	1.5
Yak-19	20.07.05	Lena	61°24'26,0"	131°07'01,7"	250	Alas	50 x 150	1.3
Yak-20	20.07.05	Lena	61°32'45,3"	130°54'18,9"	230	Th-E	400 x 800	2.0
Yak-21	22.07.05	Lena	62°00'11,3"	131°49'06,1"	208	Th-E	100 x 200	1.9
Yak-22	22.07.05	Lena	62°00'23,7"	131°43'10,0"	207	Th-E	100 x 200	1.7
Yak-23	22.07.05	Lena	62°07'54,2"	131°13'24,9"	169	Th-E	150 x 350	2.3
Yak-24	23.07.05	Lena	61°58'05,7"	132°14'49,7"	182	Alas	200 x 300	3.2
Yak-25	23.07.05	Lena	61°48'05,9"	132°04'58,8"	198	Alas	300 x 500	2.0
Yak-26	24.07.05	Lena	61°54'09,9"	132°12'22,1"	187	Alas	150 x 150	1.7
Yak-27	24.07.05	Lena	61°53'24,2"	132°09'51,3"	200	Alas	200 x 350	2.0
Yak-28	24.07.05	Lena	61°56'23,9"	132°09'55,8"	171	T	150 x 200	4.7
Yak-29	24.07.05	Lena	61°56'46,5"	132°08'39,2"	207	Alas	150 x 200	1.4
Yak-30	26.07.05	Yakutsk	61°57'60,9"	129°24'51,2"	200	Tukulan	300 x 500	4.0
Yak-31	31.07.05	Yakutsk	62°00'11,7"	129°35'57,8"	102	R-B	20 x 30	no data
Yak-32	31.07.05	Yakutsk	62°00'13,7"	129°35'58,8"	104	R-B	20 x 100	no data
Yak-33	02.08.05	Yakutsk	61°50'57,8"	129°34'10,2"	111	R-B	30 x 300	no data
Yak-34	03.08.05	Yakutsk	62°18'22,8"	129°54'29,0"	96	R-B	200 x 500	no data
Yak-35	04.08.05	Yakutsk	62°19'00,7"	129°30'20,3"	182	Alas	40 x 50	no data
Yak-36	05.08.05	Yakutsk	62°19'03,7"	129°32'58,2"	217	Alas	20 x 30	no data
Yak-37	05.08.05	Yakutsk	62°18'35,7"	129°31'18,9"	218	Alas	40 x 50	no data
Yak-38	06.08.05	Yakutsk	62°20'02,2"	129°34'50,1"	200	D	30 x 200	no data
Yak-39	06.08.05	Yakutsk	62°19'39,2"	129°33'43,2"	210	Alas	100 x 100	no data
Yak-40	09.08.05	Moma	66°20'57,7"	143°23'42,9"	220	L-D	200 x 300	no data
Yak-41	09.08.05	Moma	66°20'57,4"	143°23'37,1"	223	L-D	10 x 100	no data
Yak-42	10.08.05	Moma	66°28'33,7"	143°15'01,9"	210	K	20 x 30	no data
Yak-43	13.08.05	Moma	66°31'05,2"	143°45'26,0"	768	L-D	300 x 500	no data
Yak-44	15.08.05	Moma	66°27'22,6"	143°15'27,3"	205	A	30 x 300	no data
Yak-45	15.08.05	Moma	66°26'57,8"	143°16'00,0"	203	A	10 x 30	no data
Yak-46	16.08.05	Moma	66°16'34,2"	143°18'49,1"	220	R-B	20 x 1100	no data
Yak-47	16.08.05	Moma	66°17'11,2"	143°18'48,4"	224	R-B	30 x 1000	no data
Yak-48	17.08.05	Moma	66°00'54,4"	143°12'40,4"	270	R-B	30 x 250	no data
Yak-49	18.08.05	Moma	66°11'44,9"	143°20'49,5"	240	L-D	5 x 10	no data
Yak-50	18.08.05	Moma	66°13'18,2"	143°23'13,5"	235	L-D	2 x 5	1.0
Yak-51	19.08.05	Moma	66°14'44,2"	143°19'18,2"	222	L-D	10 x 20	1.0
Yak-52	20.08.05	Moma	66°26'22,2"	143°17'20,1"	217	L-D	5 x 5	0.5
Yak-53	20.08.05	Moma	66°26'46,4"	143°16'24,4"	203	L-D	10 x 20	1.0
Yak-54	21.08.05	Moma	66°29'14,3"	143°13'23,8"	203	L-D	10 x 30	1.0
Yak-55	21.08.05	Moma	66°28'19,8"	143°15'21,2"	211	K	5 x 10	1.0
Yak-56	21.08.05	Moma	66°27'23,1"	143°14'05,4"	199	A	10 x 200	1.0

*day/month/year

**Lena – Lena-Amga interfluve, Central Yakutia; Yakutsk – near Yakutsk, Central Yakutia; Moma – near Khonnu, NE Yakutia

***Alas – Lake in an Alas depression; D – Dyuedya; T – Tyympy; Th-E – Lake in a thermokarst valley; R-B – River branch on the floodplain; Tukulan – Dune lake; L-D – Lake in a lowland depression; A – Anthropogenic (man-made reservoir); K – Kerdyugen

Appendix III-4 (Chapter 3) Hydrochemical and stable isotope characteristics of the studied lakes and ponds

Lake №	EC* [mS/cm]	pH	O_2 [mg/l]	T_{water} [°C]	$\delta^{18}O$ [‰] VSMOW	δD [‰] VSMOW	$\delta^{13}C$ [‰] VPDP
Yak-01	1.63	8.54	3.88	24.3	-13.02	-131.7	-7.45
Yak-02	2.38	9.11	9.50	26.3	-9.97	-116.5	-5.43
Yak-03	0.82	8.71	6.50	26.1	-10.14	-116.9	-1.17
Yak-04	0.91	8.08	7.63	24.2	-13.76	-133.8	-2.98
Yak-05	1.99	9.05	9.13	24.4	-8.79	-110.9	6.19
Yak-06	5.71	9.96	5.70	18.7	-5.48	-88.7	7.98
Yak-07	4.14	9.91	14.50	21.0	-5.89	-90.7	11.00
Yak-08	0.10	7.54	7.50	20.5	-13.91	-130.0	4.68
Yak-09	0.12	7.31	6.14	19.5	-13.12	-124.4	-0.31
Yak-10	0.42	8.78	9.76	21.8	-14.36	-137.1	1.73
Yak-11	0.50	8.64	7.60	21.9	-10.12	-114.0	5.65
Yak-12	0.92	8.42	8.46	21.4	-10.20	-113.7	1.80
Yak-13	0.14	8.46	12.00	21.7	-14.48	-133.2	4.74
Yak-14	0.21	6.86	9.18	24.6	-14.12	-131.5	-1.87
Yak-15	0.16	7.55	5.75	22.9	-16.02	-141.3	-3.47
Yak-16	0.29	10.24	19.90	21.3	-11.44	-117.0	-3.90
Yak-17	0.10	6.60	2.40	20.2	-15.71	-140.8	-3.09
Yak-18	0.39	8.57	13.70	21.5	-12.90	-125.9	4.87
Yak-19	0.71	8.02	1.00	22.9	-12.36	-122.6	-1.66
Yak-20	0.81	9.00	13.30	22.6	-11.05	-117.9	2.29
Yak-21	0.33	8.19	7.40	20.0	-13.66	-128.4	-0.15
Yak-22	0.36	8.69	22.20	20.8	-15.03	-134.5	1.27
Yak-23	0.26	9.20	15.70	22.8	-14.84	-134.3	-4.73
Yak-24	0.79	8.58	38.00	21.7	-7.72	-98.7	4.89
Yak-25	0.82	8.75	n.a.	22.0	-7.86	-95.9	0.77
Yak-26	0.48	8.16	13.50	21.5	-10.56	-113.5	1.85
Yak-27	0.65	8.20	14.30	22.0	-10.46	-112.6	0.87
Yak-28	1.95	8.60	17.30	23.8	-8.18	-105.9	6.46
Yak-29	1.04	8.93	14.20	22.0	-10.37	-113.3	-1.58
Yak-30	n.a	n.a	n.a	n.a.	-12.33	-122.1	5.24
Yak-31	1.43	8.38	5.90	20.5	-11.61	-119.0	-7.55
Yak-32	1.39	8.09	6.80	20.2	-12.02	-126.7	-7.51
Yak-33	0.85	8.09	5.50	20.5	-9.76	-108.4	-2.84
Yak-34	0.49	9.05	6.80	18.5	-14.98	-133.3	-5.23
Yak-35	0.36	9.19	4.50	18.7	-10.26	-109.8	-10.62
Yak-36	0.39	7.78	2.40	16.4	-12.13	-121.9	-5.51
Yak-37	1.52	9.12	2.40	22.7	-8.75	-103.5	-4.65
Yak-38	0.59	7.58	1.50	15.0	-9.74	-105.8	-4.48
Yak-39	0.18	7.04	5.00	16.1	-11.14	-107.4	-3.82
Yak-40	0.11	7.64	4.70	17.2	-17.20	-151.4	1.04
Yak-41	0.11	6.85	5.80	17.1	-17.69	-153.3	-8.08
Yak-42	0.12	7.21	5.40	13.7	-21.66	-167.8	-9.30
Yak-43	0.12	6.00	5.80	11.4	-21.84	-169.4	n.a.
Yak-44	0.08	7.27	4.90	14.6	-20.53	-163.2	-4.22
Yak-45	0.24	6.99	1.90	12.6	-15.11	-142.4	-2.82
Yak-46	0.10	6.81	7.50	14.8	-20.64	-164.3	-5.67
Yak-47	0.09	6.89	7.40	14.4	-20.89	-165.0	-6.29
Yak-48	0.03	6.48	5.70	14.2	-21.33	-166.1	n.a.
Yak-49	0.42	7.45	4.00	13.2	-12.24	-129.7	0.00
Yak-50	0.10	7.03	5.70	11.7	-18.81	-155.0	-2.52
Yak-51	0.13	6.83	4.70	10.4	-14.98	-140.8	-7.44
Yak-52	0.13	7.09	5.30	14.2	-18.34	-148.8	-4.54
Yak-53	0.32	7.37	6.90	14.3	-16.64	-143.3	-3.38
Yak-54	0.06	6.08	5.50	8.0	-15.46	-140.8	-11.23
Yak-55	0.40	7.30	4.70	16.4	-13.62	-135.6	-7.29
Yak-56	0.93	9.08	6.20	18.9	-12.42	-129.5	-5.38

Appendix III-4 (Chapter 3) Continuation

Lake №	HCO_3 [mg/l]	Ca [mg/l]	Na [mg/l]	Cl [mg/l]	Mg [mg/l]	Sr [mg/l]	K [mg/l]	SO_4 [mg/l]
Detection limit		0.10	0.20	0.10	0.10	0.02	0.20	0.10
Yak-01	561.36	33.56	147.09	109.60	178.72	0.29	3.88	436.80
Yak-02	1269.15	24.11	267.42	199.00	305.26	0.29	4.03	424.20
Yak-03	561.36	18.64	81.08	33.82	86.23	0.18	1.26	23.98
Yak-04	475.93	17.67	100.28	83.13	65.47	0.12	7.45	35.39
Yak-05	1598.65	26.5	227.81	147.55	285.44	0.35	4.47	43.53
Yak-06	3794.51	2.17	1481.44	408.50	96.71	< 0.02	158.27	0.52
Yak-07	2581.52	1.58	1040.92	350.80	91.64	0.03	68.25	< 0.10
Yak-08	48.81	11.61	11.37	1.32	3.75	0.13	2.74	< 0.10
Yak-09	73.22	10.0	18.62	2.59	4.54	0.11	3.03	0.94
Yak-10	347.80	20.8	24.1	8.56	41.10	0.15	12.49	0.19
Yak-11	439.32	32.51	41.12	5.75	54.85	0.26	3.87	0.33
Yak-12	738.31	20.35	124.85	33.77	86.63	0.20	11.13	10.34
Yak-13	122.03	14.33	3.46	0.37	11.90	0.09	2.32	2.48
Yak-14	170.85	22.17	5.46	< 0.10	18.02	0.11	1.30	2.87
Yak-15	140.34	16.74	3.95	< 0.10	14.12	0.08	1.53	2.25
Yak-16	256.27	25.39	12.37	4.24	22.63	0.11	3.93	< 0.10
Yak-17	73.22	10.83	1.80	0.11	7.32	0.05	2.94	0.13
Yak-18	335.59	36.25	20.26	1.46	34.62	0.24	3.63	0.30
Yak-19	573.56	21.39	83.24	19.83	60.50	0.19	4.53	5.18
Yak-20	634.58	37.16	175.36	33.80	38.23	0.20	5.35	1.49
Yak-21	274.58	37.71	8.79	0.96	25.82	0.15	3.81	0.54
Yak-22	298.98	40.31	11.09	2.98	28.99	0.19	4.73	2.78
Yak-23	262.37	34.50	8.20	0.58	22.88	0.14	3.01	1.10
Yak-24	842.03	17.18	129.12	38.37	96.13	0.19	13.05	5.04
Yak-25	683.39	23.50	107.94	28.36	80.93	0.26	9.22	2.44
Yak-26	390.51	35.89	50.21	5.95	34.84	0.21	6.61	0.60
Yak-27	536.95	21.66	65.92	19.19	62.91	0.21	11.81	0.24
Yak-28	1659.66	18.10	288.97	151.35	226.77	0.27	4.09	11.20
Yak-29	683.39	4.91	180.11	110.36	64.36	0.07	17.95	6.01
Yak-30	61.02	8.29	8.11	1.18	3.67	0.13	2.13	2.70
Yak-31	524.75	56.63	189.96	187.90	74.99	0.66	18.18	168.30
Yak-32	561.36	39.02	197.36	196.90	73.59	0.53	15.08	93.19
Yak-33	305.09	40.19	103.22	143.70	43.93	0.50	7.66	33.12
Yak-34	183.05	39.23	52.75	72.29	18.80	0.39	3.81	26.41
Yak-35	274.58	16.84	28.37	7.96	27.49	0.15	16.30	2.77
Yak-36	292.88	24.37	22.94	5.65	30.93	0.17	12.20	1.03
Yak-37	976.27	15.22	202.39	87.84	155.88	0.30	7.01	203.40
Yak-38	414.92	26.17	56.77	9.88	50.61	0.27	9.35	1.95
Yak-39	122.03	3.39	24.11	4.92	11.45	0.06	14.20	< 0.10
Yak-40	73.22	14.86	4.04	0.51	4.87	0.17	2.24	5.83
Yak-41	85.42	15.08	3.83	< 0.10	5.13	0.14	0.71	0.54
Yak-42	97.63	18.14	4.45	< 0.10	5.02	0.14	0.67	0.11
Yak-43	2.44	1.17	0.64	0.12	0.37	< 0.02	< 0.20	0.68
Yak-44	61.02	11.25	2.48	0.18	4.10	0.14	0.75	< 0.10
Yak-45	183.05	26.76	12.34	1.15	12.76	0.24	5.19	1.44
Yak-46	73.22	15.41	3.07	0.16	3.80	0.09	0.27	0.46
Yak-47	85.42	14.86	2.98	0.12	3.73	0.08	0.26	0.53
Yak-48	14.79	3.62	1.32	< 0.10	1.04	< 0.02	< 0.20	< 0.10
Yak-49	341.70	40.16	27.21	1.08	30.15	0.29	5.93	10.51
Yak-50	61.02	16.65	3.24	< 0.10	3.05	0.09	< 0.20	2.53
Yak-51	109.83	16.03	5.91	0.16	7.83	0.09	1.30	< 0.10
Yak-52	85.42	16.11	5.80	0.12	8.79	0.22	2.28	0.10
Yak-53	256.27	46.71	16.00	0.30	18.11	0.39	2.61	0.12
Yak-54	35.23	12.03	0.43	< 0.10	2.71	0.09	< 0.20	< 0.10
Yak-55	335.59	55.91	17.69	2.10	21.02	0.51	6.89	< 0.10
Yak-56	329.49	26.96	119.49	171.30	42.71	0.31	44.97	16.46

Appendix III-5 (Chapter 3) Stable isotopes ($\delta^{18}O$, $\delta^{13}C$) and element ratios (Mg/Ca, Sr/Ca) of host waters and ostracod calcite. The species identification follows the key: species (candida → *C. candida*, inaequi → *F. inaequivalvis*, jakutica → *C. muelleri jakutica*, weltneri → *C. weltneri*) and sex (f → female or m → male)

Lake №	Species	$\delta^{18}O$ [‰] VSMOW water	$\delta^{18}O$ [‰] VPDP valve	$\delta^{13}C$ [‰] VPDP water	$\delta^{13}C$ [‰] VPDP valve	Mg/Ca molar water	Mg/Ca (* 10^{-2}) molar valve	Sr/Ca (* 10^{-3}) molar water	Sr/Ca (* 10^{-3}) molar valve
Yak-12	welterni_f	-10.20	-10.47	1.80	2.73	7.02	1.52	4.39	1.77
Yak-12	welterni_m	-10.20	-6.45	1.80	1.37	7.02	2.03	4.39	1.24
Yak-20	welterni_f	-11.05	-5.88	2.29	0.01	1.70	0.60	2.51	1.05
Yak-20	welterni_m	-11.05	-5.07	2.29	4.85	1.70	1.18	2.51	1.28
Yak-22	jakutica_f	-15.03	-11.27	1.27	-1.95	1.19	0.45	2.12	0.76
Yak-22	jakutica_m	-15.03	-11.64	1.27	-1.39	1.19	0.55	2.12	0.71
Yak-26	jakutica_f	-10.56	-9.52	1.85	-0.15	1.60	0.46	2.71	0.82
Yak-26	jakutica_m	-10.56	-9.72	1.85	0.24	1.60	0.53	2.71	0.90
Yak-26	welterni_f	-10.56	-8.72	1.85	-0.97	1.60	0.34	2.71	1.04
Yak-26	welterni_m	-10.56	-9.00	1.85	-0.56	1.60	0.36	2.71	1.05
Yak-27	welterni_f	-10.46	-9.79	0.87	4.15	4.79	0.89	4.35	1.71
Yak-27	welterni_m	-10.46	-9.86	0.87	3.91	4.79	0.64	4.35	1.65
Yak-31	welterni_m	-11.61	-9.09	-7.55	-5.28	2.18	0.67	5.35	1.90
Yak-33	candida_f	-9.76	-8.88	-2.84	-2.75	1.80	0.56	5.64	1.88
Yak-36	candida_f	-12.13	-10.99	-5.51	-5.75	2.09	0.57	3.24	1.23
Yak-36	welterni_f	-12.13	-7.32	-5.51	-7.77	2.09	0.58	3.24	1.20
Yak-36	welterni_m	-12.13	-9.86	-5.51	-4.49	2.09	0.55	3.24	1.14
Yak-40	candida_f	-17.20	-15.19	1.04	-3.90	0.54	0.24	5.22	2.29
Yak-45	candida_f	-15.11	-11.91	-2.82	-1.33	0.79	0.32	4.14	1.53
Yak-45	inaequi_f	-15.11	-13.18	-2.82	-2.45	0.79	0.47	4.14	1.29
Yak-45	inaequi_m	-15.11	-12.51	-2.82	-1.56	0.79	0.55	4.14	1.50
Yak-45	jakutica_f	-15.11	-15.30	-2.82	-4.87	0.79	0.52	4.14	1.27
Yak-45	jakutica_m	-15.11	-12.27	-2.82	-2.05	0.79	0.35	4.14	1.31
Yak-49	jakutica_f	-12.24	-9.51	0.00	-0.81	1.24	0.51	3.27	1.04
Yak-49	jakutica_m	-12.24	-10.08	0.00	-1.92	1.24	0.53	3.27	0.95
Yak-49	welterni_f	-12.24	-9.80	0.00	-1.06	1.24	0.33	3.27	1.07
Yak-51	inaequi_f	-14.98	-11.81	-7.44	-4.51	0.81	0.57	2.56	0.94
Yak-51	inaequi_m	-14.98	-13.11	-7.44	-5.47	0.81	0.48	2.56	0.90
Yak-52	jakutica_f	-18.34	-15.03	-4.54	-6.47	0.90	0.51	6.32	1.69
Yak-52	jakutica_m	-18.34	-15.61	-4.54	-5.38	0.90	0.59	6.32	1.86
Yak-53	inaequi_f	-16.64	-13.68	-3.38	-2.69	0.64	0.41	3.83	1.33
Yak-53	inaequi_m	-16.64	-14.05	-3.38	-2.91	0.64	0.55	3.83	1.42
Yak-55	jakutica_f	-13.62	-10.48	-7.29	-5.94	0.37	0.41	3.43	1.34
Yak-55	jakutica_m	-13.62	-9.83	-7.29	-5.49	0.37	0.47	3.43	1.22

IV References

ACIA (2005) *Arctic Climate Impact Assessment.* Symon L, Arris L and Heal B (eds.) Cambridge University Press, Cambridge and New York, 1042 pp. (published online: http://www.acia.uaf.edu)

Adams M (1807) Some account of a journey to the frozen sea, and of the discovery of the remains of a mammoth. *Philosophical Magazine* 29: 141-143

Alm G (1914) Beiträge zur Kenntnis der nördlichen und arktischen Ostracodenfauna. *Arkiv för Zoologi* 9: 1-20 (in German)

Anadón P, Moscariello A, Rodríguez-Lázarro J and Filippi ML (2006) Holocene environmental changes of Lake Geneva (Lac Léman) from stable isotopes ($\delta^{13}C$, $\delta^{18}O$) and trace element records of ostracod and gastropod carbonates. *Journal of Paleolimnology* 35: 593-616

Anderson N J and Bennike O (1997) Holocene lake sediments in West Greenland and their palaeoclimatic implications. *Geology of Greenland Survey Bulletin* 176: 89-94

Anderson PM and Lozhkin AV (2001) The Stage 3 interstadial complex (Karginskii/middle Wisconsinan interval) of Beringia: variations in paleoenvironments and implications for paleoclimatic interpretations. *Quaternary Science Reviews* 20: 93-125

Andreev AA, Schirrmeister L, Siegert C, Bobrov AA, Demske D, Seiffert M and Hubberten H-W (2002) Paleoenvironmental changes in north-eastern Siberia during the Late Pleistocene-evidence from pollen records of the Bykovsky Peninsula. *Polarforschung* 70: 13-25.

Andreev AA, Grosse G, Schirrmeister L, Kuzmina SA, Novenko EY, Bobrov AA, Tarasov PE, Kuznetsova TV, Krbetschek M, Meyer H and Kunitsky VV (2004) Late Saalian and Eemian palaeoenvironmental history of the Bol'shoy Lyakhovsky Island (Laptev Sea region, Arctic Siberia). *Boreas* 33: 319-348

Andeev AA, Grosse G, Schirrmeister L, Kuznetsova TV, Kuzmina SA, Bobrov AA, Tarasov PE, Novenko EY, Meyer H, Derevyagin AY and co-authors (2008) Weichselian and Holocene palaeoenvironmental history of the Bol'shoy Lyakhovsky Island, New Siberian Archipelago, Arctic Siberia. *Boreas* (published online: doi 10.1111/j.1502-3885.2008.00039.x)

Are F and Reimnitz E (2000) An overview of the Lena River Delta settings: Geology, tectonics, geomorphology, and hydrology. *Journal of Coastal Research* 16: 1083-1093

Arkhipov SA, Volkova VS, Zolkina VS, Krutkover AA and Kul'kova LA (2005) West Siberia. In: Velichko AA and Nechaev VP (eds.) *Cenozoic climatic and environmental changes in Russia*. The Geological Society of America Special Paper 382: 105-120

Arkhangelov AA, Plakht IR, Kolesnikov SF and Parmuzina OY (1985) Vremya formirovaniya mnogoletnei merzloty na Severnoi Chukotke (The age of permafrost formation in Northern Chukotka). In: Popov AI (ed.) *Razvitie kriolitozony Evrazii v verkhnem Kainozoe* (Development of the Cryolithozone of Eurasia in the upper Cenozoic). Nauka, Moscow, pp. 108-112 (in Russian)

Arkhangelov AA, Mikhalev DV and Nikolaev VI (1996) Rekonstruktsiya uslovii formirovaniya mnogoletnei merzloty i paleoklimatov Severnoi Evrazii (Reconstruction of formation conditions of permafrost and palaeoclimate of northern Eurasia). In: Velichko AA, Arkhangelov AA, Borisova OK, Gribchenko YN, Drenova AN, Zelikson EM, Kurenkova EN, Mikhalev DV, Nikolaev VI, Novenko EY and co-editors (eds.) *Razvitie oblasti mnnogoletnei merzloty i periglyatsial'noi zony Severnoi Evrazii i usloviya rasseleniya drevnego cheloveka* (History of permafrost regions and periglacial zones of Northern Eurasia and conditions of old human settlement). Russian Academy of Science, Institute of Geography, Moscow, pp. 85-109 (in Russian)

Astakhov V (2001) The stratigraphic framework for the Upper Pleistocene of the glaciated Russian Arctic: changing paradigms. *Global and Planetary Change* 31: 283-295

Astakhov V (2006) O khronostratigraficheskikh podrazdelenuyakh verkhnego Pleistotsena Sibiri (Chronostratigraphic subdivisions of the Siberian Upper Pleistocene). *Geologiya i Geofisika* (Geology and Geophysics) 47: 1207-1220 (in Russian)

Astakhov V and Mangerud J (2005) O vozraste kargisnkikh mezhlednikovykh sloev na Niznem Eniseee (The age of the Karginsky interglacial strata on the lower Yenisei). *Doklady RAN* (Lectures of the Russian Academy of Science) 403: 63-66 (in Russian)

Athersuch J, Horne DJ and Whittaker JE (1989) Marine and brackish water ostracods (superfamilies Cypridacea and Cytheracea). In: Kermack DM and Barnes RSK (eds.) *Synopses of the British Fauna (New Series)* № 43. EJ Brill, Leiden, New York, København, Köln, 343 pp.

Atlas Arktiki (1985) *Atlas of the Arctic*. In: Treshnikov AF, Korotkevich ES, Kruchinin YA and Markov VF (eds.). Main Administration for Geodesy and Cartography at the Ministry Council of the USSR, Moscow (in Russian)

Berger GW (2003) Luminescence chronology of late Pleistocene loess paleosol and tephra sequences near Fairbanks, Alaska. *Quaternary Research* 60: 70-83

Berglund BE and Ralska-Jasiewiczowa M (1986) Pollen analysis and pollen diagrams. In: Berglund B (ed.) *Handbook of Holocene Palaeoecology and Palaeohydrology*. Interscience, New York, pp. 455-484

Billings WD and Peterson KM (1980) Vegetational change and ice-wedge polygons through the thaw-lake cycle in Arctic Alaska. *Arctic and Alpine Research* 12: 413-432

Bobrov AA, Andreev, AA, Schirrmeister L and Siegert C (2004) Testate amoebae (Protozoa: Testacea) as bioindicators in the Late Quaternary deposits of the Bykovsky Peninsula, Laptev Sea, Russia. *Palaeogeography Palaeoclimatology Palaeoecology* 209: 165-181

Boomer I, Horne DJ and Slipper IJ (2003) The use of ostracods in palaeoenvironmental studies, or what can you do with an ostracod shell? In: Park LE and Smith AJ (eds.) *Bridging the gap: trends in the Ostracode biological and geological sciences*. The Paleontological Society Papers 9:153-179

Bosikov NP (2005) Aktivnost' termokarsta na Leno-Amgiskom mezhdurech'e (Thermokarst activity on the Lena-Anga interfluve). *Materialy tret'ei konferentsii geokryologov Rossii* (Materials of the 3rd Conference of Russian Geocryologists). Moscow State University Publishers, Moscow, pp. 17 (in Russian)

Bronshtein ZS (1947) *Fauna SSSR. Rakoobraznye*, *tom 2, vypusk 1: Ostracoda presnykh vod*. (Fauna of the USSR. Crustaceans, vol. 2, № 1: Freshwater Ostracods). Soviet Academy of Science, Zoological Institute, Moscow, 369 pp. (in Russian)

Bunbury J and Gajewski K (2005) Quantitative analysis of freshwater ostracode assemblages in southwestern Yukon Territory, Canada. *Hydrobiologia* 545: 117-128

Bunge AA (1887) Bericht über den ferneren Gang der Expedition. Reise nach den Neusibirischen Inseln. Aufenthalt auf der Grossen Ljachof-Insel. In: Schrenk LV und Maximovicz CJ (eds.) *Expedition zu den Neusibirischen Inseln und dem Jana-Lande (1885)*. Beiträge zur Kenntnis des russischen Reiches und der angrenzenden Länder vol. III, pp. 231-284 (in German)

Chersky ID (1891) *Opisanie kollektsiy posletretichnykh iskopaemykh zhivotnykh, sobrannykh Novo-Sibirskoi ekspeditsiei 1885-1886 gg* (The description of the collection of post-Tertiary mammals, collected by the New Siberian expedition in 1885-1886). Zapiski Imperatorskoi Akademii Nauk (Notes of the Russian Imperial Academy of Science) 65: 1-707 (in Russian)

Chivas AR, De Deckker P and Shelley JMG (1983) Magnesium, strontium and barium Partitioning in nonmarine ostracode shells and their use in paleoenvironmental reconstructions: A preliminary study. In: Maddocks RF (ed.) *Applications of Ostracods*. Department of Geosciences, University of Houston, Houston, pp. 238-249

Chivas AR, De Deckker P and Shelley JMG (1986) Magnesium content of non-marine ostracod shells: a new palaeosalinometer and palaeothermometer. *Palaeogeography Palaeoclimatology Palaeoecology* 54: 43-61

Chivas AR, De Deckker P, Cali JA, Chapman A, Kiss E and Shelley JMG (1993) Coupled stable-isotope and trace-element measurements of lacustrine carbonates as paleoclimatic indicators. In: Swart PK, Lohmann KC, McKenzie J and Savin S (eds.) *Climate change in continental isotopic records*. Geophysical Monograph 78:113-121

Clark ID and Fritz P (1997) *Environmental isotopes in hydrogeology*. Lewis Publishers, Boca Raton, FL, 328 pp.

Cohen AC, Dawn EP and Maddocks RF (2007) Ostracoda. In: James TC (ed.) *The Light and Smith Manual: Intertidal Invertebrates from Central California to Oregon*. Fourth Edition, University of California Press, Berkeley and Los Angeles, pp. 417-446

Craig H (1961) Isotopic variations in meteoric waters. *Science* 133: 1702-1703

Curry B and Delorme D (2003) Ostracode-based reconstruction from 23,300 to about 20,250 cal yr BP of climate, and paleohydrology of a groundwater-fed pond near St. Louis, Missouri. *Journal of Paleolimnology* 29: 199-207

De Deckker P and Forester RM (1988) The use of ostracods to reconstruct continental palaeoenvironmental records. In: De Deckker P, Colin JP and Peypouquet JP (eds.) *Ostracoda in the Earth science*. Elsevier, Amsterdam, pp 175-199

De Deckker P, Chivas A R and Shelley JMG (1999) Uptake of Mg and Sr in the euhaline ostracod *Cyprideis* determined from in vitro experiments. *Palaeogeography Palaeoclimatology Palaeoecology* 148: 105-116

Delorme LD (1967) Freshwater ostracode synonyms. *Journal of Paleontology* 41: 792-794

Delorme LD (1968) Pleistocene freshwater Ostracoda from Yukon, Canada. *Canadian Journal of Zoology* 46: 859-876

Delorme LD (1969) Ostracodes as Quaternary paleoecological indicators. *Canadian Journal of Earth Sciences* 6: 1471-1476

Delorme LD (1970a) Freshwater ostracodes of Canada. Part I. Family Cypridinae. *Canadian Journal of Zoology* 48: 153-168

Delorme LD (1970b) Freshwater ostracodes of Canada. Part II. Family Cypridopsinae. *Canadian Journal of Zoology* 48: 253-266

Delorme LD (1970c) Freshwater ostracodes of Canada. Part III. Family Candonidae. *Canadian Journal of Zoology* 48: 1099-1127

Delorme LD, Zoltai SC and Kalas LL (1977) Freshwater shelled invertebrate indicators of paleoclimate in northwestern Canada during late glacial times. *Canadian Journal of Earth Sciences* 14: 2029-2046.

Dettman DL, Smith AJ, Rea D K, Moore TC and Lohmann KC (1995) Glacial meltwater in Lake Huron inferred from single-valve analysis of oxygen isotopes in ostracodes. *Quaternary Research* 43: 297-310

Dettmann DL, Palacios-Fest M and Cohen AS (2002) Comment on G. Wansard and F. Mezquita, The response of ostracode shell chemistry to seasonal change in a Mediterranean freshwater spring environment. *Journal of Paleolimnology* 27: 487-491

Diebel K (1968) Neue Limnocythere-Arten (Ostracoda) aus dem deutschen Pleistozän. *Monatsberichte der Deutschen Akademie der Wissenschaften zu Berlin* 10: 519-538 (in German)

Diebel K and Pietrzeniuk E (1969) Ostracoden aus dem Mittelpleistozän von Süßenborn bei Weimar. *Paläontologische Abhandlungen* A III: 463-488 (in German)

Diebel K and Pietrzeniuk E (1975) Mittel- und jungpleistozäne Ostracodenfaunen des Raums Potsdam-Brandenburg.Rathenow in stratigraphischer und ökologischer Sicht. *Zeitschrift für geologische Wissenschaften* 3: 1197-1233 (in German)

Diebel K and Pietrzeniuk E (1978a) Die Ostracodenfauna des eeminterglazialen Travertins von Burgtonna in Thüringen. *Quartärpaläontologie* 3: 87-91 (in German)

Diebel K and Pietrzeniuk E (1978b) Die Ostracodenfauna aus den jungpleistozänen (weichselkaltzeitlichen) Deckschichten von Burgtonna in Thüringen. *Quartärpaläontologie* 3: 207-221 (in German)

Doerfel K (1966) *Statistik in der Analytischen Chemie*. VEB Deutscher Verlag für Grundstoffindustrie, Leipzig, 192 pp. (in German)

Dostovalov BN and Kudryavtsev VA (1967) Obshchee Merzlotovedenie (General Permafrost Studies). Moscow State University Publishers, Moscow, 403 pp (in Russian)

Drachev SS, Savostin LA, Groshev VG and Bruni IE (1998) Structure and geology of the continental shelf on the Laptev Sea, Eastern Russian Arctic. *Tectonophysics* 298: 357-393

Duff K, Laing TE, Smol JP and Lean DRS (1999) Limnological characteristics of lakes located across arctic treeline in northern Russia. *Hydrobiologia* 391: 205-222

Engstrom DR and Nelson SR (1991) Paleosalinity from trace metals in fossil ostracodes compared with observatorial records at Devils Lake, North Dakota, USA. *Palaeogeography Palaeoclimatology Palaeoecology* 83: 295-312

Epstein S, Buchsbaum R, Lowenstam HA and Urey HC (1953) Revised carbonate-water isotopic temperature scale. *Geological Society of America Bulletin* 64:1315-1326

Fartyshev AI (1993) *Osobennosti pribrezhno-shel'fovoy kriolitozony morya Laptevykh* (Characteristics of the coastal and shelf Permafrost zone of the Laptev Sea). Nauka, Novosibirsk, 135 pp. (in Russian)

Fradkina AF, Alekseev MN, Andreev AA and Klimanov VA (2005a) East Siberia. In: Velichko AA and Nechaev VP (eds.) *Cenozoic climatic and environmental changes in Russia*. The Geological Society of America Special Paper 382: 89-103

Fradkina AF, Grinenko OV, Laukhin SA, Nechaev VP, Andreev AA and Klimanov VA (2005b) North-eastern Asia. In: Velichko AA and Nechaev VP (eds.) *Cenozoic climatic and environmental changes in Russia*. The Geological Society of America Special Paper 382: 105-120

Franke D, Hinz K, Block M, Drachev SS, Neben S, Kos'ko MK, Reichert C and Roeser HA (2000) Tectonics of the Laptev Sea Region in Northeastern Siberia. *Polarforschung* 68: 51-58

Frechen M, Sierralta M, Oezen D and Urban B (2007) Uranium-series dating of peat from Central and Northern Europe. In: Sirocko F, Litt T and Claussen M (eds.) *The climate of past interglacials*. Springer, Heidelberg, pp. 92-118

French HM (1996) *The periglacial environment*. 2nd edition. Addison Wesley Longman Limited, Harlow, 341 pp.

French HM (2007) *The periglacial environment*. 3rd edition. Wiley, Chichester, 458 pp.

Frenzel P (1991) Die Ostracodenfauna der tieferen Teile der Ostsee-Boddengewässer Vorpommerns. *Meyniana* 43: 151-175 (in German)

Friedrich K and Boike J (1999) Energy and water balance of the active layer. In: Rachold V (ed.) *Expeditions in Siberia in 1998*. Berichte zur Polarforschung 315: 27-32

Fry B, Brand W, Mersch FJ, Tholke K and Garrit R (1992) Automated analysis system for coupled ^{13}C and ^{15}N measurements. *Analytical Chemistry* 64: 288-291

Froese DG, Westgate JA, Reyes AV, Enkin RJ and Preece SJ (2008) Ancient Permafrost and a Future, Warmer Arctic. *Science* 321: 1648

Fuhrmann R and Pietrzeniuk E (1990a) Die Ostrakodenfauna des Interglazials von Gröbern (Kreis Gräfenhainichen). *Altenburger Naturwissenschaftliche Forschungen* 5: 168-193

Fuhrmann R and Pietrzeniuk E (1990b) Die Ostrakodenfauna des Interglazials von Grabschütz (Kreis Delitzsch). *Altenburger Naturwissenschaftliche Forschungen* 5: 202-227

Fuhrmann R, Schirrmeister L and Pietrzeniuk E (1997) Ostrakoden und Mollusken aus den weichselspätglazialen Sedimenten des Biesenthaler Beckens, N-Brandenburg, Barnim. *Zeitschrift für geologische Wissenschaften* 25: 489-511

Fujita K, Stone DB, Layer PW, Parfenov LM and Koz'min BM (1997) Cooperative program helps decipher tectonics of northeast Russia. *Transactions of the American Geophysical Union* (Eos) 78: 252-253

Galabala RO (1987) Novye dannye o stroenii del'ty Leny (New data on the Lena Delta structure). In: Pokhilainen VP (ed.) Chetvertichniy period v Severno-Vostochoy Azii (Quaternary of North East Asia). Soviet Academy of Science, Far East Branch, Magadan, pp. 152-172 (in Russian)

Gat JR (1979) Isotope hydrology of very saline surface waters. In: International Atomic Energy Agency IAEA (ed.) *Isotopes in Lake Studies*. IAEA, Vienna, pp. 151-162

Gat JR (1981) Chapter 9: Lakes. In: Gat JR and Gonfiantini R (eds.) *Stable Isotope Hydrology–Deuterium and Oxygen-18 in the Water Cycle*. Technical report series No. 210, IAEA, Vienna, pp. 203-219

Gavrilova MK (1969) Mikroklimaticheskii i teplovoi regime ozera Tyungyulyu (Microclimatic and heat regime of Tyungyulyu lake). *Voprosy Geografii Yakutii* (Questions on Yakutian Geography) 5: 57-72 (in Russian)

Gavrilova MK (1973) *Klimat Tsentral'oi Yakutii* (Climate of Central Yakutia). Yakutian Book Publishers, Yakutsk, 120 pp. (in Russian)

Gavrilova MK (1998) *Klimaty kholodnykh regionov zemli* (Climates of cold regions in the world). Russian Academy of Science, Siberian Branch, Permafrost Institute Yakutsk, 206 pp. (in Russian)

Geocryological Map (1991) *Geokriologicheskaya karta SSSR, masstab 1: 2,500 000* (Geocryological map of the USSR, scale 1:2,500 000). Moscow State University, Geological Faculty, Department of Geocryology (in Russian)

Gravis GF (1978) Cyclicity of thermokarst at the coastal lowlands during the late Pleistocene and Holocene. In: *Publications of the 3rd International Permafrost Conference*. July 10-13, 1978, Edmonton, Alberta, Canada vol. 1, pp. 283-287

Griffiths HI (1995) *European Quaternary freshwater ostracoda: A biostratigraphic and paleobio-geographic primer*. Scopolia 34: 1-168

Griffiths HI and Holmes JA (2000) *Non-marine ostracods and Quaternary paleoenvironment*. Technical Guide 8, Quaternary Research Association, London, 179 pp.

Griffiths HI, Pietrzeniuk E, Fuhrmann R, Lennon JL, Martens K and Evans JG (1998) *Tonnacypris glacialis* (Crustacea, Cyprididae): taxonomic position, (paleo-) ecology and zoogeography. *Journal of Biogeography* 25: 515-526

Grigoriev MN (1993) *Kriomorfogenez ust'evoi oblasti reki Leny* (Cryomorphogenesis of the Lena River mouth). Russian Academy of Science, Siberian Branch, Permafrost Institute Yakutsk, 174 pp. (in Russian)

Grigoriev MN, Imaev VS, Koz'min BM and co-authors (1996) *Geologiya, seismichnost' i kriogenye protsessy arkticheskikh raionov zapadnoi Yakutii* (Geology, seismicity and cryogenic processes of the Arctic areas of western Yakutia). Russian Academy of Science, Siberian Branch, Permafrost Institute Yakutsk, 80 pp (in Russian)

Grigoriev MN, Rachold V, Bolshiyanov DY, Pfeiffer EM, Schirrmeister L, Wagner D, and Hubberten H-W (eds.) 2003. *Russian-German Cooperation SYSTEM LAPTEV SEA: The Expedition LENA 2002*. Berichte zur Polar- und Meeresforschung 466: 341 pp.

Grimm E (1991) *Tilia and Tiliagraph*. Illinois State Museum, Springfield, Illinois, USA

Grimm E (2004) *Tilia, Tilia·Graph and TGView 2.0.2*. Illinois State Museum, Springfield, USA

Grosse G, Schirrmeister L, Siegert C, Kunitsky VV, Slagoda EA, Andreev AA and Dereviagin AY (2007) Geological and geomorphological evolution of a sedimentary periglacial landscape in Northeast Siberia during the Late Quaternary. *Geomorphology* 86: 25-51

Guthrie RD (2001) Origin and causes of the mammoth steppe: a story of cloud cover, woolly mammal tooth pits, buckles, and inside-out Beringia. *Quaternary Science Reviews* 20: 549-574

Hansen K (1961) Lake types and lake sediments. *Verhandlungen der internationalen Vereinigung für Limnologie* 14: 285-290

Hammarlund D, Edwards TWD, Björk S, Buchardt B and Wohlfahrt B (1999) Climate and environment during the Younger Dryas (GS-1) as reflected by composite stable isotope records of lacustrine carbonates at Torreberga, southern Sweden. *Journal of Quaternary Science* 14: 17-28

Hastings DA, Dunbar PK, Elphingstone GM, Bootz M, Murakami H, Maruyama H, Masaharu H, Holland P, Payne J, Bryant NA, Logan TL, Muller JP, Schreier G and MacDonald JS (eds.) (1999) *The global land one-kilometer base elevation (GLOBE) digital elevation model*, version 1.0. NOAA, National Geophysical Data Center, Boulder, CO

Heaton THE, Holmes JA and Bridgwater ND (1995) Carbon and oxygen isotope variations among lacustrine ostracods: implications for palaeoclimatic studies. *Holocene* 5: 428-434

Hiller D (1972) Untersuchungen zur Biologie und zur Ökologie limnischer Ostracoden aus der Umgebung von Hamburg. *Archiv für Hydrobiologie* 40: 400-497 (in German)

Hinzman LD, Bettez ND, Bolton WR, Chapin FS, Dyurgerov MB, Fastie CL, Griffith B, Hollister RD, Hope A, Huntington HP and co-authors (2005) Evidence and implications of recent climate change in northern Alaska and other arctic regions. *Climate Change* 72: 251-298

Holmes JA (1996) Trace-element and stable-isotope geochemistry of non-marine ostracod shells in Quaternary palaeoenvironmental reconstructions. *Journal of Paleolimnology* 15: 223-235

Holmes JA, Hales PE and Street-Perrott F A (1992) Trace-element chemistry of non-marine ostracods as a means of palaeolimnological reconstruction: An example from the Quaternary of Kashmir, North India. *Chemical Geology* 95: 177-186

Holmes JA and Chivas AR (2002) Ostracod shell chemistry - overview. In: Holmes JA and Chivas AR (eds.) *The Ostracoda: Applications in Quaternary Research*. Geophysical Monograph 131: 185-204

Hopkins DM (1982) Aspects of the paleogeography of Beringia during the Late Pleistocene. In: Hopkins DM, Matthews JV Jr, Schwerger CE and Young SB (eds.) *Paleoecology of Beringia*. Academy Press, New York, London, pp. 3-27

Horne DJ, Cohen A and Martens K (2002) Taxonomy, morphology and biology of Quaternary and living Ostracoda. In: Holmes JA and Chivas A (eds.) *The Ostracoda: Applications in Quaternary research*. Geophysical Monograph 131: 5-36

Horne DJ (1998). Non-marine Ostracod Database of Europe. University of Greenwich, Chatham.

Horne DJ (2007) A mutual temperature range method for Quaternary palaeoclimatic analysis using European nonmarine Ostracoda. *Quaternary Science Reviews* 26: 1398-1415

Hubberten H-W, Andreev A, Astakhov VI, Demidov I, Dowdeswell JA, Henriksen M, Hjort C, Houmark-Nielsen M, Jakobsson M, Kuzmina S and co-authors (2004) The periglacial climate and environment in northern Eurasia during the last glaciation. *Quaternary Science Reviews* 23: 1333-1357

Igarashi Y, Fukuda M, Nagaoka D and Saljo K (1995) Vegetation and climate during accumulating period of Yedoma, inferred from pollen records. In: Takahashi K, Osawa A and Kanazawa Y (eds.) *Proceedings of the third symposium on the joint Siberian permafrost studies between Japan and Russia in 1994*. Hokkaido University Press, Sapporo, pp. 139-146.

Ilyashuk BP, Andreev AA, Bobrov AA, Tumskoy VE and Ilyashuk EA (2006) Interglacial history of a palaeo-lake and regional environment: A multi-proxy study of a permafrost deposit from Bol'shoi Lyakhovsky Island, Arctic Siberia. *Journal of Paleolimnology* 36: 855-872

Ingram BL, De Deckker P, Chivas AR, Conrad ME and Byrne AR (1998) Stable isotopes, Sr/Ca, and Mg/Ca in biogenic carbonates from Petaluma Marsh, northern California, USA. *Geochimica et Cosmochimica Acta* 62: 3229-3237

IPCC (2007) Intergovernmental Panel on Climate Change. *Climate Change 2007: The Physical Science Basis. Contribution of Working Group I to the Fourth Assessment*. Solomon S, Qin D, Manning M, Chen Z, Marquis M, Averyt KB, Tignor M and Miller HL (eds.). Cambridge University Press, Cambridge, United Kingdom and New York, NY, USA, 996 pp

Ito E, De Deckker P and Eggins SM (2003) Ostracodes and their shell chemistry: implications for paleohydrologic and paleoclimatologic applications. In: Park LE and Smith AL (eds.) *Bridging the gap: trends in ostracode biological and geological sciences*. The Paleontological Society Papers 9: 119-151

Ivanov OA (1972) Stratigrafiya i korrelatsiya Neogenykh i Chetvertichnykh otlozheniyakh subarkticheskikh ravnin Vostochnoi Yakutii (Stratigraphy and correlation of Neogene and Quaternary deposits of subarctic plains in Eastern Yakutia). In: *Problemy izucheniya Chetvertichnogo perioda* (Problems of the Quaternary studies). Nauka, Moscow, pp. 202-211 (in Russian)

Janz H (1994) Zur Bedeutung des Schalenmerkmals 'Marginalrippen' der Gattung *Ilyocypris*, Ostracoda, Crustacea. *Stuttgarter Beiträge zur Naturkunde Serie B* 206: 1-19 (in German)

Jeppesen E, Christofferson K, Malmquist HJ, Faafeng B and Hansson LA (2002) Ecology of five Faroese lakes: summary and synthesis. *Annales Societatis Scientiarum Faeroensis Supplementum* 36: 126-139

Kaplina TN, Giterman RE, Lakhtina OV, Abrashov BA, Kiselyov SV and Sher AV (1978) Duvannyi Yar – opornyi razrez pozdnepleistotsenovykh oltozhenii Kolymskoi nizmenosti (Duvannyi Yar – a key section of Upper Pleistocene deposits of the Kolyma lowland). *Byulleten' komissii po izucheniyu chetvertichnogo perioda* (Bulletin of the Commission on Quaternary Research) 48: 49-65 (in Russian)

Kaplina TN, Sher AV, Giterman RE, Zazhigin VS, Kiselyov SV, Lozhkin AV and Nikitin VP (1980) Opornyi razrez pleistotsenovykh otlozhenii na reke Allaikha - nizov'ya Indigirki (Key section of Pleistocene deposits on the Allaikha River - lower reaches of the Indigirka). *Byulleten' komissii po izucheniyu chetvertichnogo perioda* (Bulletin of the Commission on Quaternary Research) 50: 73-95 (in Russian)

Katamura F, Fukuda M, Bosikov NP, Desyatkin RV, Nakamura T and Moriizumi J (2006) Thermokarst formation and vegetation dynamics inferred from a palynological study in Central Yakutia, Eastern Siberia, Russia. *Arctic Antarctic and Alpine Research* 38: 561-570

Katasonov EM (1954) *Litologia merzlykh chetvertichnykh otlozhenii / Kriolitologia / Yanskoi primorskoi nizmenosti* (Lithology of frozen Quaternary deposits / Cryolithology / of the Yana lowland). PhD thesis, Moscow State University, Moscow, 224 pp.

Katasonov EM, Ivanov MS, Siegert C, Katasonova EG and Pudov GG (1979) *Struktura i absolutnya geokhonologiya alasnykh otlozhenii Tsentralnoi Yakutii* (Structure and absolute geochronology of Alas deposits in Central Yakutia). Nauka, Novosibirsk, 96 pp. (in Russian)

Kayalainen VI and Kulakov YN (1966) K voprosy paleogeografii Yana-Indigirskoi nizmenosti v Neogeno-Chetvertichnom periode (To the questions of Paleogeography of the Yana-Indigirka coastal lowland during the Neogene-Quaternary period). In: In: Saks VN (ed.) *Chetvertichnyi period v Sibiri* (Quaternary period of Siberia). Nauka, Moscow, pp. 274-283 (in Russian)

Kaz'mina TA (1975) *Stratigrafiya i ostrakody pliotsena i rannego pleystotsena yuga Zapadno-Sibirskoy ravniny* (Pliocene and Early Pleistocene stratigraphy and ostracodes in the south of the West-Siberian lowlands). Nauka, Novosibirsk, 108 pp. (in Russian)

Keatings KW, Heaton THE, Holmes JA (2002) Carbon and oxygen fractionation in non-marine ostracods: Results from a 'natural culture' environment. *Geochimica et Cosmochimica Acta* 66: 1701-1711

Keatings KW, Hawkes I, Holmes JA, Flower RJ, Leng MJ, Abu-Zied RH and Lord AR (2006a) Evaluation of ostracod-based palaeoenvironmental reconstruction with instrumental data from the arid Faiyum Depression, Egypt. *Journal of Paleolimnology* 38: 261-283

Keatings KW, Holmes JA and Heaton THE (2006b) Effects of pre-treatment on ostracod valve chemistry. *Chemical Geology* 235: 250-261

Kelts K and Talbot MR (1990) Lacustrine carbonates as geochemical archives of environmental change and biotic/abiotic interactions. In: Tilzer MM, Serruya C (eds.) *Large lakes: ecological structure and function*. Science and Technology Publishers, Madison, pp. 288-315

Kempf EK (1967) Ostracoden aus dem Holstein-Interglazial von Tönisberg, Niederrheingebiet. *Monatsberichte der Deutschen Akademie der Wissenschaften zu Berlin* 9: 119-139

Kesling RV (1951) The morphology of ostracod moult stages. *Illinois Biological Monographs* 21: 1-126

Kienast F, Schirrmeister L, Siegert C and Tarasov P (2005) Palaeobotanical evidence for warm summers in the East Siberian Arctic during the last cold stage. *Quaternary Research* 63: 283-300

Kienast F, Tarasov P, Schirrmeister L, Grosse G and Andreev AA (2008) Continental climate in the East Siberian Arctic during the last interglacial: implications from palaeobotanical records. *Global and Planetary Change* 60: 535-562

Kim ST and O'Neil JR (1997) Equilibrium and nonequilibrium oxygen isotope effects in synthetic carbonates. *Geochimica et Cosmochimica Acta* 61: 3461-3475

Kind NV (1974) *Geokhronologia pozdnego Antropogena po izotopnym dannym* (Geochronology of the late Anthropogene based on isotope data). Nauka, Moscow, 256 pp. (in Russian)

Kiselyov SV (1981) *Pozdnekainozoiskie zheskokrylie Severo-Vostoka Sibiri* (Late Cenozoic Coleoptera of North-east Siberia). Nauka, Moscow, 116 pp. (in Russian)

Kloss AL (2008) *Water isotope geochemistry of recent precipitation in Central and North Siberia as a proxy for the local and regional climate system*. Unpublished diploma thesis, Institute for Physical Geography and Landscape Ecology, Leibniz University of Hannover, Germany, 107 pp.

Kondrat'eva KA and Solov'ev VA (1989) *Zakonomernosti formirovaniya i osobennosti rasprostraneniya kriogennykh protsessov i obrazovanii* (Development and occurrence of cryogenic processes and materials). In: Yershov YD (ed.) Kriolitologiya SSSR - Srednyaya Sibir' (Cryolithology of the USSR - Middle Siberia). Nedra, Moscow, 414 pp. (in Russian)

Konishchev VN and Kolesnikov SF (1981) Osobennosti stroeniya i sostava pozdnekainozoiskikh otlozheniyakh b obnazhenii Oyagosskii Yar (Specifics of structure and composition of late Cenozoic deposits in the section of Oyogossky Yar). In: Problemy Kriolitologii (Problems of Cryolithology) vol. IX, Moscow State University Publishers, Moscow, pp. 107-117 (in Russian)

Krbetschek MR, Gonser G and Schwamborn G (2002) Luminescence dating results on sediment sequences of the Lena Delta. *Polarforschung* 70: 83-88

Krstić N (1972) *Rod Candona (Ostracoda) iz Kongerijskikh Slojeva Juzhnog dela Panonskog Basena* (The genus Candona (Ostracoda) from Congeria Beds of the southern Pannonian Basin). Monographs of the Serbian Academy of Sciences and Arts (Section of Natural and Mathematical Sciences) 39: 1-145 (in Serbian)

Kumke T, Ksenofontova M, Pestryakova L, Nazarova L and Hubberten H-W (2007) Limnological characteristics of lakes in the lowlands of Central Yakutia, Russia. *Journal of Limnology* 66: 40-53

Kunitsky VV (1989) *Kriolitologiya nizov'ya Leny* (Kryolithogenesis of the lower Lena). Russian Academy of Science, Siberian branch, Permafrost Institute Yakutsk, 164 pp. (in Russian)

Kunitsky VV (1996) Khimicheskii sostav ledinykh zhil ledovogo kompleksa (Chemical content of ice wedges of the Ice complex). In: *Razvitie kriolitozony v Evrazii v verkhnem Kenozoe* (Development of the Cryolithozone of Eurasia during the upper Cenozoic). Russian Academy of Science, Siberian branch, Permafrost Institute Yakutsk, pp. 93-117 (in Russian)

Kunitsky VV (1998) Ledovyi kompleks i krioplanatsionnye terrasy ostrova Bol'shogo Lyakhovskogo (Ice Complex and cryoplanation terraces of the Bol'shoy Lyakhovsky Island) In: Kamensky RM, Kunitsky VV, Olovin BA and Shepelev VV (eds.) *Problemy Geokriologii* (Problems of Geocryology). Russian Academy of Science, Siberian branch, Permafrost Institute Yakutsk, pp. 60-72 (in Russian)

Kunitsky VV and Grigoriev MN (2000) Boulders and cobble roundstones near the Svyatoy Nos Cape and on Big Lyakhovsky Island. In: *Fourth QUEEN Workshop*, Lund, Sweden, April 7-10, 2000. Abstracts, pp. 62

Kurashov EA (1995) Rakushkovye raki, Podklass Ostrakoda (Conchostraca, sub-class Ostracoda). In: Tsalolikhin SY (ed.) *Opredelitel' presnovodnykh bespozvonochnykh Rossii i sopredel'nykh territorii* tom 2 (Key to Freshwater invertebrates of Russia and adjacent areas: Crustacea, vol. 2). Russian Academy of Science, Zoological Institute St. Petersburg, pp. 131-156 (in Russian)

Kuzmina S and Sher A (2006) Some features of the Holocene insect faunas of northeastern Siberia. *Quaternary Science Reviews* 25: 1790-1820

Kuznetsova TV, Sulerzhitsky LD, Andreev A, Siegert C, Schirrmeister L and Hubberten H-W (2003) Influence of Late Quaternary paleoenvironmental conditions on the distribution of mammals in the Laptev Sea Region. In: Storer JE (ed.) Third International Mammoth Conference Yukon, Canada, Program and Abstracts. *Occasional Papers in Earth Sciences* 5: 58-60

Lemke P, Ren J, Alley RB, Allison I, Carrasco J, Flato G, Fujii Y, Kaser G, Mote P, Thomas RH and Zhang T (2007) Observations: Changes in Snow, Ice and Frozen Ground. In: Solomon S, Qin D, Manning M, Chen Z, Marquis M, Averyt KB, Tignor M and Miller HL (eds.) *Climate Change 2007: The Physical Science Basis. Contribution of Working Group I to the Fourth Assessment Report of the Intergovernmental Panel on Climate Change*. Cambridge University Press,Cambridge, United Kingdom and New York, NY, USA, pp. 337-383

Leng M and Marshall JD (2004) Palaeoclimate interpretation of stable isotope data from lake sediment archives. *Quaternary Science Reviews* 23: 811-831

Lopez CML, Brouchkov A, Nakayama H, Takakai F, Fedorov AN and Fukuda M (2007) Epigenetic salt accumulation and water movement in the active layer of central Yakutia in eastern Siberia. *Hydrological Processes* 21: 103-109

Lozkhin AV, Anderson PM, Matrosova TV and Minyuk P (2007) The pollen record from El'gygytgyn Lake: implications for vegetation and climate histories of northern Chukotka since the late middle Pleistocene. *Journal of Paleolimnology* 37: 135-153

Lungersgauzen GF (1961) Geologicheskaya istoriya srednei Leny i nekotorye voprosy stratigrafii chetvertichnykh otlozhenii vostochnoi Sibiri (Geological history of the middle Lena and some questions of Quaternary deposits stratigraphy in East Siberia). In: *Materialy vsesoyusnogo soveshchaniya po izucheniyu chetvertichnogo perioda* tom 3. (Contributions to the all-union Conference on the study of the Quaternary period, vol. 3, Soviet Academy of Science, Moscow, pp. 209-217 (in Russian)

Lüttig G (1955) Die Ostracoden des Interglazials von Elze. *Paläontologische Zeitschrift* 29: 146-169 (in German)

Lüttig G (1959) Die Ostracoden des Spätglazials von Tatzmannsdorf (Burgenland). *Paläontologische Zeitschrift* 33: 185-197 (in German)

Mangerud JM, Jacobsson M, Alexanderson H and Astakhov V (2004) Ice-dammed lakes and rerouting of the drainage of northern Eurasia during the Late Glaciation. *Quaternary Science Reviews* 23: 1313-1332

Martens K, Schön I, Meisch C and Horne DJ (2007) Global diversity of ostracods (Ostracoda, Crustacea) in freshwater. *Hydrobiologia* 595: 185-193

Mazepova GF (2001) Ostracody (Ostracods). In: Timoshkin OA (ed.) *Annotirovannyi spisok fauny ozera Baikal i ego vodosbornogo basseina*, tom 1 (Index of animal species inhabiting Lake Baikal and its catchments area, vol. 1). Nauka, Novosibirsk, pp. 510-557 (in Russian)

McGuire AD, Chapin III FS, Wirth C, Apps M, Bhatti J, Callaghan TV, Christensen TR, Clein JS, Fukuda M, Maximov T, Onuchin A and co-authors (2007) Responses of high latitude ecosystems to global change: potential consequences for the climate system. In: Canadell JG, Pataki DE and Pitelka LF (eds.) *Terrestrial Ecosystems in a Changing World*. Springer, London, pp. 297-310

Meisch C (2000) *Freshwater Ostracoda of Western and Central Europe*. Spektrum Akademischer Verlag, Heidelberg, Berlin, 522 pp.

Meyer H, Schönicke L, Wand U, Hubberten H-W and Friedrichsen H (2000) Isotope studies of hydrogen and oxygen in ground ice - Experiences with the equilibration technique. *Isotopes in Environmental and Health Studies* 36: 133-149

Meyer H, Dereviagin AY, Siegert C and Hubberten H-W (2002a) Paleoclimate studies on Bykovsky Peninsula, North Siberia - hydrogen and oxygen isotopes in ground ice, *Polarforschung* 70: 37-51

Meyer H, Dereviagin AY, Siegert C, Schirrmeister L and Hubberten H-W (2002b) Paleoclimate reconstruction on Big Lyakhovsky Island, North Siberia - Hydrogen and oxygen isotopes in ice wedges. *Permafrost and Periglacial Processes* 13: 91-105

Meyer H (2003) Studies on recent cryogenesis. In: Grigoriev MN, Rachold V, Bolshiyanov DY, Pfeiffer EM, Schirrmeister L, Wagner D and Hubberten H-W (eds.) *Russian-German Cooperation System Laptev Sea. The Expedition LENA 2002*. Berichte zur Polar- und Meeresforschung 466: 29-48

Mischke S (2001) *Mid and Late Holocene paleoenvironment of the lakes Eastern Juyanze and Sogo Nur in NW China, based on ostracod species assemblages and shell chemistry*. Berliner Geowissenschaftliche Abhandlungen Serie E 35, 131 pp.

Mischke S and Wünnemann B (2006) The Holocene salinity history of Bosten Lake (Xinjiang, China) inferred from ostracod species assemblages and shell chemistry: Possible palaeoclimatic implications. *Quaternary International* 154/155: 100-112

Mischke S, Herzschuh U, Massmann G and Zhang C (2007) An ostracod-conductivity transfer function for Tibetan lakes. *Journal of Paleolimnology* 38: 509-524

Mischke S, Kramer M, Zhang C, Shang H, Herzschuh U and Erzinger J (2008) Reduced early Holocene moisture availability in the Bayan Har Mountains, northeastern Tibetan Plateau, inferred from a multi-proxy lake record. *Palaeogeography Palaeoclimatology Palaeoecology* 267: 59-76

Murton JB (2001) Thermokarst sediments and sedimentary structures, Tuktoyaktuk Coastlands, western Arctic Canada. *Global and Planetary Change* 28: 175-192

Murton JB (2005) Ground-ice stratigraphy and formation at North Head, Tuktoyaktuk coastlands, Western Arctic Canada: a product of glacier–permafrost interactions. *Permafrost and Periglacial Processes* 16: 31-50

Nadeau MJ, Schleicher M, Grootes PM, Erlenkeuser H, Gottdang A, Mous DJW, Sarnthein JM and Willkomm H (1997) The Leibniz-Labor facility at the Christian-Albrecht-University, Kiel, Germany. *Nuclear Instruments and Methods in Physics Research* 123: 22-30

Nadeau MJ, Grootes PM, Schleicher M, Hasselberg P, Rieck A and Bitterling M (1998) Sample throughput and data quality at the Leibniz-Labor AMS facility. *Radiocarbon* 40: 239-245.

Nagaoka D, Saijo K and Fukuda, M (1995) Sedimental environment of the Yedoma in high Arctic eastern Siberia. In: *Proceedings of the third symposium on the joint Siberian permafrost studies between Japan and Russia in 1994*. Hokkaido University Press, Sapporo, pp. 8-13.

Neale JW (1969) The Freshwater Ostracode *Candona harmsworthi* SCOTT from Franz Josef Land and Novaya Zemlya. In: Neale JW (ed.) *The taxonomy, morphology and ecology of recent ostracoda*. Oliver and Boyd, Edinburgh, pp. 222-236

Nemchinov AG (1958) O periodicheskikh kolebaniyakh urovnya ozer Tsentral'noi Yakutii. (About periodic lake level changes in Central Yakutia). *Nauchnye otchety Yakutskogo otdeleniya Sovietskoi Akademii Nauk* (Scientific reports of the Yakutsk branch of the Soviet Academy of Science) 1: 30-37 (in Russian)

Nikolsky PA and Basilyan A E (2004) Mys Svyatoi Nos - Opornyi razrez chetvertichnykh otlozhenii severa Yana-Indigiskoi nizmenosti (Mys Svyatoi Nos - a Quaternary key section of the northern Yana-Indigirka lowland). In: *Estestvenaya istoriya rossiskoi vostochnoi Arktiki v Pleisotsene i Golotsene* (Natural history of the Russian Eastern Arctic during the Pleistocene and Holocene). GEOS, Moscow, pp. 5-13 (in Russian)

Oberman NG and Mazhitova GG (2001) Permafrost dynamics in the northeast of European Russia at the end of the 20th century. *Norwegian Journal of Geography* 55: 241-244

Opel T, Dereviagin AY, Meyer H and Schirrmeister L (in preparation) Paleoclimatic information from stable water isotopes of Holocene and recent ice wedges at the Oyogos Yar coast region (Northeastern Siberia). *Permafrost and Periglacial Processes*, Special Issue in 2009 "Isotope and Geochemical characteristics of permafrost"

Parfenov LM (1991) Tectonics of the Verkhoyansk-Kolyma Mesozoides in the context of plate tectonics. *Tectonophysics* 199: 319-342

Park LE, Cohen AS, Martens K and Bralek R (2003) The impact of taphonomic processes on interpreting paleoecologic changes in large lake ecosystems: ostracodes in Lakes Tanganyika and Malawi. *Journal of Paleolimnology* 30: 127-138

Palacios-Fest MR and Dettman DL (2001) Temperature controls monthly variation in ostracode valve Mg/Ca: *Cypidopsis vidua* from a small lake in Sonora, Mexico. *Geochimica et Cosmochimica Acta* 65: 2499-2507

Palacios-Fest MR, Carreño AL, Ortega-Ramírez JR and Alvarado-Valdéz G (2002) A paleontological reconstruction of Laguna Babícora, Chihuahua, Mexico based on ostracode paleoecology and trace element shell chemistry. *Journal of Paleolimnology* 27: 185-206

Pestryakova LA (2005) Diatomovye vodorosli v osadkakh ozer Verkhnei Tatty (Diatoms in Surface Sediments from Lakes at the Upper Tatta River). In: Savvinov DD, Mironova SI, Bosikov NP, Anisimova NP, Averenskii AI, Gavril'eva LD, Gogoleva PA, Dmitriev AI, Zhirkov FH, Isaev AP and co-editors (eds.) *Alasnye Ekosystemy: Struktura, Funktsionalnost', Dinamika* (Alas Ecosystems: Structures, Functionality, Dynamics). Nauka, Novosibirsk, pp. 101-107 (in Russian)

Pestryakova LA, Bosikov NP and Ksenofontova MI (2007) Diatomovye kompleksy i khimism vody termokarstovykh ozer Ukechinskogo polygona (Diatom complexes and water chemistry of thermokarst lakes at the Ukechinskiy site). *Nauka i Obrazovanie* (Science and Education) 2: 19-24 (in Russian).

Péwé TL (1975) *Quaternary Geology of Alaska*. Geological Survey Professional Paper 835. U.S. Government Printing Office, Washington DC, 145 pp.

Pietrzeniuk E (1977) Ostracoden aus Thermokarstseen und Altwässern in Zentral-Jakutien. *Mitteilungen des Zoologischen Museums zu Berlin* 53: 331-362 (in German)

Pietrzeniuk E (1983) *Bericht über die Untersuchung der Ostracoden aus Schlämmrückständen von 5 Bohrungen an den Alassen Enjor und Mjurju (Jakutien)*. Naturkundemuseum Berlin, 6 pp. (unpublished report in German)

Pietrzeniuk E (1984) *Bericht über die Untersuchung der Ostrakoden aus 3 Proben vom Mammutberg (Jakutien)*. Naturkundemuseum Berlin, 3 pp. (unpublished report in German)

Pietrzeniuk E (1986) *Bericht über die Untersuchung von fünf Ostracodenproben aus Zentral- und Nordjakutien*. Naturkundemuseum Berlin, 4 pp. (unpublished report in German)

Pirumova LG (1968) Diatomovye vodorosli v chetvertichnykh otlozheniyakh Yana-Indigiskoi nizmenosti i Bol'shogo Lyakhovskogo ostrova (Diatoms in Quaternary sediments of northern Yana- Indigirka lowland and Bol'shoy Lyakhovsky Island). In: Zhuze AP (ed.) *Iskopaemye diatomovye vodorosli SSSR* (Fossil diatoms of the USSR). Nauka, Moscow, pp. 80-83 (in Russian)

Pitulko VV, Nikolsky PA, Girya EY, Basilyan AE, Tumskoy VE, Koulakov SA, Astakhov SN, Pavlova EY and Anisimov MA (2004) The Yana RHS site: humans in the Arctic before the Last Glacial Maximum. *Science* 303: 52-56

Poberezhnaya AE, Fedotov AP, Ya T, Sitnikova Yu, Semenov M, Ziborova GA, Otinova EL and Khabuev AV (2006) Paleoecological and paleoenvironmental record of the Late Pleistocene Record of lake Khubsugul (Mongolia) based on ostracod remains. *Journal of Paleolimnology* 36: 133-149

Popp S, Beloyubsky I, Lehmkuhl F, Prokopiev A, Siegert C, Spektor V, Stauch G and Diekmann B (2007) Sediment provenance of late Quaternary morainic, fluvial and loess-like deposits in the southwestern Verkhoyansk Mountains (eastern Siberia) and implications for regional palaeoenvironmental reconstructions. *Geological Journal* 42: 477-497

Porter SC, Sauchyn DJ and Delorme LD (1999) The ostracode record from Harris Lake, southwestern Saskatchewan: 9200 years of local environmental change. *Journal of Paleolimnology* 21: 35-44

Rachold V (ed.) (1999) *Expeditions in Siberia in 1998*. Berichte zur Polar- und Meeresforschung 315, 268 pp.

Rachold V and Grigoriev MN (eds) (2001) *Russian-German Cooperation System Laptev Sea 2000: The Expedition LENA 2000*. Berichte zur Polar- und Meeresforschung 388, 135 pp.

Reimer PJ, Baillie MGL, Bard E, Bayliss A, Beck JW, Bertrand C, Blackwell PG, Buck CE, Burr G, Cutler KB, and co-authors (2004) INTCAL04 terrestrial radiocarbon age calibration, 0-26 cal kyr BP. *Radiocarbon* 46: 1029-1058

Richter-Menge J, Overland J, Svoboda M, Box J, Loonen MJJE, Proshutinsky A, Romanovsky V, Russell D, Sawatzk CD, Simpkins M and co-authors (2008). *Arctic Report Card 2008*. National Oceanic and Atmospheric Administration, Washington DC, 61 pp. (published online: http://www.arctic.noaa.gov/reportcard)

Ricketts RD, Johnson TC, Brown ET, Rasmussen KA and Romanovsky VV (2001) The Holocene paleolimnology of Lake Issyk-Kul, Kyrgyzstan: trace element and stable isotope composition of ostracodes. *Palaeogeography Palaeoclimatology Palaeoecology* 176: 207-227

Rivas-Martínez S (2007) *Global bioclimatics*. Data set. Phytosociological Research Center, Madrid, Spain (published online: http://www.globalbioclimatics.org)

Romanovskii NN (1958a) Novye dannye o stroenii chetvertichnykh otlozhenii ostrova Bol'shogo Lyakhovskogo, Novosibirskie ostrova (New data about Quaternary deposits structure on the Bol'shoy Lyakhovsky Island, New Siberian Islands). *Nauchnye doklady vysshei shkoly. Seriya geologogeograficheskaya* (Scientific notes of the higher school. Geological-geographical series) 2: 243-248 (in Russian)

Romanovskii NN (1958b) Paleogeograficheskie usloviya obrazovaniya chetvertichnykh otlozhenii ostrova Bol'shogo Lyakhovskogo, Novosibirskie ostrova (Paleogeographical conditions of formation of the Quaternary deposits on the Bol'shoy Lyakhovsky Island, New Siberian Islands). Voprosy fizicheskoi geografii polyarnykh stran (Questions of Physical Geography in Polar regions) vol. I: pp. 80-88 (in Russian)

Romanovskii NN (1958c) Merzlotnye structury oblekaniya v chetvertichnykh otlozheniyakh (Permafrost structures in Quaternary deposits. *Nauchnye doklady vysshei shkoly. Seriya geologogeograficheskaya* (Scientific notes of the higher school. Geological-geographical series) 3: 185-189 (in Russian)

Romanovskii NN, Gavrilov AV, Tumskoy VE, Kholodov AL, Siegert C, Hubberten H-W and Sher AV (2000) Environmental evolution in the Laptev Sea region during Late Pleistocene and Holocene. *Polarforschung* 68: 237-245

Romanovskii NN and Hubberten H-W (2001) Results of Permafrost Modelling of the Lowlands and Shelf of the Laptev Sea Region, Russia. *Permafrost and Periglacial Processes* 12: 191-202

Romanovskii NN, Hubberten H-W, Gavrilov AV, Tumskoy VE and Kholodov AL (2004) Permafrost of the east Siberian Arctic shelf and coastal lowlands. *Quaternary Science Reviews* 23: 1359-1369

Sars GO (1898) The Cladocera, Copepoda and Ostracoda of the Jana expedition. *Annuaire du Musée Zoologique de l'Académie Impériale des Sciences de Saint-Pétersbourg* 3: 324-358.

Schirrmeister L, Kunitsky V, Grosse G, Kuznetsova T, Kuzmina S and Bolshiyanov D (2001) Late Quaternary and recent environmental situation around the Olenyok Channel (western Lena Delta) and on Bykovsky Peninsula. In: Rachold V and Grigoriev MN (eds.) *Russian-German cooperation SYSTEM LAPTEV SEA 2000: The Expedition LENA 2000*. Berichte zur Polar- und Meeresforschung 388: 85-135

Schirrmeister L, Siegert C, Kunitsky VV, Grootes PM and Erlenkeuser H (2002a) Late Quaternary ice-rich Permafrost sequences as a paleoenvironmental archive for the Laptev Sea Region in northern Siberia. *International Journal of Earth Sciences* 91: 154-167

Schirrmeister L, Siegert C, Kuznetsova T, Kuzmina S, Andreev AA, Kienast F, Meyer H and Bobrov AA (2002b) Paleoenvironmental and paleoclimatic records from permafrost deposits in the Arctic region of Northern Siberia. *Quaternary International* 89: 97-118

Schirrmeister L, Oezen D and Geyh MA (2002c) ^{230}Th/U Dating of Frozen peat, Bol'shoy Lyakhovsky Island (Northern Siberia). *Quaternary Research* 57: 253-258

Schirrmeister L, Grosse G, Schwamborn G, Andreev AA, Meyer H, Kunitsky VV, Kuznetsova TV, Dorozhkina MV, Pavlova EY, Bobrov AA and Oezen D (2003) Late Quaternary history of the accumulation plain north of the Chekanovsky Ridge (Lena Delta, Russia): a multidisciplinary approach. *Polar Geography* 27: 277-319

Schirrmeister L (ed.) (2004) *Expeditions in Siberia in 2003*. Berichte zur Polar- und Meeresforschung 489, 231 pp.

Schirrmeister L, Grosse G, Kunitsky V, Magens D, Meyer H, Dereviagin A, Kuznetsova T, Andreev A, Babiy O, Kienast F and co-authors (2008a) Periglacial landscape evolution and environmental changes of Arctic lowland areas for the last 60 000 years (western Laptev Sea coast, Cape Mamontov Klyk). *Polar Research* 27: 249-272

Schirrmeister L, Kunitsky VV, Grosse G, Kuznetsova T, Meyer H, Derevyagin A, Wetterich S and Siegert S (2008b). The Yedoma Suite of the Northeast Siberian Shelf Region – Characteristics and Concept of Formation. In: Kane DL and Hinkel KM (eds.) *Proceedings of the 9th International Conference on Permafrost (NICOP)*. University of Alaska Fairbanks, Institute of Northern Engineering, pp. 1595-1601

Schirrmeister L, Wetterich S, Kunitsky V, Tumskoy V, Dobrynin D, Dereviyagyn A, Opel T, Kienast F, Kuznetsova T and Gorodinski A (in press). Palaeoenviromental studies on the Oyogos Yar coast. In: Boike J, Bol'shiyanov DY, Schirrmeister L and Wetterich S (eds.) *The Expedition LENA - NEW SIBERIAN ISLANDS 2007 during the International Polar Year (IPY) 2007/2008*. Berichte zur Polar- und Meeresforschung

Schwalb A (2003) Lacustrine ostracodes as stable isotope recorders of late-glacial and Holocene environmental dynamics and climate. *Journal of Paleolimnology* 29: 267-351

Schwalb A, Burns SJ and Kelts K (1999) Holocene environments from stable isotope stratigraphy of ostracods and authigenic carbonate in Chilean Altiplano Lakes. *Palaeogeography Palaeoclimatology Palaeoecology* 148:153-168

Schwamborn G, Rachold V and Grigoriev MN (2002) Late Quaternary sedimentation history of the Lena Delta. *Quaternary International* 89: 119-134

Sedenko SV, Sedenko EG and Vasil'ev SP (2001) Skhematicheskaya geologicheskaya karta Respubliki Sakha (Yakutia) (Schematic geological map of the Sakha Republic (Yakutia)). In: Parfenov LM and Kuzmin MI (eds.) *Tektonika, geodinamika i metallogeniya territorii Respubliki Sakha (Yakutia)* (Tectonics, Geodynamics and Metallogeny of the Sakha Republic (Yakutia)). Maik Nauka / Interperiodica, Moscow, 571 pp. (in Russian)

Semenova LM (2003) Vidovoi sostav i rasprostranenie ostrakod (Crustacea, Ostracoda) v vodoemakh arkhipelaga Novaya zemlya i ostrova Vaigach (Species occurrence and distribution of ostracods (Crustacea, Ostracoda) on Novaya Zemlya Archipelago and Vaigach Island). *Biologiya Vnutrennikh Vod* (Biology of Inland waters) 2: 20-26 (in Russian)

Semenova LM (2005) Fauna i rasprostranenie ostracod (Crustacea, Ostracoda) vo vnytrennikh vodoemakh Rossii i sopredel'nykh gosudarstv (Fauna and distribution of ostracods (Crustacea, Ostracoda) in inland waters of Russia and adjacent states). *Biologiya Vnutrennikh Vod* (Biology of Inland waters) 3: 17-26 (in Russian)

Serreze MC, Walsh JE, Chapin III FS, Osterkamp T, Dyurgerov M, Romanovsky V, Oechel WC, Morison J and Zhang T and Barry RG (2000) Observational evidence of recent change in the northern high-latitude environment. *Climatic Change* 46: 159-207

Shagedanova M (2002) The climate at present and in the historical past. In: Shagedanova M (ed.) *The physical geography of northern Eurasia*. Oxford University Press, Oxford, pp. 70-102

Sher AV (1971) *Mlekopitayushchie i stratigrafia pleistotsena krainego Severo-Vostoka SSSR i Severnoi Ameriki* (Pleistocene mammals and stratigraphy of the far Northeast USSR and North America). Nauka, Moscow, 310 pp. (in Russian)

Sher AV, Kaplina TN and Ovander MG (1987) Unifitsirovanaya regional'naya stratigraficheskaya skhema chetvertichnykh otlozhenii Yano-Kolymskoi nizmenosti i ee gornogo obramleniya (Unified regional stratigraphic chart for the Quaternary deposits in the Yana-Kolyma Lowland and its mountainous surroundings). In: *Ob'yasnatel'naya zapiska – Resheniya mezhvedomstvogo stratigraficheskogo soveshaniya po chetvertichnoi sisteme Vostoka SSSR* (Explanatory Note – Decisions of Interdepartmental Stratigraphic Conference on the Quaternary of the Eastern USSR). Soviet Academy of Science, Far East Branch, Magadan, pp. 29-69 (in Russian)

Sher AV, Kuzmina SA, Kuznetsova TV and Sulerzhinsky LD (2005) New insights into the Weichselian environment and climate of the East Siberian Arctic, derived from fossil insects, plants, and mammals. *Quaternary Science Reviews* 24: 533-569

Sher AV and Kuzmina SA (2007) Beetle records / Late Pleistocene of Northern Asia. In: Elias S (Ed.) *Encyclopaedia of Quaternary Science*, vol. 1, Elsevier, Amsterdam, pp. 246-267.

Siegert C, Schirrmeister L and Babiy O (2002) The sedimentological, mineralogical and geochemical composition of Late Pleistocene deposits from the Ice Complex on the Bykovsky Peninsula, Northern Siberia. *Polarforschung* 70: 3-11

Sirocko F, Claussen M, Sánchez Goñi FM and Litt T (eds.) (2007) *The Climate of Past Interglacials*. Developments in Quaternary Science 7, Elsevier, Amsterdam, 622 pp.

Slagoda EA (1993) Genesis i mikrostruktura krilolitogennykh otlozhenii Bykovskogo polostrova i ostrova Muostakh (Genesis and microstructure of cryolithogenic deposits at the Bykovsky Peninsula and the Muostakh Island). Russian Academy of Science, Siberian Branch, Permafrost Institute Yakutsk, 218 pp. (in Russian)

Smith GL (1997) Late Quarternary climates and limnology of the Lake Winnebago basin, Wisconsin, based on ostracodes. *Journal of Paleolimnology* 18: 249-260

Smith LC, Sheng Y, MacDonald GM and Hinzman LD (2005) Disappearing Arctic lakes. *Science* 308: 1429

Smol JP, Wolfge A, Birks HJB, Douglas MSV, Jones VJ, Korhola A, Pienitz R, Rühland K, Sorvari S, Antoniades D and co-authors (2005) Climate-driven regime shifts in the biological communities of arctic lakes. *Proceedings of the National Academy of Sciences* (PNAS) 102: 4397-4402

Smol JP and Douglas MSV (2007) Crossing the final ecological threshold in high Arctic ponds. *Proceedings of the National Academy of Sciences* (PNAS) 104: 12395-12397

Sohn IG (1958) Chemical constituents of ostracodes; some applications to paleontology and paleoecology. *Journal of Paleontology* 32:730-736

Soloviev PA (1959) *Kriolitozona severnoi chasti Leno-Amgiskogo mezhdurech'ya* (The cryolithozone of the northern part of the Lena-Amga-interfluve). Soviet Academy of Science, Moscow, 144 pp. (in Russian)

Soloviev PA (1973) Thermokarst phenomena and landforms due to frost heaving in Central Yakutia. *Biuletyn Peryglacjalny* 23: 135-155

Stuiver M and Polach HA (1977) Discussion: Reporting of ^{14}C data. *Radiocarbon* 19: 355-363

Stuiver M, Reimer PJ, Bard E, Beck JW, Burr GS, Hughen KA, Kromer B, McCormac G, van der Plicht J and Spurk M (1998) INTCAL98 radiocarbon age calibration, 24,000-0 cal BP. *Radiocarbon* 40: 1041-1083

Svenning MA, Klemetsen A and Olsen T (2006) Habitat and food choice of Arctic char in Linnevatn on Spitsbergen, Svalbard: the first year-round investigation in a High Arctic lake. *Ecology of Freshwater Fish* 16: 70-77

Swain FM (1963) Pleistocene ostracodes from Gubic Formation, Arctic coastal plain, Alaska. *Journal of Paleontology* 37: 798-834

Tarasov P, Granoszweski W, Bezrukova E, Brewer S, Nita M, Abzaeva A and Oberhänsli H (2005) Quantitative reconstruction of the last interglacial vegetation and climate based on pollen record from Lake Baikal, Russia. *Climate Dynamics* 25: 625-637

Tomirdiaro SV (1982) Evolution of lowland landscapes in northern Asia during Late Quaternary time. In: Hopkins DV, Matthews JV Jr, Schweger CE and Young SB (eds.) *Paleoecology of Beringia*. Academic Press, New York, pp. 29-37.

Tomirdiaro SV and Chernenky BI (1987) *Kriogenno-eolovye otlozheniya vostochnoy arktiki i subarktiki* (Cryogenic deposits of East Arctic and Subarctic). Soviet Academy of Science, Far East Branch, Moscow, 198 pp. (in Russian)

Triebel E (1941) Die ersten Ostracoden aus der Paludinenbank. Zeitschrift für Geschiebeforschung 17: 61-75 (in German)

Tumel N (2002) Permafrost. In: Shahgedanova M (ed.) *The Physical Geography of Northern Eurasia*. Oxford University Press, Oxford, pp. 149-168

Turpen JB and Angell RW (1971) Aspects of moulting and calcification in the ostracod *Heterocypris*. *Biological Bulletin, Marine Biological Laboratory, Woods Hole* 140: 331-338

Tumskoy VE and Basilyan AE (2006) Opornyi razrez chetvertichnykh otlozhenii ostrova Bol'shoy Lyakhovsky (Key section of Quaternary deposits on Bol'shoy Lyakhovsky Island) In: *Problemy korrelatsii pleistotsenovykh sobytii na Russkom Severe COPERN* (Correlation problems of Pleistocene Events in the Russian North) COPERN abstracts. December 4-6, 2006, St. Petersburg, pp. 106-107 (in Russian)

van Everdingen R (ed.) (1998, revised May 2005) *Multi-language glossary of permafrost and related ground-ice terms*. Boulder, CO: National Snow and Ice Data Center/World Data Center for Glaciology (published online: http://nsidc.org/fgdc/glossary/)

van Harten D (2000) Variable noding in *Cyprideis torosa* (Ostracoda, Crustacea): an overview, experimental results and a model from Catastrophe Theory. *Hydrobiologia* 419: 131-139

Vartanyan S L, Garutt V E and Sher A V (1993) Holocene dwarf mammoths from Wrangel Island in the Siberian Arctic. *Nature* 362: 337-340

Vasil'chuk YK (1992) *Izotopno-kislorodnyi sostav podzemnykh l'dov – Opyt paleogeokriologicheskikh rekonstrultsii* (Oxygen isotope composition of ground ice – Application to paleogeocryological reconstructions). Moscow State University Publishers, Moscow, 420 pp. (in Russian)

Velichko AA, Curry B and Ehlers J (2005) Main Quaternary chronostratigraphical units used in Siberia, East-European Plain, West Europe and North America. In: Velichko AA and Nechaev VP (eds.) *Cenozoic climatic and environmental changes in Russia*. The Geological Society of America Special Paper 382: pp. XVII

Velichko AA and Nechaev VP (eds.) (2005) *Cenozoic Climatic and Environmental Changes in Russia*. Geological Society of America Special Paper 382, 226 pp.

Vereshchagin VN (ed.) (1982) *Stratigraficheskii slovar' SSSR*. Paleogen, Neogen i Chetvertichnaya sistema (Stratigraphical dictionary of the USSR. Palaeogene, Neogene, Quaternary system). Nauka, Moscow, 128 pp. (in Russian)

Vesper B (1975) To the problem of noding on *Cyprideis torosa* (JONES, 1850). *Bulletins of American Paleontology* 58: 205-216

Viehberg FA (2002) A new and simple method for qualitative sampling of meiobenthos-communities. *Limnologica* 32: 350-351

Viehberg FA (2006) Freshwater ostracod assemblages and their relationship to environmental variables in waters from northeast Germany. *Hydrobiologia* 571: 213-224

von Grafenstein U, Erlenkeuser H and Trimborn P (1999) Oxygen and carbon isotopes in modern fresh-water ostracod valves: Assessing vital offsets and autecological effects of interest for palaeoclimate studies. *Palaeogeography Palaeoclimatology Palaeoecology* 148: 133-152

von Toll EV (1897) *Iskopaemye ledniki Novo-Sibirskikh ostrovov, ikh otnoshenie k trupam mamontov i k lednikovomu periodu* (Ancient glaciers of New Siberian Islands, their relation to mammoth corpses and the Glacial period). Zapiski Imperatorskogo Russkogo Geograficheskogo obshestva po obshei geografii (Notes of the Russian Imperial Geographical Society) 32: 1-137 (in Russian)

Walsh J, Anisimov O, Hagen JOM, Jakobsson T, Oerlemans J, Prowse TD, Romanovsky V, Savelieva N, Serreze M, Shiklomanov A and co-authors (2005) Cryosphere and hydrology. In: Symon L, Arris L and Heal B (eds.) *Arctic Climate Impact Assessment (ACIA)*. Cambridge University Press, Cambridge and New York, pp. 183-242 (published online: http://www.acia.uaf.edu)

Wansard G, De Deckker P and Julià R (1998) Variability in ostracod partition coefficients D(Sr) and D(Mg): Implications for lacustrine palaeoenvironmental reconstructions. *Chemical Geology* 146: 39-54

Wansard G, Roca JR and Mezquita F (1999) Experimental determination of strontium and magnesium partitioning in calcite of the freshwater ostracod Herpetocypris intermedia. *Archiv für Hydrobiologie* 145: 237-253

Wansard G and Mezquita F (2001) The response of ostracod shell chemistry to seasonal change in a Mediterranean freshwater spring environment. *Journal of Paleolimnology* 25: 9-16

Wetterich S, Schirrmeister L and Pietrzeniuk E (2005) Freshwater ostracodes in Quaternary permafrost deposits in the Siberian Arctic. *Journal of Paleolimnology* 34: 363-374

Wetterich S, Schirrmeister L, Meyer H, Viehberg FA and Mackensen A (2008a) Arctic freshwater ostracods from modern periglacial environment in the Lena River Delta (Siberian Arctic, Russia): geochemical applications for palaeoenvironmental reconstructions. *Journal of Paleolimnology* 39: 427-449

Wetterich S, Herzschuh U, Meyer H, Pestryakova L, Plessen B, Lopez CML and Schirrmeister L (2008b) Evaporation effects as reflected in freshwaters and ostracod calcite from modern environments in Central and Northeast Yakutia (East Siberia, Russia). *Hydrobiologia* 614:171-195

Wetterich S, Kuzmina S, Andreev AA, Kienast F, Meyer H, Schirrmeister L, Kuznetsova T and Sierralta M (2008c) Palaeoenvironmental dynamics inferred from late Quaternary permafrost deposits on Kurungnakh Island, Lena Delta, Northeast Siberia, Russia. *Quaternary Science Reviews* 27: 1523-1540

Wetterich S, Schirrmeister L, Meyer H and Siegert C (2008d) Thermokarst lakes in Central Yakutia (East Siberia) as habitats of freshwater ostracods and archives of palaeoclimate. In: Kane DL and Hinkel KM (eds.) *Proceedings of the 9th International Conference on Permafrost (NICOP).* University of Alaska Fairbanks, Institute of Northern Engineering, pp. 1945-1950.

Wetterich S, Viehberg FA, Pienitz R and Schirrmeister L (2008e). Ecological training set of freshwater ostracods in Canadian and Siberian periglacial regions. European Geosciences Union (EGU) General Assembly, April 13-18, 2008, Vienna, Austria. Geophysical Research Abstracts, vol. 10, EGU2008-A-01983 (SRef-ID: 1607-7962/gra/ EGU2008-A-01983)

Wetterich S and Schirrmeister L (2009) Limnological studies in the Dimitrii-Laptev-Strait region. In: Boike J, Bol'shiyanov D Yu, Schirrmeister L and Wetterich S (eds.) *The Expedition LENA - NEW SIBERIAN ISLANDS 2007 during the International Polar Year (IPY) 2007/2008*. Berichte zur Polar- und Meeresforschung 584: 155-163

Wetterich S and Schirrmeister L (in preparation) Limnological studies in modern periglacial waters on the lower Kolyma plain. In: Schirrmeister L, Wetterich S and Kholodov A.L. (eds.) *The joint Russian-German Expedition BERINGIA/KOLYMA 2008 during the International Polar Year (IPY) 2007/2008*. Berichte zur Polar- und Meeresforschung

Wille C, Kobabe S and Kutzbach L (2003) Energy and water budget of permafrost soils – long time soil survey station on Samoylov Island. In: Grigoriev MN, Rachold V, Bolshiyanov DY, Pfeiffer EM, Schirrmeister L, Wagner D and Hubberten H-W (eds.) *Russian-German Cooperation System Laptev Sea: The Expedition LENA 2002*. Berichte zur Polar- und Meeresforschung 466: 17-28

Wrona FJ, Prowse TD, Reist J, Beamish R, Gibson, JJ Hobbie J, Jeppesen E, King J, Koeck G, Korhola A and co-authors (2005) Freshwater ecosystems and fisheries. In: Symon L, Arris L and Heal B (eds.) *Arctic Climate Impact Assessment (ACIA)*. Cambridge University Press, Cambridge and New York, pp. 353-452 (published online: http://www.acia.uaf.edu)

Xia J, Haskell BJ, Engstrom DR and Ito E (1997a) Holocene climate reconstructions from tandem trace-element and stable-isotope composition of ostracodes from Coldwater Lake, North Dakota, U.S.A. *Journal of Paleolimnology* 17: 85-100

Xia J, Ito E and Engstrom DR (1997b) Geochemistry of ostracode calcite 1: an experimental determination of oxygen isotope fractionation. *Geochimica et Cosmochimica Acta* 61: 377-382

Xia J, Engstrom DR and Ito E (1997c) Geochemistry of ostracode calcite 2: effects of the water chemistry and seasonal temperature variation on *Candona rawsoni*. *Geochimica et Cosmochimica Acta* 61: 383-391

Yershov YD (1990) *Obshchaya geokriologiya* (General Geocryology). Nedra, Moscow, 559 pp.

Yoshikawa K and Hinzman L (2003) Shrinking thermokarst ponds and groundwater dynamics in discontinuous permafrost near Council, Alaska. *Permafrost and Periglacial Processes* 14: 151-160

Yurtsev BA (2001) The Pleistocene "Tundra-Steppe" and the productivity paradox: the landscape approach. *Quaternary Science Reviews* 20: 165-174

Zhang T (2003) Distribution of seasonally and perennially frozen ground in the northern Hemisphere. In: *Proceedings of the 8th International Conference on Permafrost (EICOP)*. 21-25 July, 2003. Zurich, Switzerland, pp. 1289-1294

Note: The reference list has been updated and arranged according to the structure of the thesis. Therefore, slight differences to citations in the already published original papers (Chapters 2 and 3; Appendices I and II) may occur.

Acknowledgements

During the last years many people from my scientific and private environment helped realise and finally accomplish my dissertation. To all of them my warmest thanks.

I would like to thank Prof. Hans-Wolfgang Hubberten for providing the opportunity to work at the Alfred Wegener Institute in Potsdam (AWI), for supervision of the thesis and helpful thoughts in special permafrost and stable isotope related questions. He supported my participation in conferences and several expeditions to Siberia and Alaska where I could not only collect samples and data for my research, but also got to know fascinating places of the Arctic.

Since my beginning at the institute as student assistant I was supported by Dr. Lutz Schirrmeister who attended and guided my research in many ways. Thanks to his enthusiasm and ongoing interest, many ideas for research, fieldwork and interpretation were not only created but also realised. Lutz contributed a lot to the 'hot' final phase of my PhD and hopefully our collaboration will be continued under auspices of new projects.

I am grateful to my colleagues from the AWI interested in my work. I really benefited by discussions, advices and experience. In particular, Dr. Christine Siegert gave me the first ideas of permafrost science and Dr. Hanno Meyer was an always critical and constructive counterpart. I really enjoyed discussions in his basement office. Taking into account the multidisciplinary character of the thesis publications my research benefited from contributions of my co-authors whose work gave a broader context and fresh ideas to the ostracod data. The publications benefited by English language correction and valuable comments from Dr. Candace O'Connor (UAF, Fairbanks, Alaska) and Nicole Couture (McGill University, Montreal, Canada). Furthermore, Candace, and Thomas Opel, Dr. Hanno Meyer and Dr. Georg Schwamborn (all from AWI) are acknowledged for their rapid proof-reading of the final version.

First insights into ostracod research gave me Dr. Erika Pietrzeniuk (formerly from the Museum of Natural History Berlin). Later I became familiar with the ostracodologist's community and continued fruitful exchange especially with Dr. Finn Viehberg (University of Braunschweig), Prof. Steffen Mischke (Free University Berlin) and Dr. Claude Meisch (National Museum of Natural History Luxembourg) who also kindly hosted a study stay at his affiliation in summer 2006.

Fieldwork in 2002, 2005, 2007 and 2008 was performed with financial support of the German Federal Ministry of Education and Research for the Russian-German Cooperation SYSTEM LAPTEV SEA and the German Research Foundation (DFG) within the framework of several grants. Any of my expeditions to the Arctic was characterised by a trustful teamwork of Russian and German participants. For me it was a great experience to realise fieldwork in

cooperation with my Russian colleagues Dr. Lyudmila Pestryakova (Yakutsk State University), Dr. Viktor Kunitsky (Permafrost Institute Yakutsk), Aleksandr Derevyagin, Dr. Vladimir Tumskoy and Dmitry Dobrynin (all from Moscow State University). Based on their experience in scientific and common expedition tasks exciting fieldwork was possible. Furthermore, the German commitment during expeditions is honourable mentioned. In this course, my special thanks go to Dr. Lutz Schirrmeister, Dr. Frank Kienast, Thomas Opel and Prof. Ulrike Herzschuh (all from AWI).

Analytical work would not be possible without the engagement of the people in the labs. I would like to thank for their support Antje Eulenburg, Ute Bastian, Lutz Schönicke, Beate Hollmann, Torben Lübbe, Judith Walter, Dr. Hanno Meyer, Prof. Andreas Mackensen (all from AWI) as well as Sabine Tonn, Dr. Helga Kemnitz, Prof. Jörg Erzinger, and Dr. Birgit Plessen (all from GFZ) who all helped in their own field of competence and gave me the chance to learn about sedimentological, geochemical and SEM methods.

During the PhD my work was also promoted by several funds from the DFG and the International Permafrost Association (IPA) which gave me the possibility to participate in international conferences. The German Academic Exchange Service (DAAD) provided a grant for a four-month research stay in Russia kindly hosted by Prof. Anatoly Bobrov in Moscow and Prof. Dmitry Subetto in St. Petersburg.

I really enjoyed the time in Potsdam at the Alfred Wegener Institute where I could work in a friendly face-to-face atmosphere. Actions of the Jungforscher community helped during hard times.

Finally, my private thanks remain private thus not expressed in particular here.